CHAPTER 1

TOXIC POTENTIALS OF HETEROGENEOUS CHEMICAL MIXTURE EXPOSURE ON TOXIC MANIFESTATION INDICATORS

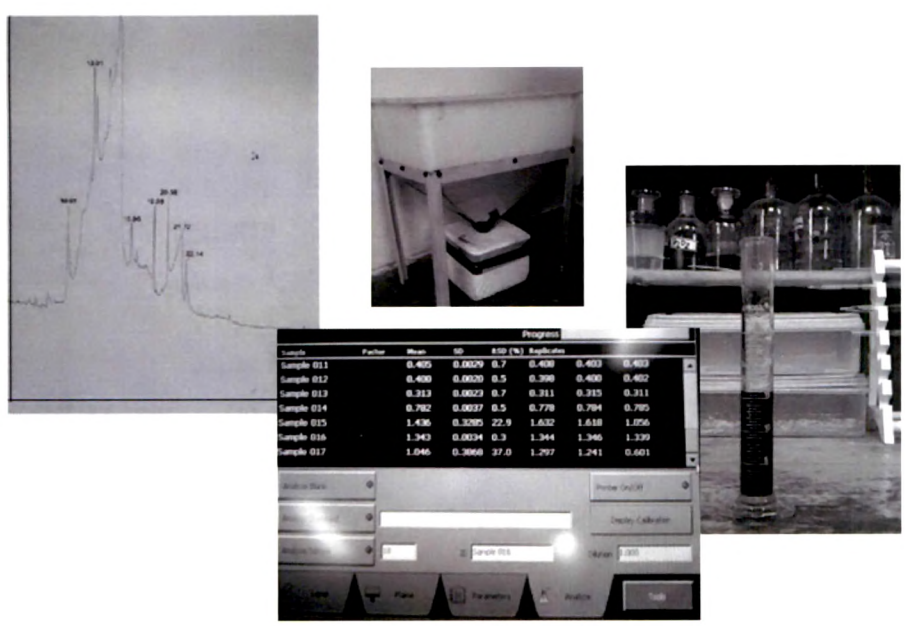

The tremendous increase in the use of large varieties of chemicals over past few decades has inevitably resulted in an increased flux of harmful substances in our environment. Evidences suggest that the presence of these chemicals has had deleterious effects on life (Jarup, 2002; Toft *et al.,* 2004; Schecter *et al.,* 2005; Jurewicz and Hanke, 2011; Linos *et al.,* 2011). Humans are exposed to mixture of combination of chemicals at low doses throughout their life. Therefore, it is necessary to evaluate the exposure outcome of chemical mixture. Animal studies are major element of the safety assessment of many compounds, including insecticides, pharmaceuticals and industrial chemicals. Until recently, about 95% of all chemical toxicity studies were performed on different animals with individual chemicals (Simmons, 1995; Groten *et al.*, 1999). The goal of the present study was to study the toxicological effects of heterogeneous chemical mixture (HCM) at low doses for longer time period. The following factors were tasted: clinical signs, daily food and water intake, body weight gain; hematological parameters, blood toxicant content or level, with level of two trace essential element Zn and Se.

Clinical Signs, Body Weight and Food and Water Consumption

There was no mortality observed in any of the group throughout the study duration. Physical observations of all the groups of animals indicated that none of them showed general signs and symptoms of toxicity such as changes in skin and fur, respiratory function, walking disproportion or dragging of legs, hyperactivity or lethargy *etc.* except some uneasiness noticed in high dose heterogeneous chemical mixture (HCM) treated group towards the end of the experimental schedule.

Average consumption of water and food in healthy adult rats (control groups) were increased gradually along with the gradual increment in the body weight, while in HCM treated groups significant decrement in water and food consumption were noted towards the end of 60 day experimentation with a decrement in body weight. Table 1 and Fig. 1 describe the rate of water consumption per week during the experimental regimen (17 weeks

approximately). The values are expressed in the weakly means as millilitres of water per rat per week. In high dose group, towards the end of experimentation of HCM treatment and initiation of recovery schedule there was significant decrement in water intake. The recovery started from the 3rd week post exposure of high dose experimentation schedule. The similar pattern of water intake and decrement was also observed in low dose HCM treatment, but the decrement was only significant at the end of 60 day experimentation schedule (Group V) and recovery was observed from the very first week of recovery schedule (Group IX) (Table 1, Fig. 1).

Table 2 lists the rate of food consumption during the experimental schedule and the values are expressed as gram of food intake per animal per week. There was a significant decrease in food consumption observed in high dose HCM treated groups near the end of experimentation. Significant decrement of food consumption was started in the 5th week of 60 days of experimentation schedule and it continued in recovery groups for 3 consecutive weeks. In low dose HCM treatment schedule decrement in food intake was observed in 8th week (Table 2, Fig. 2).

Table 3 describes the changes in body weight per week per animal of all the experimental groups and the values are expressed as mean and standard error for the 17 weeks approximately of the experimental regimen. The results clearly demonstrated that after initiation of experiment all the animals of control groups showed weight gain. The percentage increment in the body weight measured on day 60 and 120 of non treated control animals were found to be 12.7 and 14.01 % and vehicle treated control animals were found 16.15 and 11.67 %, respectively (Tables 4, 5, Fig. 3). However, the percentage changes in high dose HCM treated animals were found to be -8.21 and 13.38 % and in the low dose treated animal were -8.08 and 16.04 % for day 60 and 120 respectively. The result indicated that following the treatment of HCM the animals exhibited loss of weight in both high and low dose groups and in 60 days withdrawal group (Tables 4, 5, Fig. 3). The body weight of group VIII (high dose) and IX (Low dose) animals did not recover as

compared to control groups VII and VIII but, it can be assumed that the treated animal exhibited a pattern of recovery during the withdrawal phase of the experiment (Tables 3, 4, 5).

Hematological Analysis

The changes in the mean red blood cell (RBC) count, Hemoglobin concentration (Hb), hematocrite (HCT), Mean corpuscular volume (MCV), mean corpuscular hemoglobin (MCH), mean corpuscular hemoglobin concentration (MCHC), Platelet count, Platelet, white blood cell (WBC) count and differential white blood cell count of treated and untreated rats are presented in Table 6, Fig.6.

In rats treated with high dose HCM; the RBC, Hb and HCT values showed significant decrease while no significant changes were found in RBC, Hb and HCT values of rats treated with low dose of HCM compared with the values obtained from the 60 day vehicle treated group. Similarly no changes in above haematological parameter were observed in both recovery groups when compared with their respective controls. Moreover, no marked differences were observed in the values of all the control groups. On the other hand, no statistically significant changes were observed in the values of MCV, MCH and MCHC in any of the groups. High and low dose HCM treatment marginally increased the WBC values of all the treated rats though not significantly ($P>0.05$) when compared with the values of control groups (Table 6, Fig. 6). The changes in the differential WBC count following HCM administration to rats at high and low doses were not significant and all the values were found to be within the normal range. HCM exposure caused increase in blood Platelet count though the increment was not statistically significant when compared with controls. Furthermore, no toxicological meaningful differences were observed between controls and recovery groups with respect to WBC, differential WBC and Platelet counts.

Detection of Cadmium and Chromium in Blood, Tissues and Urine Samples

Cadmium and chromium level were determined in blood, liver, kidney, testis, epididymis and urine by means of ICP (Tables 7, 8 and Fig.s. 7, 8). The results revealed that approximately more than 2 fold increments in cadmium (Cd) and chromium (Cr) levels were observed in groups IV and V in all the analyzed samples. While the levels of Cd and Cr was normal in all the other recovery and control groups. The increment of cadmium concentration was significant in blood, liver, testis and urine in group IV (high dose HCM) while insignificant increments were observed in kidney and epididymis samples. At low dose HCM administration, the significant increment of cadmium concentration was observed only in urine sample. Chromium concentration data showed its significant increment in urine and testis sample at high dose HCM treated group when compared with control group III and rest showed insignificant increment when compared with control group III.

Detection of Metabolites of Organic Compounds in Blood, Tissues and Urine Samples

The detection of DCB and PE metabolites after sixty days HCM administration at doses of 1/100 and 1/1000 of their individual LD_{50} values, in blood, urine and tissues are presented in Fig.s 10-15. The chief metabolites identified of 1, 2 DCB in urine at high dose (1/100) were 2, 3-dichlorophenol, 3, 4-dichlorophenol and 3, 4-dichlorobenzenethiol. But no such metabolites were detected in urine at low dose (1/1000) HCM exposure. Similarly, no metabolites of DCB could be detected in samples of blood, liver, kidney, testis and epididymis.

Phthalic acid monobutyl ester was detected as the metabolite of PE. It was detected in all the samples (blood, tissues, and urine) at both the doses of HCM.

Detection of Zinc and Selenium in Blood, Tissues and Urine Samples

The effects of cadmium, chromium, 1, 2-dichlorobenze and phthalic acid dibutyl ester mixture on selenium and zinc levels are depicted in Tables 9, 10 and Fig.s. 9, 10. Results indicated that concurrent exposure to these toxic chemicals increased selenium and zinc levels significantly in serum after 60 day treatment and non significantly in recovery groups when compared with their respective controls. Tissues zinc and selenium concentration decreased in HCM treated groups when compared with control group III. Tissues zinc and selenium level restored toward the normal values in recovery groups i.e. in group VIII and IX when compared with HCM exposed and control groups (Tables 9, 10 and Fig.s. 9, 10).

DISCUSSION

Chemicals in combination at low doses may have sub lethal effects at cellular and organ levels. Gravimetric analysis and haematological profile in experimental studies are proven to be sensitive indices and can provide quantifiable indications of disturbance for the evaluation of growth rate and physiology under stressed condition due to any kind of toxic insult (Stevens and Gallo, 1989; Gur and Waner, 1993; Abadin *et al.,* 1998). Studies have shown that exposures to chemical mixture disturb the normal physiology and these are reflected in the values of one or more parameters of the haematology and gravimetric analysis with clinical signs (Groten *et al.,* 1997; Adeyemi *et al.,* 2007). However, there are very less studies available demonstrating the changes in blood indices and gravimetric analysis of rats exposed to a heterogeneous nature of chemical mixture at low doses. Hence the aim of this study was to investigate the changes in clinical sings, gravimetric analysis and hematological profile in Wistar rat influenced by mixture of selected chemicals at NOAELs.

Clinical Signs, Body Weight and Food and Water Consumption

HCM treated rats, consumed significant less water and food as compared to control and also a marked decrease in body weight gain within

the 60 days experimental period was observed. Decrement in body weight gain is an expression of general toxicity or decrease in food consumption. However this is very difficult to predict precisely that whether the observed body weight decrement is due to decreased caloric consumption of diet or due to the nature of HCM. Our results, to some extent, support the observations reported by Jadhav *et al.,* 2007 who showed that mixture of eight heavy metals administration depress the weight gain along with water consumption. Withdrawal from HCM treatment in recovery groups improves the water and food intake and body weight gain.

Hematological analysis

A complete blood count provides detailed information about three types of blood cell: RBC, WBC and Platelets. Blood cell responses are important indicators of changes in the internal environment of animal. Changes in the blood parameter, which occur because of injuries of the organs or tissues, can be used to determine and confirm the dysfunction in the body induced by industrial compounds, heavy metals, pesticides, pharmaceutical products *etc.* (Abadin *et al.,* 1998; Institoris *et al.,* 1999; Mansour and Mossa, 2005; Sayim *et al.,* 2005; Asagba and Eriyamremu, 2007;).

The effects are very much dependent on concentration of chemicals and duration of exposure and can cause certain reversible and other irreversible changes in the homeostasis mechanisms of the animal. The results of the present study indicated that high dose and sub chronic HCM exposure induce significant haematological changes in rats such as decrement in red blood cell (RBC) count, Hemoglobin concentration (Hb), and hematocrite (HCT). RBC's are very important for the oxygen transport to the tissues and Hb concentration is directly correlated with the count of RBC's (Blackman and Rey, 2005). Literature has reported the induction of anaemia like condition with experimental exposure to chemicals (Abadin *et al.,* 1998) and its diagnosis is partly made through the determination of RBC's count, Hb and HCT (Yang, 1993; Mugahi *et al.,* 2003; Aziz and Zabut, 2011; Sharma *et*

al., 2007). Low RBC's count may be linked to reduction in formation rate or increased breakdown rate of RBC's. Starek et al. (2010) and Ita and Udofia, (2011) suggested that the decrease in RBC count is indicative of inadequate production of RBC's or the selective hemolysis of the aged erythrocytes leaving a population of young RBC's.

This study shows that mean hemoglobin in the vehicle treated control for 60 day was 14.89 ±0.34 and in high dose treated HCM was 13.22 ±0.38. A decrease in the concentration of Hb in the blood may be caused by the effect of toxic compounds as observed by other researchers, as well as decrease in RBC's and HCT value, also suggests the condition of anaemia in the body or confirms toxic impact of HCM in rats. Moreover, the heme biosynthesis has already been reported to be affected by exposure to heavy metals and other chemical compounds, which contributed towards the decrement in RBC's and Hb (Awad and William, 1997). Other red blood cell indices used to determine anaemia includes mean corpuscular volume (MCV), mean corpuscular hemoglobin (MCH) and mean corpuscular hemoglobin concentration (MCHC).

The slight increase in the number of WBC's of the HCM treatment group that was observed in group IV agrees with the other reports that chemicals individually or in a mixture cause an increase in WBC's (Prekeyi and Akinjokun, 2008; Ambali *et al.,* 2010). Activation of the immune system as an animal's defence mechanism may result in the increment in WBC count, as a result of an infection, toxic response to chemical or in cancer (Aziz *et al.,* 2006). NTP (1993) reported that after exposure to a chemical mixture of 25 ground water contaminants (at formulated concentration 378 ppm) WBC count of female rats was higher than the control after 26 week exposure. Thus the present findings are indicative of toxic manifestations following HCM exposure in male rats. However, the toxicity potentials of the toxicant mixture at present doses and duration of exposure are low.

Toxicant uptake and bioaccumulation in tissues

The selected four compounds are widely used chemicals. A very long term exposure study of these four chemicals individually in rats and mice showed a significant increase in systemic and reproductive alterations. Toxicant accumulation can occur if the homeostatic mechanisms cannot maintain properly i.e. the intake and excretion ratios to maintain the constant blood concentrations. In order to investigate the relation between metabolism and toxicity of selected compounds, the biotransformation (especially for organic compounds), tissue distribution, blood and urinary concentration at two different oral dose levels were investigated.

After HCM administration cadmium and chromium concentration increased more than two fold in all analysed samples. Interestingly, cadmium levels in testis and kidneys were high even following the recovery phase while the improvements in chromium levels in most of the tissues following the recovery phase very only marginal, particularly in the higher dose group. The findings, therefore, clearly indicate bioaccumulation of the toxic metals.

In urine, after 24 h of last administration of high dose of HCM (experiment day 61), the major metabolites of 1, 2-DCB and PE identified were 2, 3-dichlorophenol, 3, 4-dichlorophenol, 3, 4-dichlorobenzenethiol and phthalic acid monobutyl ester respectively. The identified metabolites were confirmed with the reports of other authors (Tanaka *et al.,* 1978; Hissink *et al.,* 1996; Kumagai and Matsunaga, 1997; Blount *et al.,* 2000). Following sixty days HCM exposure, only phthalic acid (one of the metabolites of dibutyl phthalic ester) was detected in extracted blood and tissues samples. These results may indicate that 1, 2 DCB readily metabolized than PE and this is strongly evident from the absence and/ or below detection level of metabolites of 1, 2 DCB. The compounds and their metabolites were previously shown to be positively associated with the adverse changes in the tissues which are indicative of over production of reactive oxygen species, DNA damage and condition of oxidative stress.

Therefore, significant increase in concentrations of metals and presence of organic metabolites recorded in HCM exposed groups compared to control may suggest cytotoxic conditions. And these findings are supported by observed alterations in hematological indices of HCM exposed rats.

Cadmium, chromium, DCB and PE are toxic compounds that may interact metabolically with nutritional essential elements like zinc and selenium. In a point of fact, an inadequate level of zinc and selenium has been shown to cause degenerative changes in tissues (Jeyaprakash and Chinnaswamy, 2005). It can be postulated that after HCM, the body level of zinc and selenium gradually diminished because of its excretion due to toxic action at different levels. This explanation conveys the obvious impression that after combined administration, selenium and zinc are gradually excreted from the body but the administered toxicants retained inside the body in sufficient amount to produce the toxic effect in different tissues.

CONCLUSION: The findings indicate potensial intoxication following HCM exposure for 60 days at both the doses and were reversible to near normal within next 60 days of withdrawal phase. The experimental toxicants and/or their metabolites were detected in the blood, tissues and urine of the exposed animals clearly indicating the toxicity due to these chemicals.

Experimental Groups

Groups	Treatment	Autopsy day
I	Zero (initial) day control	01
II	Control (No treatment)	61
III	Control (Vehicle treatment)	61
IV	Heterogeneous chemical mixture treated group (1% of LD_{50} dose/ animal/ day - NOAEL dose level)	61
V	Heterogeneous chemical mixture treated group (0.1% of LD_{50} dose/ animal/ day)	61
VI	Control (No treatment)	121
VII	Control (Vehicle treatment)	121
VIII	Heterogeneous chemical mixture treated group (1% of LD_{50} dose/ animal/ day) for 60 days followed by withdrawal phase of 60 days - NOAEL dose level.	121
IX	Heterogeneous chemical mixture treated group (0.1% of LD_{50} dose/ animal/ day) for 60 days followed by withdrawal phase of 60 days.	121

Values in all the following Tables are Mean± SE and statistical significance is considered and presented for (*) $P<0.05$, (+) $P<0.01$ and (#) $P<0.001$ compared withrespective vehicle control.

Table 1: Average water intake per week per animal in ml

	G II	G III	G IV	G V
7th	211.9 ±1.47	201.2 ±3.22	191.6 ±9.09	191.7 ±3.45
14th	213.3 ±0.93	204.9 ±4.99	187.3 ±9.90	190.7 ±4.24
21st	213.9 ±0.83	203.5 ±4.01	186.8 ±11.25	189.5 ±3.83
28th	212.2 ±1.34	203.0 ±4.49	183.4 ±11.61	193.5 ±3.70
35th	211.5 ±3.07	205.2 ±5.05	181 ±11.41	188.2 ±9.17
42nd	209.1±2.204	204.6 ±3.40	172.5 ±6.87*	186.2 ±7.69
49th	214.2 ±5.05	203.5 ±6.03	165.0 ± 8.37*	185.3 ±7.96
56th	213.5± 5.02	202.7 ±4.66	166.2 ±7.56*	171.1 ±7.38*
60th	123.2 ±3.12	117.3 ±1.29	96.99 ±5.23*	104.3 ±3.52
	G VI	**GVII**	**GVIII**	**G IX**
67th	219.2 ±7.90	212.0 ±2.00	178.1 ±4.41*	195.1 ±4.29
74th	229.2 ±12.31	233.0 ±3.00	189.0 ±1.53*	198.3 ±5.19
81st	239.7 ±12.40	231.0 ±7.00	199.9 ±6.66	205.7 ±5.50
88th	232.1 ±6.95	228.0 ±5.93	211.4 ±9.44	203.9 ±6.16
95th	243.1 ±6.57	252.7 ±8.66	206.6 ±12.48	215.8 ±8.90
102nd	252.4 ±7.52	258.7 ±5.94	228.8 ±12.08	235.7 ±5.01
109th	255.9 ±6.07	248.8 ±3.2	227.5 ±9.88	247.1 ±9.97
116th	255.3 ±7.20	251.6 ±1.6	239.3 ±5.33	245.3 ±11.6
120th	144.5 ±8.76	147.6 ±1.41	127.8 ±0.20	141.0 ±4.49

Fig. 1: Average water intake per week by the animals.

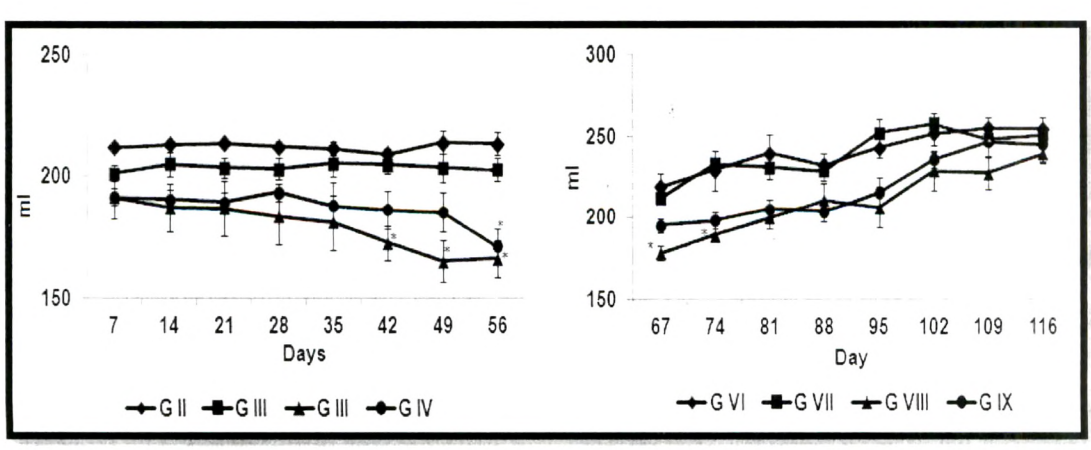

Table 2: Average food consumption per week per animal in grams

Day	G II	G III	G IV	G V
7th	144.0 ± 4.62	137.1 ±5.00	130.2 ±3.81	127.9 ±3.91
14th	141.1 ±4.35	136.0 ±3.34	131.2 ±4.46	128.9 ±3.58
21st	151.3 ±6.83	137.4 ±1.60	125.6 ±3.14	131.2 ±3.95
28th	143.2 ±6.36	140.1 ±1.83	129.3 ±4.40	128.7 ±1.96
35th	152.6 ±5.44	140.8 ±1.44	123.2 ±2.37*	127.7 ±2.78
42nd	146.3 ±3.31	139.3 ±2.22	119.8 ±4.36*	127.0 ±2.42
49th	152.1 ±4.81	140.8 ±2.14	111.2 ±4.30#	125.8 ±2.79
56th	147.0 ±3.27	142.6 ±0.89	107.6 ±4.27#	125.2 ±3.44*
60th	91.47 ±3.14	80.50 ±1.39	61.36 ±2.81#	70.44 ±1.79
	G VI	GVII	GVIII	G IX
67th	148.3 ±1.67	140.5 ±5.50	104.0 ±2.31*	117.4 ±8.55
74th	151.4 ±2.73	146.5 ±5.50	112.2 ±4.04*	123.3 ±6.66
81st	150.3 ±0.88	150.0 ±3.00	113.3 ±3.53#	118.0 ±4.16+
88th	160.3 ±5.28	160.0 ±9.99	129.8 ±6.58	135.3 ±5.33
95th	162.2 ±6.19	150.7 ±7.66	129.3 ±7.45	136.8 ±5.20
102nd	156.6 ±4.30	161.5 ±11.5	130.1 ±7.56	134.7 ±5.28
109th	160.3 ±5.28	165.7 ±7.33	140.6 ±5.30	140.1 ±3.98
116th	161.1 ±1.90	165.7 ±7.33	134.0 ±3.05	140.2 ±7.36
120th	104.5 ±6.60	91.17 ±7.83	79.06 ±3.30	82.11 ±5.53

Fig. 2: Average food consumption per week by the animals.

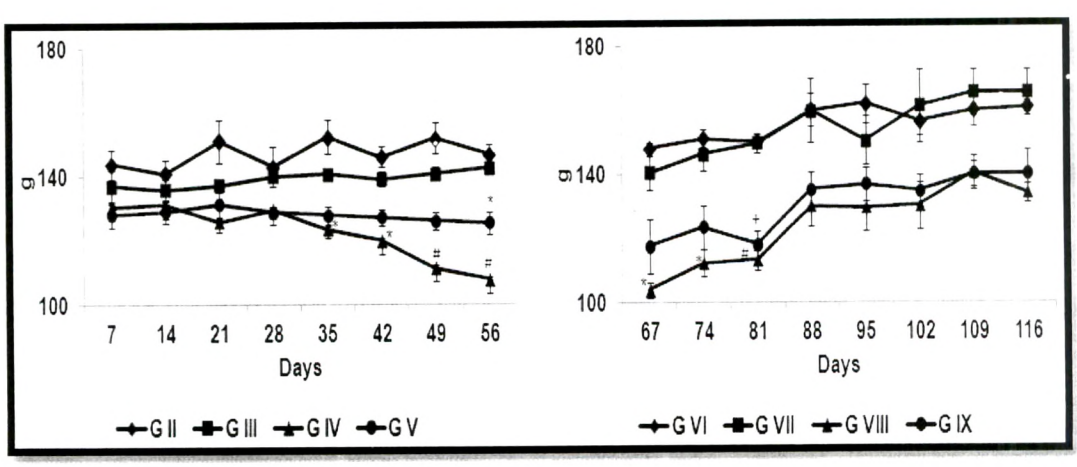

Table 3: Average body weight of the animals

Days	G II	G III	G IV	G V
Initial weight	299.0 ±2.67	305.0 ±4.23	324.5 ±4.91	339.5 ±3.37
7th	299.8 ±3.45	306.3 ±2.94	317.5 ±3.95	327.3 ±3.35
14th	307.3 ±2.98	315.0 ±2.50	311.0 ±4.08	323.8 ±3.22
21st	311.8 ±2.91	322.5 ±2.24	306.8 ±4.09	320.8 ±3.08
28th	317.0 ±2.65	329.4 ±1.98	304.8 ±4.19	317.3 ±3.23
35th	321.3 ±2.46	335.3 ±2.68	297.3 ±4.65	312.3 ±3.21
42nd	323.5 ±2.67	340.9 ±2.51	297.6 ±4.04	309.8 ±2.98
49th	327.0 ±2.60	345.3 ±2.52	295.8 ±3.69	306.8 ±2.44
56th	331.8 ±2.60	350.9 ±2.38	292.4 ±3.55	302.5 ±2.75
60th	338.0 ±2.60	357.5 ±2.46	291.3 ±3.26	302.8 ±2.87
	G VI	GVII	GVIII	G IX
67th	345.0 ±2.11	370.0 ±3.27	296.5 ±3.95	317.5 ±4.61
74th	351.5 ±1.83	375.6 ±3.59	302.0 ±3.82	325.5 ±4.56
81st	353.0 ±2.38	380.6 ±3.59	310.0 ±4.22	333.0 ±5.49
88th	359.0 ±2.21	385.6 ±3.83	316.0 ±3.06	342.0 ±5.33
95th	364.5 ±2.03	390.0 ±4.33	320.5 ±4.44	346.5 ±6.19
102nd	371.0 ±1.63	395.6 ±4.38	327.5 ±4.03	353.5 ±6.37
109th	377.5 ±1.86	403.1 ±4.62	333.5 ±3.66	362.0 ±5.83
116th	385.0 ±1.29	409.4 ±4.27	341.0 ±3.40	369.0 ±5.15
120th	395.5 ±2.03	409.4 ±4.27	341.0 ±3.40	369.0 ±5.15

Table 4: Average percentage change in body weight of the animals

	G II & G VI	G III & G VII	G IV & G VIII	G V & G IX
% change after 60 day treatment	12.7±0.90	16.15±0.67	-8.21±1.32#	-8.08±0.50#
% change after 60 day recovery period	14.01±0.71	11.67±0.45	13.38±1.37	16.04±0.35+
Over all % chance at end of experiment	24.39±0.73	25.89±1.31	5.57±0.74#	8.31±0.79#

Table 5: Average percentage change in body weight / week / animal

Days	G II	G III	G IV	G V
7th	1.58 ±0.35	2.11 ±0.48	0.41 ±0.32*	0.01 ±0.31#
14th	2.46 ±0.43	2.78 ±0.45	-2.12 ±0.40#	-1.08 ±0.30#
21st	1.44 ±0.28	2.32 ±0.40	-1.41 ±0.38#	-0.94 ±0.29#
28th	1.66 ±0.27	2.09 ±0.24	-0.68 ±0.32#	-1.12 ±0.33#
35th	1.33 ±0.26	1.74 ±0.32	-2.60 ±0.47#	-1.61 ±0.24#
42nd	0.68 ±0.35	1.65 ±0.23	0.27 ±1.50	-0.81 ±0.41
49th	1.07 ±0.28	1.26 ±0.30	-0.58 ±0.33#	-0.96 ±0.33#
56th	1.42 ±0.35	1.61 ±0.18	-1.12 ±0.37#	-1.43 ±0.28#
60th	1.85 ±0.24	1.83 ±0.25	-0.33 ±0.32#	0.07 ±0.19#
	G VI	GVII	GVIII	G IX
67th	1.44 ±0.43	1.69 ±0.22	-0.43 ±1.78	2.00 ±0.46
74th	1.85 ±0.37	1.49 ±0.39	1.82 ±0.46	2.46 ±0.25
81st	0.41 ±0.21	1.31 ±0.01	2.56 ±0.34	2.21 ±0.49
88th	1.67 ±0.40	1.29 ±0.43	1.93 ±0.54	2.64 ±0.30
95th	1.51 ±0.25	1.11 ±0.50	1.35 ±0.49	1.25 ±0.50
102nd	1.75 ±0.40	1.42 ±0.28	2.15 ±0.46	1.98 ±0.22
109th	1.71 ±0.39	1.86 ±0.23	1.81 ±0.44	2.37 ±0.30
116th	1.95 ±0.29	1.53 ±0.38	2.21 ±0.25	1.92 ±0.32
120th	2.64 ±0.28	0.61 ±0.23	0.73 ±0.32	0.42 ±0.21

Fig. 3:Average percentage change in body weight of animals

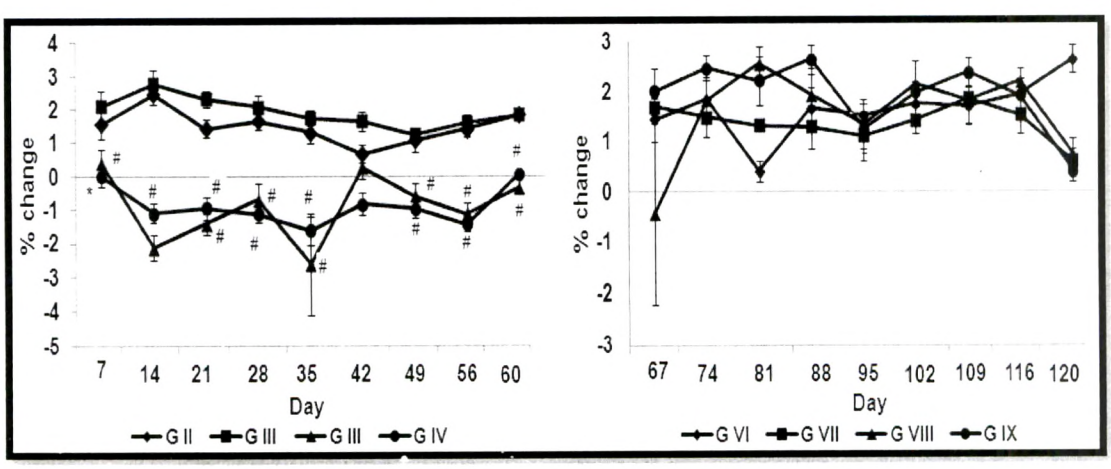

Table 6a: Analysis of haematological parameters

Groups	RBC (10^6/µl)	Hb (g/dL)	HCT (%)
I	8.30 ±0.21	14.21 ±0.30	43.21 ±0.92
II	8.59 ±0.27	15.21 ±0.23	45.49 ±0.69
III	8.55 ±0.23	14.89 ±0.34	45.12 ±0.82
IV	7.15± 0.21*	13.22 ±0.38$^+$	39.58 ±1.26$^+$
V	9.20 ±0.22	14.10 ±0.28	42.71 ±0.87
VI	8.60 ±0.33	14.80 ±0.21	44.36 ±0.72
VII	8.65 ±0.25	15.61 ±0.38	46.74 ±1.20
VIII	8.90 ±0.21	15.36 ±0.13	46.40 ±0.59
IX	8.80 ±0.40	15.32 ±0.19	45.80 ±0.58

Fig. 6a: Analysis of haematological parameters

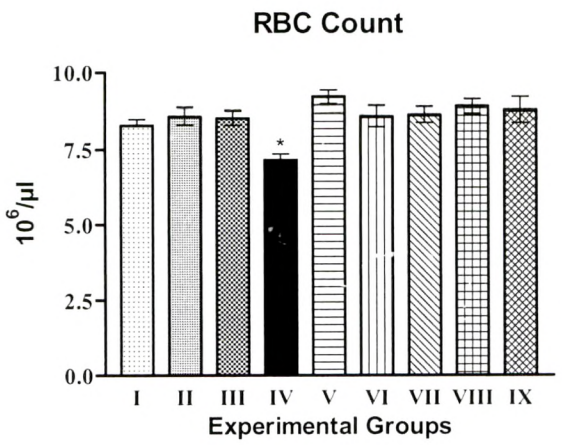

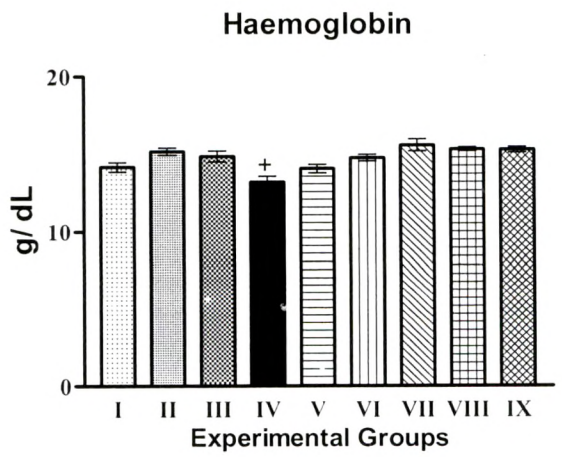

Table 6b: Analysis of haematological parameters

Groups	MCV (fL)	MCHC (g/dL)	MCH (pg)
I	52.21 ±1.40	32.88 ±0.18	17.16 ±0.45
II	53.17 ±1.40	33.44 ±0.26	17.80 ±0.58
III	52.96 ±1.37	33.02 ±0.57	17.47 ±0.44
IV	55.36 ±0.71	33.44 ±0.37	18.51 ±0.33
V	46.53 ±1.01	33.02 ±0.29	15.36 ±0.35
VI	52.16 ±2.52	33.39 ±0.55	17.38 ±0.75
VII	54.30 ±2.03	33.41 ±0.25	18.13 ±0.64
VIII	52.36 ±1.73	33.13 ±0.24	17.33 ±0.51
IX	52.64 ±2.12	33.46 ±0.29	17.60 ±0.68

Fig. 6b: Analysis of haematological parameters

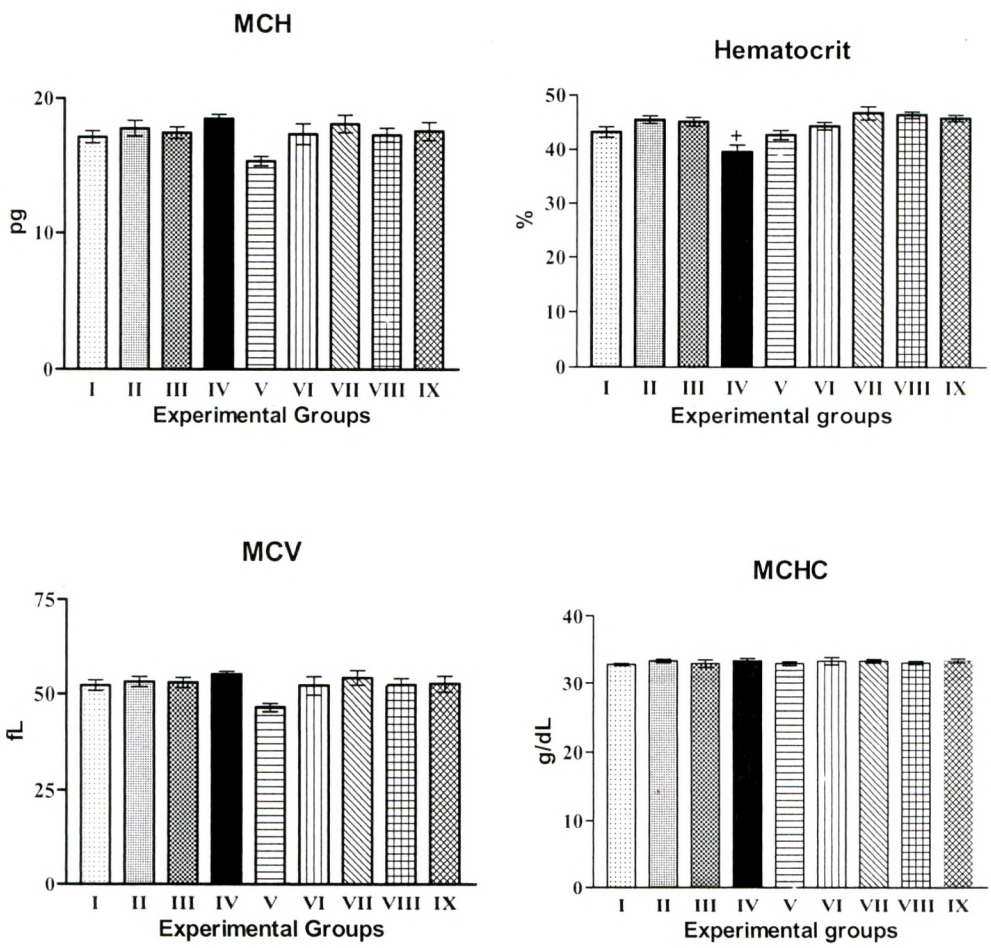

Table 6c: Analysis of haematological parameters

Groups	Platelets (10^3/ul)	WBC (10^3/µl)
I	743.60 ±57.57	8.80 ±0.23
II	803.10 ±61.58	9.31 ±0.33
III	845.40 ±63.33	8.64 ±0.43
IV	908.70 ±68.13	9.99 ±0.65
V	902.30 ±64.61	9.54 ±0.85
VI	899.60 ±105.5	9.21 ±0.54
VII	769.00 ±46.92	8.37 ±0.56
VIII	938.10 ±31.96	10.77 ±0.4
IX	1003.0 ±100.3	10.25 ±0.38

Fig. 6c: Analysis of haematological parameters

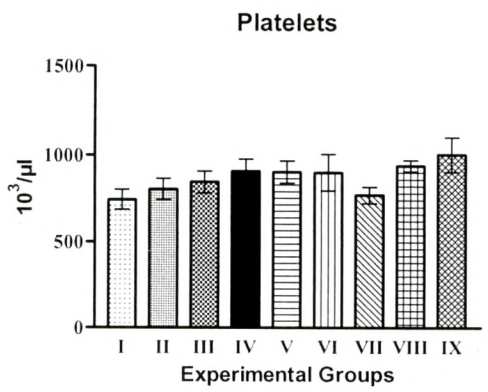

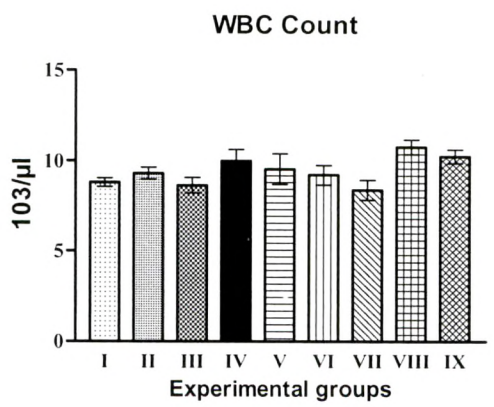

Table 6d: Analysis of haematological parameters

Groups	Differential count				
	N (%)	L (%)	E (%)	M (%)	B (%)
I	37.43±0.90	55.71±0.68	4.29±0.47	2.57±0.30	0
II	39.29±1.95	55.57±2.00	2.57±0.43	2.57±0.30	0
III	38.57±1.43	55.86±1.18	3.57±0.30	2.00±0.22	0
IV	34.00±1.22	60.71±1.61	3.43±0.57	1.86±0.26	0
V	39.00±1.40	55.57±1.48	3.14±0.51	2.29±0.36	0
VI	41.00±0.76	53.14±1.08	3.29±0.36	2.57±0.30	0
VII	39.71±0.71	55.43±0.57	3.00±0.53	1.86±0.34	0
VIII	40.71±1.71	53.86±1.71	3.57±0.30	1.86±0.14	0
IX	41.29±1.19	53.57±0.95	3.57±0.30	1.57±0.20	0

Table 7: Cadmium concentration in Blood, Urine and Tissue

Groups	Blood (ppm)	Urine (ppm)	Liver (µg/g)	Kidney (µg/g)	Testis (µg/g)	Epididymis (µg/g)
III	0.012 ±0.005	0.007 ±0.002	0.011 ±0.003	0.009 ±0.002	0.013 ±0.004	0.034 ±0.020
IV	0.063 ±0.019*	0.035 ±0.008+	0.053 ±0.010+	0.041 ±0.007	0.050 ±0.006#	0.043 ±0.009
V	0.047 ±0.014	0.046 ±0.007#	0.030 ±0.009	0.060 ±0.003	0.037 ±0.003	0.013 ±0.004
VII	0.007 ±0.002	0.009 ±0.005	0.010 ±0.002	0.016 ±0.006	0.006 ±0.002	0.034 ±0.013
VIII	0.004 ±0.002	0.002 ±0.001	0.015 ±0.001	0.097 ±0.048	0.050 ±0.028	BDL
IX	0.008 ±0.001	0.003 ±0.001	0.026 ±0.012	0.035 ±0.002	0.080 ±0.033	0.004 ±0.001

Fig. 7: Cadmium concentration in Blood, Urine and Tissue

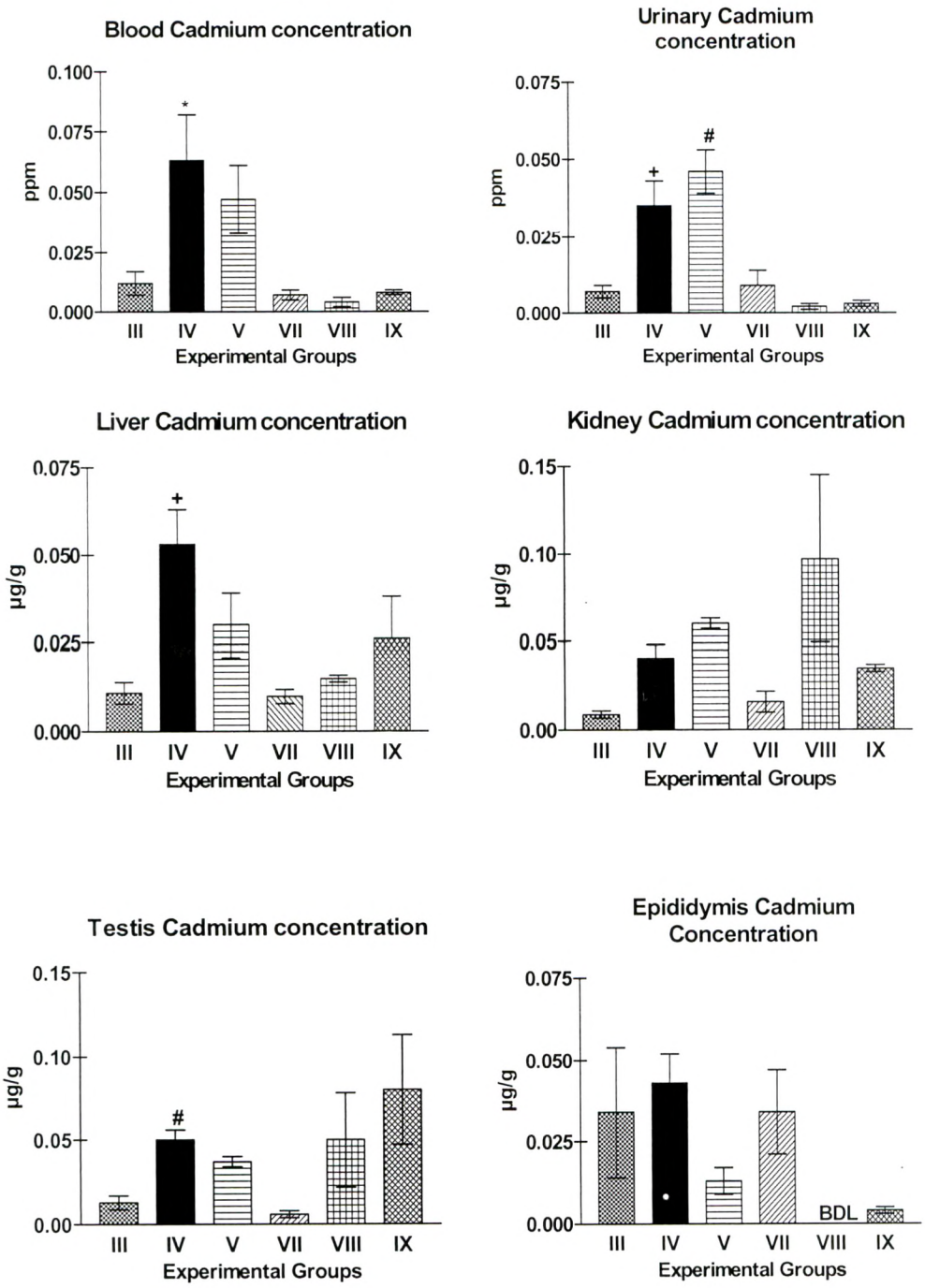

Table 8: Chromium concentration in Blood, Urine and Tissue

Groups	Blood (ppm)	Urine (ppm)	Liver (µg/g)	Kidney (µg/g)	Testis (µg/g)	Epididymis (µg/g)
III	0.096 ±0.021	0.130 ±0.023	0.104 ±0.055	0.034 ±0.004	0.037 ±0.006	0.035 ±0.002
IV	0.185 ±0.047	0.360 ±0.036^{+}	0.156 ±0.014	0.107 ±0.050	0.094 ±0.013^{+}	0.047 ±0.006
V	0.079 ±0.019	0.233 ±0.054	0.146 ±0.021	0.102 ±0.025	0.086 ±0.014	0.058 ±0.005
VII	0.033 ±0.033	0.156 ±0.064	0.110 ±0.026	0.047 ±0.009	0.044 ±0.007	0.027 ±0.007
VIII	0.120 ±0.120	0.119 ±0.029	0.129 ±0.021	0.055 ±0.015	0.030 ±0.007	0.038 ±0.013
IX	0.125 ±0.072	0.133 ±0.019	0.096 ±0.016	0.064 ±0.017	0.048 ±0.011	0.049 ±0.021

Fig. 8: Chromium concentration in Blood, Urine and Tissue

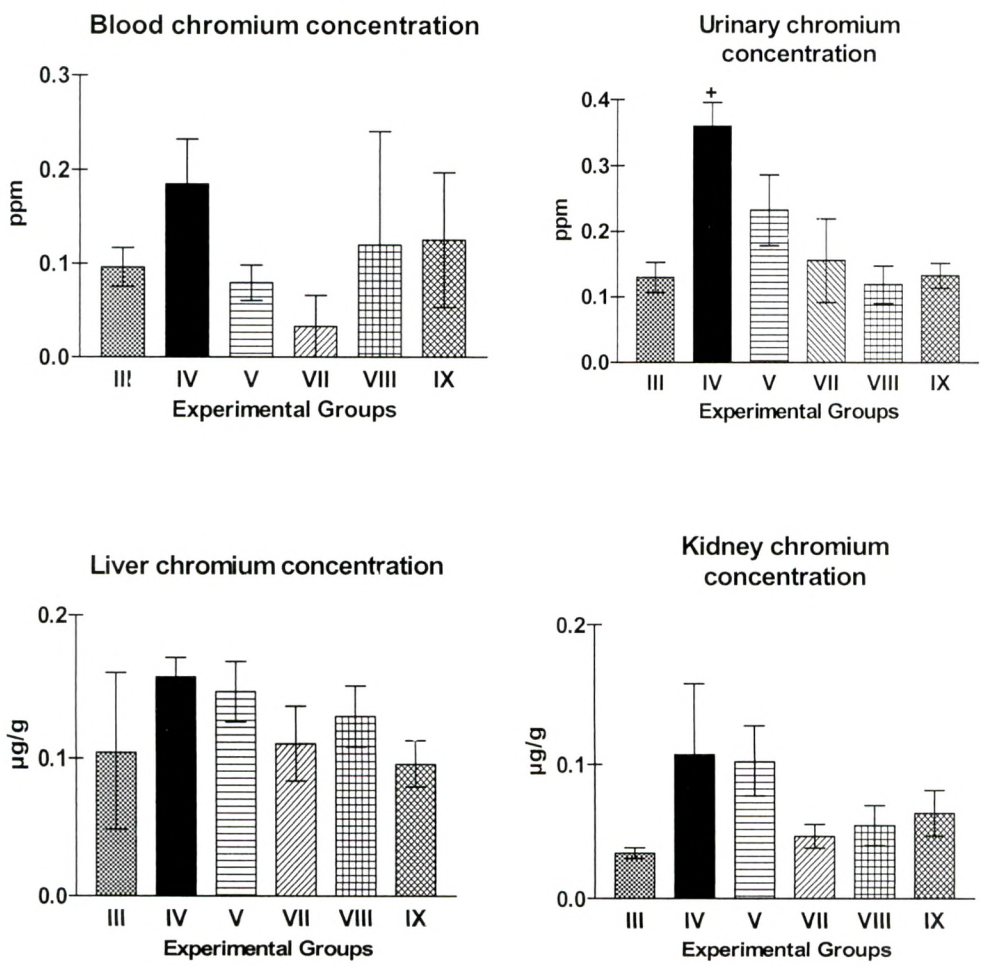

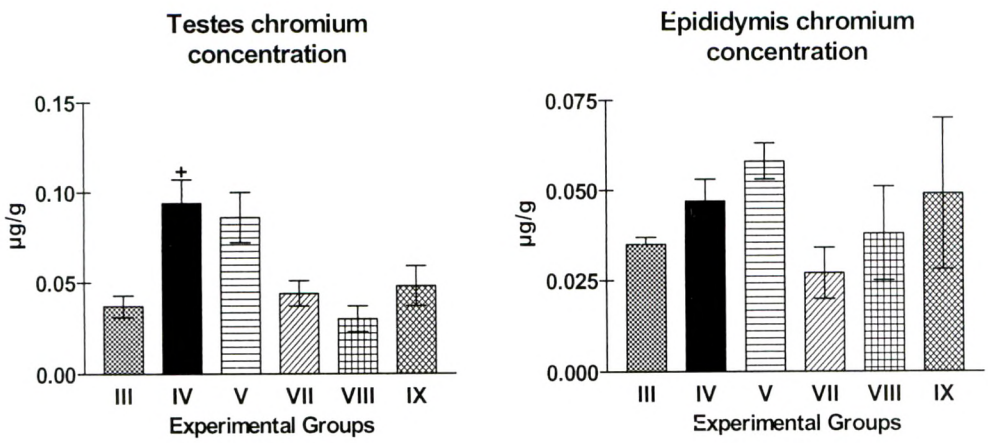

Table 9: Zinc concentration in Blood, Urine and Tissue

Groups	Blood (ppm)	Urine (ppm)	Liver (µg/g)	Kidney (µg/g)	Testis (µg/g)	Epididymis (µg/g)
III	51.20 ±2.11	23.09 ±3.67	76.49 ±1.24	65.74 ±2.05	44.66 ±1.79	29.73 ±2.01
IV	50.10 ±1.49	32.86 ±2.40	52.02 ±1.48^{+}	44.97 ±6.40*	35.02 ±3.08	18.03 ±1.92^{+}
V	56.67 ±1.31	33.57 ±2.53	59.09 ±2.75	58.11 ±1.88	39.13 ±5.97	24.57 ±3.21
VII	47.95 ±2.91	18.64 ±3.38	62.93 ±4.06	57.65 ±3.01	47.49 ±1.34	21.07 ±1.31
VIII	44.92 ±0.69	14.24 ±1.61	58.27 ±5.94	58.62 ±3.28	28.56 ±2.54	16.36 ±1.32
IX	48.79 ±2.86	14.60 ±1.45	62.09 ±5.41	50.44 ±6.30	35.91 ±4.85	20.55 ±1.30

Fig. 9: Zinc concentration in Blood, Urine and Tissue

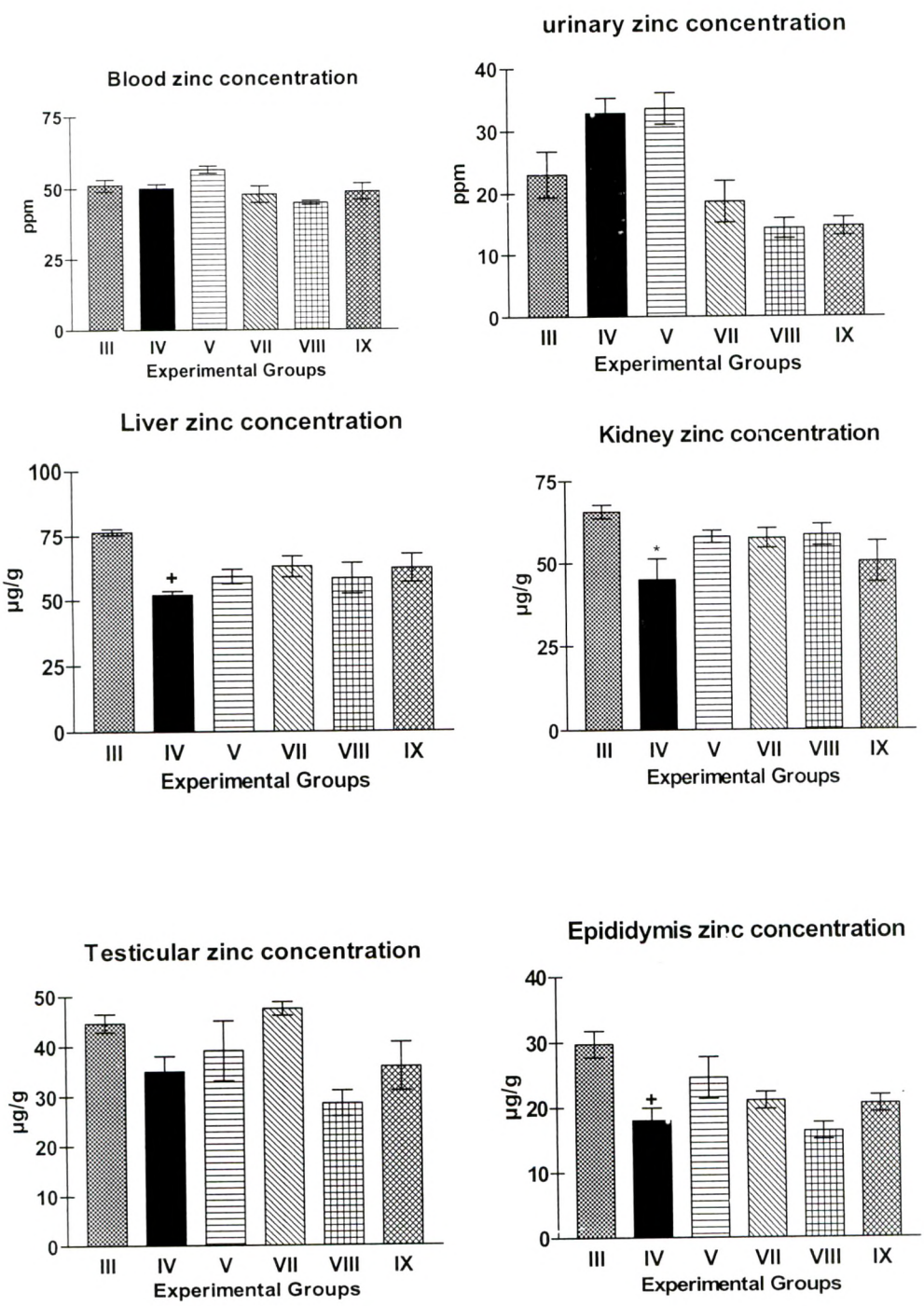

Table 10: Selenium concentration in Blood, Urine and Tissue

Groups	Blood (ppm)	Urine (ppm)	Liver (µg/g)	Kidney (µg/g)	Testis (µg/g)	Epididymis (µg/g)
III	0.35 ±0.036	0.15 ±0.028	0.65 ±0.033	0.59 ±0.017	0.38 ±0.015	0.29 ±0.016
IV	0.51 ±0.015^{+}	0.21 ±0.026*	0.34 ±0.001$^{\#}$	0.24 ±0.002$^{\#}$	0.16 ±0.027$^{\#}$	0.14 ±0.006$^{\#}$
V	0.57 ±0.026$^{\#}$	0.27 ±0.026	0.45 ±0.037$^{\#}$	0.51 ±0.042	0.21 ±0.002^{+}	0.21 ±0.001
VII	0.39 ±0.024	0.14 ±0.002	0.72 ±0.023	0.54 ±0.001	0.38 ±0.024	0.31 ±0.024
VIII	0.49 ±0.016	0.16 ±0.024	0.58 ±0.020^{+}	0.43 ±0.001*	0.30 ±0.027	0.17 ±0.018$^{\#}$
IX	0.52 ±0.022	0.19 ±0.023	0.65 ±0.001	0.51 ±0.024	0.32 ±0.060	0.20 ±0.025^{+}

Fig. 7: Selenium concentration in Blood, Urine and Tissue

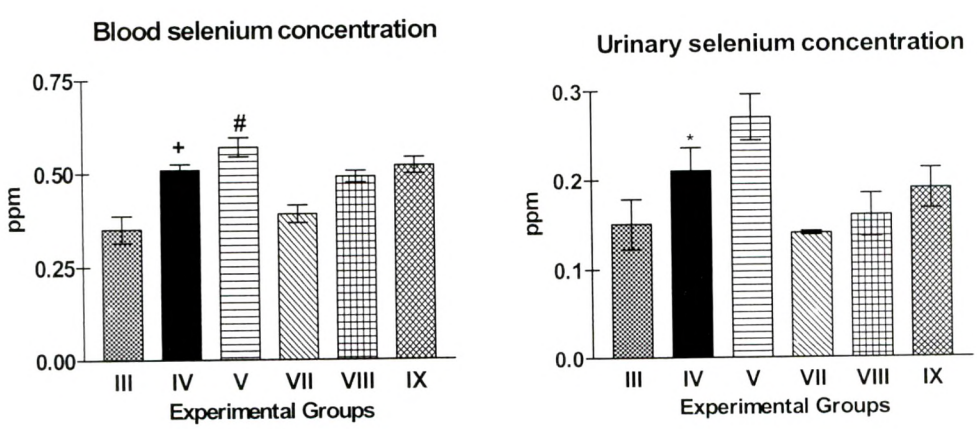

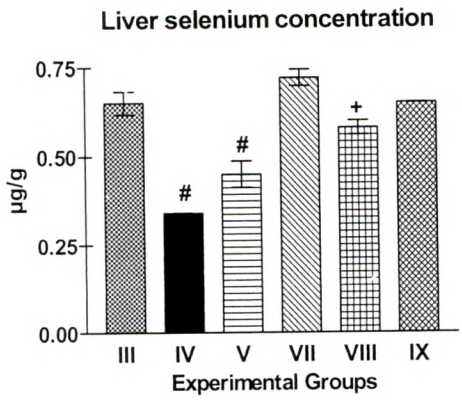
Liver selenium concentration
0.75
0.50
0.25
0.00
µg/g
#
#
+
III
IV
V
VII
VIII
IX
Experimental Groups

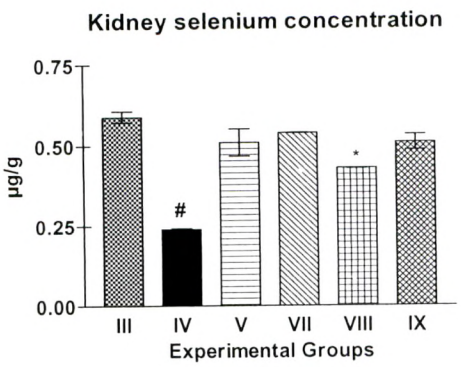
Kidney selenium concentration
0.75
0.50
0.25
0.00
µg/g
#
*
III
IV
V
VII
VIII
IX
Experimental Groups

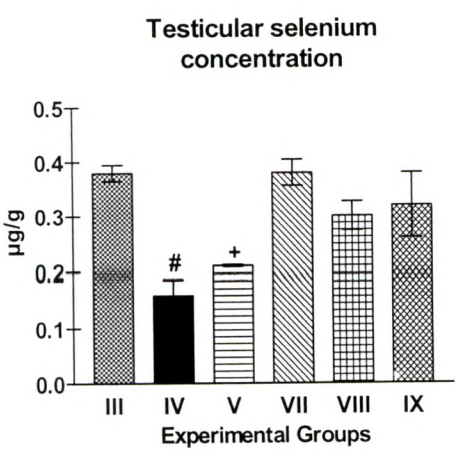
Testicular selenium concentration
0.5
0.4
0.3
0.2
0.1
0.0
µg/g
#
+
III
IV
V
VII
VIII
IX
Experimental Groups

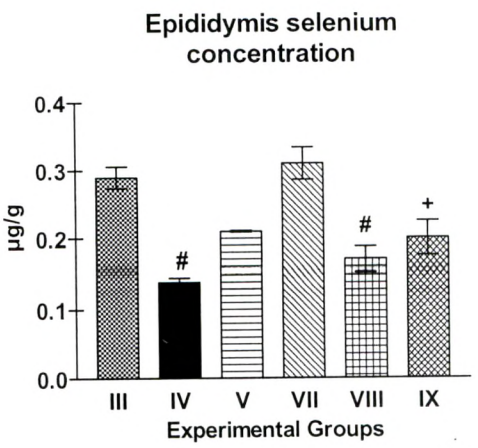
Epididymis selenium concentration
0.4
0.3
0.2
0.1
0.0
µg/g
#
#
+
III
IV
V
VII
VIII
IX
Experimental Groups

Fig. 10a: Representative GC/MS chromatogram of processed blood samples in sixty days high dose treated HCM group

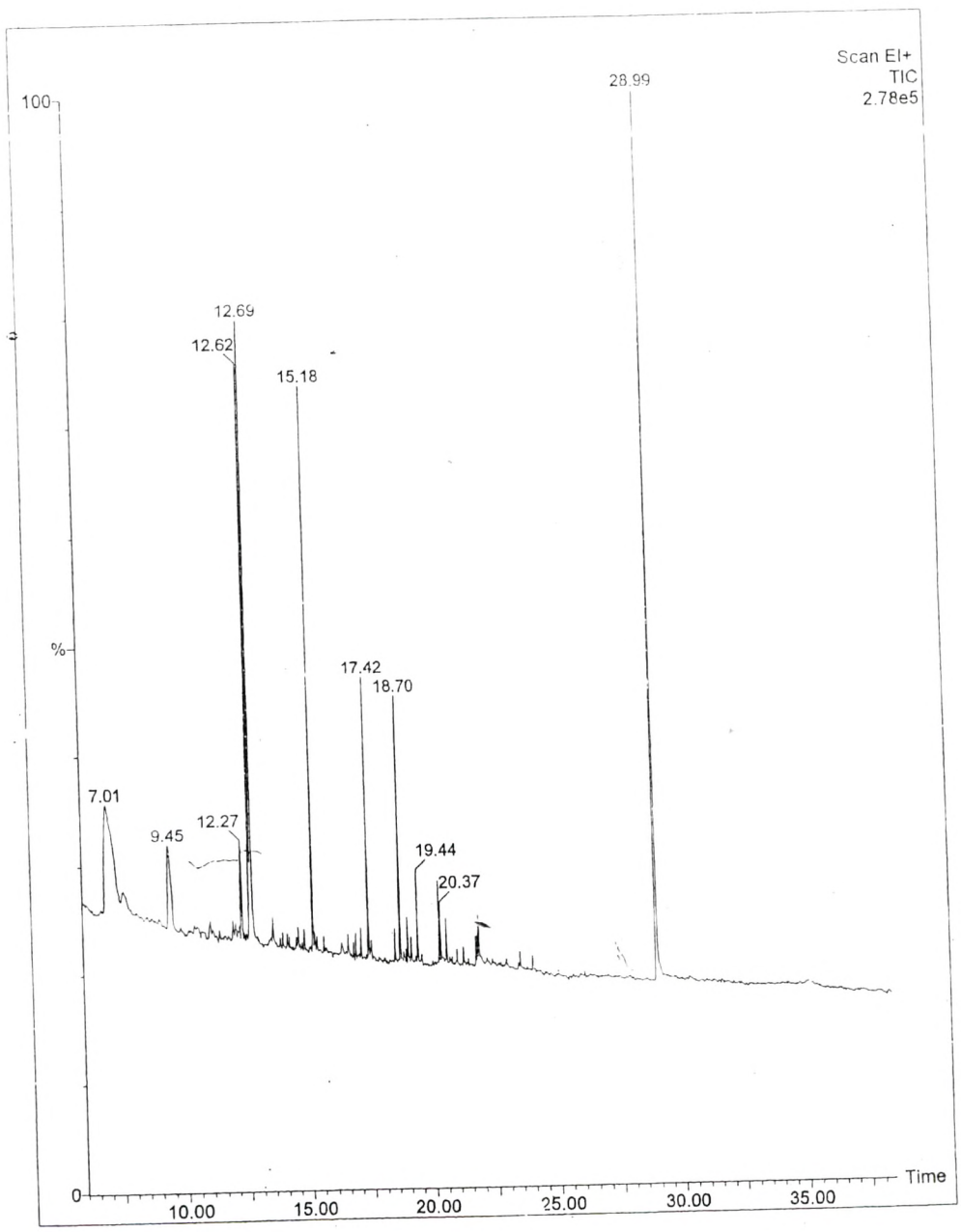

Fig. 10a 1: Mass Spectra of peak identified as 12.69 and corresponding metabolites of HCM

Identified as Benzene (1-Methoxy-4-(2-propenyl)

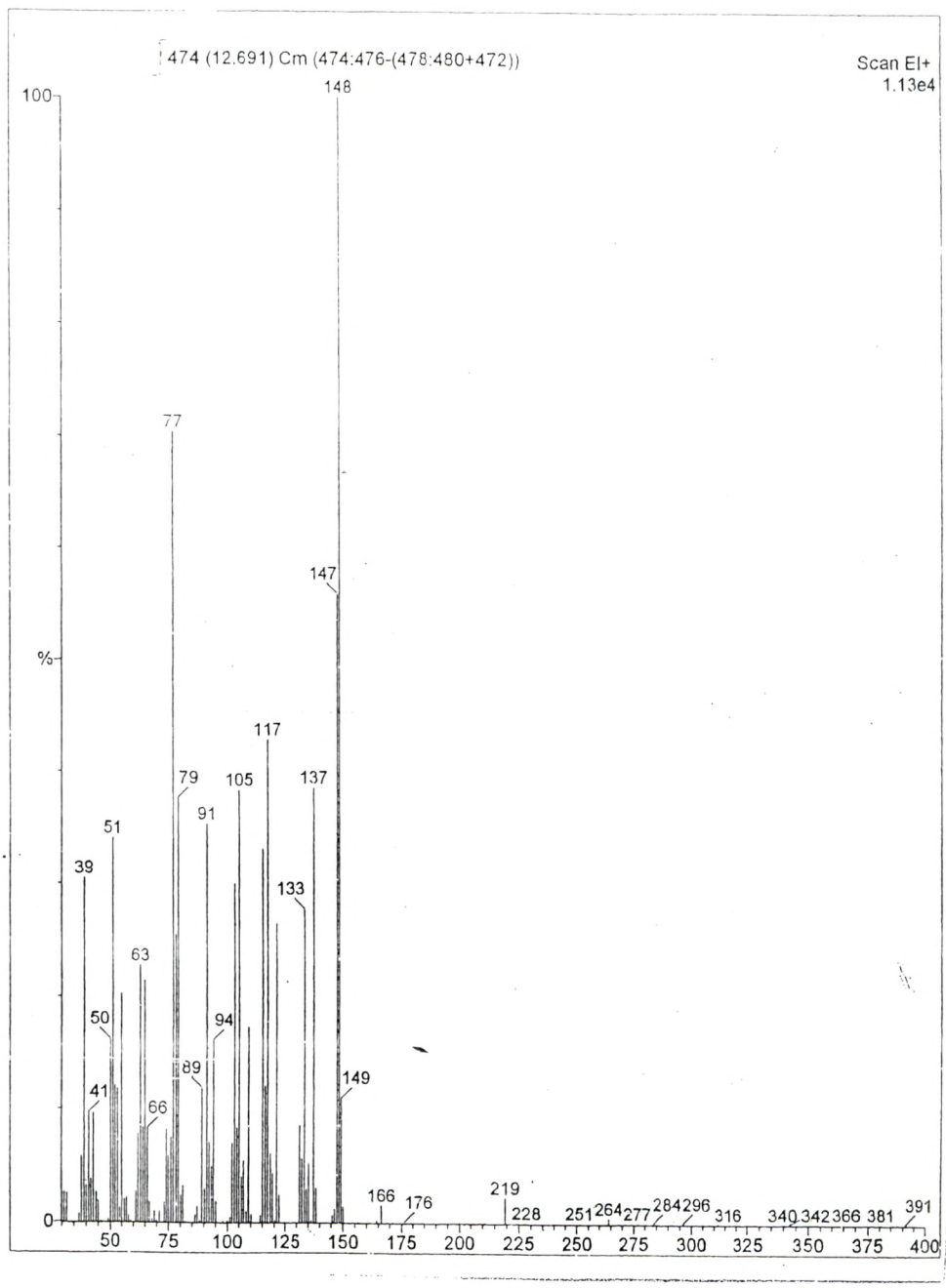

Fig. 10b: Representative GC/MS chromatogram of processed blood samples in sixty days low dose treated HCM group

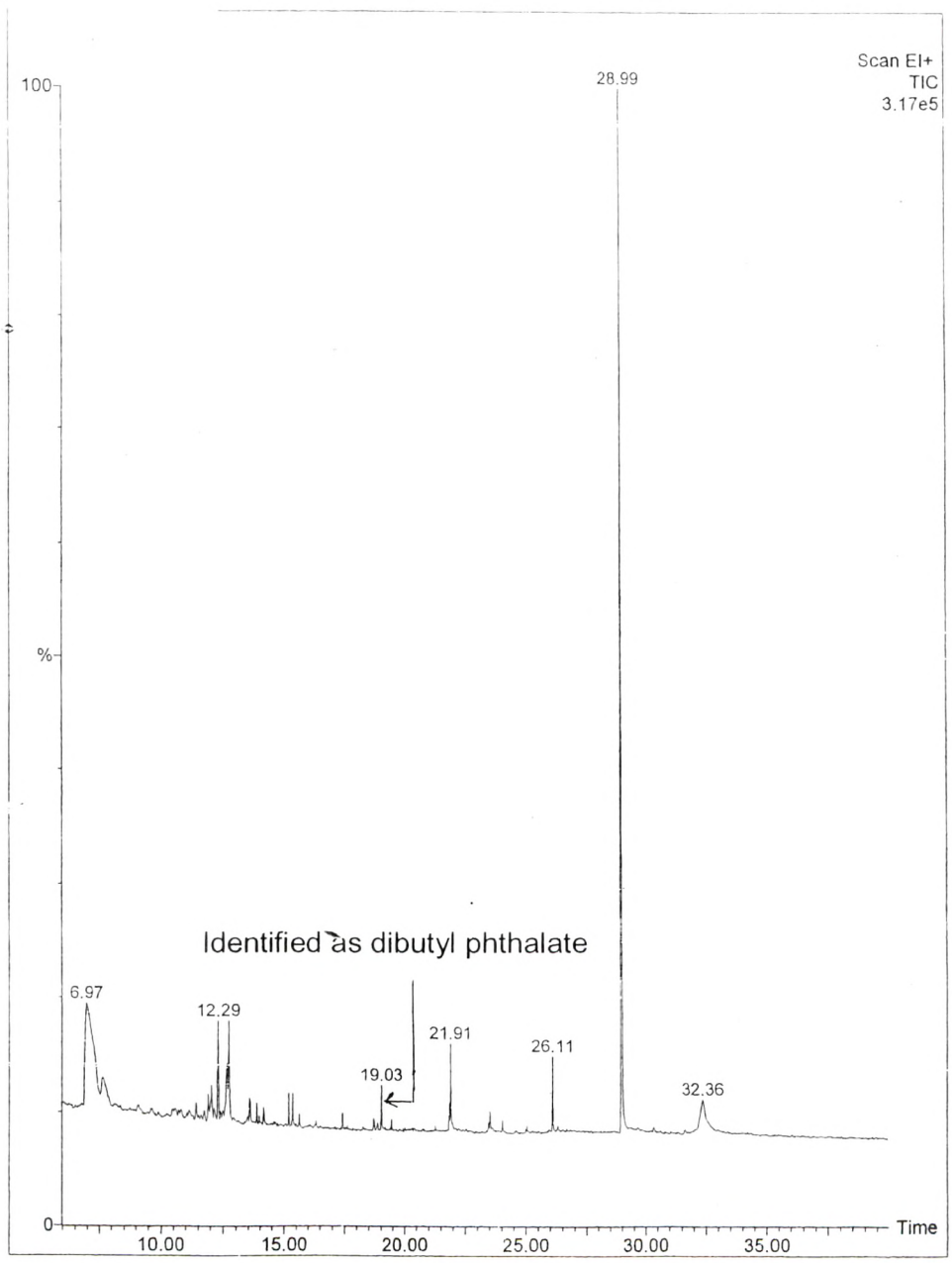

Fig. 11a: Representative GC/MS chromatogram of processed urine samples in sixty days high dose treated HCM group

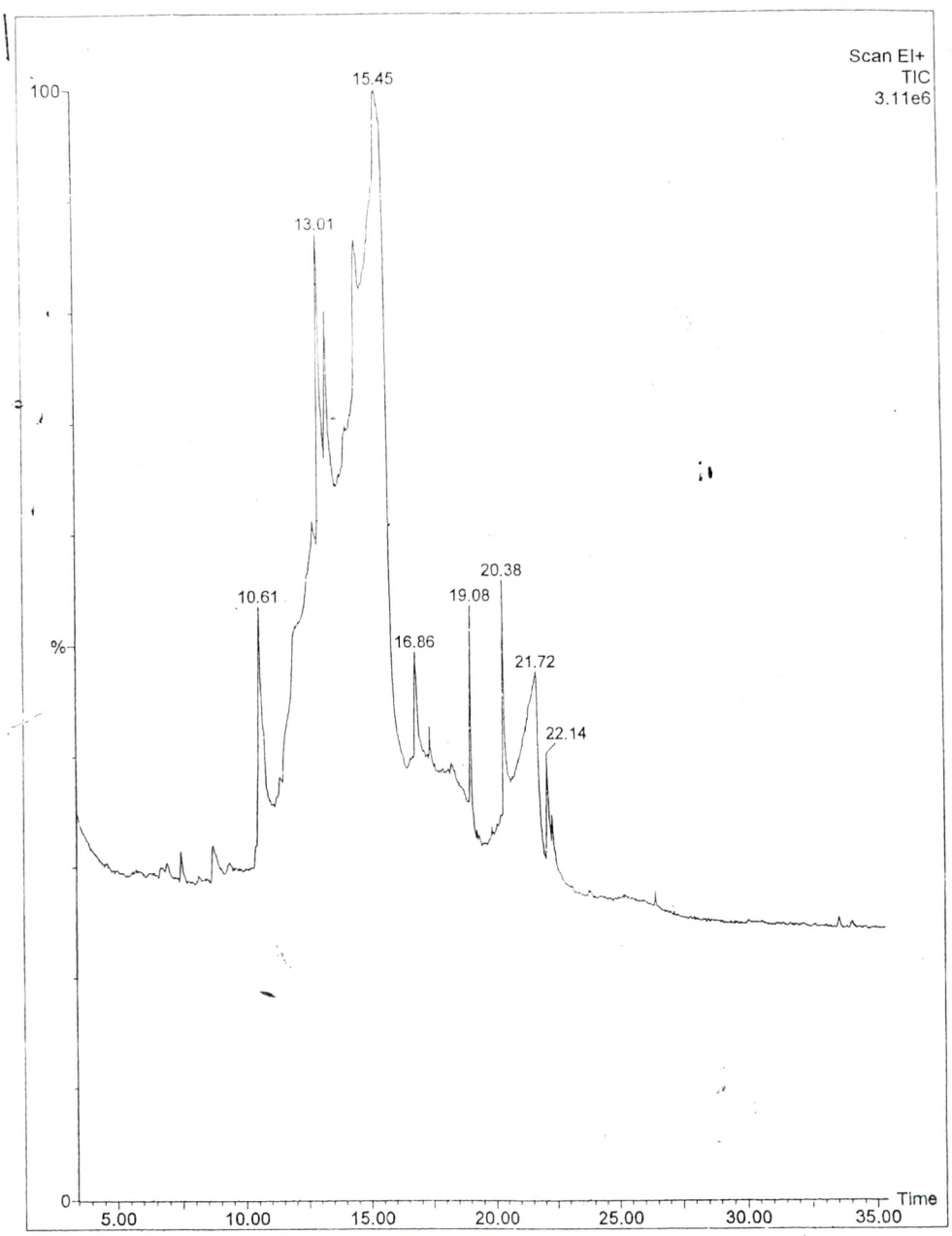

Fig. 11a 1: Mass Spectra of peak identified as 10.61, 13.35, 14.58 and 19.08 corresponds to metabolites of phthalic acid dibutyl ester and 1, 2-dichlorobenzene

Identified as 2, 3-dichlorophenol

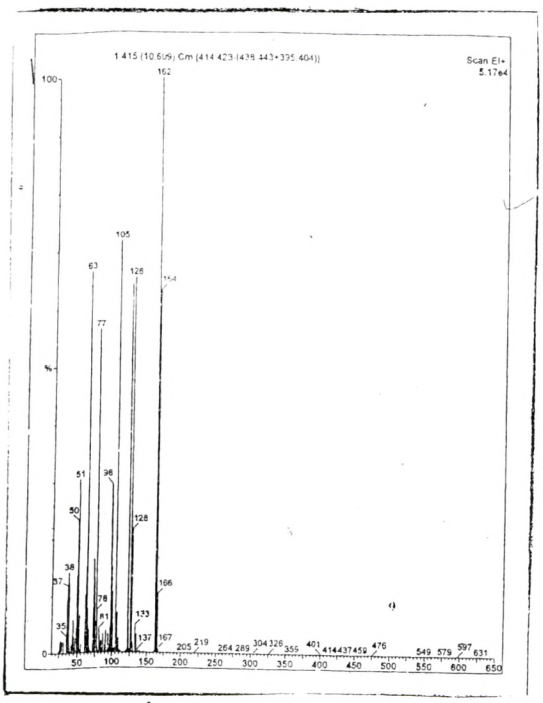

Identified as 3, 4-dichlorobenzenethiol

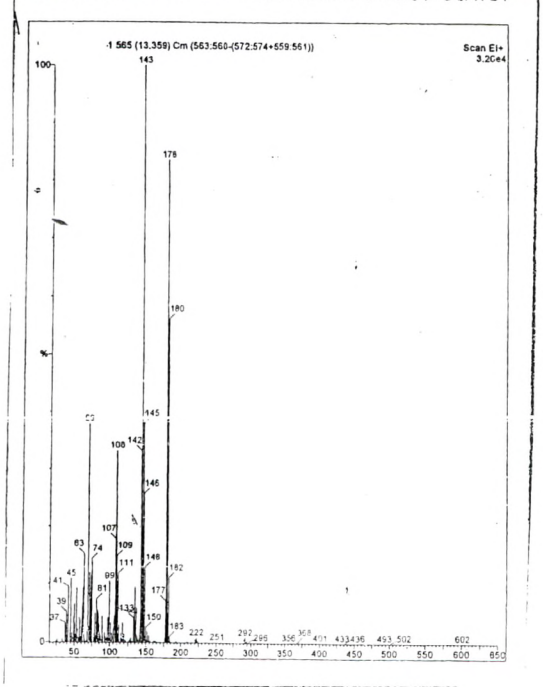

Fig. 11a 1: Mass Spectra of peak identified as 10.61, 13.35, 14.58 and 19.08 corresponds to metabolites of phthalic acid dibutyl ester and 1, 2-dichlorobenzene

Identified as Phthalic acid monobutyl ester

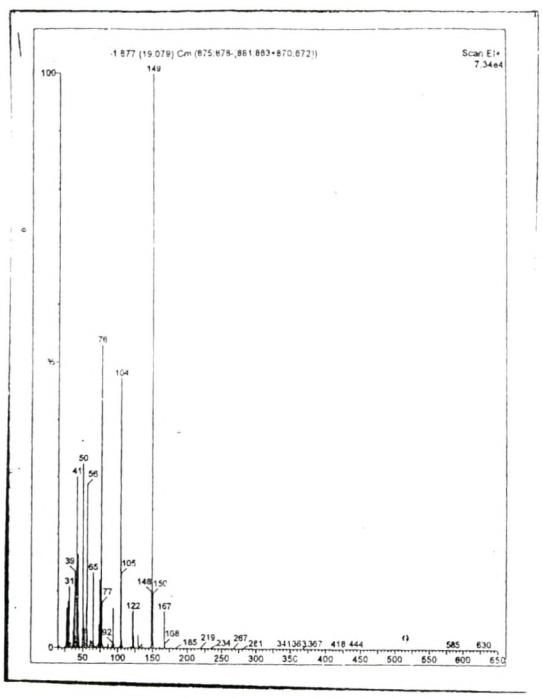

Identified as 3, 4-dichlorophenol

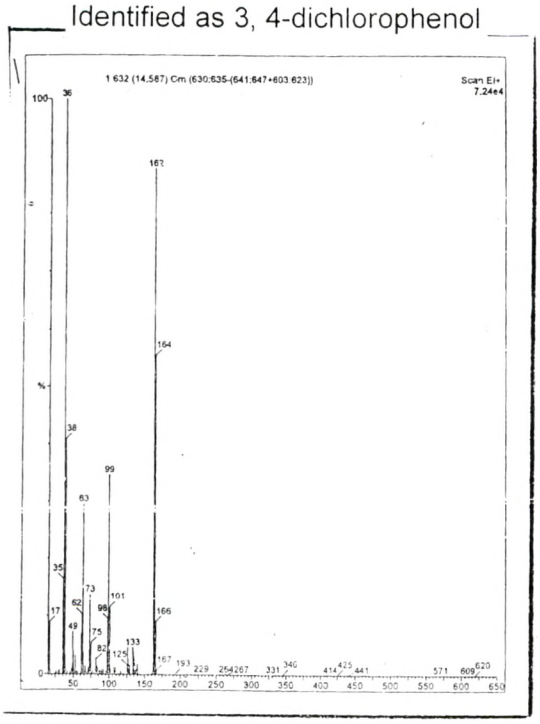

Fig. 11b: Representative GC/MS chromatogram of processed urine samples in sixty days low dose treated HCM group

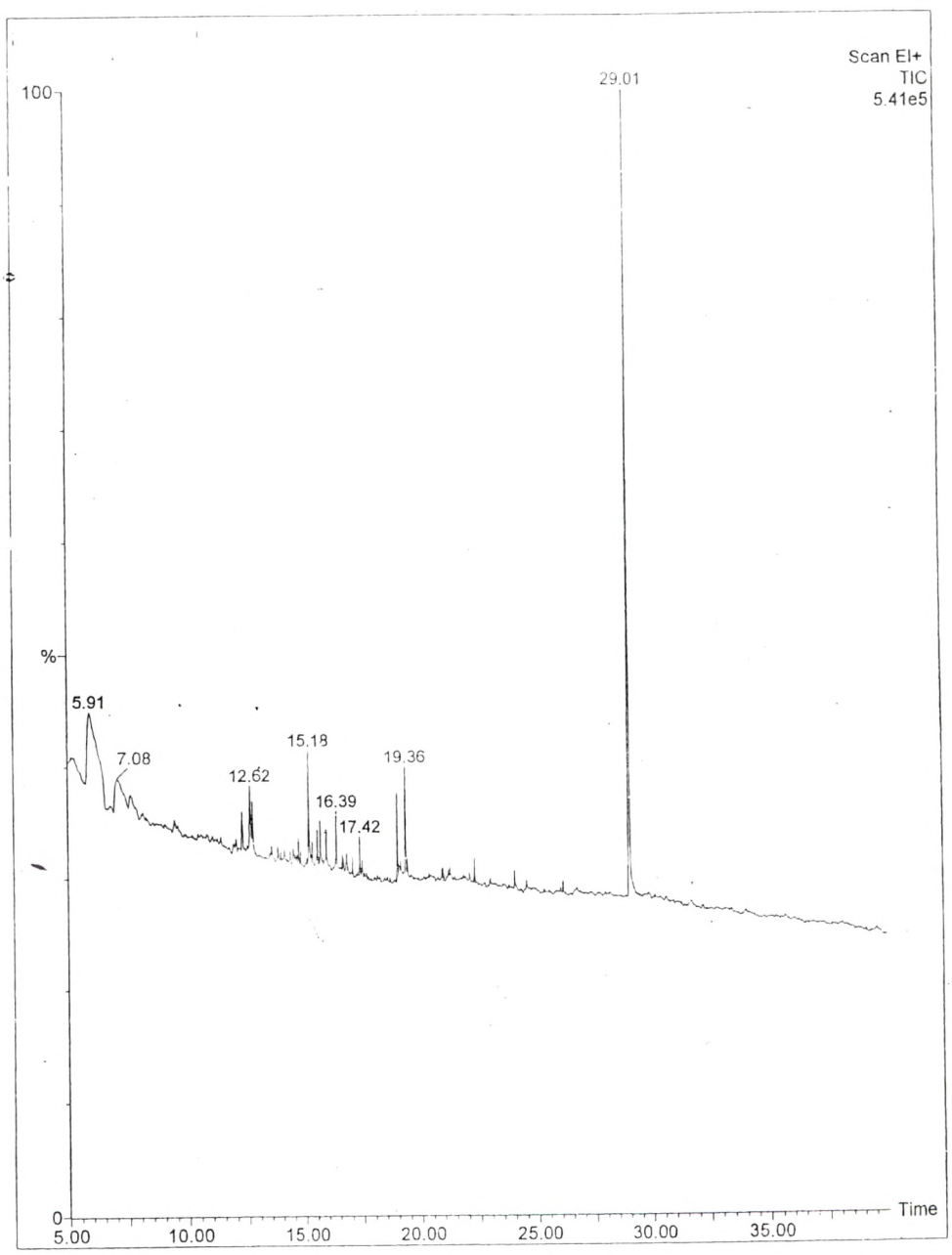

Fig. 11b 1: Mass Spectra of peak identified as 5.90 and 16.39 corresponds to compounds/ metabolites of phthalic acid dibutyl ester and 1, 2-dichlorobenzene

Identified as dichlorobenzene

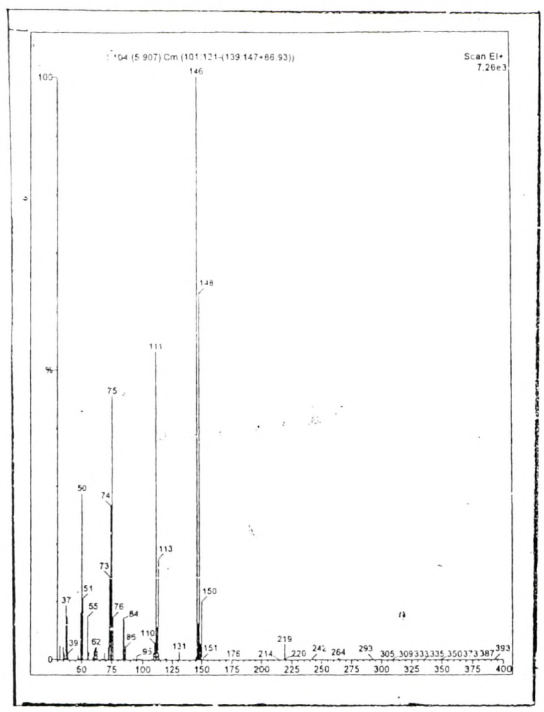

Identified as Benzene (1-MethoxyDecyl)

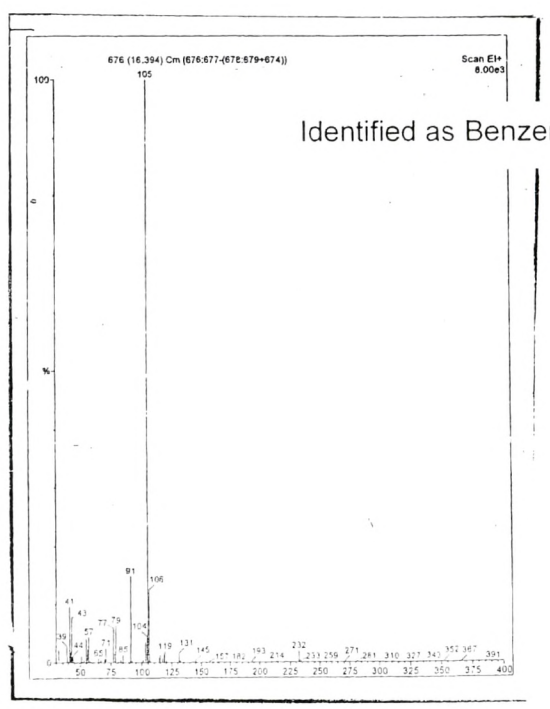

Fig. 12a: Representative GC/MS chromatogram of processed liver samples in sixty days high dose treated HCM group

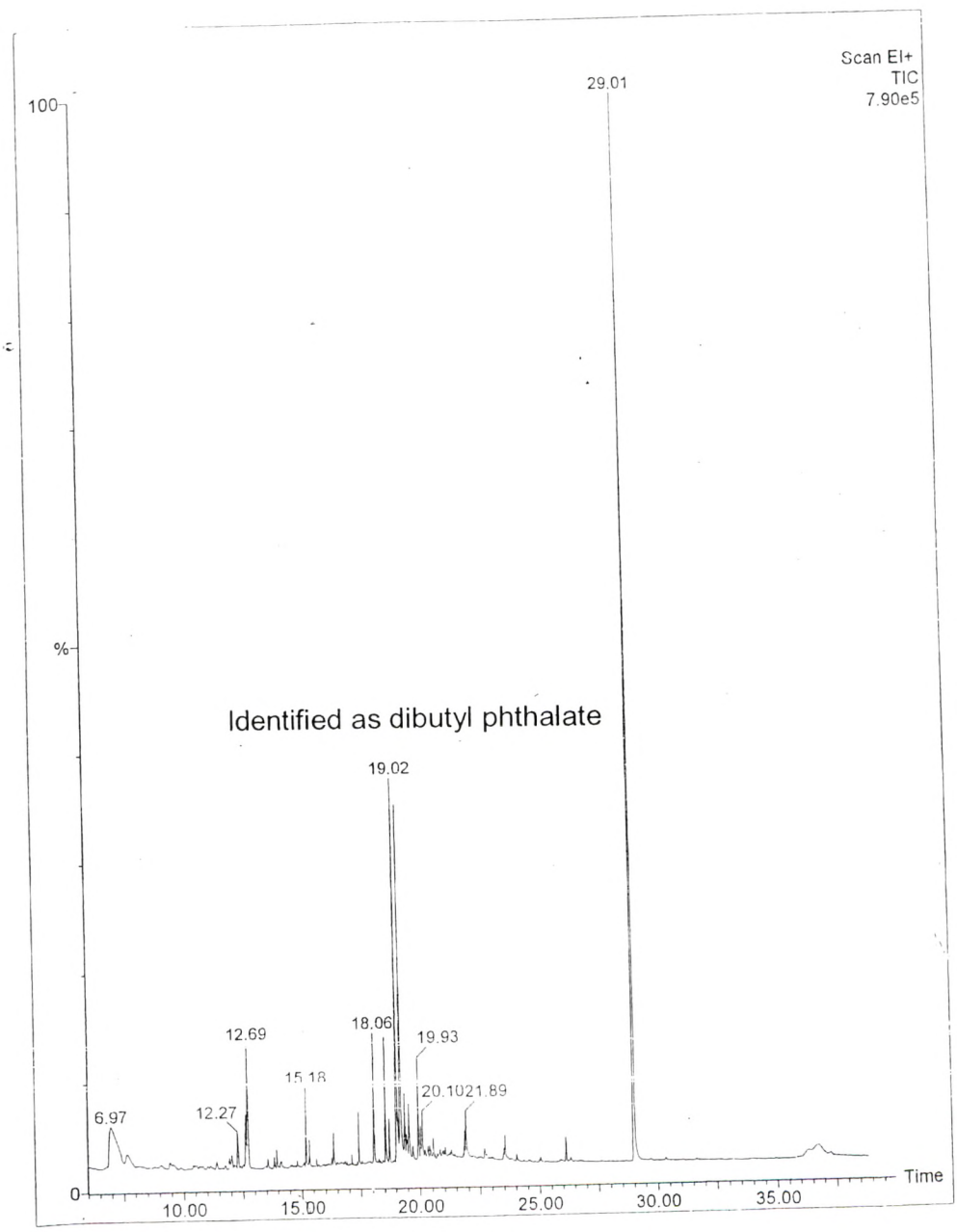

Fig. 12a 1: Mass Spectra of peak identified as 19.19 and 18.53 corresponds to metabolites of phthalic acid dibutyl ester

Identified as dibutyl phthalate

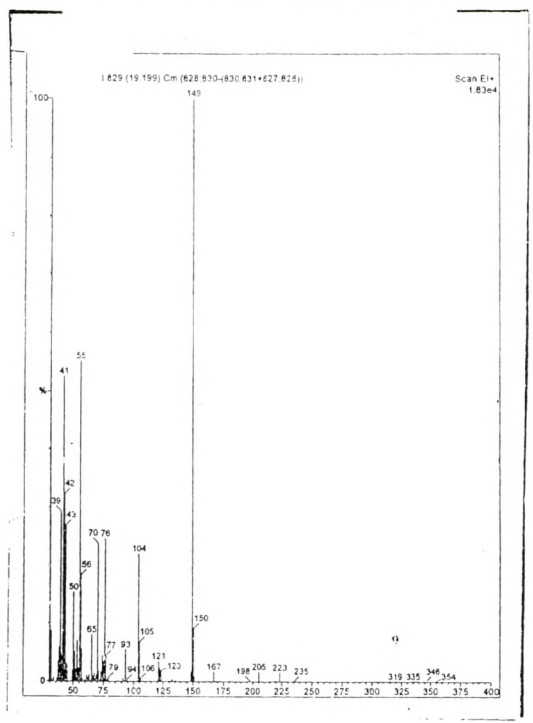

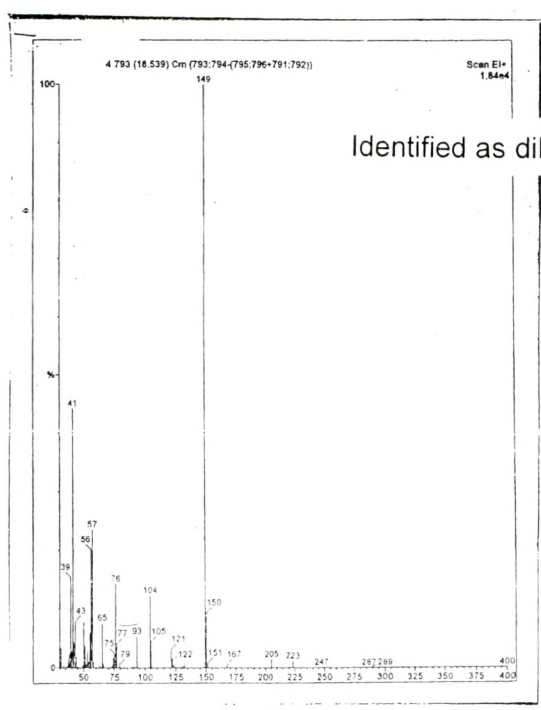

Identified as dibutyl phthalate

Fig. 12b: Representative GC/MS chromatogram of processed liver samples in sixty days low dose treated HCM group

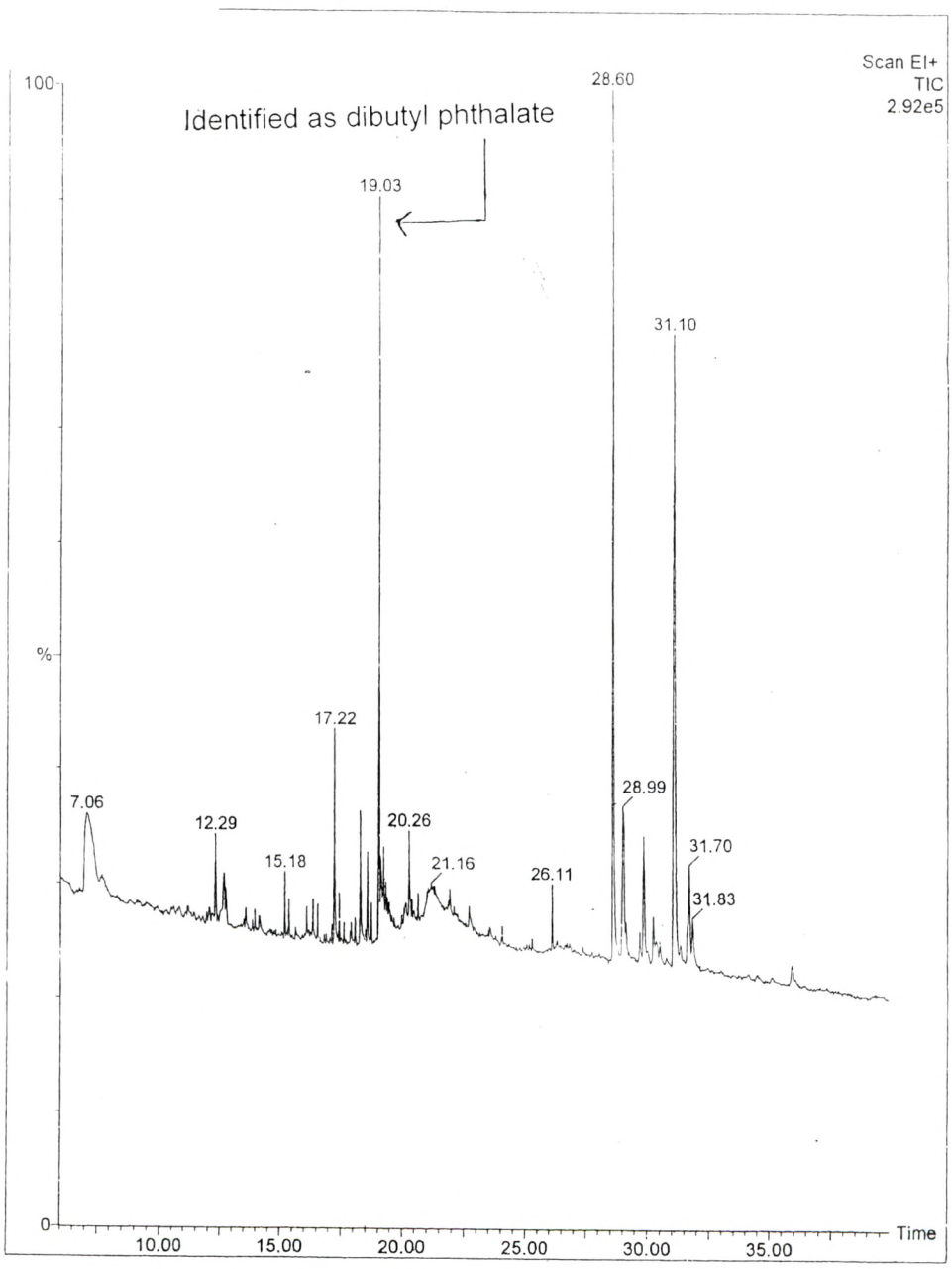

Fig. 13a: Representative GC/MS chromatogram of processed kidney samples in sixty days high dose treated HCM group

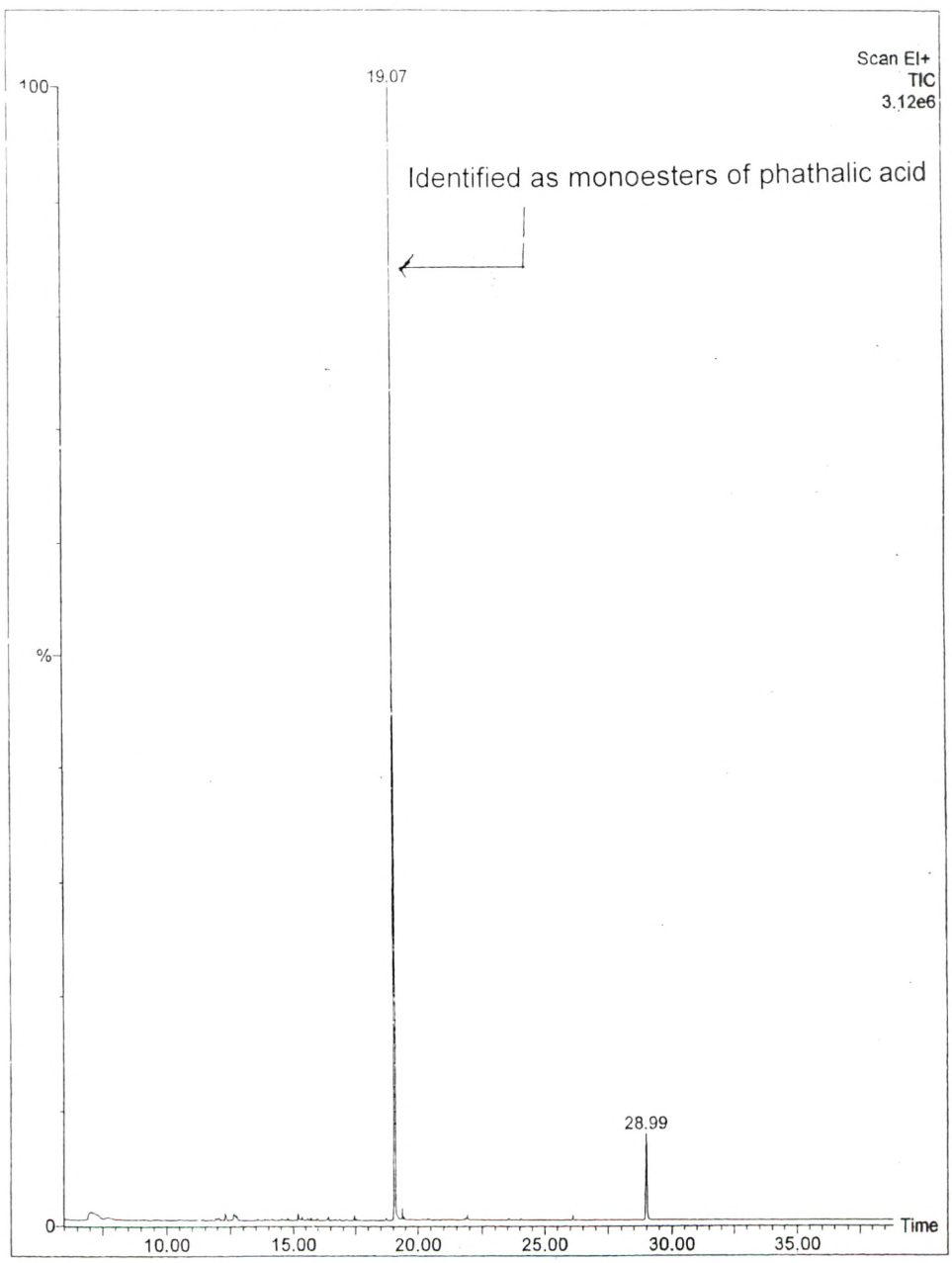

Fig. 13b: Representative GC/MS chromatogram of processed kidney samples in sixty days low dose treated HCM group

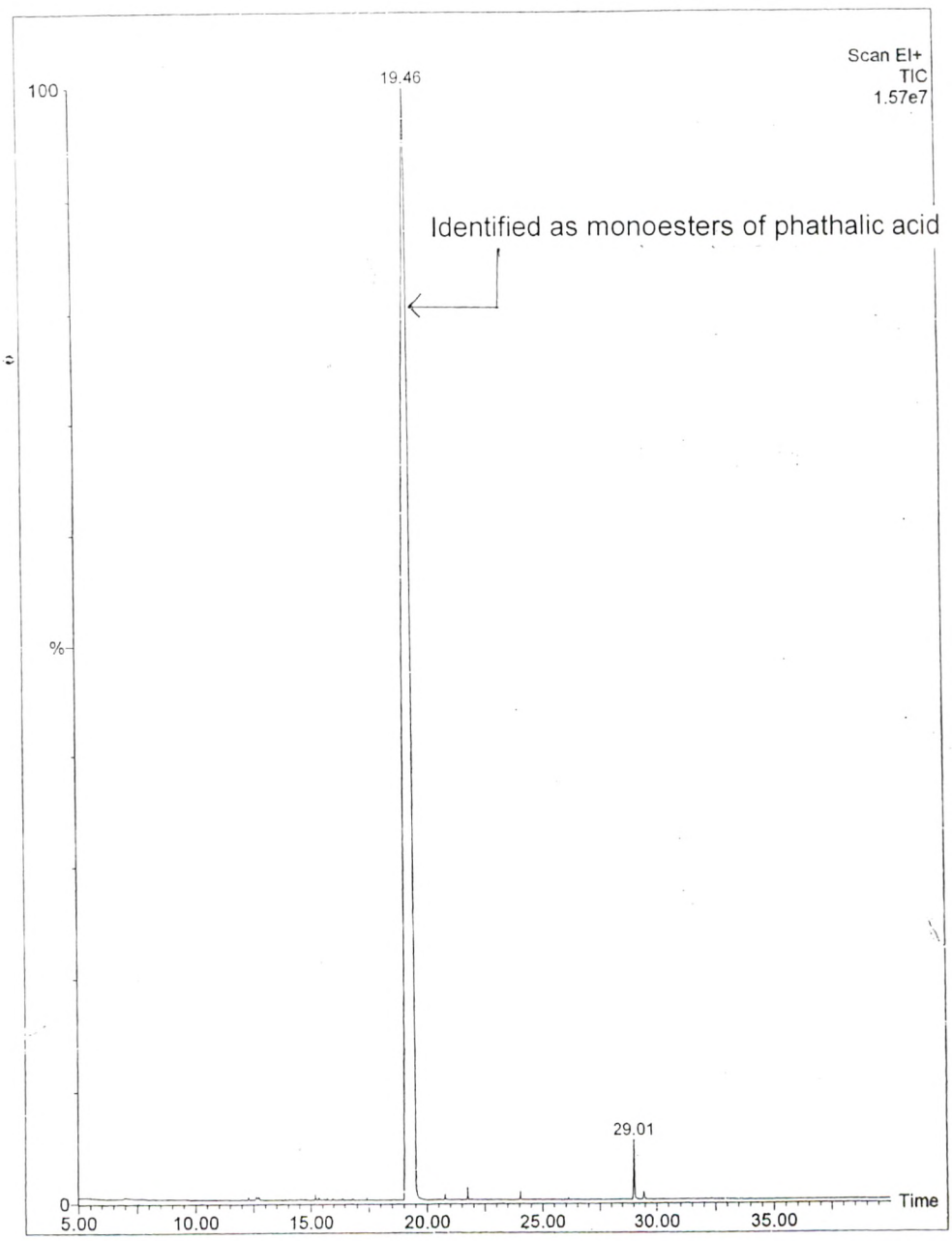

Fig. 14a: Representative GC/MS chromatogram of processed testis samples in sixty days high dose treated HCM group

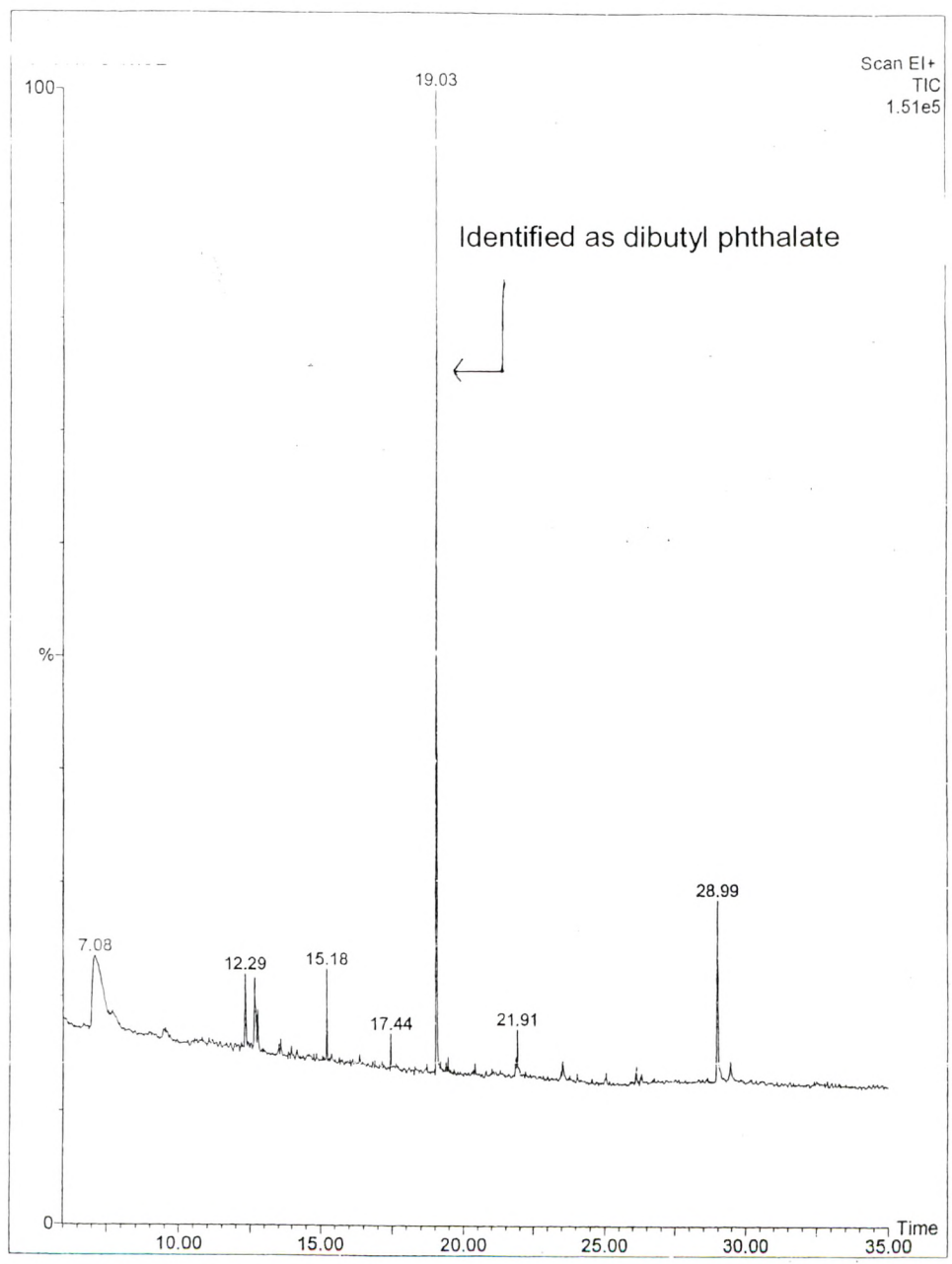

Fig. 14b: Representative GC/MS chromatogram of processed testis samples in sixty days low dose treated HCM group

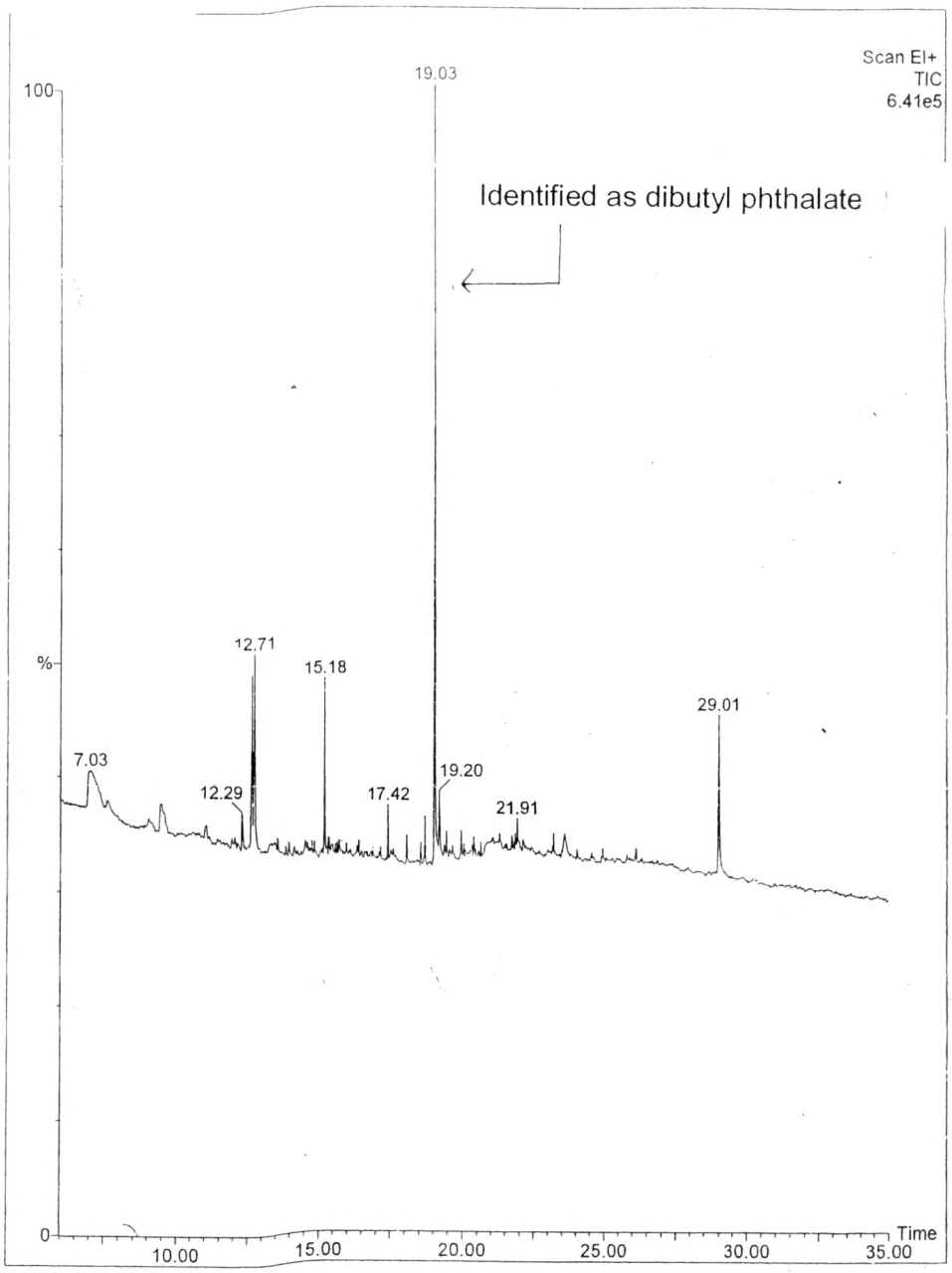

Fig. 15a: Representative GC/MS chromatogram of processed epididymis samples in sixty days high dose treated HCM group

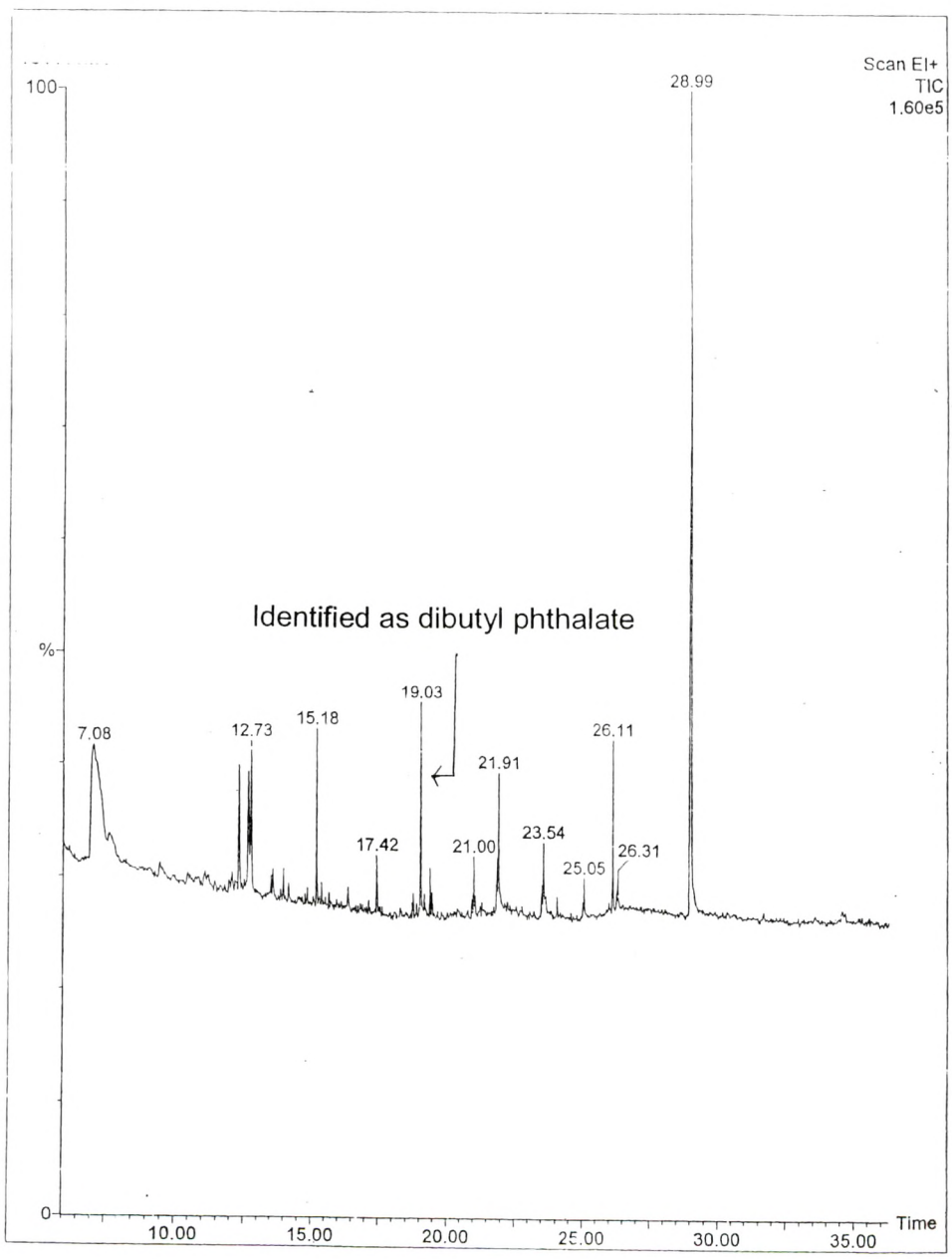

Fig. 15b: Representative GC/MS chromatogram of processed epididymis samples in sixty days low dose treated HCM group

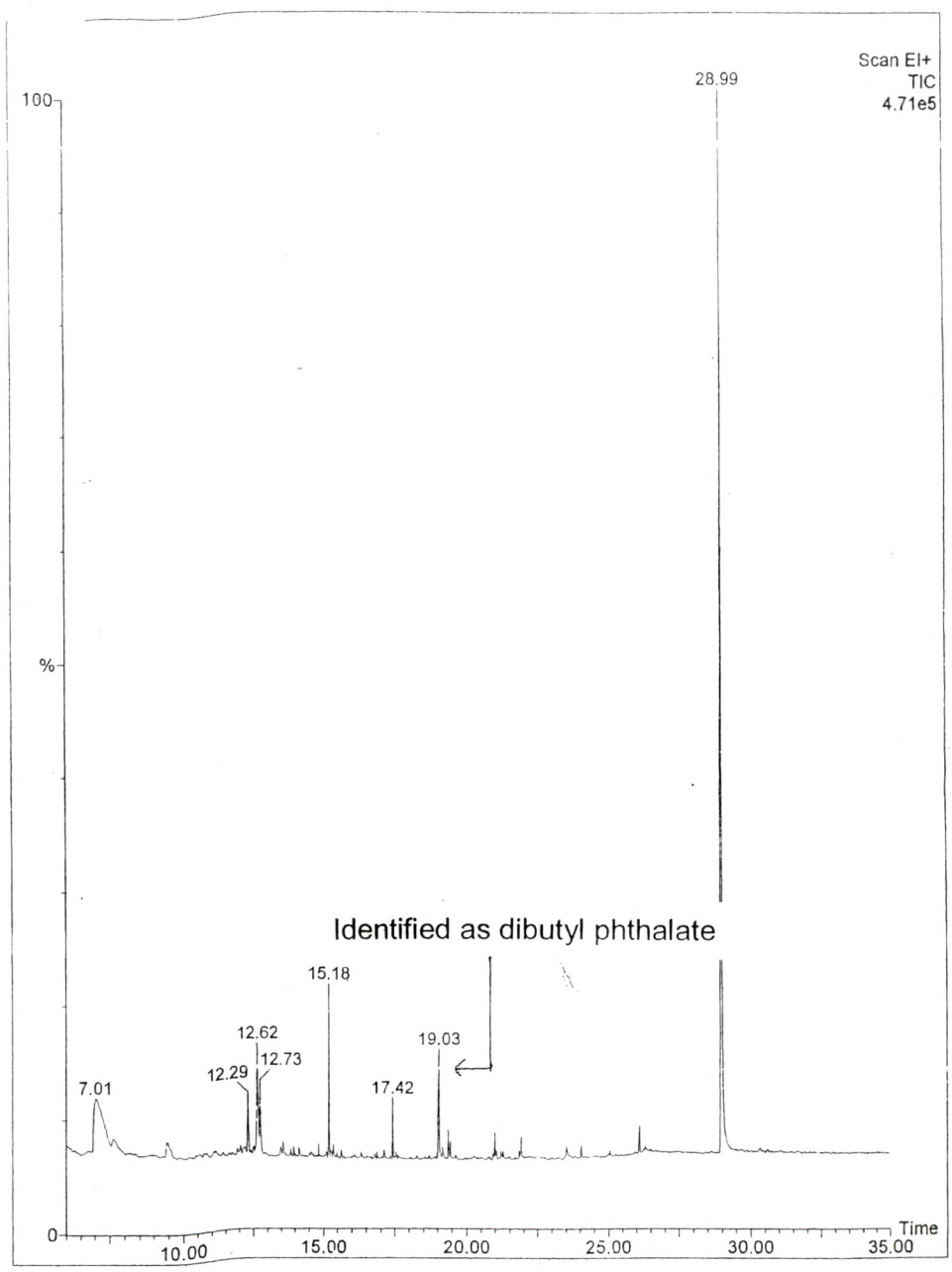

CHAPTER 2

TOXIC POTENTIALS OF HETEROGENEOUS CHEMICAL MIXTURE EXPOSURE ON THE LIVER

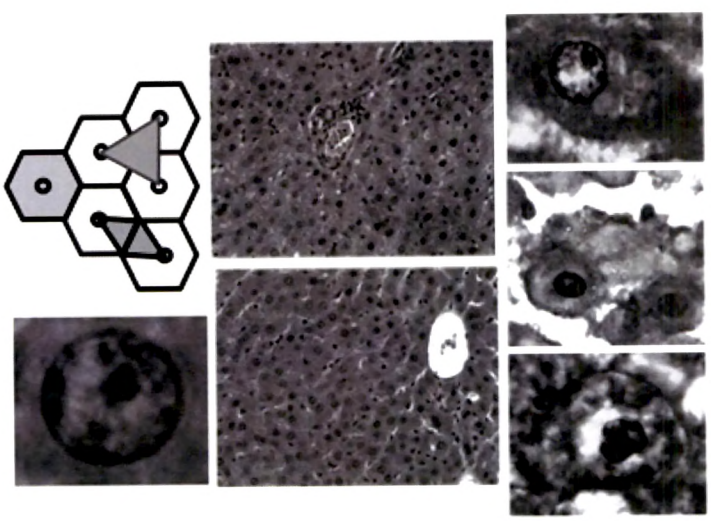

Liver is considered to be one of the most vital organs that function as a centre of metabolism of nutrient and excretion of waste metabolites. Additionally, it is also involved in metabolism and excretion of drugs and xenobiotics thereby providing sufficient protection against any harmful foreign substances. Therefore, Liver damage can impact almost all body systems because of its so many pivotal functions. Globally, one in ten persons suffers with some type of liver and bile duct diseases (Al-Attar, 2011). These diseases represent the liver response to diverse chronic insult such as exposure to toxic pollutants, viral and parasitic infection, nutritional health status *etc.* Simultaneous exposure to more than one chemical may modify the biological activity of other chemical and such interaction might result in potentiating, decreasing or nullifying of the ultimate effect of that chemical mixture (Eaton and Klaassen, 2001). Hence, there is an ever increasing need for evaluation of chemical mixture on liver to understand the cellular and molecular mechanisms responsible for the development and progression of the toxic insult.

Therefore, toxicity study was performed with a chemically defined mixture of four different compounds of industrial origin, using dosage level very much comparable and/or below to no observable adverse effect level (NOAEL) on the normal functions of liver. The selection of these compounds was based on their frequency of occurrence in the industrial effluent. The mixture contained two organic compounds, Phthalic acid dibutyl ester and 1, 2 dichlorobenzene and two metal, cadmium and chromium. The study was performed to explore the interaction among organicals and metals in the induction of stress and the focus of this study was to assess the toxicity of heterogeneous chemical mixture (HCM) for sixty days and to check the possibility of recovery after HCM withdrawal for another sixty days.

Most of the hepatotoxic chemicals damage liver cells mainly by inducing lipid peroxidation (Poli, 1993). Abnormal levels of antioxidants in chemical induced toxicity further verify the role of free radical in cellular damage (Batt and Ferrari, 1995; Jaeschke, 1995). The levels of enzymatic and non enzymatic antioxidant are altered in majority of toxicity studies. In

order to find out the mechanism of action of any toxicant on liver, it is important to assess its effect on oxidative-redox status along with parameters of liver function test.

To examine oxidative stress in hepatic cells caused by HCM treatment, the effect of HCM at different doses on activities on Superoxide dismutase (SOD), Glutathione peroxidase (GPx), Catalase (CAT), Glutathione S transferase (GST), reduced glutathione level (GSH), ascorbic acid, and lipid peroxidation (LPO) together with histology and parameters of liver function tests were performed.

RESULTS

Effect on liver weight

No significant changes were observed in absolute and relative liver weight at any dose of HCM and the weight remains within the normal range in experimental rats of all groups (Table 1, Fig. 1).

Effect on serum biochemical parameters of liver function test

The effect of HCM administration on liver marker enzymes and total bilirubin content are given in Table 2 and 3. Activities of SGPT and GGT were increased significantly following high dose HCM exposure to rats for sixty days. Low dose HCM treatment also caused increase in the activity of SGPT and GGT enzymes but the elevation was insignificant when compared with control. The activities of SGPT, and GGT restored towards the normal value in withdrawal groups (VIII and IX) when compared to rats exposed to HCM (group IV and V). However, these enzymes (SGPT and GGT) activities remained high in recovery groups as compared to their control. The activity of serum SGOT showed a significant ($P<0.01$ and $P<0.001$) increase in high and low dose HCM treated rats compared to vehicle treated control group and also remained significantly ($P<0.05$) high in recovery group VIII (high dose HCM + recovery).

Insignificant elevated activity of ALP was observed in the HCM exposed groups. Similarly no significant change in the level of total bilirubin was observed in any of the HCM treated groups. The activity of LDH showed a significant ($P<0.01$ and $P<0.05$) increase in HCM (high and low dose respectively) treated rats when compared to vehicle treated control. Here again the activity of LDH restored towards the normal value in withdrawal groups (VIII and IX) when compared to rats exposed to HCM (group IV and V). But, activity remained significantly high in groups VIII (high dose HCM + recovery) when compared with control group VII.

Effect on serum lipid profile

Table 4 shows the significant increase in serum cholesterol (CHO), Triglyceride (TG), low density lipoprotein (LDL) and very low density lipoprotein (VLDL) in group IV (high dose HCM) as compared to group III (vehicle treated group). The low dose HCM treatment caused only significant increment in CHO level while the elevated difference in TG, LDL and VLDL level were insignificant with control group. The level of CHO, LDL and VLDL were reduced in group VIII and IX i.e. elevated level reduced after withdrawal from HCM exposure. The variation in high density lipoprotein (HDL) level was non significant in HCM exposed as well as in recovery groups.

Effect on liver SDH, ALP and ACP activities

Table 5 shows the activities of succinate dehydrogenase (SDH) acid phosphatase (ACP) and alkaline phosphatase (ALP) and cholesterol level in liver of rats exposed to HCM. Treatment with high dose HCM for sixty days caused significant ($P<0.05$) decrease in the activity SDH and its significant ($P<0.05$) increase, in recovery groups (VIII and IX). Treatment with low dose HCM caused no significant change in the activity of SDH enzyme in liver. However, there was no significant change in the enzymes ACP and ALP activities. Treatment with high dose HCM caused significant ($P<0.01$) decrease in the liver cholesterol level.

Effect on protein content

Protein content of liver decreased in sixty days HCM exposed groups (Table 6). The decrease was statistically significant in high dose HCM treated group IV, as compared with vehicle treated control group III. Withdrawal of the treatment for another sixty days showed recovery towards normalization.

Effect on Lipid Peroxidation (LPO)

Administration of HCM caused change in the level of LPO (Table 6, Fig. 6). LPO levels were found to be significantly elevated in high and low dose HCM exposed rats when compared with vehicle treated control rats. The elevated LPO level restored toward the normal values in recovery groups VIII and IX when compared with HCM exposed and control groups.

Effect on enzymatic and non enzymatic antioxidants

The results of oxidative stress parameters revealed that the administration of HCM caused significant damage as evident by marker enzymes of antioxidant defence system. Table 6 and 7 depicts that the content of non enzymatic antioxidants such as GSH, ascorbic acid and activities of enzymatic antioxidants such as SOD, CAT and GST were declined significantly upon HCM treatment (group IV and V) when compared with vehicle treated control (group III). While no statistically significant differences existed in the activity of GPx between the treated and control rats. Withdrawal of the HCM treatment for sixty days showed recovery in few antioxidant parameters, except CAT and GST in group VIII (high dose HCM treated + recovery), which were not recovered compared to 120 days control group VII.

Effect on the histoarchitecture of liver

The major cell type of liver is polygonal hepatocyte arranged in hepatic cords between the central vein and portal triad. The hepatic cords are

separated by capillary sinusoids. The cytoplasmic properties of the hepatocytes are dependent upon the metabolic status since the sequestration of various metabolites; e. g. glycogen and various forms of lipids, is very significant for general function of liver and other bodily requirements. The bile canaliculi are formed between the two adjacent hepatic cords and drain into the bile duct located at the hepatic triad. The connective tissue stroma is formed of a fine meshwork of reticulin fibres. The sinusoids are lined by a discontinuous, fenestrated endothelium, devoid of basement membrane and which is separated from the hepatocytes by a narrow space of Disse, which drains into the lymphatic of the portal tracts. This is also the region where from the exchange of material between the sinusoid and hepatocyte occurs. The liver sinusoids receive blood from terminal branches of both the hepatic portal vein and hepatic artery. The Kupffer cells that form part of the monocyte-macrophage defence system are scattered along the lining of sinusoids. The third cell type, known as stellate cells, Ito cells or hepatic lipocytes, have the dual functions of vitamin A storage and production of extracellular matrix and collagen. The hepatic artery, hepatic vein and the bile duct form triad. Structurally, the liver is divided into classical polygonal lobules which has central vein in the centre and hepatic triads at the ends (Fig. 8). However, now this is not considered as the unit of liver. The portal lobule was also proposed as the unit but it represents mostly the structures inclusive of bile canaliculi and ducts, thus representing the exocrine functions of the tissue (Fig. 8). The hepatic acinus is physiologically more appropriate unit of liver, although it cannot be represented correctly in the light microscope. The acinus is located between two central veins and two portal triads encompassing the hepatic cords distributed in between (Fig. 8). The acinus is divided into zones 1, 2 and 3 and the hepatocytes in these zones have different metabolic functions. Zone 1 is closest to the portal tract and receives the most oxygenated blood, while zone 3 is furthest away and receives least oxygen.

In the control animals, the liver exhibited normal arrangement of hepatic cords and all the cell types (Plate 1). The hepatocytes were prominently stained and their nuclei were distinct. The endothelial lining of the

sinusoids and central vein were also distinct indicating appropriate structural integrity. The Kupffer cells were randomly distributed along the sinusoids (Plate 2). Administration of high doses of HCM for 60 days leads to moderate to severe changes in different regions of the liver (Plates 3-6). The hepatocytes in region 1 of acini, the periportal region, exhibited severe vacuolation which varied from minute homogeneously distributed vacuoles to large perinuclear vacuoles (Plate 4). The endothelial lining of the central veins and sinusoids were disrupted. The hepatic cord's arrangement was disorganized and several hepatocytes were isolated from the cords indicating loss of junction complexes between the adjacent cells. The margins of the hepatocytes were wavy and showed blebbing and probable potential leakage of the material from the cells. This is also supposed to distort the integrity of bile canaliculi. The Kupffer cell hyperplasia was noticeable particularly in the zone 3 of acinus, the pericentral region as well as along the highly vacuolated hepatocytes in region 1 of acinus (Plates 4, 5). Higher magnification observations showed that the hepatocytes were swollen and fluffy. The disorganization of hepatic cord arrangement is suggestive of damage to the connective tissue stroma.

Following low dose HCM administration the effects were quite similar but comparatively less than the high dose treatment group (Plate 7). The swelling of hepatocytes was prominent but the vacuolation was not as conspicuous. In the recovery groups on day 120, following high dose treatment the hepatocyte swelling was seen almost in the entire lobule with prominence in the zone 1 (periportal region) of the hepatic acinus (Plate 8,9). Interestingly, several binucleate and polyploid cells were observed both in the low and high dose groups (Plates 9-11). The cytoplasmic dissolution, hepatocyte membrane damage and leakage of cytoplasmic material into the space of Disse as well as within the sinusoid were still prominent on day 120 (Plates 9-11).

DISCUSSION

Organisms in the environment often experience many chemical stressors simultaneously. The present study aimed to investigate the effect of treatment of HCM. Animals treated with daily dose of HCM for sixty days induced elevation in liver biomarker enzymes glutamic oxaloacetic transaminase (SGOT), serum glutamic pyruvic transaminase activities (SGPT), Gamma glutamyl transpeptidase (GGT) and Lactate dehydrogenase (LDH) when compared with control. These elevated enzymes activities were considered indicative criteria for damage to hepatocytes in rats (Dias *et al.*, 2009). All these liver enzymes, in small amounts, are usually found in blood circulation because of hepatic growth and repair.

As a liver specific enzyme SGPT significantly elevate only in damaged condition of hepatocytes or in hepatobiliary disease; however, an increase in level of SGPT and LDH can occur in connection with damages to other organs like muscle as well as of liver parenchyma (Moss and Henderson, 1996). The available reports on chemical toxicity suggested that increase in activity of liver biomarker enzymes in serum could be due to possible leakage of these enzymes across damaged plasma membrane (Kumar *et al.*, 2005; Zaki *et al.*, 2011). In present study, the histoarchitecture of liver in HCM treated groups clearly demonstrated the damage to hepatocyte membrane. Intoxication with many toxicants either individually or in mixture form, induced elevation in plasma SGOT, SGPT, GGT and LDH resulted from leakage of enzymes from damaged tissues of liver (Sturgill and Lambert, 2000; Khan *et al.*, 2008; Wadaan, 2009). Consequently, elevated biomarker enzymes observed in the current study in response to HCM treatment were common signs of impaired function of liver. The liver cells play an important role in synthesis and secretion of ALP and its location is within the sinusoidal and bile canalicular membranes (Kako *et al.*, 1980). The non significant increment in serum alkaline phosphatase (ALP) activity caused by sixty day HCM treatment again suggests the damaged condition of hepatocytes. Nevertheless, the activity of SGPT and GGT were reduced in serum after withdrawal of HCM treatment for sixty days in both of the recovery groups

when compared to sixty day HCM treated groups towards the controls level. The toxicity induced by HCM treatment was lowered during recovery period but the cellular injuries still persist as indicated by higher level of SGOT, ALP and LDH in the serum of recovery groups and the histological observations.

Lipid is an integral part of cell membrane. It is useful in production of several hormones and important for other cellular functions. Lipoproteins enable the transport of cholesterol within the blood stream. Therefore, the measurement of serum cholesterol levels can be considered as valuable indicator of lipid metabolism disruption. Also liver is known to be involved in the synthesis of triglyceride and cholesterol (Dentine *et al.,* 2005). Results showed that HCM exposure altered the hepatic cellular function in the treated rats by inducing significant increase in the serum TG and cholesterol levels. However, the rise in TG level in HCM exposed group may be due to inhibitory effect of mixture on the activity of lipoprotein lipase in blood vessel which breaks up the TG (Gupta *et al.,* 2008). LDL and HDL particles tend to transport cholesterol into the artery wall and away from the arteries back to the liver, respectively (Nielsen., 1996; Brown, 2007). Several studies have shown that higher levels of LDL particles promote health problems and cardiac disease (Joven *et al.,* 1997; Selvan *et al.,* 2008; Tsimihodimos *et al.,* 2011). The increased LDL levels are also associated with hepatic dysfunction and risk of atherosclerosis as increased level starts the formation of plaques in artery wall (Spady, 1999; Christ-Crain *et al.,* 2004). In histological preparations, the extensive vacuolation in the hepatocytes actually suggest lipid accumulation, thus corroborate with the biochemical findings in present and earlier studies (Selvan *et al.,* 2008; Israni *et al.,* 2010).

Oral administration of HCM for sixty days caused significant reduction in the activity of Succinate dehydrogenase (SDH) in the liver. The effect was comparatively more pronounced in high dose HCM treated group than that of low dose. SDH is a key enzyme in the mitochondrial Kreb cycle, and is more active than any other enzyme of Kerb cycle dehydrogenase (Hederstedt and Rutberg 1981). Therefore, reduction in SDH activity clearly indicates reduction in aerobic metabolism, which might be the result of reduction of oxygen

transport to the tissues. Activities of marker enzymes viz alkaline phosphatase (ALP) and acid phosphatase (ACP) are considered functional indicators of hepatic tissue (Ksheerasagar *et al.,* 2011). The present study demonstrated that 60 days exposure of HCM to male rats at high dose resulted in decreased activities of ALP and ACP which reflect the suppression of liver function.

The organ liver has a number of characteristic consistent with oxidative injuries and various studies have reported the effect of toxicants either individually or in combination, on the oxidative stress in rats (Stohs and Bagchi, 1995; Anane and Creppy, 2001; Rao *et al.,* 2006; Koyuturk *et al.,* 2007; Jain et al 2009). It has been linked with enhanced reactive species of oxygen and nitrogen generation (Valko *et al.,* 2005; Aly and Domenech, 2009). Lipid peroxidation (LPO) is viewed as a complicated biochemical reaction and is the focus of intense activity in relation to its possible involvement in health status (Muriel, 2009; Chouhan and Flora, 2010). The significant elevated level of LPO in sixty days HCM treated groups are in strong favour of oxidative stress. Similar increases in liver LPO have been previously reported following other toxicant exposures. The reactive oxygen species are very well known to counteract by an interacting network of enzymatic and non enzymatic antioxidant system, thus preventing the cells from oxidative damage (Ji, 1995).

Oxidative stress/process generated superoxide radical is first converted to hydrogen peroxide and further reduced to give water molecule. This detoxification pathway is the result of several enzymes, with superoxide dismutase catalyse in the first step and Glutathione peroxidase the next one, where glutathione and catalase help removing hydrogen peroxide (Aitken and Roman, 2008). Glutathione S Transferase (GST) activity detoxifies endogeneous compounds such as peroxidised lipid and breakdown product of xenobiotics and may also bind to many toxicants directly and function as transport protein. GST also catalyses the conjugation of reduced glutathione to wide variety of substrates and thus the enzyme activity is closely associated with oxidative stress (Baars and Breimer, 1980). Ascorbic acid one

of the important antioxidants reacts with oxidants of the ROS such as hydroxyl radical (Rao *et al.,* 2006).

The cellular macromolecules are prevented from lipid peroxidation and DNA damage by enzymatic and non enzymatic antioxidant via scavenging the generated ROS (Stohs and Bagchi, 1995; Anane and Creppy, 2001; Aitken and Roman, 2008). The administration of HCM resulted in the depletion of enzymatic antioxidant (SOD, GPx, CAT and GST) and non enzymatic antioxidant (GSH and ascorbic acid). The depletion in antioxidant enzymes could be attributed to the exhaustive mobilization of these antioxidants to scavenge the ROS associated with HCM hepatocellular toxicity. This decrease of enzymatic antioxidants activity in sixty day treated HCM groups further may result in the deficiency of essential antioxidants to prevent the cell from the attack of ROS. The non enzymatic antioxidant system complements the activity of enzymatic antioxidant system in preventing cells from oxidative stress. There was a significant decrease in the concentration of GHS and ascorbic acid following HCM treatment for 60 days at both the doses. Again the decrease in concentration of these non enzymatic antioxidants could be attributed to exhaustion in scavenging ROS. Though the recovery from HCM treatment has no significant effect on GSH and ascorbic acid level when compared with control but withdrawal groups still shows the decrement in these two antioxidants concentration. The withdrawal from HCM attenuated decreased activity of enzymatic antioxidants (SOD and GPX) and a subsequent recovery towards normalization was observed. The withdrawal of treatment as reported helped in partial recovery in all parameters, where as no changes were observed in the CAT and GST activity. It is interesting to note that the histological preparations distincly showed that the recovery was partial only. The presence of binucleate cells and polyploid nuclei are indicative of active growth and rapid nuclear divisions for repair and regeneration. However, the metabolic potentials and structure-function correlates like the membrane integrity and leakages across the membrane are sufficient indicators of persistent functional impairment.

The HCM treatment enhances oxidative stress and was accompanied by decrease in protein level. It has been shown that many industrial toxicants reduce the content of protein and causes thiol protein oxidation in liver (Narayan and Roy, 1992; Moustafa, 2003). So HCM probably reduces the protein levels of antioxidant enzymes as a marked inhibitory effect of the drug on the synthesis of protein has been demonstrated in the liver of rat. Therefore, the HCM treatment induced decreases in antioxidant defence systems makes the animal more susceptible to oxidative damage and compromise the ROS scavenging capacity of antioxidants in the liver.

CONCLUSION

The increased serum liver marker enzyme activities and decreased endogenous antioxidant levels suggested that HCM exposure below NOAEL significantly hampers the normal function of liver. This can be very well correlated with increased CHO, LDL and VLDL level because these particles appear harmless until they are in blood vessel walls and oxidised by free radicals. Thus, HCM exposure has a definite effect on liver function. However, the HCM induced changes are reversible and could be effectively reversed by withdrawal of treatment for longer duration of time.

Experimental Groups

Groups	Treatment	Autopsy day
I	Zero (initial) day control	01
II	Control (No treatment)	61
III	Control (Vehicle treatment)	61
IV	Heterogeneous chemical mixture treated group (1% of LD_{50} dose/ animal/ day - NOAEL dose level)	61
V	Heterogeneous chemical mixture treated group (0.1% of LD_{50} dose/ animal/ day)	61
VI	Control (No treatment)	121
VII	Control (Vehicle treatment)	121
VIII	Heterogeneous chemical mixture treated group (1% of LD_{50} dose/ animal/ day) for 60 days followed by withdrawal phase of 60 days - NOAEL dose level.	121
IX	Heterogeneous chemical mixture treated group (0.1% of LD_{50} dose/ animal/ day) for 60 days followed by withdrawal phase of 60 days.	121

Values in all the following Tables are Mean± SE and statistical significance is considered and presented for (*) $P<0.05$, (+) $P<0.01$ and (#) $P<0.001$ compared withrespective vehicle control.

Table 1: Gravimetric analysis of liver

Groups	Liver weight (g)	Relative Liver weight (g/ 100 g animal)
I	11.29 ±0.38	3.50 ±0.11
II	11.62 ±0.26	3.46 ±0.07
III	11.83 ±0.30	3.37 ±0.09
IV	10.64 ±0.30	3.72 ±0.09
V	10.98 ±0.21	3.73 ±0.08
VI	12.99 ±0.29	3.28 ±0.07
VII	12.88 ±0.18	3.15 ±0.06
VIII	12.02 ±0.31	3.52 ±0.07
IX	12.45 ±0.24	3.38 ±0.09

Fig. 1:Gravimetric analysis of liver

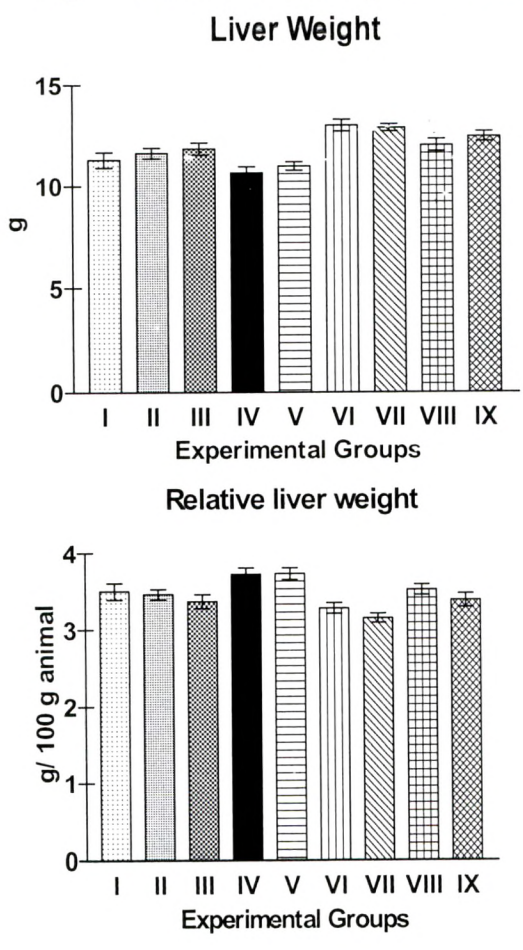

Table 2: Serum markers of liver function

Groups	Serum SGPT (U/L)	Serum SGOT (U/l.)	Serum GGT (U/L)
I	34.44 ±2.75	81.43 ±2.79	7.36 ±0.40
II	39.63 ±2.42	85.86 ±3.16	7.24 ±0.35
III	37.22 ±2.10	80.71 ±2.31	8.62 ±0.43
IV	50.49 ±3.30*	105.80 ±3.80^{+}	12.47 ±0.84$^{\#}$
V	47.41 ±3.91	108.40 ±4.32$^{\#}$	10.49 ±0.58
VI	37.55 ±1.17	93.67 ±4.47	9.38 ±0.29
VII	33.62 ±3.07	95.00 ±3.88	9.58 ±0.39
VIII	43.45 ±1.09	115.00 ±4.36*	10.18 ±0.47
IX	47.45 ±1.33*	106.80 ±5.34	9.45 ±0.42

Fig. 2: Serum markers of liver function

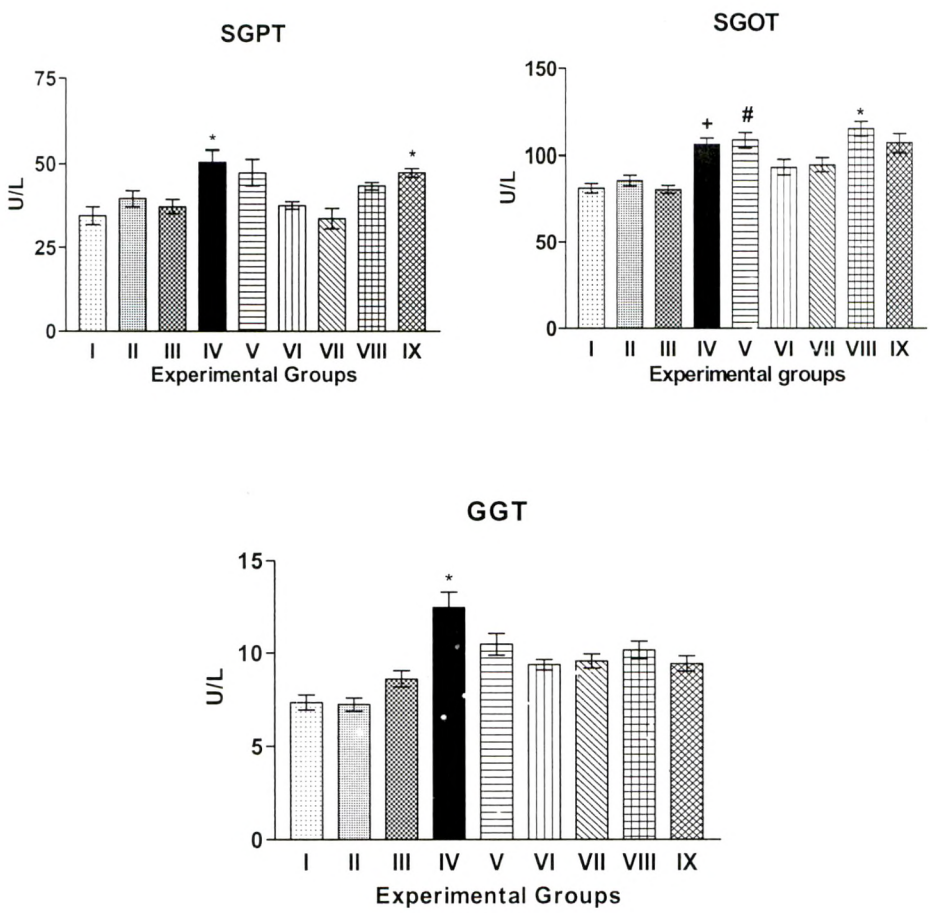

Table 3: Serum markers of liver function

Groups	Serum ALP (U/L)	Serum LDH (U/L)	Serum Bilirubin (mg/dL)
I	98.87±3.46	1352 ±51.28	0.33 ±0.15
II	104.80±4.90	1534 ±31.42	0.12 ±0.02
III	106.40±4.26	1410 ±21.45	0.15 ±0.02
IV	125.40±7.86	1653 ±42.30^{+}	0.24 ±0.04
V	119.70±5.46	1600 ±17.36*	0.20 ±0.05
VI	112.90±3.29	1408 ±47.83	0.09 ±0.01
VII	109.50±2.51	1411 ±23.09	0.11 ±0.02
VIII	131.40±6.80	1587 ±22.73*	0.13 ±0.04
IX	130.10±6.61	1493 ±51.99	0.09 ±0.01

Fig. 3: Serum markers of liver function

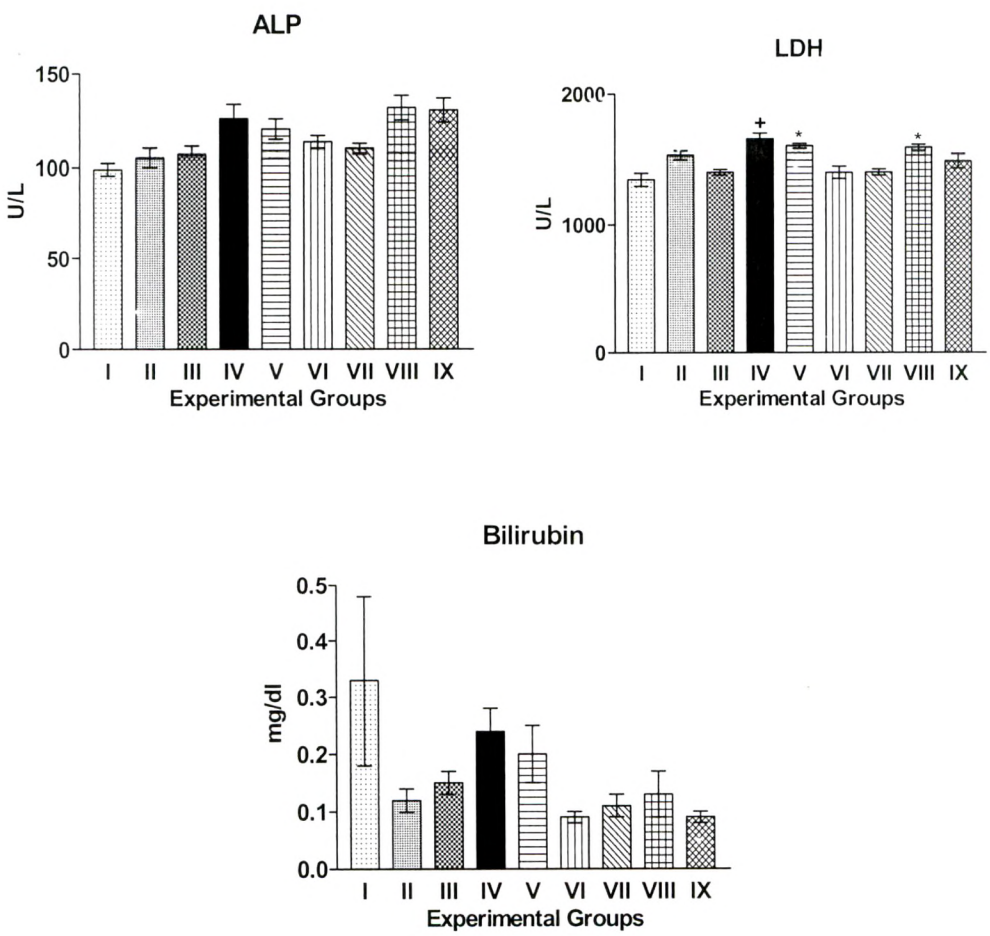

Table 4: Serum markers of liver function

Groups	Serum Cholesterol (mg/dl)	Serum Triglyceride (mg/dl)	Serum HDL-cholesterol (mg/dl)	Serum LDL-cholesterol (mg/dl)	Serum VLDL-cholesterol (mg/dl)
I	78.67 ±2.32	52.29 ±2.44	42.15 ±1.13	26.06 ±2.27	10.46 ±0.49
II	80.51 ±2.69	55.11 ±2.65	46.11 ±0.97	23.37 ±3.39	11.02 ±0.53
III	83.17 ±2.60	56.36 ±2.83	44.65 ±1.70	27.25 ±3.39	11.27 ±0.57
IV	108.30 ±3.52#	69.21 ±1.29*	41.17 ±1.14	53.27 ±4.26#	13.84 ±0.26*
V	96.45 ±3.13*	58.50 ±1.61	43.23 ±1.48	41.52 ±3.23	11.70 ±0.32
VI	86.22 ±2.40	53.43 ±2.70	40.51 ±1.21	35.02 ±1.79	10.69 ±0.54
VII	85.13 ±2.45	51.78 ±2.36	43.47 ±2.30	31.30 ±3.90	10.36 ±0.47
VIII	88.10 ±3.07	51.06 ±3.18	39.10 ±3.27	38.79 ±4.95	10.21 ±0.64
IX	82.15 ±2.32	49.66 ±2.78	42.20 ±1.80	30.02 ±4.00	9.93 ±0.55

Fig. 4: Serum markers of liver function

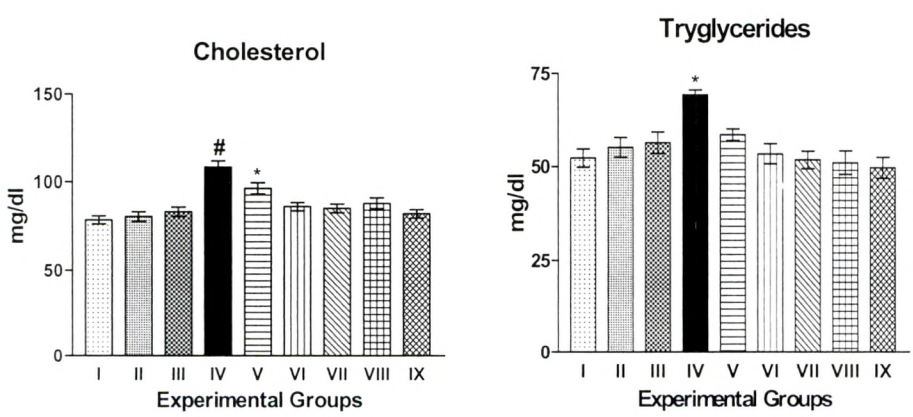

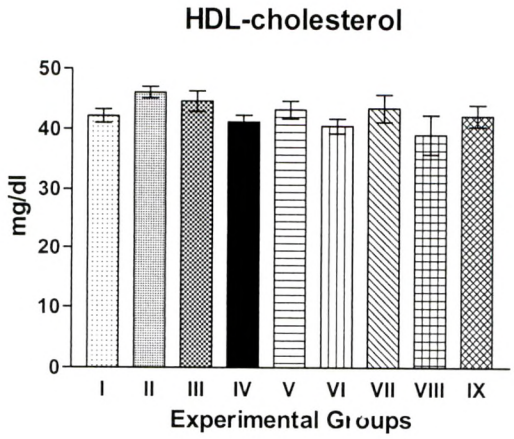
HDL-cholesterol
mg/dl
50
40
30
20
10
0
I II III IV V VI VII VIII IX
Experimental Groups

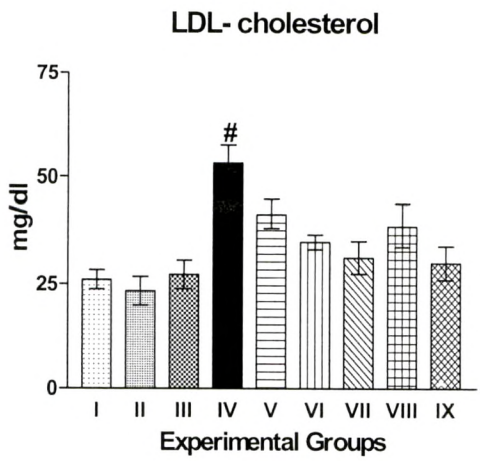
LDL- cholesterol
mg/dl
75
50
25
0
#
I II III IV V VI VII VIII IX
Experimental Groups

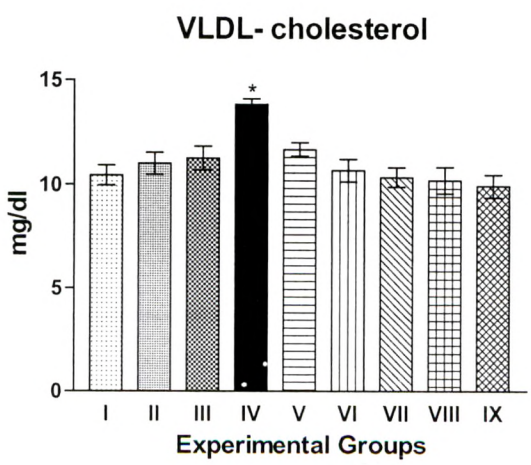
VLDL- cholesterol
mg/dl
15
10
5
0
*
I II III IV V VI VII VIII IX
Experimental Groups

Table 5: Enzymes and metabolites of general liver function

Groups	SDH (µg formazan formed/ mg protein)	ACP (µ moles of p-nitrophenol released/ mg protein/ min)	ALP (µ moles of p-nitrophenol released/ mg protein/ min)	Cholesterol (mg/ 100 mg tissue)
I	18.65 ±2.21	0.26 ±0.011	0.12 ±0.007	0.44 ±0.02
II	21.71 ±2.63	0.28 ± 0.009	0.13 ±0.003	0.46 ±0.03
III	20.35 ±0.97	0.25 ±0.013	0.11 ±0.005	0.50 ±0.04
IV	11.67 ±0.71*	0.23 ±0.019	0.10 ±0.007	0.28 ±0.03^{+}
V	19.25 ±1.23	0.21 ±0.014	0.11 ±0.007	0.43 ±0.03
VI	18.73 ±1.51	0.26 ±0.010	0.13 ±0.008	0.44 ±0.02
VII	18.29 ±1.94	0.26 ±0.018	0.14 ±0.010	0.54 ±0.03
VIII	26.66 ±1.03*	0.28 ±0.017	0.14 ±0.012	0.47 ±0.04
IX	27.75 ±1.29^{+}	0.21 ±0.019	0.11 ±0.010	0.40 ±0.07

Fig. 5: Enzymes and metabolites of general liver function

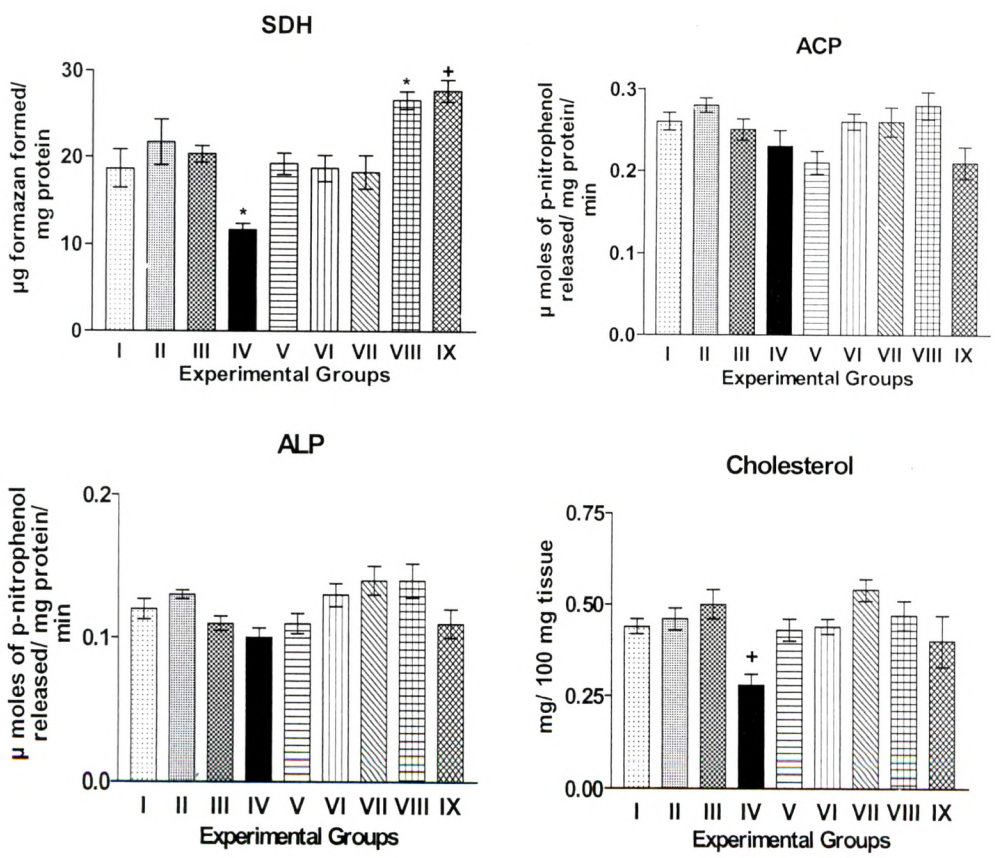

Table 6: Oxidative stress indicators of liver function

Groups	LPO (n mole MDA/ 100mg tissue)	GSH (µg of GSH/ mg protein)	Ascorbic acid (µg/ mg tissue)	Protein (mg/ 100mg tissue)
I	79.04 ±7.01	6.66 ±0.56	0.46 ±0.05	21.04 ±0.85
II	77.42 ±7.67	6.79 ±0.44	0.50 ±0.06	20.79 ±0.52
III	71.90 ±5.71	7.07 ±0.63	0.49 ±0.07	21.75 ±0.60
IV	111.00 ±5.17^{+}	3.09 ±0.40$^{\#}$	0.22 ±0.03*	17.77 ±0.37*
V	102.70 ±2.14*	4.43 ±0.26*	0.22 ±0.03*	19.14 ±0.96
VI	87.20 ±9.74	7.14 ±0.55	0.47 ±0.06	21.20 ±0.90
VII	89.07 ±4.38	6.49 ±0.56	0.39 ±0.05	21.31 ±1.02
VIII	99.26 ±5.79	6.81 ±0.50	0.37 ±0.07	19.23 ±1.00
IX	114.2 ±7.58	7.28 ±0.55	0.36 ±0.06	20.03 ±0.57

Fig. 6: Oxidative stress indicators of liver function

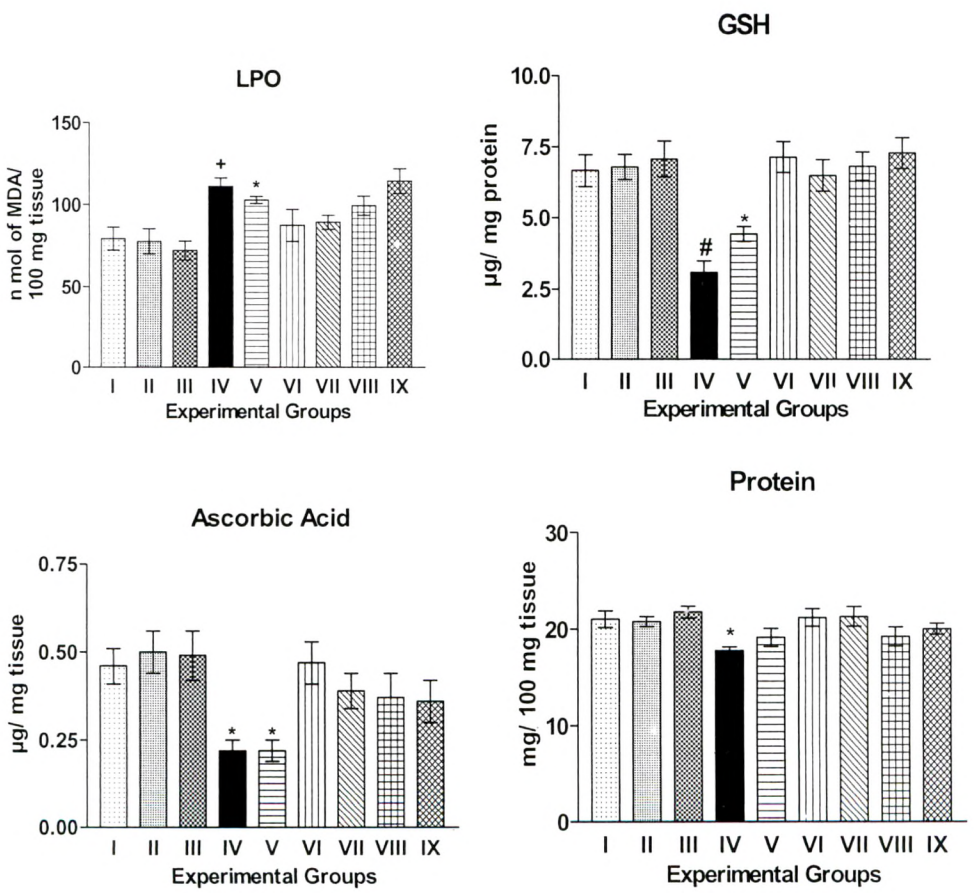

Table 7: Oxidative stress marker enzymes as indicators of liver function

Groups	SOD (Unit/ mg protein)	GPx (µg of GSH utilize/ min/ mg protein)	CAT (µ mole of H_2O_2 consumed/ min/ mg protein)	GST (µ mole CDNB-GSH conjugate formed /min/ mg protein)
I	13.19 ±0.97	10.59 ±0.65	58.96 ±2.68	7.41 ±0.45
II	12.04 ±1.21	9.89 ±0.67	63.81 ±5.82	8.50 ±0.39
III	13.35 ±0.45	9.41 ±0.53	68.16 ±8.03	8.01 ±0.42
IV	8.18 ±0.77*	6.22 ±0.46	39.61 ±2.43^{+}	3.29 ±0.20$^{\#}$
V	10.19 ±1.32	8.25 ±0.72	38.41 ±3.03^{+}	4.65 ±0.55^{+}
VI	13.89 ±0.88	9.96 ±0.70	62.82 ±5.17	8.51 ±0.73
VII	11.01 ±1.17	10.13 ±0.69	58.99 ±3.39	9.04 ±0.64
VIII	14.27 ±0.89	11.72 ±0.88	36.17 ±4.03*	6.24 ±0.65*
IX	12.98 ±0.67	9.84 ±0.76	48.15 ±4.59	7.26 ±0.64

Fig. 7: Oxidative stress marker enzymes as indicators of liver function

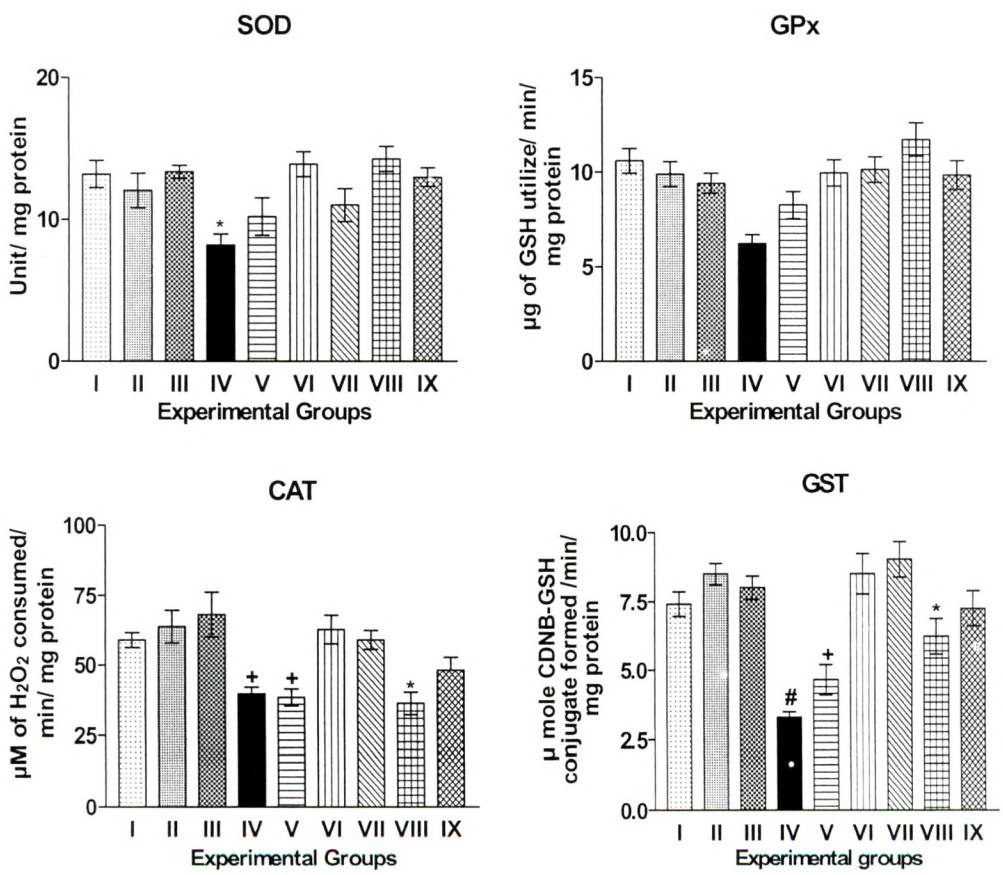

Fig. 8: Diagrammatic representation of the histological unit structure of liver

1. **Aninus zone one: Periportal region, 2. Acinus zone two: Mid zonal region, 3. Acinus zone three: Pericentral region**

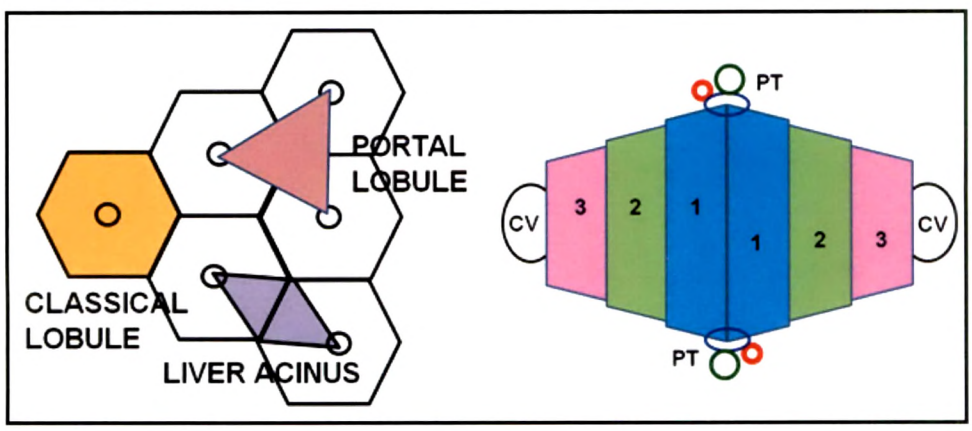

PLATE-1

Transverse sections of liver of control animals.

a Showing parenchymatous appearance of the liver. The hepatic cords are arranged along the central vein (CV) and have distinct sinusoidal spaces. The nuclei of hepatocytes are prominent. Kupffer cell are lined along the sinusoids. This shows Zone-3 of acinus. 200X

b Region of liver showing the portal triad (PT). The portal vanule, hepatic artery and bile duct are clearly seen. A few lymphocytes (L) are also present around the portal triad. The inset shows typical histological feature of the hepatocyte nucleus which has a few distinct nucleoli and almost clear nucleoplasm. This shows Zone-1 of acinus. 200X

c Showing the Zone-2 of acinus between the central vein and portal triad regions. The sinusoids (S) and kupffer cells (K) are distinct. 400X

PLATE 1

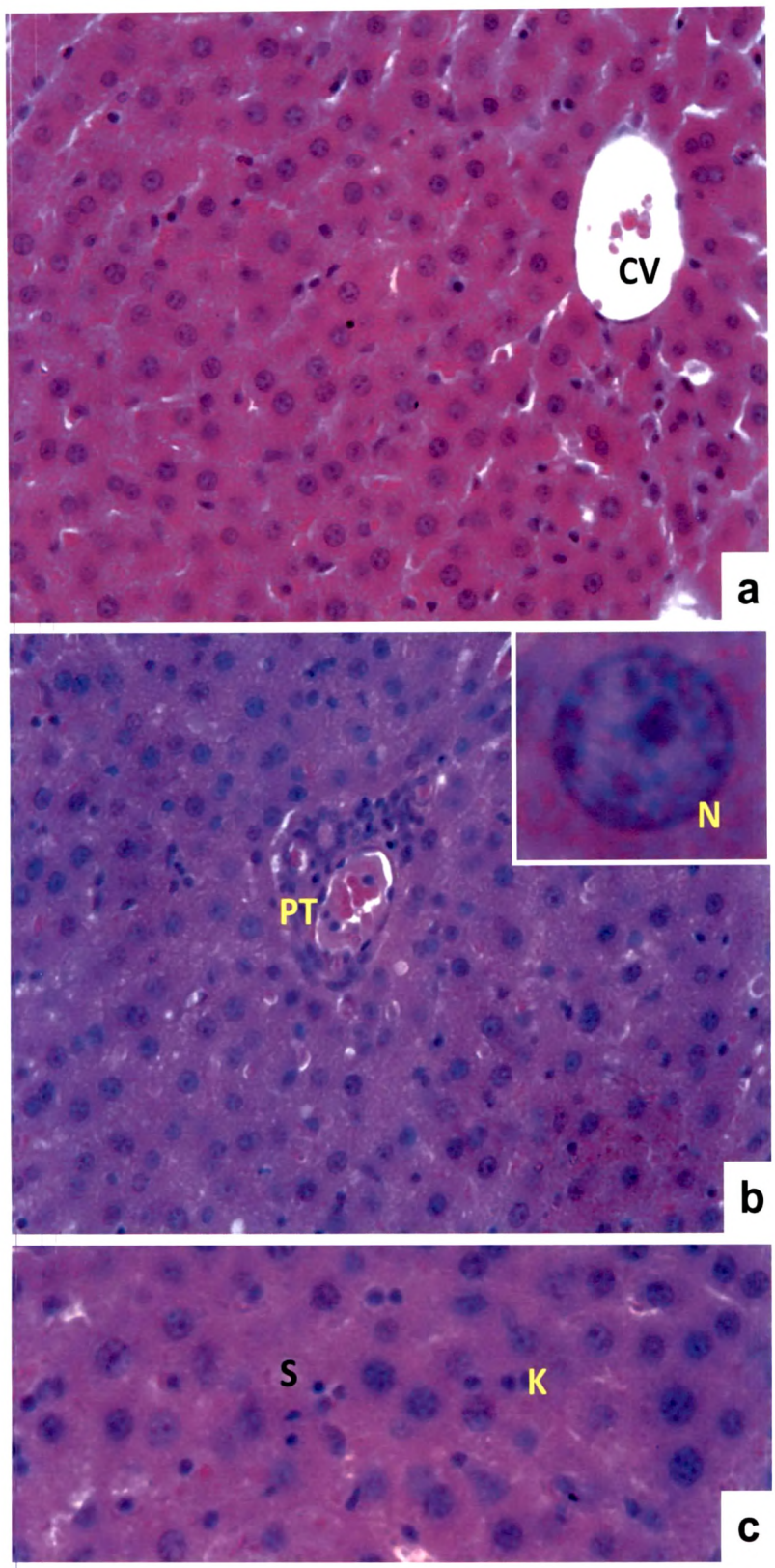

PLATE 2

Transverse sections of liver of control animals

a Showing the Zone 3 of acinus around the central vein (CV). The endothelial lining of the central vein is prominent and intact (arrow). The arrangements of marginal hepatocytes are also appropriate. The bile canali (BC) is distinctly seen between the two adjacent hepatocytes. 400X

b Showing the details of Zone-1 of the hepatic acinus. The portal vein (PV), hepatic artery (HA) and the bile duct (BD) are clearly seen. The cuboidal epithelium of bile duct is distinct and normal. The hepatocytes around portal triad also appear normal. 400X

c Showing the Zone-2 of hepatic acinus. The hepatocytes appear normal. The nuclei are distinct and the cytoplasm is prominently granular. In between small sinusoidal spaces are also seen. One Kuffer cell exhibiting prominently stained nucleus along the sinusoid (S). 1000X

PLATE 2

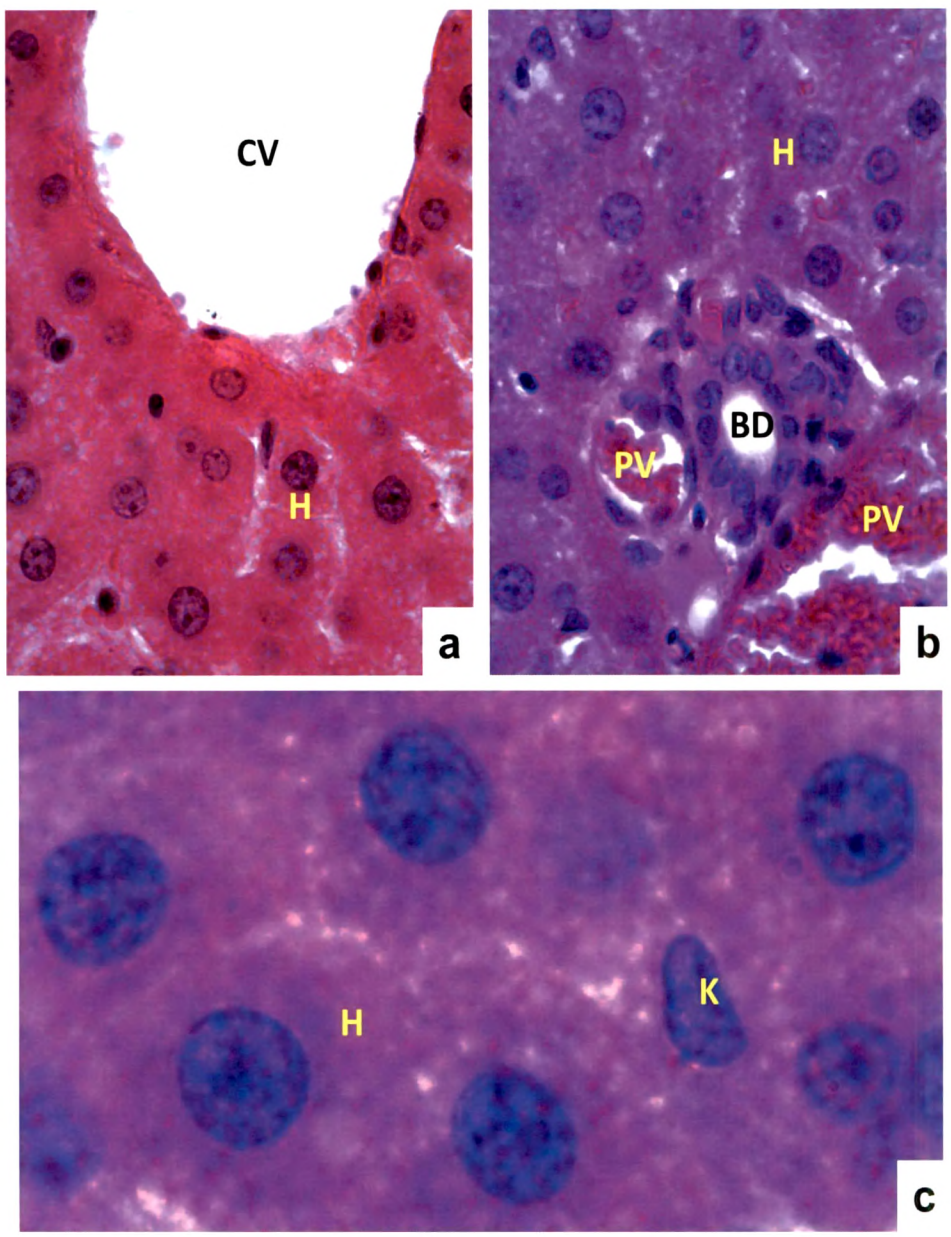

PLATE-3

Showing the transverse sections of liver exposed to high dose of heterogeneous mixture exposed for 60 days.

a and c Depicting Zone-1 of acinus, the portal triad (PT) region. The hepatocytes are highly vacuolated although the cytoplasm is prominently granular. 200X

b the zonal degenerative pattern of the hepatocytes is clear. The cells of Zone-1 are highly vacuolated, that of Zone-2 moderately affected and that of Zone-3 least vacuolated. The cytoplasm of Zone-3 hepatocytes is however, comparatively more eocinophilic. 200X

d showing the hepatocytes of Zone-2 where the vacuolation is quite less. The sinusoids are wider. Nuclear changes are not seen. However, cytoplasm is eosinophilic. 300X

e Showing Zone-3 of acinus where marginal Kupffer cell hyperplasia can be seen. Most of the hepatocyte show minute cytoplasmic vacuoles. 400X

PLATE 3

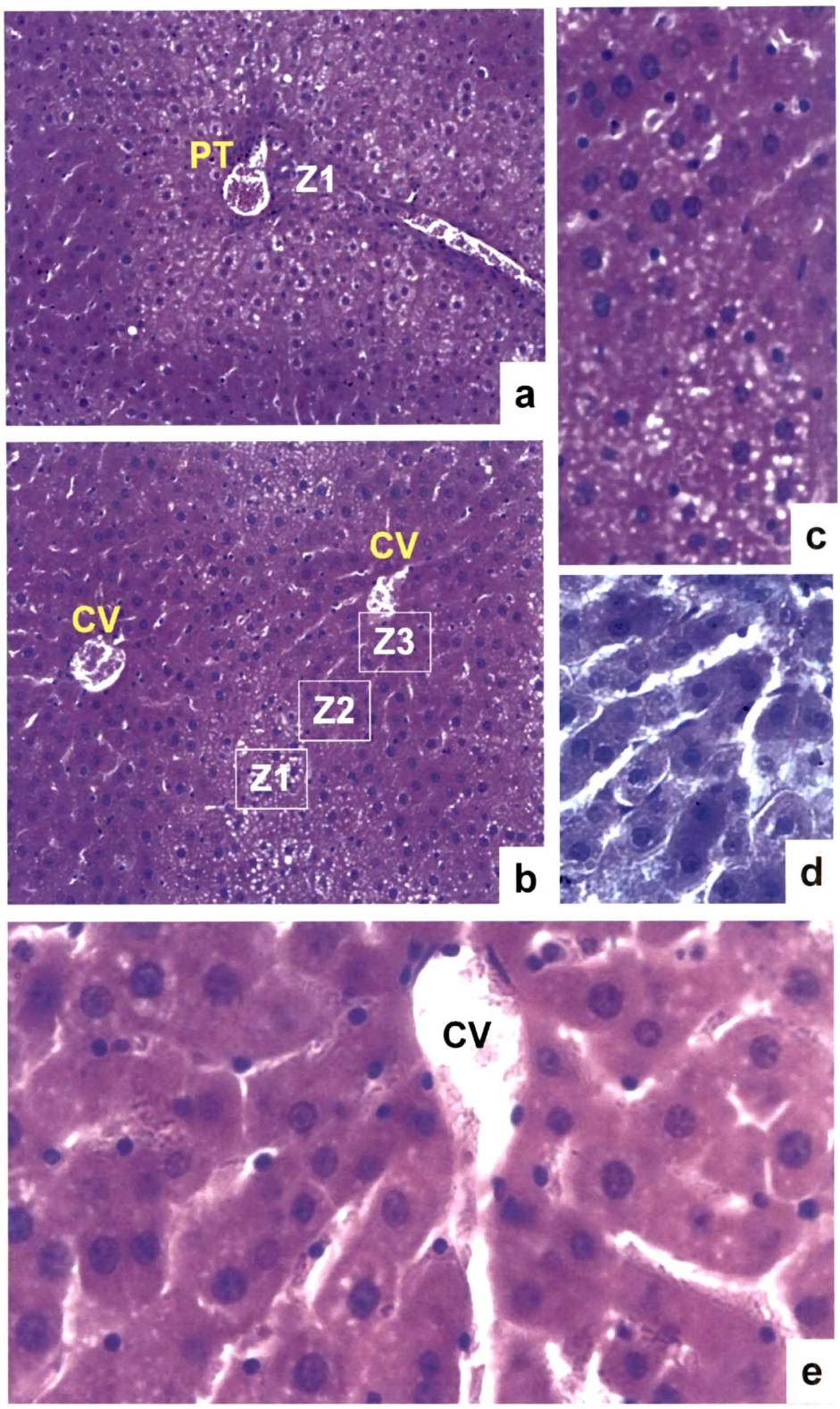

PLATE 4

a, b and c Showing the pattern and extent of cytoplasmic vacuolation particularly in Zone 1 as well in Zone 2. The hepatocytes are swollen and hence the sinusoidal spaces are constricted. In photoGraph C, marginal hyperplasia of Kuffer cell is also clear and the variation in the extent of cytoplasmic vacuolation in the hepatocytes is also clear. a: 200X b,c : 400X

d and e Showing the prominence of cytoplasmic vacuolation in the hepatocytes of Zone 3. The cellular margins of hepatocytes appear quite thick which is actually due to fluid accumulation in the perihepatocyte region or the space of disse (arrow) d: 650X e: 1000X

PALTE 4

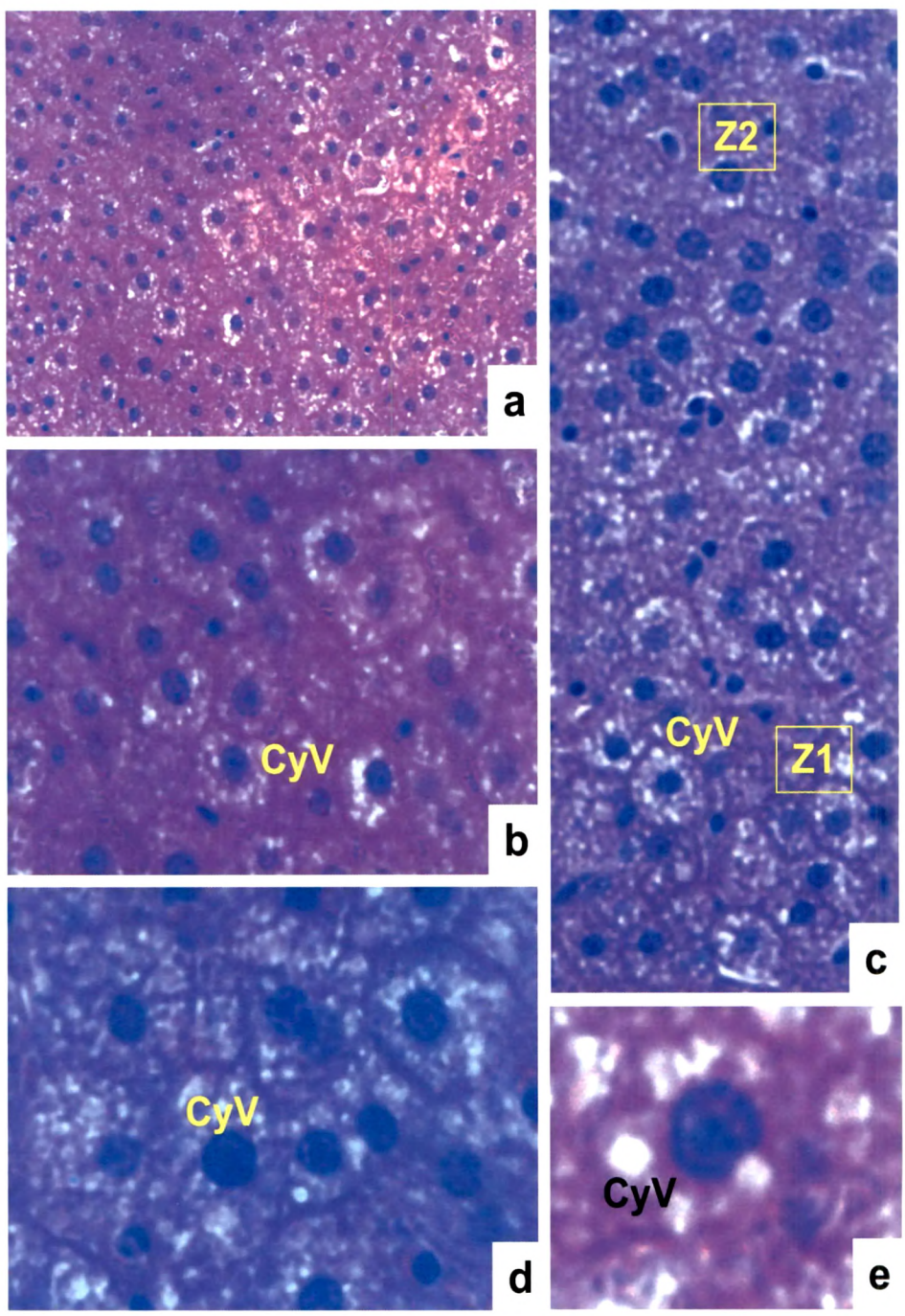

PLATE-5

a Showing the Zone-1 of acinar where in theper portal region lymphocytic infiltration is seen. The sinusoids are marginally edematous and contain the cytoplsmic debris and the fluid that probably has leaked from the hepatocyets. 400X

b Showing the Zone-3 of acinus where Kupffer cell hyperplasia and cytoplasmic debris in the sinusoidal region are seen. The hepatocyte are vacuolated. 200X

c Showing the Zone-2 of acinus. In the mid portion of the photoGraph swelling of hepatocyte and their wavy margine are seen. The prominence of extensive small vacuoles is also obvious. 200X

d Showing the hepatocytes at the margin of Zone-2 and Zone -3 where the variations in the extent and pattern of vacuolization as well as the intensity of granular cytoplasm can be clearly seen in most of the hepatocytes are normal. 400X

PLATE 5

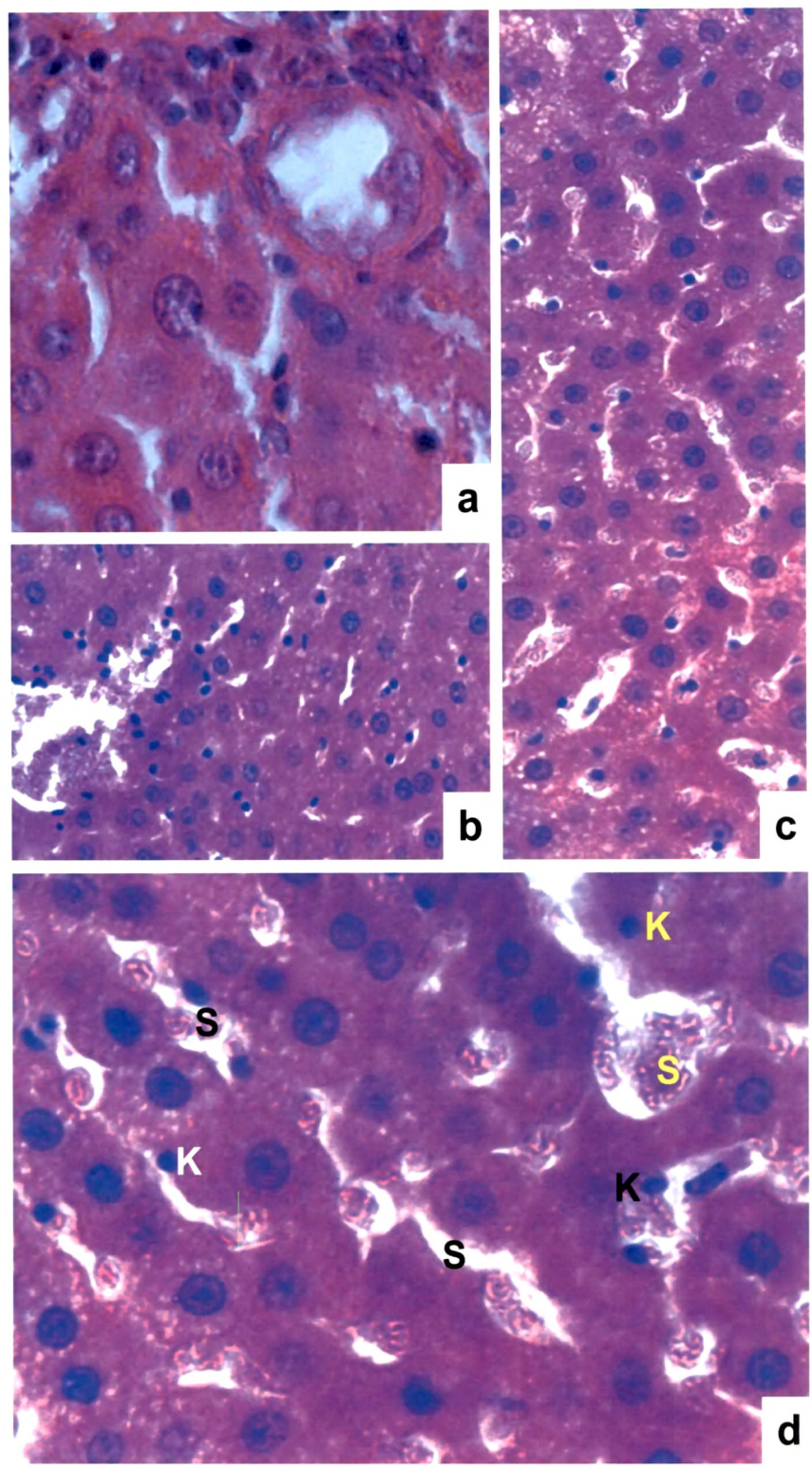

PLATE 6

a The swelling of hepatocytes is prominently seen. The variation in the vacuolation is Zone 2 and Zone 3 is also clear. It can be noted that the hepatocytes of the Zone 3 are more swollen and have less vacuoles compared to that of Zone 2. 200X

b, c, d and e Showing the prominent features of cell damaged to hepatocytes. The cells are swollen. Cytoplasmic blebbing is prominent (arrow) and the cell exudates in the sinusoids are also seen. b, e: 1000X c, d: 650X

PLATE 6

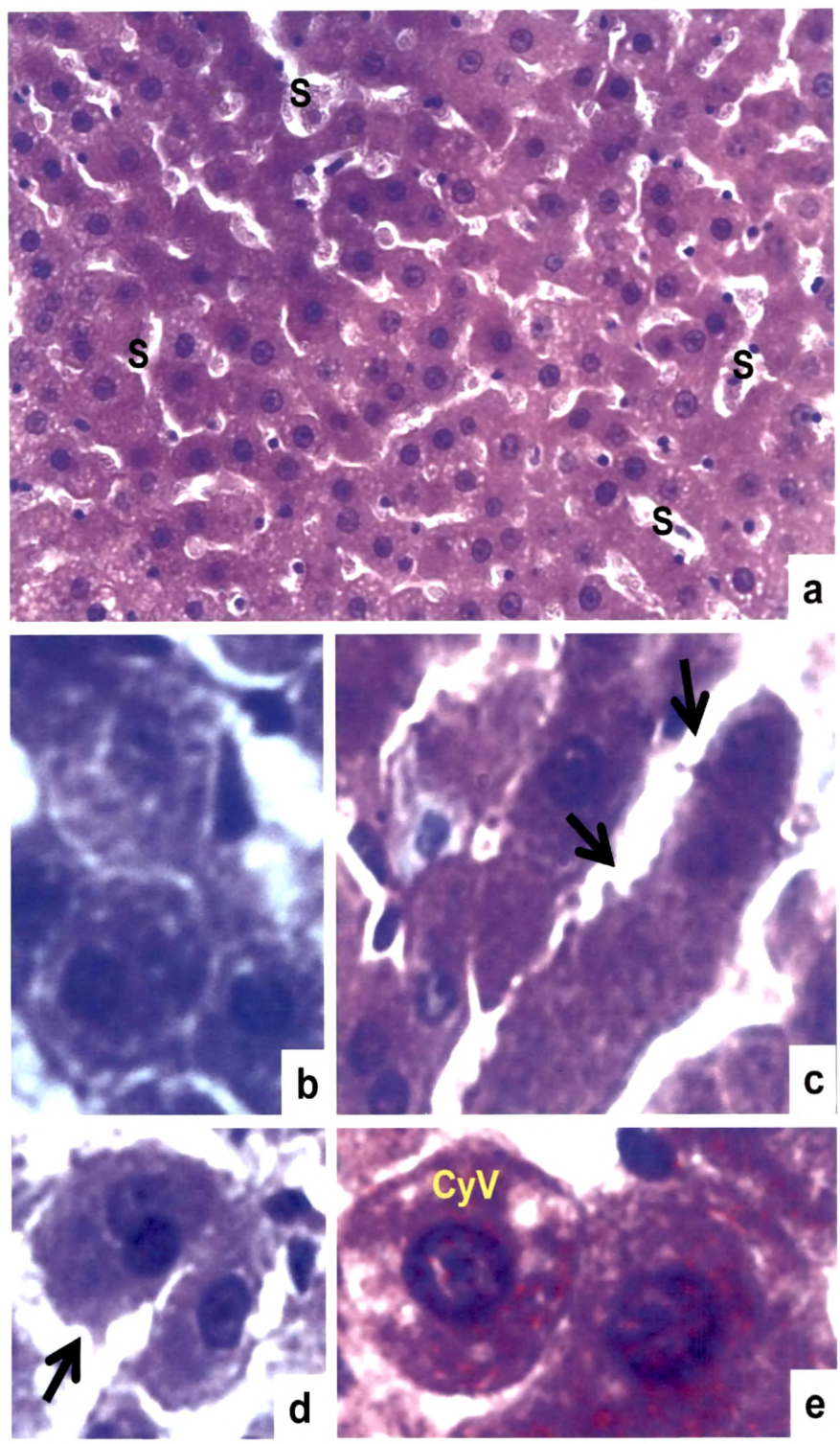

PLATE-7

Showing the transverse sections of liver exposed to low dose of hetrogenous mixture for 60 days.

a and b Showing different zones of acinus exhibiting comparatively less prominent toxic effect.200X.

c and d The degenerative changes are prominent among the hepatocytes of Zone- 1.The vacuoles in most of the cases are perinuclear and much larger. The nuclei are deformed.400X.

e and f The nuclear picnosis and deformation of margine is shown for the hepatocytes.The kupffer nucleus is also intensely stained.In one of the hepatocyte perinuclear vacuolation is prominent which is expected to lead to further degenerative changes.1000X.

PLATE 7

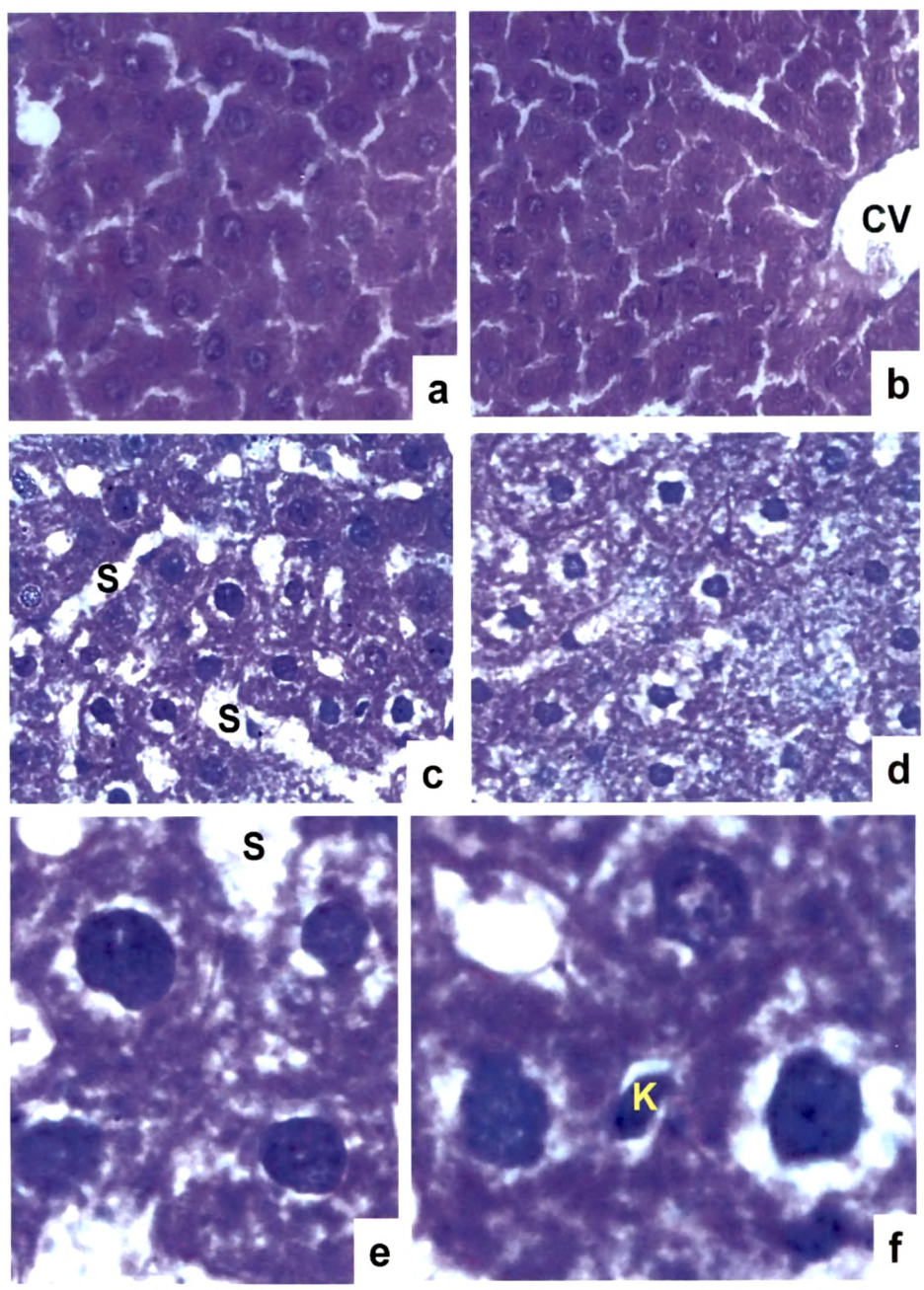

PLATE 8

a Showing the discharge of cytoplasmic exudates in the central vein through sinusoids (Star). At the periphery, a much swollen hepatocyte is undergoing degenerative apoptotic changes and is lined by other hepatocytes with less prominent cellular changes. This kind of arrangement appears as a nodular formation, although the margin of this so called nodular form is not exhibiting any sign of fibrosis. However, the outer margin of the peripheral cells is quite thick. 400X

b, c and d Prominent nuclear changes noted in the toxicant mixture exposed to. In b, the single nuclei is absolutely deformed. In c and d, actually atleast 3 different nuclei are seen as a clump. 1000X, d is further enlarged.

e and f The cytoplasmic blebbing and release of cellular exudate in sinusoidal region is seen. In e, the nuclei undergoing mitotic division appear normal. 1000X

PLATE 8

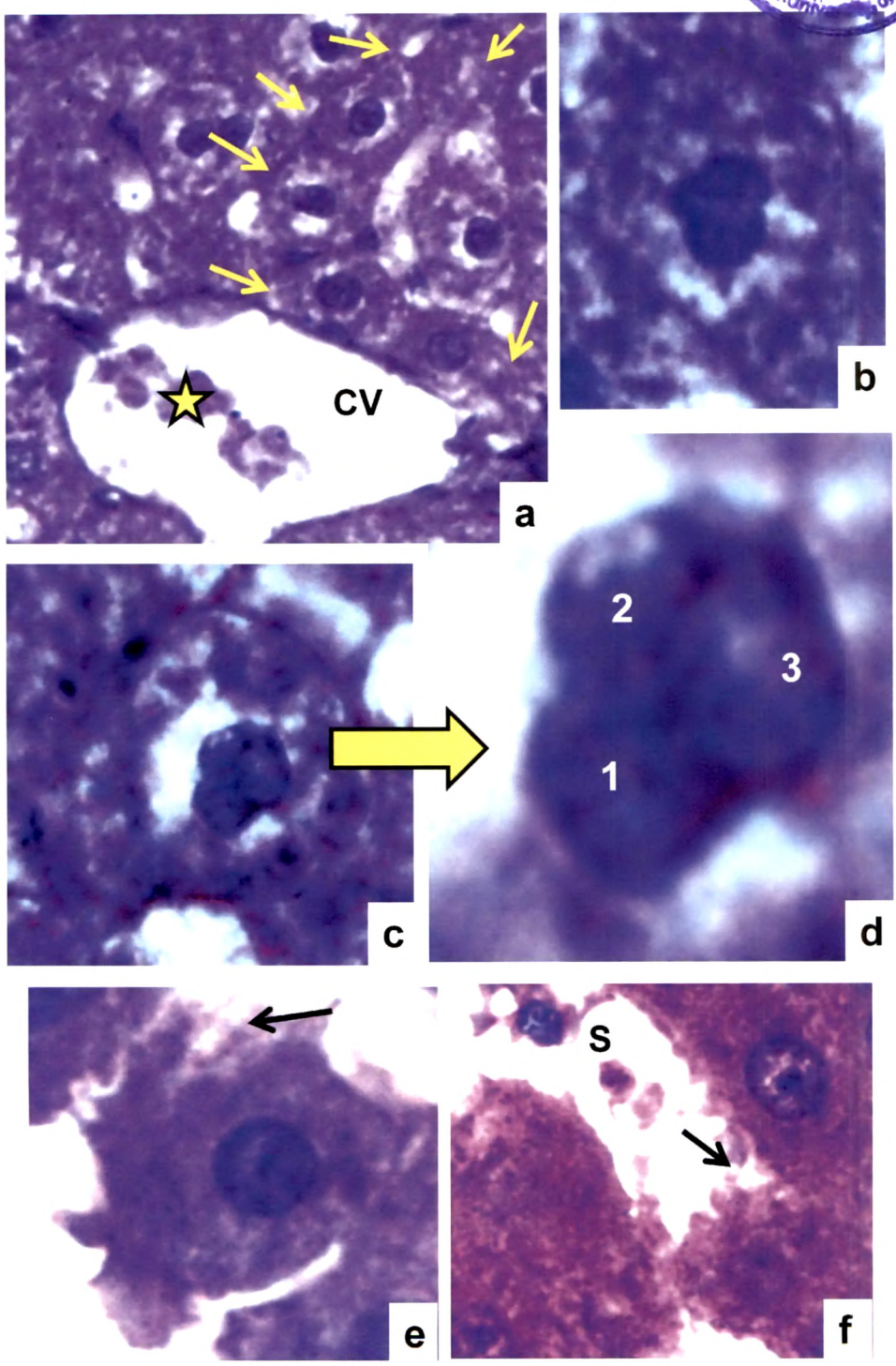

PLATE-9

Showing the transaction of the liver of the rat exposed to high dose of the heterogenous chemical mixture for 60 days followed by 60 days withdrawal.

a and b The hepatocytes are swollen but the sinusoids are the prominent and wide. In photoGraph a, the demage to the hepatocyte cytoplasmic membrane is clearly seen. A.600X, b.400X

c At higher magnification, the cytoplamic vacuolation and the membrane demage are obvious. In general the cytoplasm is highly granulomatous and more eosinophilic. 1000X

d Showing the Zone-1 of acinus including the portal triad and the hepatic cords. Some hepatic cords show normal arrangement while in other the epatocyte are separated indicating the demage to the stroma connective tissue. 200X

PLATE 9

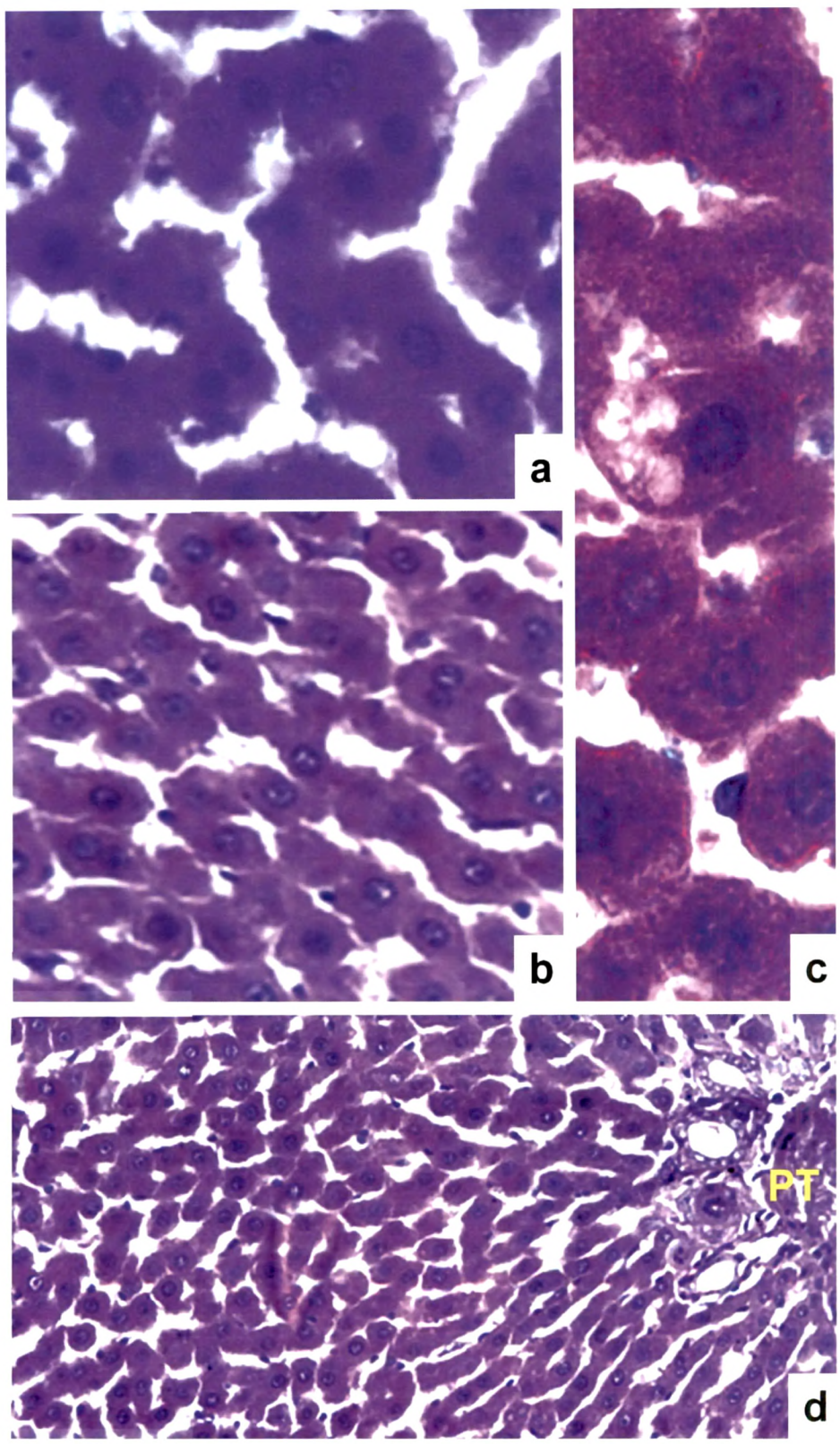

PLATE 10

a and b In Zone 2 of acinus the hepatocytes appear quite normal since the nuclei and cytoplasmic staining are appropriate. The cytoplasmic exudates are seen in some of the sinusoidal spaces (star).The kuffer cells are normal in density and distribution. a: 200X, b: 400X

c, d, e and f The nuclei of the hepatocytes from the different zones of acinus appear quite normal. However, cytoplasmic changes, especially vacuolation, are prominently seen. It was more conspicuous in Zone 1 followed by Zone 3 and Zone 3, respectively. The Kuffer cell nuclei also appear normal. The bile canaliculus (BC) is also seen prominently. 1000X

PLATE 10

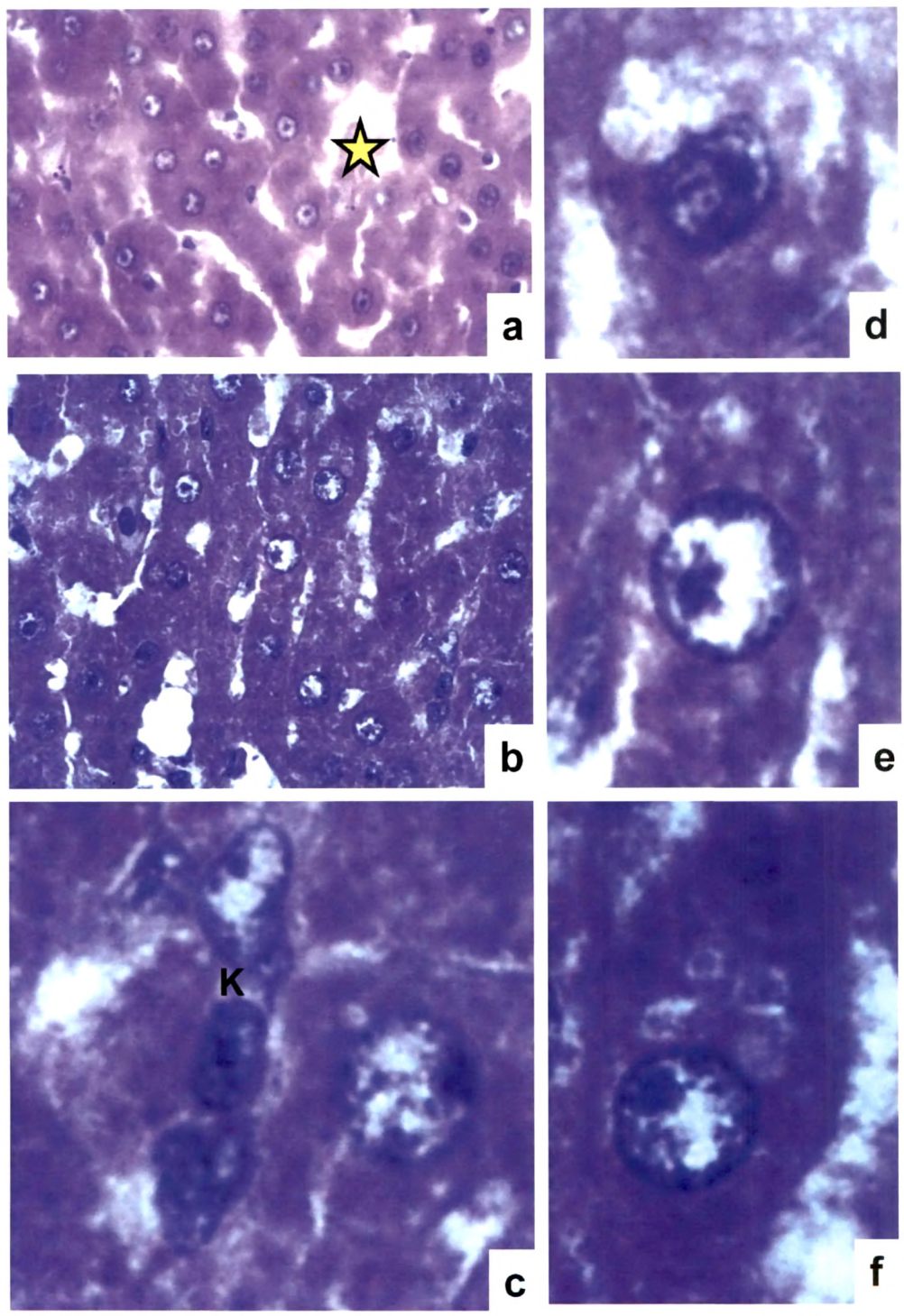

PLATE-11

a and b Several binucleate hepatocytes are seen where some of the case cytoplasm is also normal. This is generally considered as a feature of hepatic regeneration. 400X

c Region of hepatoytes in the Zone-1 of acinus showing much improved histological picture. 400X

d The exudates leaked from the hepatocytes are present in the extensively extended space of disse seen between the hepatocytes and the margin of the sinusoid. The kupffer cells lining the sinusoids are also clearly seen. 1000X

e,f and g Variations in the histological features of the binucleate hepatocytes is shown where in e and f, the cell appear to be normal while in g, it is highly vacuolated, the cytoplasm concentrated in the periphery. 1000X

PLATE 11

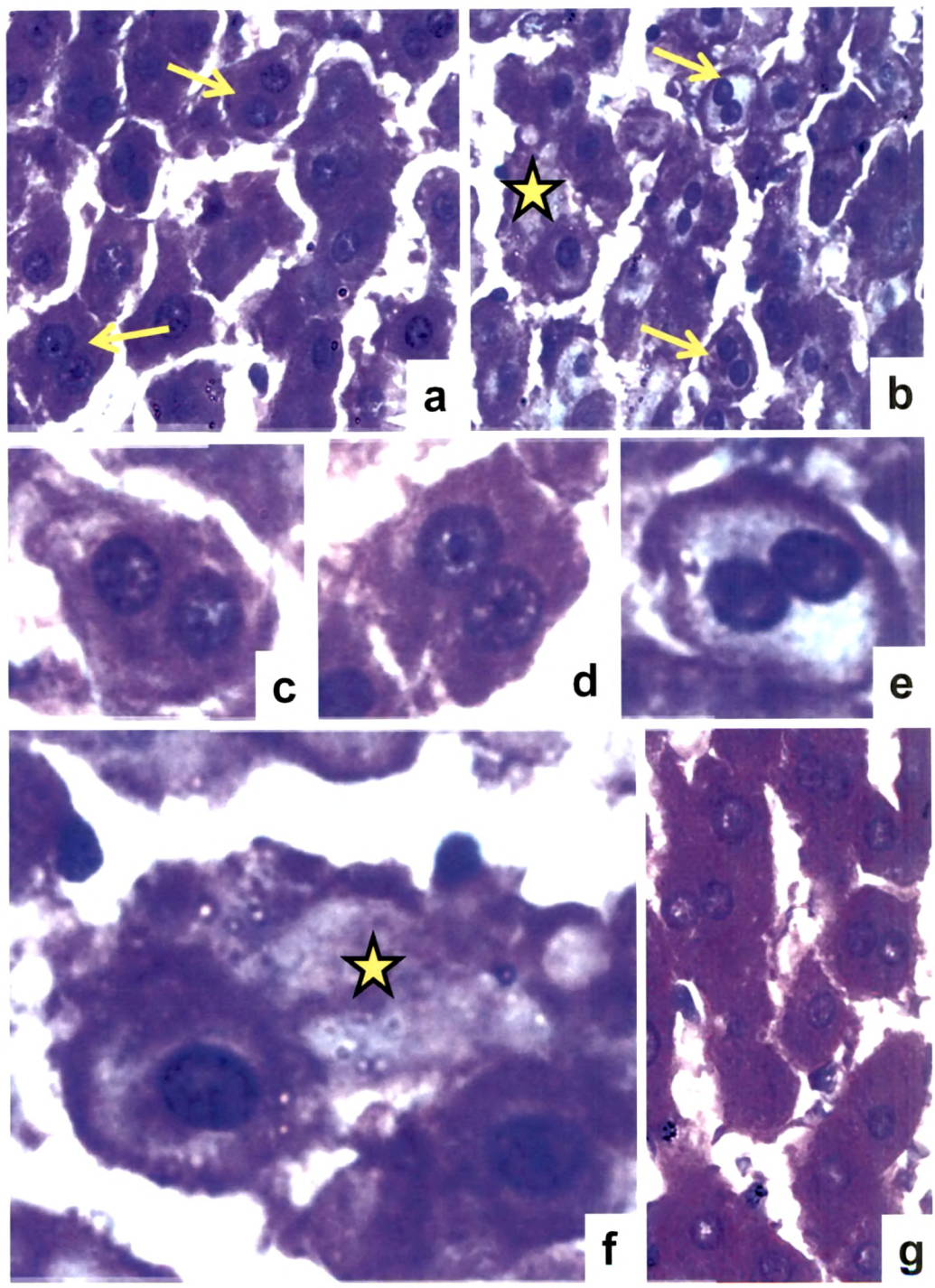

PLATE 12

Showing the histological features of liver of the rat exposed to low dose of heterogenous chemical mixture for 60 days followed by withdrawal phase of 60 days.

a and b Showing marked improvement in the histoarchitecture of hepatic parenchyma of Zone 3 (a) and Zone 1 (b) of the liver. In Zone 3 hepatocytes the prominence of minute cytoplasmic vacuoles is seen while in the Zone 1 the vacuoles are comparatively larger. In Figureb, the large sized hepatocytes nuclei actually show the polyploid status. 400X

c and d Some of the hepatocytes are swollen in Figurec while there appropriate arrangement in the hepatic cords is seen in Figured. c: 200X, d: 400X

PLATE 12

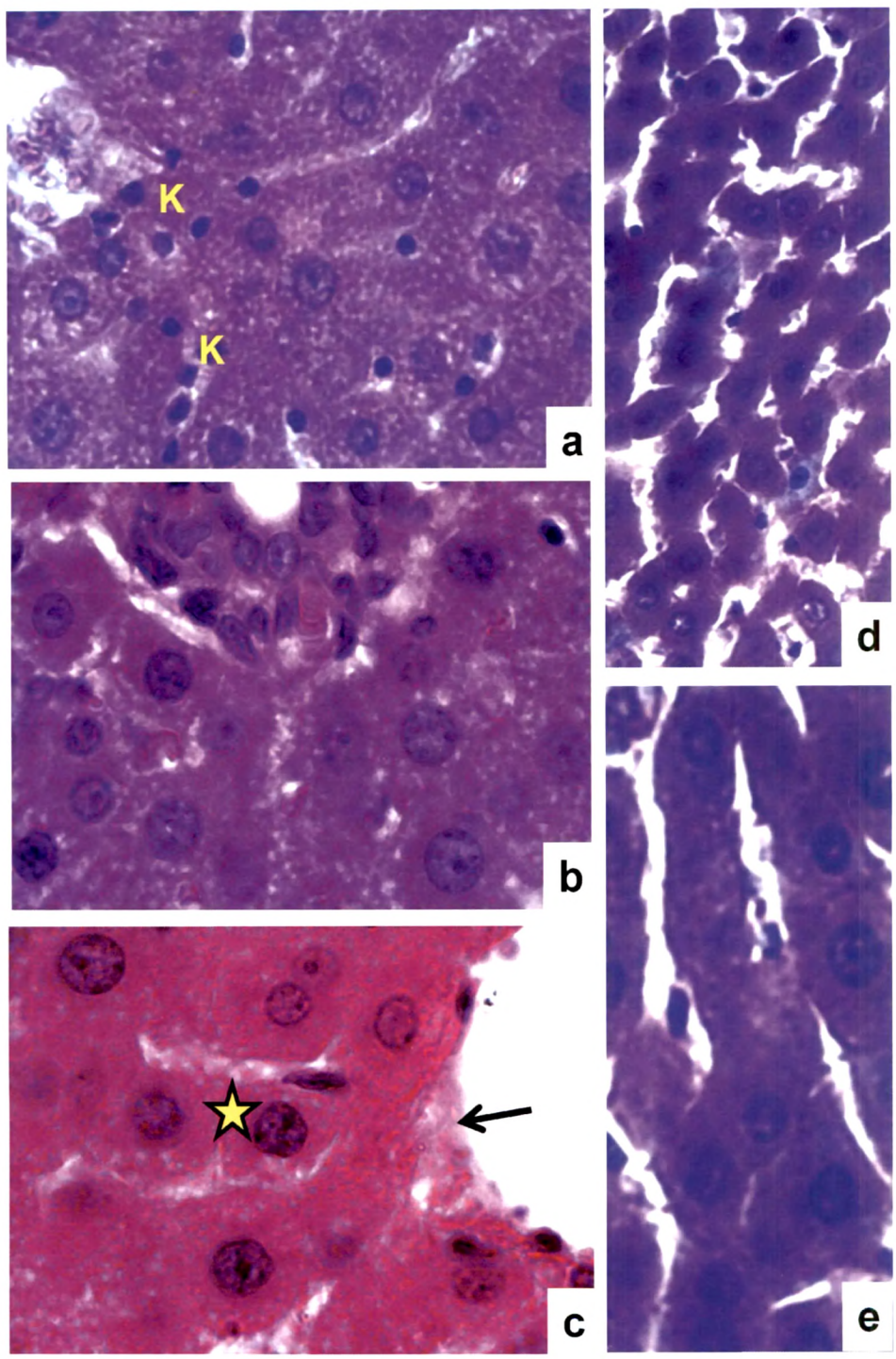

CHAPTER 3

TOXIC POTENTIALS OF HETEROGENEOUS CHEMICAL MIXTURE EXPOSURE ON THE KIDNEY

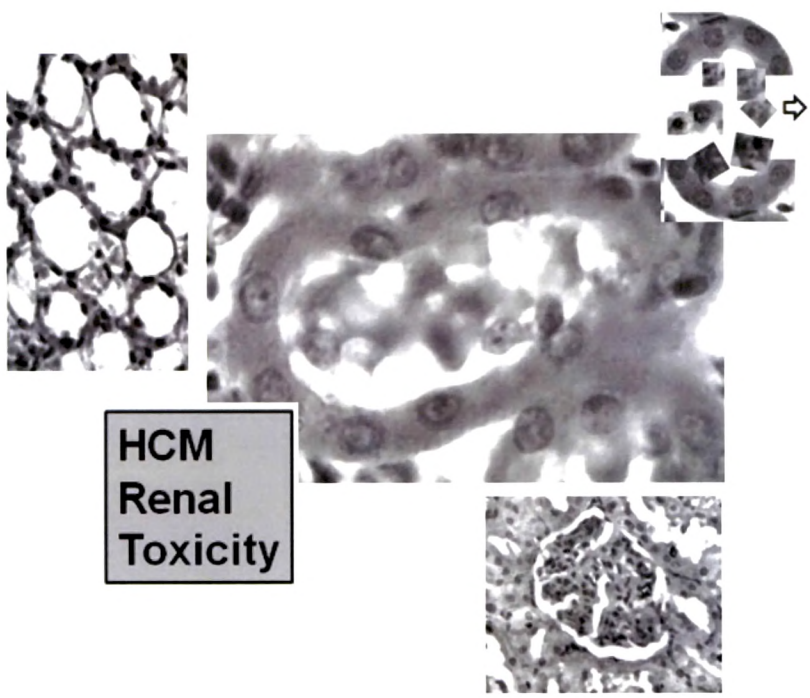

Scientist's interest in the cumulative health effects of environmental pollutants exposure continues to grow as information and multifarious facts increases about the probability for multiple exposures to varieties of chemicals. There is strong evidence available that mixture of chemicals can produce effects that are larger than the effect of individual chemical (Freidig *et al.,* 2001; Jadav *et al.,* 2006 and 2007; Shalaby and El-Mageed, 2010, Syberg *et al.,* 2008). But most of the studies have been conducted with mixture of same class of compounds or compounds with similar mode of action. These have been reported to cause systemic toxicity with development of cellular lesion (Jadhav *et al.,* 2007; Rhman *et al.,* 2011). Therefore, organ kidney was selected to identify the potential hazards from exposure to heterogeneous chemical mixture (HCM) at or below No Observable Adverse Effect Level (NOAEL).

Kidney is composed of different types of cells with varying sensitivities to substances. They filter, cleanse, and rid the body of toxic chemical wastes. The process of urine formation begins with filtration of blood at the glomerulus, re-absorption of essential elements and elimination of the formed urine by the renal collecting system. Changes in any of these processes can result in the clinical picture of rapidly deteriorating renal function (Epstein, 1997). The Kidneys also take part in regulating the body's acid base balance and blood pressure, secrete hormone and produce active form of vitamin D (Epstein, 1997; Koeppen, 1998; DeLuca, 2004) and thus kidney plays significant role in maintaining the homeostasis. Injury in kidney because of toxicants and their metabolites can leads to number of complications (Lash, 1994; Perazella, 2009). Chemicals exposures can cause extensive free radical generation that lead to improper cellular functioning in the tissues (Poovala *et al.,* 1999; Sabolic, 2006; Uboh *et al.,* 2011). Detoxification program cannot be done without the supporting system of the kidneys (Lock and Reed, 1998). When the function of this organ become sluggish as a result of toxicity of chemicals, the toxic wastes cannot be fully flushed out from the body and so is circulated in the bloodstream. An over load of toxins can

produce even more severe abnormalities and the whole body may become more vulnerable to other diseases and infections.

Therefore, with the possibility that the collective effect of the mixture could have greater adverse impact on kidney function, the current study examines the effect of a mixture of four environmentally persistent contaminants on kidney functioning in adult male rats. To study the changes in renal function several important biochemical parameters were compared along with measurement of urine volume, glomerular filtration rate, blood electrolyte concentration and histological examination.

RESULTS

Effect on kidney weight

The difference in the absolute kidney weight at the end of experiment between the groups was not statistically significant (Table 1, Fig. 1). Relative kidney weight, although increased marginally in the HCM exposed rats, was not statistically different from vehicle treated control rats.

Effect on parameters of kidney function test in serum and urine

The effect of HCM administration on parameters of kidney function test in serum and urine are given in Table 2 and Fig. 2. Serum and urinary creatinine level increased significantly after sixty days HCM exposure in group IV and V as compared to control group III. However, withdrawal from HCM treatment showed recovery to almost the same levels as in control rats (group VII). A mild increase (statistically insignificant) in serum urea level was observed in both HCM exposed and withdrawal groups. In toxicity study of HCM, a statistically significant ($P<0.01$) decrease in 24 hours urine volume was found in high dose group IV, whereas a mild decrease in urine volume observed in low dose group V was found to be statistically insignificant. A

slight decrease in glomerular filtration rate (GFR) was found in sixty days HCM treated groups.

Effect on serum electrolyte and mineral levels

Tables 3, 4 and Fig.s. 3, 4 compare the results of serum electrolytes level of HCM exposed and recovery groups with control. In toxicity and recovery study, serum calcium concentration was not changed to significant level when compared with control groups. A significant ($P<0.001$) rise in the serum sodium concentration was observed in the sixty days HCM treated rats. At the end of withdrawal period the serum sodium concentration was comparable to that of control group VII. In HCM toxicity study, the level of serum potassium increased insignificantly in high dose treated group, whereas significant ($P<0.01$) increase was observed in low dose treated group. Serum chloride data showed a significant ($P<0.05$) increase in its level in high dose HCM exposed group IV when compared with control group III. Here again at the end of withdrawal period serum potassium and chloride levels were comparable to that of control group, except serum chloride level in high dose HCM treated recovery group, that showed a significant increase ($P<0.05$) (Tables 3, 4, Fig.s. 3,4).

Effect on kidney SDH, ALP and ACP activities

Table 5 depicts the results of activities of enzymes SDH, ALP and ACP in HCM exposed and recovery groups. No significant changes were observed in the activities of SDH and ACP in both toxicity and recovery groups. However a mild decrease in the activity of SDH was observed in HCM treated group IV and V. In toxicity study, a statistically significant ($P<0.01$) decrease in ALP activity was observed in high dose HCM treated rats, where as a mild decrease (statistically significant) in ALP activity was observed in low dose HCM treated group. Similarly, in recovery group, the ALP activity was decreased ($P<0.05$) significantly in group VIII and insignificantly in group IX when compared with 120 day control group VII (Table 5, Fig. 5).

Effect on protein content

A comparison among toxicity and recovery study with control group showed that protein content of kidney was not changed to significant level (Table 6, Fig. 6). A mild decrease (insignificant) in protein content was observed in low dose HCM treated group V when compared with control group III.

Effect on Lipid Peroxidation (LPO)

In toxicity study, high dose HCM treated rats exhibited a significant higher LPO compared to normal rats (Table 6, Fig. 6). But the increase was non significant in low dose HCM treated and recovery groups (VIII and IX) when compared with their respective controls. Thus withdrawal from HCM treatment showed recovery pattern in membrane lipid peroxidation when compared with HCM treated toxicity study groups.

Effect on enzymatic and non enzymatic antioxidants

Tables 6, 7 and Fig.s. 6, 7 show the level/ activity of enzymatic and non enzymatic antioxidants in rats exposed to HCM in toxicity and recovery study. In toxicity study, a small decrease in GSH and ascorbic acid level was observed in the sixty days HCM groups in comparison to control group III. A statistically significant ($P<0.05$) decrease in the SOD activity was found in high dose treated HCM group IV, whereas an insignificant decrease in the activity was observed in low dose treated HCM group V. A statistically highly significant decrease in the activities of GPx and CAT were observed in HCM treated groups. Kidney GST activity was decreased ($P<0.05$) significantly in high dose HCM treated group whereas the decrease was non significant in low dose HCM treated group. Among recovery groups, significant ($P<0.05$) decrease in ascorbic acid content was observed in group VIII (high dose HCM treated+ recovery) whereas no significant difference was noted in GSH level when compared with control group VII. In recovery group, withdrawal from

HCM treatment for sixty days showed recovery in all antioxidant parameters, except CAT in group VIII (high dose HCM treated + recovery) which showed a significant decrease ($P<0.05$) when compared to 120 days control group VII (Tables 6, 7 and Fig.s. 6, 7).

Effect on histoarchitecture of kidney

The functional and structural unit of the kidney, the nephron, consists of a renal corpuscle (including the glomerulus) plus a long folded renal tubule. It is divided into cortex and medulla regions. The renal corpuscle are distributed throughout the cortex and referred as cortical or juxta medullary corpuscles (Plate 1). The nephron is subdivided into tubular segments like proximal convoluted and straight tubule (PCT), descending and ascending thin limbs and thick ascending limb of Henle (LH), macula densa- located within the final portion of the thick ascending limb, distal convoluted tubule (DCT), connecting and collecting tubule (CT) (Plate 2).

The afferent arteriole enters Bowman's capsule at the vascular pole of the renal corpuscle and branches to form an anastomosing network of glomerular capillaries, where each major branch gives rise to a lobule. The space between the capillary loops is filled by mesangial cells. The other cell type is podocyte which wrap the capillaries by their branched processes, the pedicels. Under light microscopy the prominently stained oblong nucleus of the podocyte can be clearly seen (Plate 2). The Bowman's capsule is lined by simple squamous epithelium, the parietal layer and internally the epithelium, the visceral layer, covers the capillary tuft (Plate 2). Between the visceral and parietal layers of Bowman's capsule is Bowman's space, which fills up with the filtrate. The filtrate formed in Bowman's space flows towards the urinary pole to enter the proximal tubule. The proximal tubule consists of an initial convoluted portion (the proximal convoluted tubule) and a distal straight portion (the pars recta). In cross section, the tubular epithelial cells are simple cuboidal cells, with a prominent brush border (microvilli). The PCTs often

have star-shaped lumens, which are generally larger in diameter than the distal tubules. Cells of the PCT are generally more eosinophilic than cells of other tubules in the kidney (Plate 2).

The exposure to heterogeneous chemical mixture at high doses for 60 days led to severe changes both in the cortical and medullary regions of the kidney. The glomeruli had distorted capillary lobes where both the parietal and visceral epithelia were significantly disintegrated (Plate 3). Due to this prominent shrinkage of the capillary tuft was seen. Of all the animals studied, one of the animals exhibited the mesengial cell hyperplasia and degeneration of the epithelia lining the corpuscle (Plate 3). Most severe degenerative changes were observed in the proximal convoluted tubules where the loss of brush border, cytoplasmic blebbing, cytoplasmic dissolution and sloughing of nuclei were typically observed (Plates 3, 4). The degenerated mass of cytoplasm/ nuclei accumulated in the tubular lumen and blocked the passage (Plate 4). The cells of the Loop of Henle, distal convoluted tubules and the collecting ducts also exhibited necrotic changes where the tubules were significantly depopulated and the height of the epithelium quite diminished (Plates 3, 4).

The changes in the low dose exposure group on day 60 were much comparable with those noted in the high dose exposure group; however, these were less severe. Glomerular epithelial damage, mesengial cell hyperplasia, necrotic changes of the distal convoluted tubule Macula Densa at the juxta glomerular region were also seen in the low dose exposure group (Plate 5). Some of the glomeruli showed hypertrophy of the parietal epithelium and significant cytoplasmic blebbing in that region (Plate 5).

Following withdrawal for next 60 days, the recovery was seen in the low dose group but not significantly in the high dose group (on day 120). The cortical glomeruli were still damaged while the medullary glomeruli were comparatively normal; although several of these exhibited podocyte and mesengial cell damage (Plates 6, 7). The epithelium of the tubular cells also

exhibited significant recovery and the degenerative changes noted on day 60 were conspicuously diminished on day 120 in the low dose exposure group (Plates 6-9). It was interesting to note that the lumen of most of the tubular cross sections were free from cellular debris. Such a picture was apparent in the low dose exposure group (Plates 8, 9).

The proximal tubule consists of three discrete segments: the S1 (pars convoluta), S2 (transition between pars convoluta and pars recta), and S3 (the pars recta) segments. The S1 segment is the initial portion of the proximal convoluted tubule and is characterized by a tall brush border and a well-developed vacuolar lysosomal system. The basolateral membrane is extensively interdigitated and many long mitochondria fill the basal portion of the cell, characteristic of Na^+-transporting epithelia. The S2 segment comprises the end of the convoluted segment and the initial portion of the straight segment. These cells possess a shorter brush border, fewer apical vacuoles and mitochondria, and less basolateral interdigitation compared to the S1 cells. The S3 segment comprises the distal portion of proximal segments and extends to the junction of the outer and inner stripe of the outer medulla. The S3 cells have a well-developed brush border but fewer and smaller lysosomes and mitochondria than S1 and S2 cells.

DISCUSSION

Impairment of the renal functions may be caused by exposure to different toxic substances, in addition to certain diseased conditions. The administration of HCM brings about an impairment of renal function which is evident by decrease in urine volume and decrease in glomerular filtration rate. The decrease in 24 hours urine volume after HCM treatment could be due to decrease in fluid intake (Janicka and Cempel, 2003). A non significant decrease in the glomerular filtration rate further supports the fact that HCM causes renal damage and that a reduced GFR is due to renal inadequacy (Stevens *et al.*, 2006). The decline in GFR may result from tubular cell injury

and its loss in lumen resulting in tubular obstruction and back leak of glomerular filtrate (Fig. 8). Besides, the damage to vasculature and oxidative stress generated following toxicant mixture exposure also induce functional alterations leading to impaired glomerular filtration. It was clear from present studies that the glomurular capillary epithelia as well as the podocytes were structurally damaged and hence can lead to structural disruption of the filtration unit (the slit formed by pedicels of podocytes and the capillary fenestrae) (Diamond and Zalups, 1998). Although this can be confirmed only by electron microscopic evaluation, light microscopic findings and the function analysis in present studies are also appropriate indicators of such disruptive changes, as described in Fig. 8.

It is significant to note that the epithelial damage, particularly in the PCT, resulted into sloughing of cells and disruption of cytoplasmic blabs which blocked the tubular lumen, again importantly in the PCT. Such a blockage would lead to back leak of the filtrate and hence the glomerular functions are further altered (Fig. 9). This feature was prominently seen on day 60, particularly in the higher dose HCM treatment group, and significant recovery was noted on day 121 indicating the restoration of the structural and functional integrity of the glomerular and tubular epithelium (Fig. 9).

Increased serum creatinine is reported to be one of the important risk factor for kidney damage which may results in renal failure (Graves, 2008). Therefore, elevations in serum creatinine in HCM treated rats can be associated with impairment of renal function. These results are in agreement with the research reports available on toxicity of metals and organicals which indicated that the exposure to these toxicants induced severe physiological and also biochemical disturbances in animals (Kertai *et al.,* 2000; Aiso *et al.,* 2005; Sujatha *et al.,* 2011).

Minerals and electrolytes are involved in multiple functions of cells. They have a strong role in holding fluids in different compartments of cell and thus ultimately maintain the acid base balance of the body (Chan, 1983;

Epstein, 1997). The elevated serum levels of Na+ and K+ in HCM treated group in comparison to control group may indicate reduced ability of the normal kidney function or interference in reabsorption processes of ions or may be caused because of less water intake. However, the calculated Na+/K+ ratio depicts no significant changes in HCM groups which indicate that system tries to maintain its Na+/K+ ratio in stress condition.

Also, several other studies showed that metals and organic compounds induced histopathological alterations in liver and kidney. Jadhav et al. (2007) showed that metals mixture intoxication led to severe effects on the structure of kidney, covering epithelium degeneration of the cells of renal tubule, and damages in renal glomeruli, especially to podocytes, as well as infiltrations. In present study oral HCM exposure causes damage to the kidneys and its cell types, mostly our findings are an indicative of the damage in the cortical region of kidney, proximal and distal tubules epithelium, and glomerulus.

In present investigation, many renal tubules of kidney showed marked degenerative lesions under toxic effect of HCM. This is justifiable since the tubules are sensitive to toxic influences because they have vulnerable enzyme system and complicated transport mechanism that may be used for elimination of toxicants and may be damaged by such toxicants. These findings reinforce those of Herak-Kramberger and Sabolic, (2001) and Cristofori *et al.,* (2007) who found that many chemicals had a direct toxic action and exerted their effects principally on the proximal convoluted tubules.

The possible mechanism for the tubular lesions may be the direct toxic effect on the cell function. The presence of histopathological lesions may be correlated to the altered activity of ALP and SDH (Jarrar and Mahmoud, 2002). Damage to the brush border and leakage of ALP, which are associated with the brush border of renal tubules, as a result of toxicant action are considered as an early marker of tubular insult (Teichert-Kuliszewska and Nicholls, 1985). SDH is a mitochondrial enzyme bound to its inner membrane and participates in aerobic oxidation in citric acid cycle (Hederstedt and

Rutberg 1981). The marginal decrease in SDH activity due to HCM treatment might indicate altered mitochondrial function and reduction in carbohydrates oxidation. Our results are in agreement with the biochemical findings of Ksheerasaga *et al.,* (2011) which suggest that industrial wastewater have adverse effects on kidney functions leading to physiological impairment.

Other possible mechanism for histopathological alterations may involve reactive intermediates and oxidative stress (Adewole *et al.,* 2007). Biologically reactive intermediates are electron deficient compound that bind to cellular electron rich compounds like proteins and lipids and thus interfere with normal activity (Aleynik *et al.,* 1997). Oxidative stress is induced by increasing production of ROS. ROS can induce lipid peroxidation, inactivate cellular enzymatic and non enzymatic antioxidants and induce DNA breakages (Patel and Katyare, 2004; Adewole *et al.,* 2007). This study also demonstrates that withdrawal of HCM treatment appears to moderate the renal damage caused by HCM.

Water reabsorption is through a passive iso-osmotic process, driven primarily by Na+ reabsorption, mediated by the Na+, K+-ATPase localized in the basolateral plasma membrane of the tubular cells. The proximal tubule reabsorbs electrolytes, such as Na+, K+, HCO3−, Cl–, PO43−, Ca2+, and Mg2+. The proximal tubule also reabsorbs virtually all the filtered low molecular weight proteins. The different segments of the proximal tubule exhibit marked biochemical and physiologic heterogeneity. Oxygen consumption, Na+, K+-ATPase activity, and gluconeogenic capacity are greater in the S1 and S2 segments than in the S3 segment. Catabolism and apical transport of glutathione (GSH) occurs to a much greater extent in the S3 segment, where the brush-border enzyme γ -glutamyl transpeptidase is present in greater amounts (Lash, 1994). Variations in toxicant induced injury to distinct proximal tubular segments can be correlated to their segmental differences in biochemical properties. Approximately 25% of the filtered Na+ and K+ and 20% of the filtered water are reabsorbed by the segments of the loop of Henle. Therefore, damage to the epithelium is associated with

differences in the absorption of the electrolytes and the water reabsorption in present studies.

The anatomic position of macula densa is suited for a feedback mechanism where in normal physiologic conditions, increased solute delivery or concentration at the macula densa results in to afferent arteriolar constriction leading to decreases in GFR and hence decreased solute delivery. The Juxta glomerular appartus is involved in the regulation of arterial flow, arterial pressure and the process of ultrafiltration. In present studies, the area of mesenchymal cells and macula densa showed clear signs of loss of structural integrity suggestive of possible functional impairment leading to alterations in glomerular filtration rate.

Conclusion

HCM intoxication induces alterations in the structure and functions of kidney impairing the excretion of the toxicants and thus permitting bioaccumulation in target/non target organs. HCM administration causes renal tubular damage, chiefly the proximal tubular region, and ultrafiltration impairment, thus indicating that the alterations in reabsorption processes due to damaged integrity of brush border membrane may contribute to the alterations in normal renal functions.

Experimental Groups

Groups	Treatment	Autopsy day
I	Zero (initial) day control	01
II	Control (No treatment)	61
III	Control (Vehicle treatment)	61
IV	Heterogeneous chemical mixture treated group (1% of LD_{50} dose/ animal/ day - NOAEL dose level)	61
V	Heterogeneous chemical mixture treated group (0.1% of LD_{50} dose/ animal/ day)	61
VI	Control (No treatment)	121
VII	Control (Vehicle treatment)	121
VIII	Heterogeneous chemical mixture treated group (1% of LD_{50} dose/ animal/ day) for 60 days followed by withdrawal phase of 60 days - NOAEL dose level.	121
IX	Heterogeneous chemical mixture treated group (0.1% of LD_{50} dose/ animal/ day) for 60 days followed by withdrawal phase of 60 days.	121

Values in all the following Tables are Mean± SE and statistical significance is considered and presented for (*) $P<0.05$, (+) $P<0.01$ and (#) $P<0.001$ compared withrespective vehicle control.

Table 1: Gravimetric analysis of kidney

Groups	Kidney (both) weight (g)	Relative Kidney weight (g/ 100 g animal)
I	2.57 ±0.069	0.79 ±0.020
II	2.47 ±0.076	0.74 ±0.022
III	2.66 ±0.082	0.76 ±0.020
IV	2.43 ±0.089	0.85 ±0.030
V	2.44 ±0.098	0.83 ±0.032
VI	2.78 ±0.064	0.70 ±0.015
VII	2.85 ±0.070	0.70 ±0.021
VIII	2.50 ±0.067	0.73 ±0.019
IX	2.57 ±0.059	0.69 ±0.014

Fig. 1: Gravimetric analysis of kidney

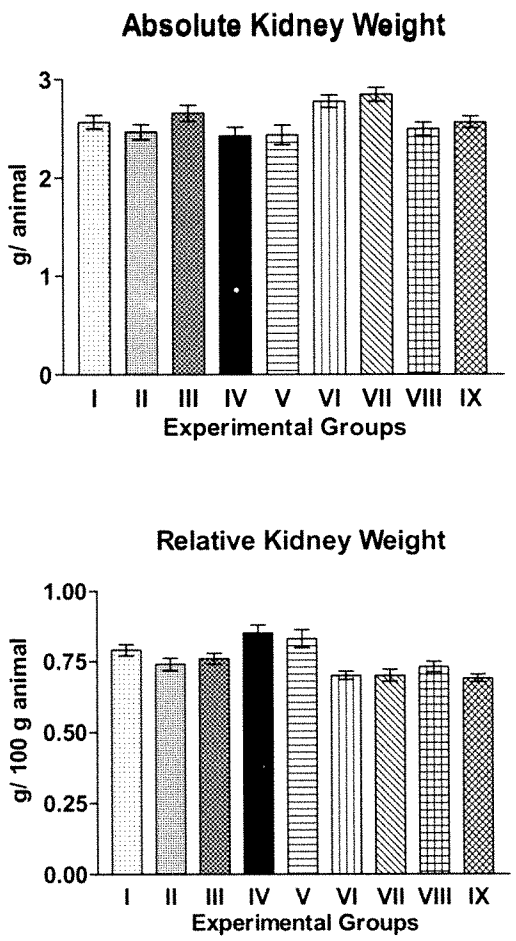

Table 2: Analysis for kidney function indicators

Groups	Serum Urea (mg/dL)	Serum Creatinine (mg/dL)	Urine Creatinine	Urine Volume (ml)	Glomerular filtration rate
I	20.82 ±0.45	0.40 ±0.021	11.23 ±0.22	10.93 ±0.12	0.64 ±0.07
II	20.61 ±0.96	0.53 ±0.057	11.01 ±0.58	12.01 ±0.71	0.57 ±0.09
III	21.52 ±0.80	0.49 ±0.038	12.58 ±0.81	11.40 ±0.29	0.61 ±0.05
IV	23.97 ±0.93	0.88 ±0.044$^{\#}$	20.67 ±0.81$^{\#}$	8.03 ±0.17^{+}	0.49 ±0.03
V	24.82 ±1.74	0.69 ±0.025*	17.35 ±1.03^{+}	9.60 ±0.53	0.56 ±0.04
VI	21.04 ±0.84	0.49 ±0.021	12.6 ±0.82	13.62 ±0.21	0.58 ±0.03
VII	21.48 ±0.59	0.51 ±0.021	12.9 ±1.03	14.00 ±0.71	0.57 ±0.07
VIII	24.80 ±1.01	0.58 ±0.051	12.28 ±0.63	12.80 ±0.54	0.68 ±0.08
IX	25.00 ±0.58	0.49 ±0.041	11.57 ±0.39	13.00 ±0.68	0.59 ±0.03

Fig.2: Analysis for kidney function indicators

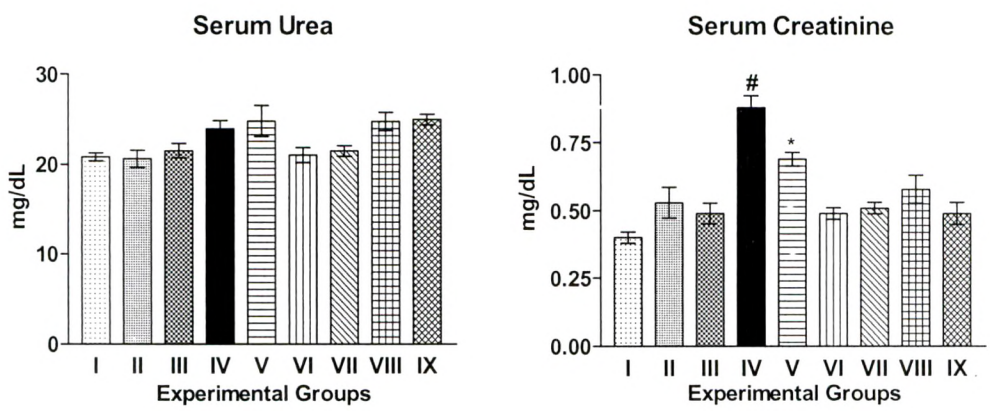

Fig.2 (Contd): Analysis for kidney function indicators

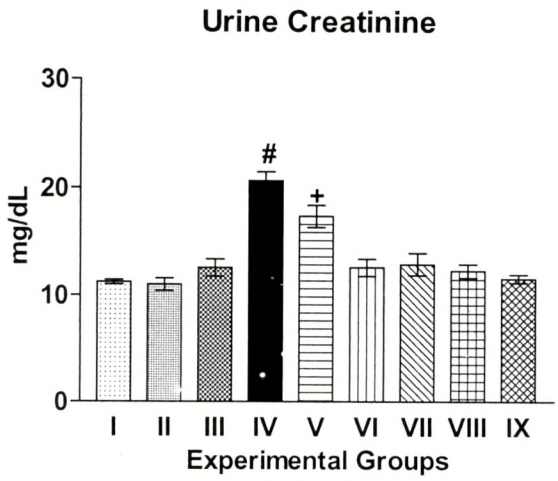

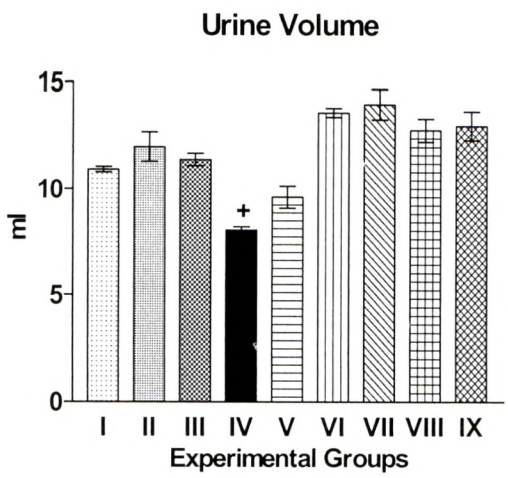

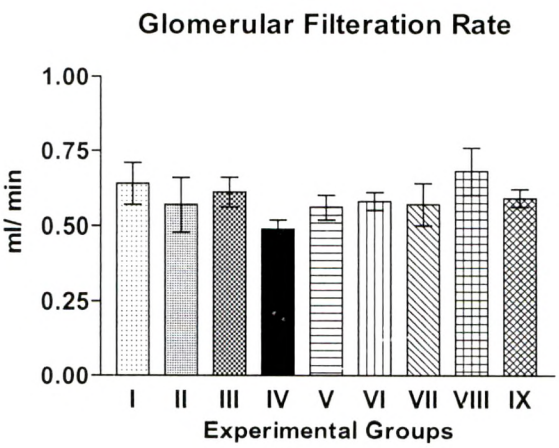

Table 3: Serum analysis for electrolyte concentrations

Groups	Serum Sodium (mmol/L)	Serum Potassium (mmol/L)	Sodium/ potassium ratio
I	142.90 ±1.30	4.57 ±0.11	31.45 ±0.93
II	141.90 ±0.84	4.29 ±0.26	35.04 ±2.26
III	140.80 ±0.81	4.55 ±0.14	30.96 ±1.18
IV	152.00 ±1.01#	5.03 ±0.19	30.59 ±1.46
V	154.20 ±1.35#	5.69 ±0.29+	27.91 ±1.48
VI	141.80 ±1.79	5.27 ±0.11	26.94 ±0.48
VII	144.30 ±1.99	5.33 ±0.15	27.26 ±1.40
VIII	145.00 ±1.36	5.12 ±0.27	28.83 ±1.91
IX	145.10 ±2.03	5.43 ±0.27	26.16 ±1.37

Fig. 3: Serum analysis for electrolyte concentrations

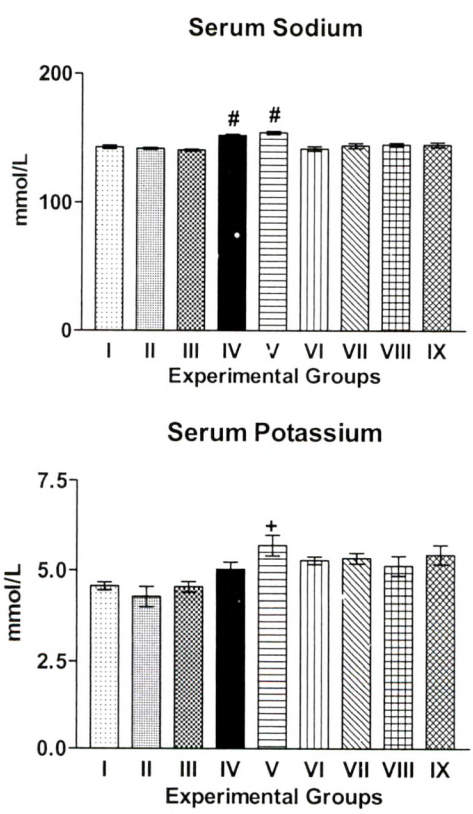

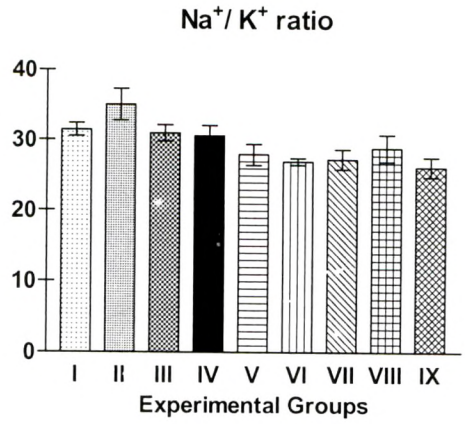

Table 4: Serum analysis for electrolyte concentrations

Groups	Serum Calcium (mg/dl)	Serum Chloride (mmol/L)
I	10.06 ±0.14	104.90 ±4.47
II	9.45 ±0.15	100.30 ±2.88
III	9.74 ±0.07	102.90 ±4.39
IV	9.63 ±0.24	124.00 ±3.72*
V	10.02 ±0.23	109.70 ±5.05
VI	9.62 ±0.17	108.00 ±2.45
VII	9.45 ±0.25	99.83 ±5.39
VIII	9.32 ±0.20	120.60 ±4.35*
IX	9.77 ±0.10	111.00 ±2.66

Fig. 4: Serum analysis for electrolyte concentrations

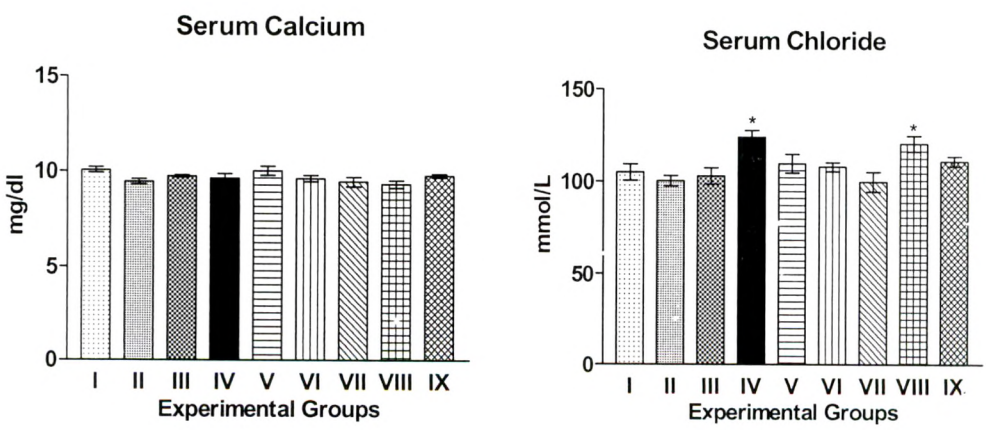

Table 5: Enzymatic and metabolites of general kidney functions

Groups	SDH (µg formazan formed/ mg protein)	ACP (µ moles of p-nitrophenol released/ mg protein/ min)	ALP (µ moles of p-nitrophenol released/ mg protein/ min)	Cholesterol (mg/ 100 mg tissue)
I	13.47 ±1.12	0.16 ±0.021	0.11 ±0.012	0.24 ±0.024
II	14.71 ±2.05	0.13 ±0.011	0.10 ±0.007	0.27 ±0.015
III	14.10 ±1.10	0.12 ±0.013	0.10 ±0.004	0.24 ±0.039
IV	9.72 ±2.11	0.13 ±0.015	0.05 ±0.004^{+}	0.22 ±0.019
V	12.68 ±1.57	0.13 ±0.013	0.07 ±0.010	0.31 ±0.044
VI	12.55 ±1.58	0.14 ±0.006	0.10 ±0.006	0.30 ±0.039
VII	13.33 ±1.67	0.13 ±0.016	0.12 ±0.006	0.31 ±0.034
VIII	11.41 ±1.57	0.10 ±0.007	0.08 ±0.005*	0.26 ±0.033
IX	13.44 ±1.55	0.11 ±0.006	0.11 ±0.006	0.29 ±0.039

Fig. 5: Enzymatic and metabolites of general kidney functions

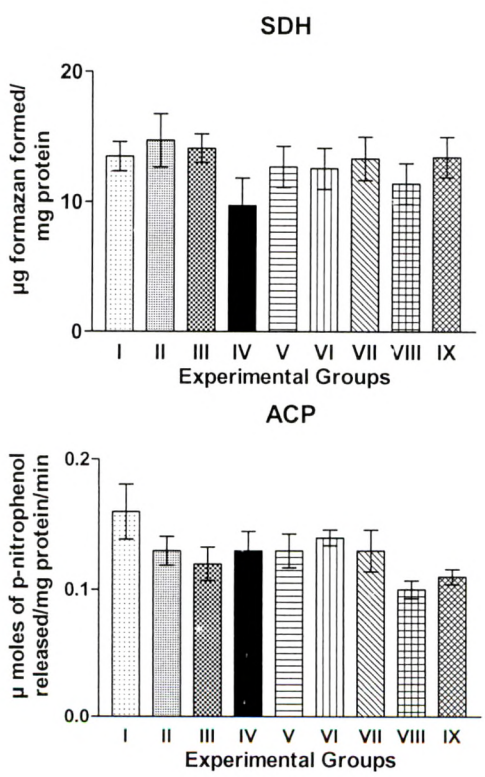

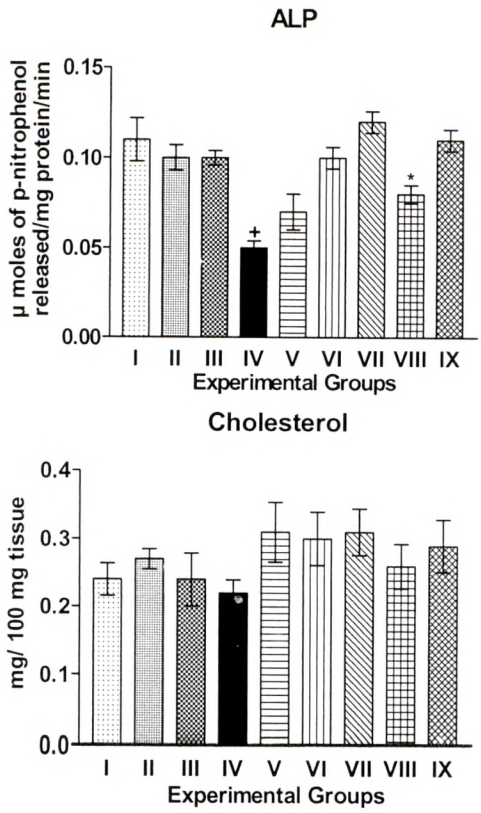

Table 6: Oxidative stress indicators of kidney function

Groups	LPO (n mole MDA/ 100 mg tissue)	GSH (μg of GSH/ mg protein)	Ascorbic acid (μg/ mg tissue)	Protein (mg/ 100mg tissue)
I	92.25 ±8.44	5.27 ±0.73	0.37 ±0.033	16.49 ±1.04
II	100.90 ±4.60	4.86 ±0.45	0.39 ±0.039	17.18 ±0.45
III	98.94 ±8.38	5.42 ±0.46	0.35 ±0.017	16.95 ±1.02
IV	148.60 ±5.86#	4.59 ±0.67	0.31 ±0.034	16.01 ±0.85
V	122.70 ±4.03	4.61 ±0.93	0.31 ±0.047	15.82 ±1.04
VI	106.70 ±9.94	4.77 ±0.73	0.41 ±0.036	17.16 ±0.42
VII	114.40 ±6.34	4.92 ±0.31	0.38 ±0.048	17.17 ±0.84
VIII	131.20 ±4.83	4.13 ±0.33	0.20 ±0.023*	17.78 ±0.63
IX	122.10 ±9.71	4.63 ±0.61	0.37 ±0.018	16.87 ±0.56

Fig. 6: Oxidative stress indicators of kidney function

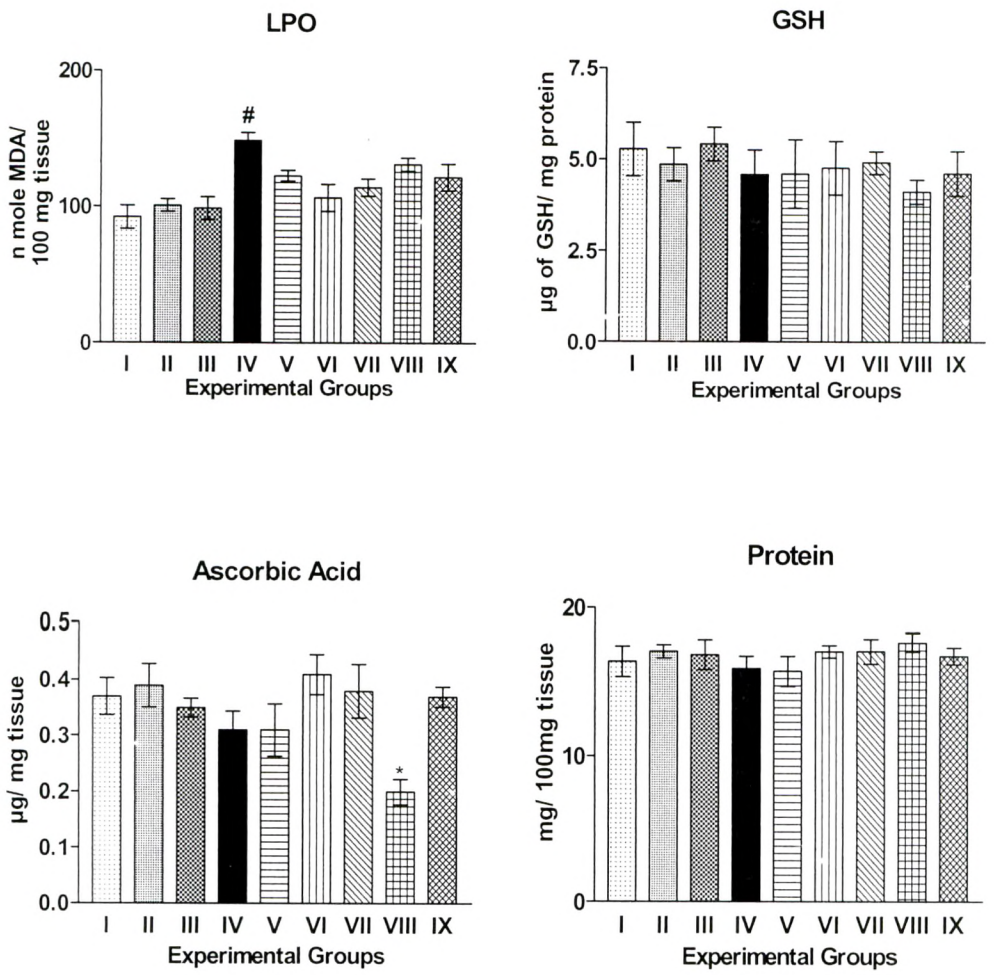

Table 7: Oxidative stress marker enzymes as indicators of kidney function

Groups	SOD (Unit/ mg protein)	GPx (µg of GSH utilize/ min/ mg protein)	CAT (µ mole of H_2O_2 consumed/ min/ mg protein)	GST (µ mole CDNB-GSH conjugate formed /min/ mg protein)
I	8.03 ±0.85	7.77 ±0.92	37.65 ±2.07	4.45 ±0.70
II	7.12 ±0.74	7.98 ±0.51	44.71 ±3.72	3.49 ±0.45
III	8.09 ±0.72	6.72 ±0.30	41.56 ±4.77	3.61 ±0.32
IV	3.97 ±0.34*	2.39 ±0.45#	19.98 ±2.47#	1.39 ±0.09*
V	6.15 ±0.68	2.64 ±0.30#	24.84 ±3.35+	3.14 ±0.52
VI	8.51 ±1.00	6.14 ±0.38	42.51 ±2.91	3.33 ±0.55
VII	7.84 ±0.71	6.48 ±0.56	40.49 ±2.58	3.24 ±0.21
VIII	5.81 ±0.46	4.96 ±0.68	25.70 ±1.56*	3.01 ±0.33
IX	7.50 ±1.04	4.57 ±0.65	34.40 ±2.69	3.07 ±0.47

Fig. 7: Oxidative stress marker enzymes as indicators of kidney function

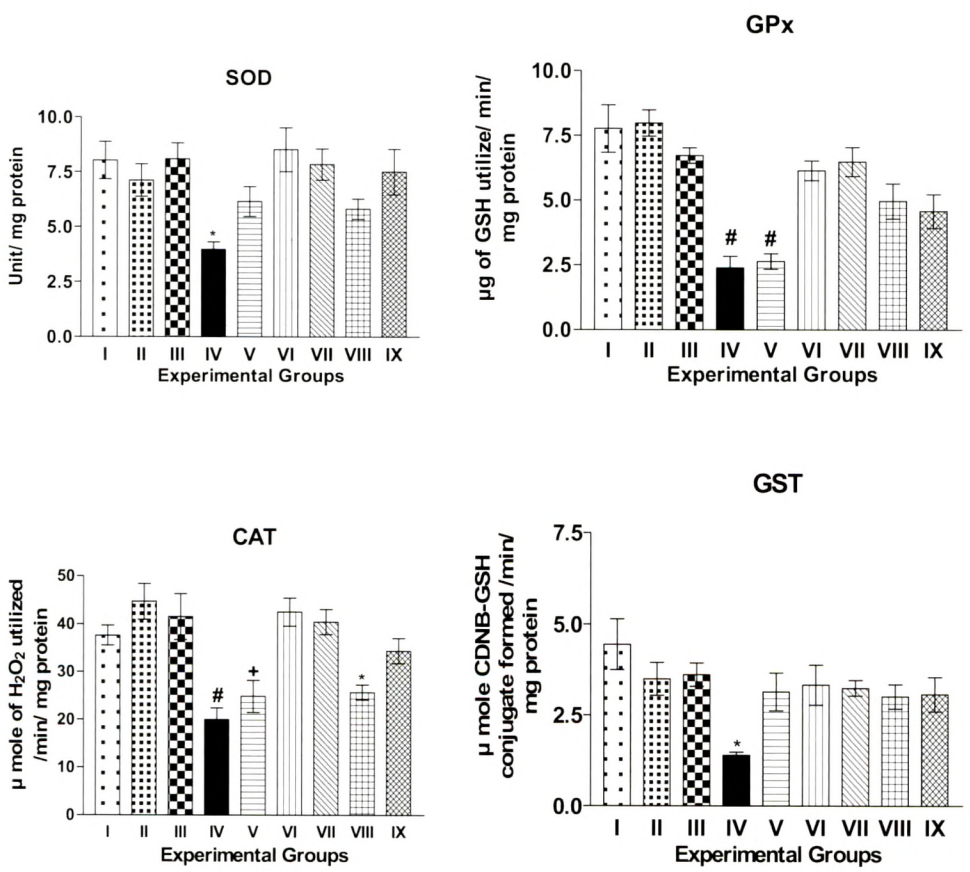

PLATE 1

The tranasections of kidney of control rat.

a A low power photomicroGraph depicting the distribution of glomeruli (G) in the cortical (Cort G) and juxtamedullary (Jx Med G)

b and c Showing the cortex and medullary regions of kidney. 100X

PLATE 1

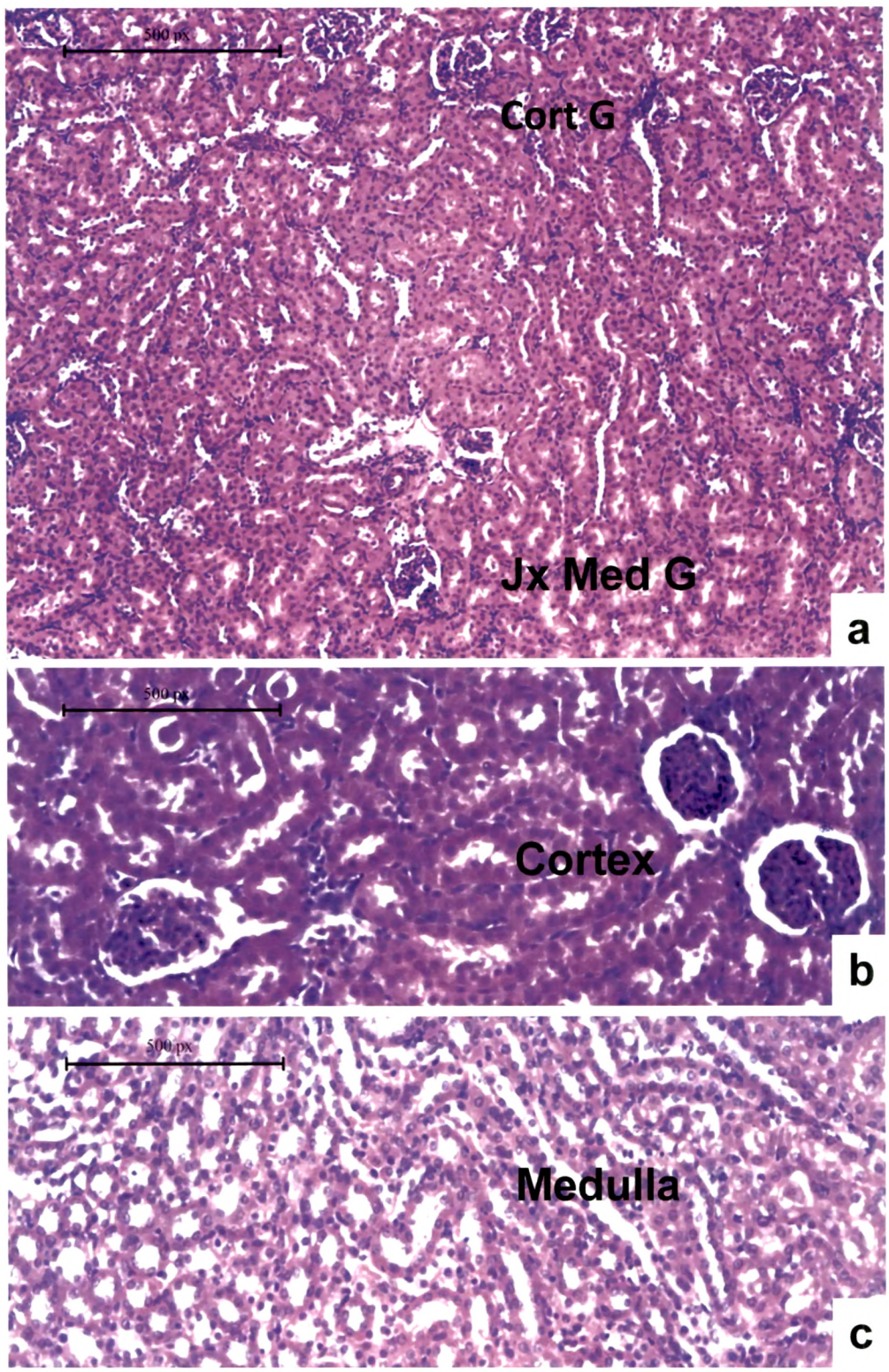

PLATE 2

a Showing the details of histoarchitecture of the renal glomeruli. The glomeruli are lined by parietal epithelilum (PE) while the tuft of blood capillaries (Cap) is lined by visceral epithelium (VE). The glomerular capillary tuft distinctly shows the lobule formation; atleast 4 lobes are clearly seen(L1-L4).the darkly stained nuclei of podocytes (POD) in the capillary lobes are seen.400X

b and c Showing the transverse section of proximal convoluted tubule(PCT). In c, the brush border lining of the cuboidal epithelium is prominently seen.400X

d and e Showing the distal convoluted tubule(DCT). The lumen is comparatively wider, nuclei prominent and the microvilli are absent. 400X

f, g and h Showing the collecting duct (CT) and the loop of henle (LH).the cuboidal epithelium are comparatively smaller than PCT and DCT regions and hence the lumen of collecting duct is wider. 400X

g and h Showing the thick and thin limbs of loop of henle. In the thick limb the epithelium is small cuboidal while in the thin limb it is almost squamosal. 400X

PLATE 2

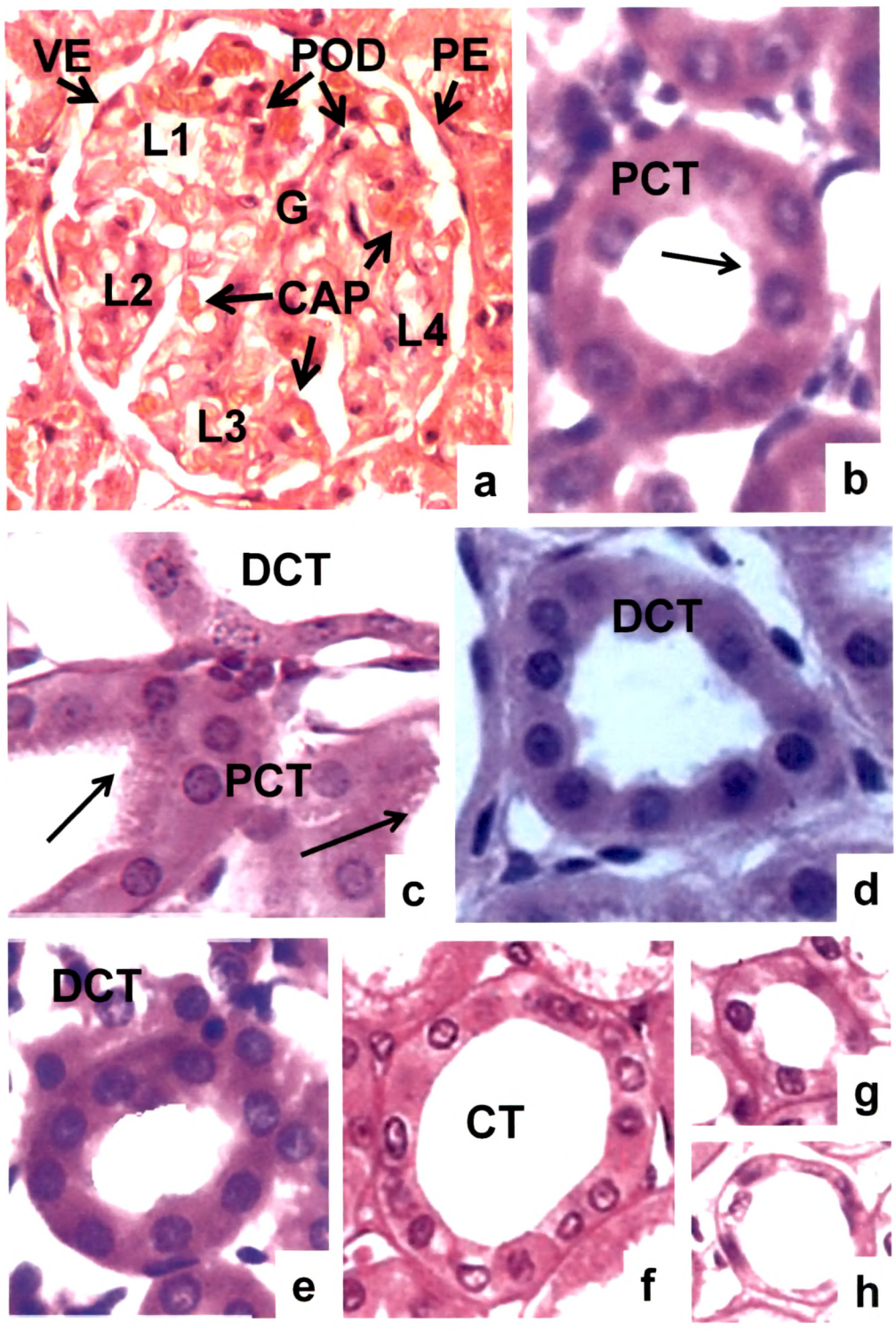

PLATE 3

Transection of kidney from rats exposed to high doses of heterogenous chemical mixture for 60 days.

a Showing the external cortical region (cortical glomaruli). The glomaruli are shrunken therefore exhibiting a wider gap in the bowmen's capsule. The stromal connective tissue exhibited loosening and some extent of degenerative changes. Some of the tubules are severely damaged. 200X.

b and c the glomeruli exhibit moderate damage where the perital epithelium of the bowmen's capsule exhibits disintegration. In photoGraph b, the distal convoluted tubule adjacent to glomaruli shows extensive degeneration. 200X

d The degenerative changes in the glomaruli and the tubules in its periphery are seen where proximal convoluted tubule shows epithial damage while the uiriniferous space of the bowmen's capsule is filled with cytoplasmic exudates and cell debris. 200X (Further enlarged).

PLATE 3

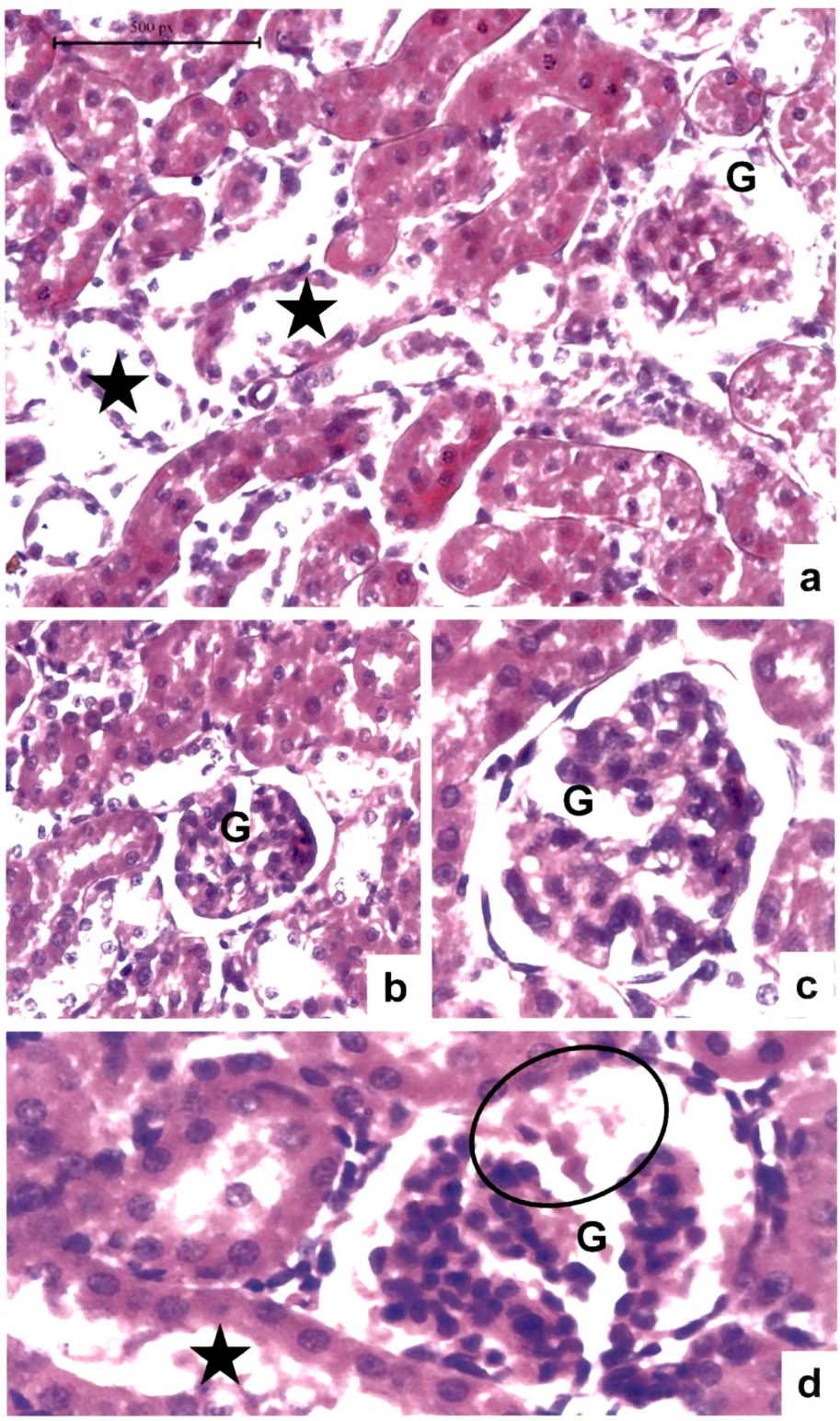

PLATE 4

a Showing the prominent changes in the glomeruli and in the tubules. The structure of integrity of the glomerular tuft is disorganized and therefore, the tufts are disproportionately distributed in the Bowman's capsule. The darkly stained nuclei are planty which indicate mesengial cell (MC) hyperplasia. The macula densa and te adjacent extra glomerular mesengial cells (EGMC) are also seen. Thus, this photoGraph shows hyperplasia of intra and etra glomerular mesengial cells. 200X

b, c and d. The damage to proximal convoluted tubule was conspicuous. Cytoplasmic blebbing and cell sloughing were prominent features of damage. Such degenerated cytoplasmic masses and the nuclei accumulated in the tubular lumen (star). The microvilli were extensively damaged and in most of the cells the luminal epithelial lining were simple and devoid of prominent brush border.400X

PLATE 4

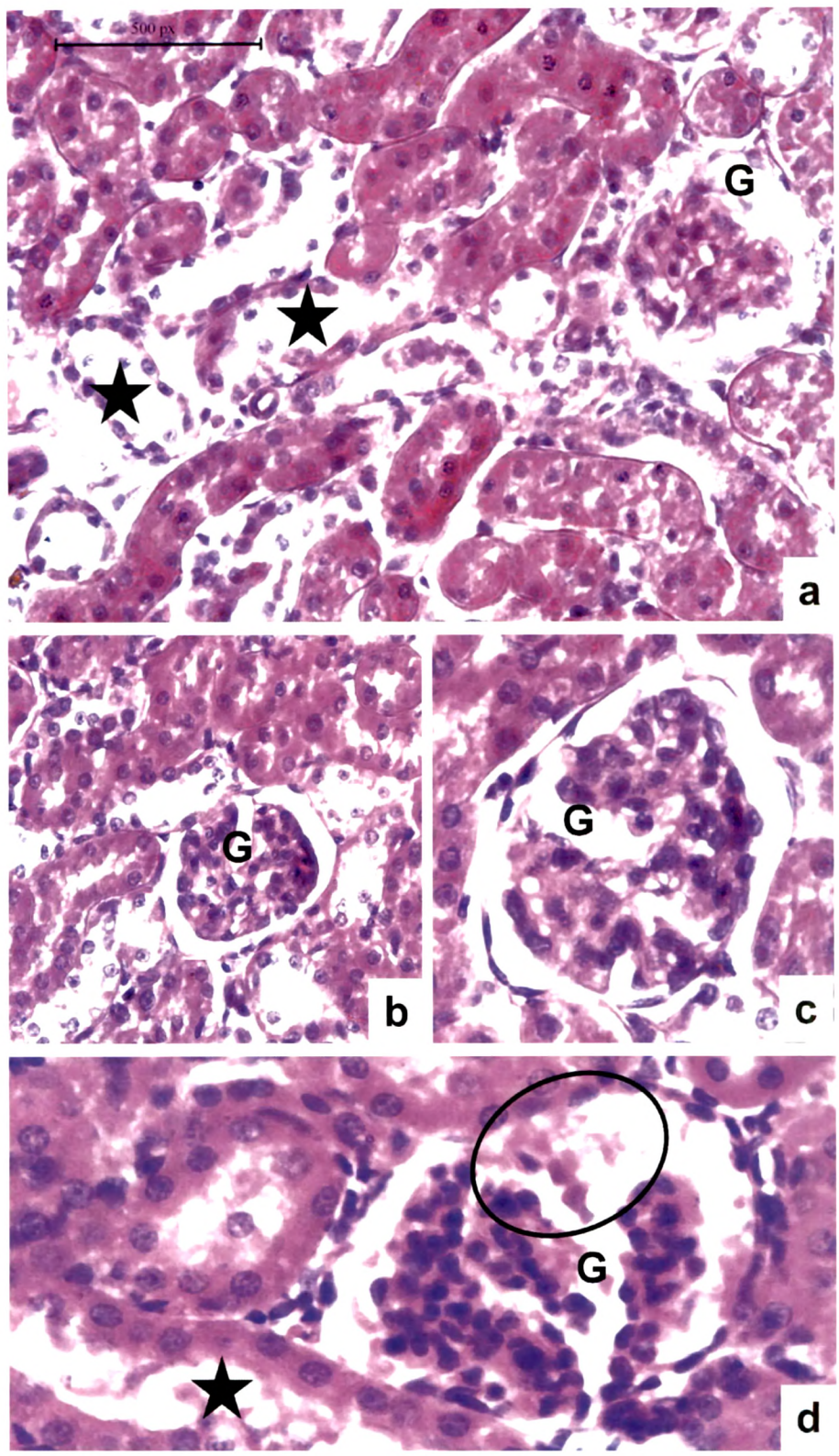

PLATE 5

Transections of kidney from rat exposed to low dose of heterogenous toxicant mixture for 60 days.

a Showing the response of renal cortical region to the toxicant exposure where cortical glomeruli exhibit mesengial cell hypertrophy and damage to the tubular epithelium. 200X

b and c. Showing the glomerulus specific changes where the integrity of the mesengial stroma and therefore that of capillary tuft is adversely affected leading to capillary lobular disintegration integration. In FigureC, the parietal epithelium of Bowman's capsule exhibit epithelial hypertrophy. It is a probable that the accumulation of cell debris on the parietal epithelium might induce further responses by parietal epithelial cell (arrow). A proximal convoluted tubule is shown accumulating cellular debris in the lumen. In Figureb, the visceral epithelium is also prominently damaged. The podocytes structural integrity with that of the capillaries seems to be disintegrated. 400X

PLATE 5

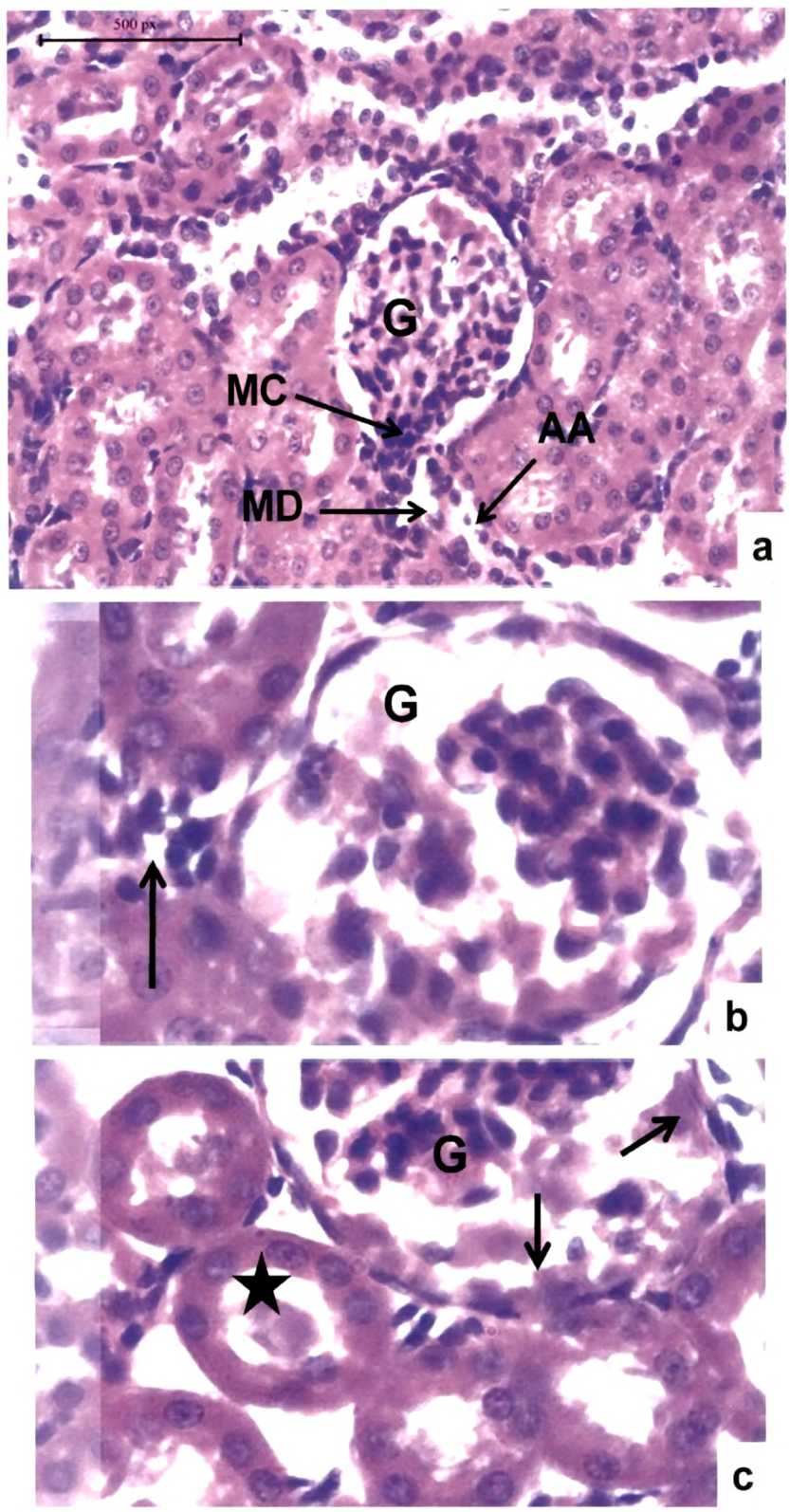

PLATE 6

Transection of kidney from rats exposed to high dose of heterogeneous chemical mixture for 60 days followed by withdrawal for further 60 days.

a Glomarular capillary tuft is conspicuously constricted in the external cortical region. The mesangial cells are atrophic and hence a central region amid the lobes of capillary tuft shows wide gaps. This is indicative of the visceral epithelial demage. Thickning of perital epithelium is also seen. Although, the cell exudates and debris are present in the tubular lumen, these have been largely cleared off from the lumen compared to that observed in day 60. 400X

b Showing the glomaruli and the tubules in the juxtamedullary region. The glomaruli appear comparatively normal and several lobules of the capillary tufts are seen. The intense staining of the podocyte/mesengeal cell nuclei, however, indicate persistent damage. The convoluted tubular epithelium exhibited cytoplasmic blebbing and cell sloughing. The nuclei of collecting duct were prominently stained and hight of epithelium was reduced. 200X

PLATE 6

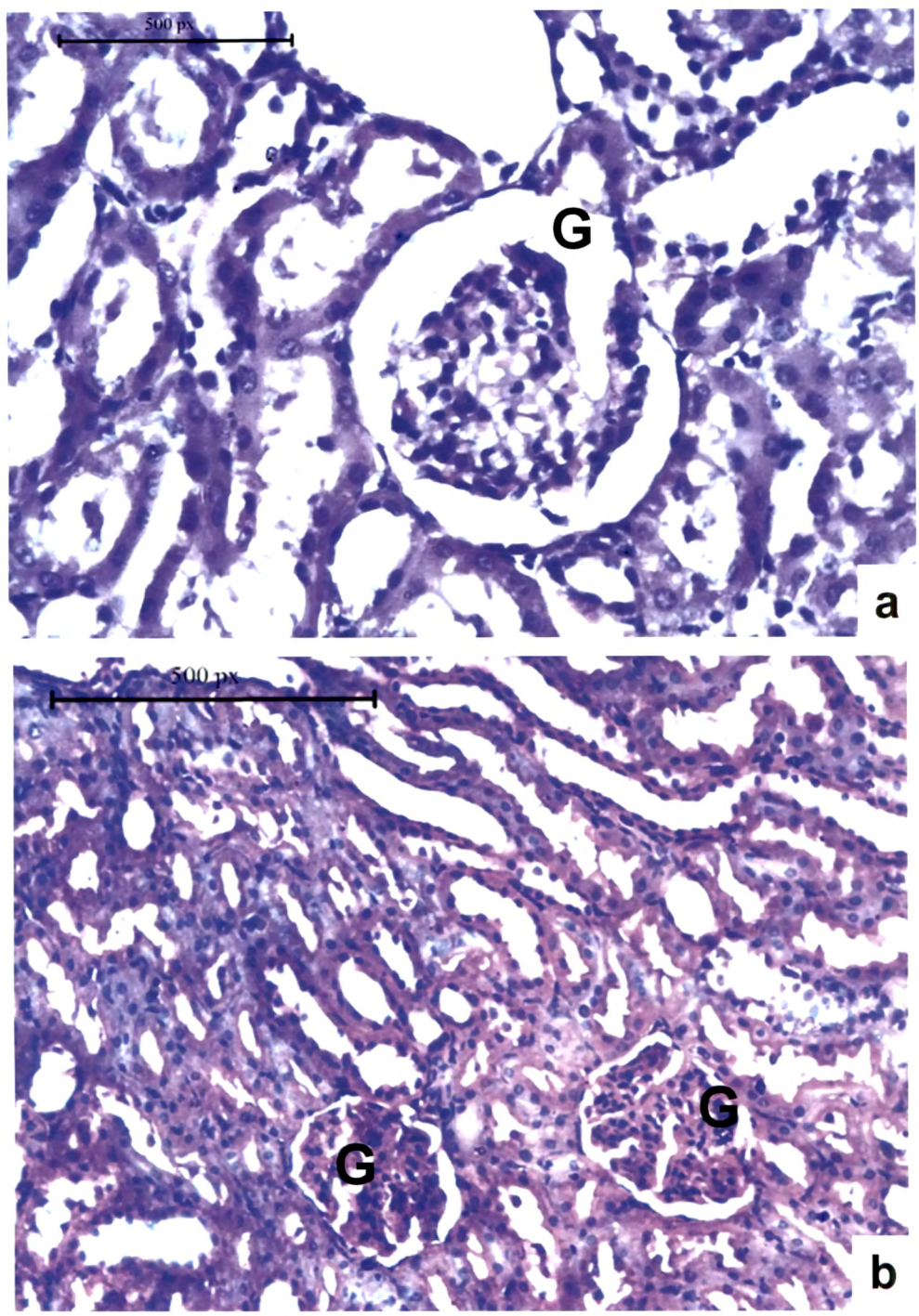

PLATE 7

Transection of kidney from the rat exposed to high dose of heterogenous chemical mixture for 60 days followed by recovery phase for further 60 days.

a Showing the medullary region where the epithelia of collecting duct and loop of henle appear comparatively normal. However, in several tubules the cytoplasm was much intensely stained suggestive of degenerative changes. 200X

b The glomeruli of the juxtamedullary region shows several capillary tuft globules. However, mesangial hyperplasia is also seen. 200X

c and d. In several proximal convoluted tubules, cytoplasmic blebbing and cell sloughing is still seen (arrow). 400X

e In cortical glomeruli the cytological damage was still seen where the disorganized cellularity and disintegrated epithelium resulted into loss of structural features. The dissolution of both the visceral and parietal membranes leads to diffusion of cell exudate from the glomeruli to the stromal connective tissue region. 400X

PLATE 7

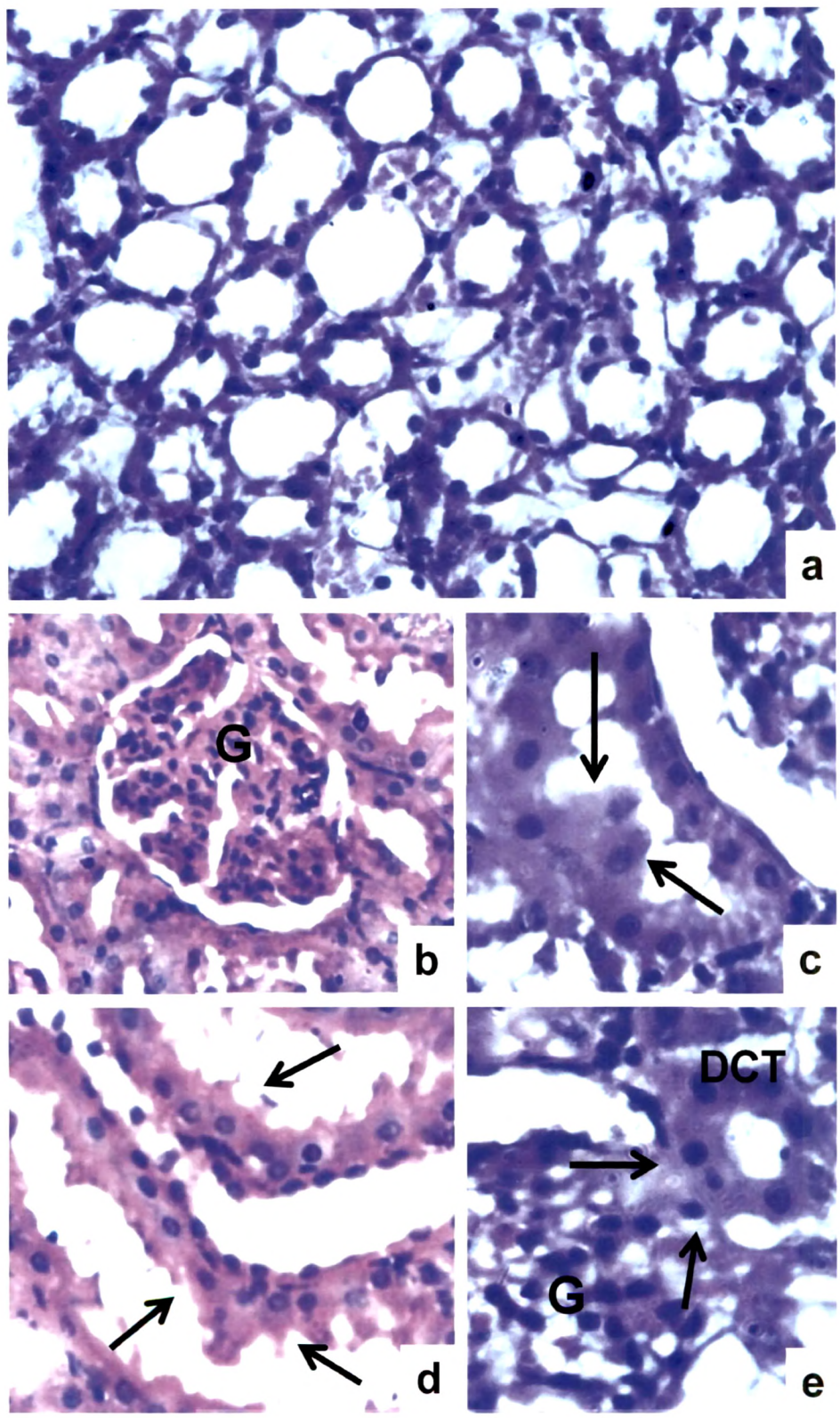

PLATE 8

Transactions of kidney from rats exposed to low dose of heterogenous chemical mixture for 60 days followed by recovery phase for 60 days.

a and b Although the glomeruli appeared quite normal without any significant feature if shrinkage or swelling or prominent hyperplasia of any cell type, they were not absolutely normal. a: 200X , b: 400X

c and d showing the improvement in the histoarchitecture features of the tubules in the cortical region (C) and the medullary region (D). 400X

PLATE 8

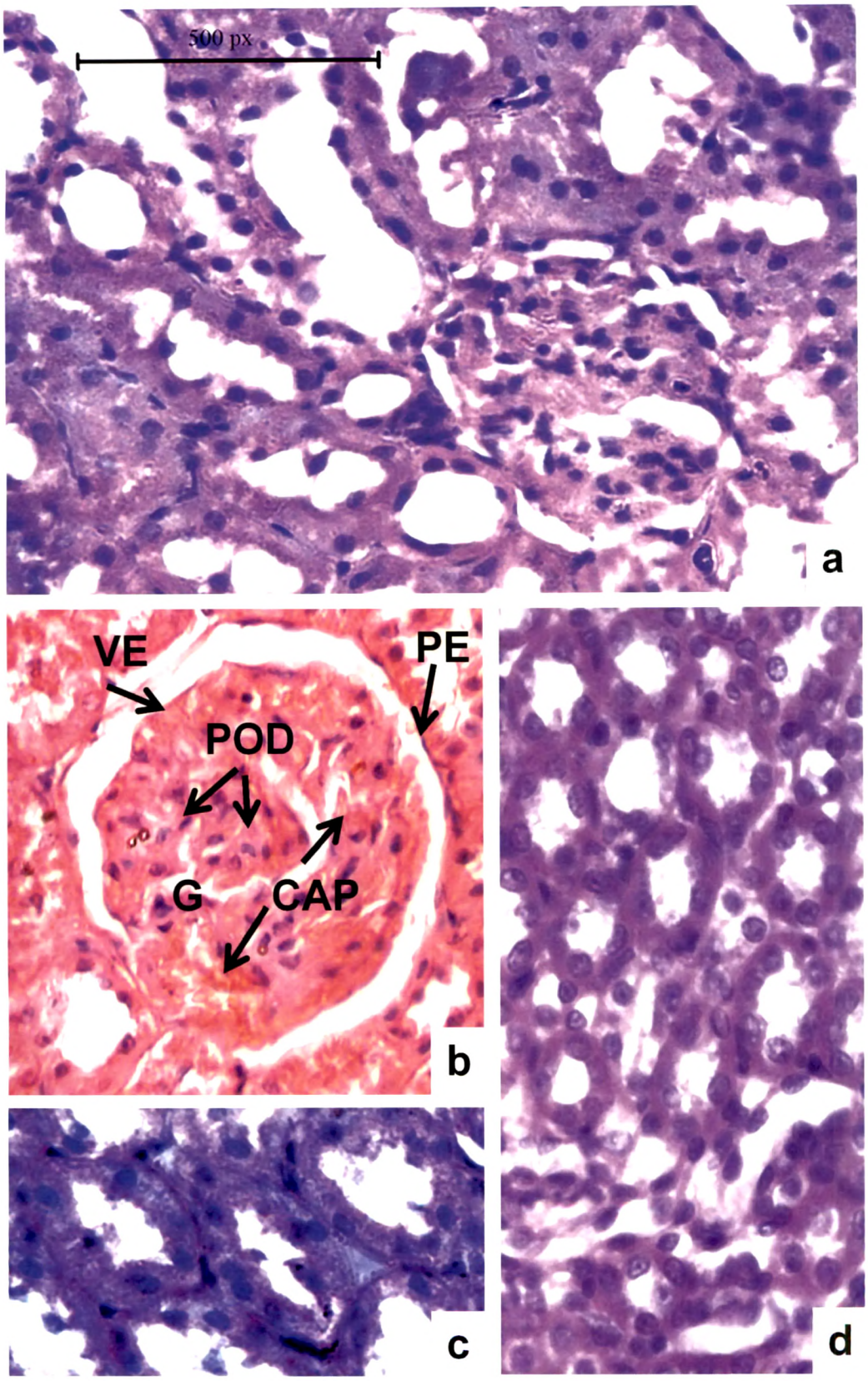

PLATE 9

Transection of kidney from rat exposed to low dose of heterogenous chemical mixture for 60 days followed by withdrawal for further 6o days.

a and b Most of the renal tubular length appear normal. However, in some region, chiefly the proximal convoluted tubule cytoplasmic degeneration and cell sloughing were seen. The microvilli brush border was also clearly seen lining several cells. 400x

c and d demonstrate the normal epithilial lining of distal convoluted tubule and collecting duct. The lumen is completely devoid of cytoplasmic debris or exudates. 400X

e showing the tubules in the medullary region where the collecting duct and loop of Henle were histologically comparable to normal. 400x

PLATE 9

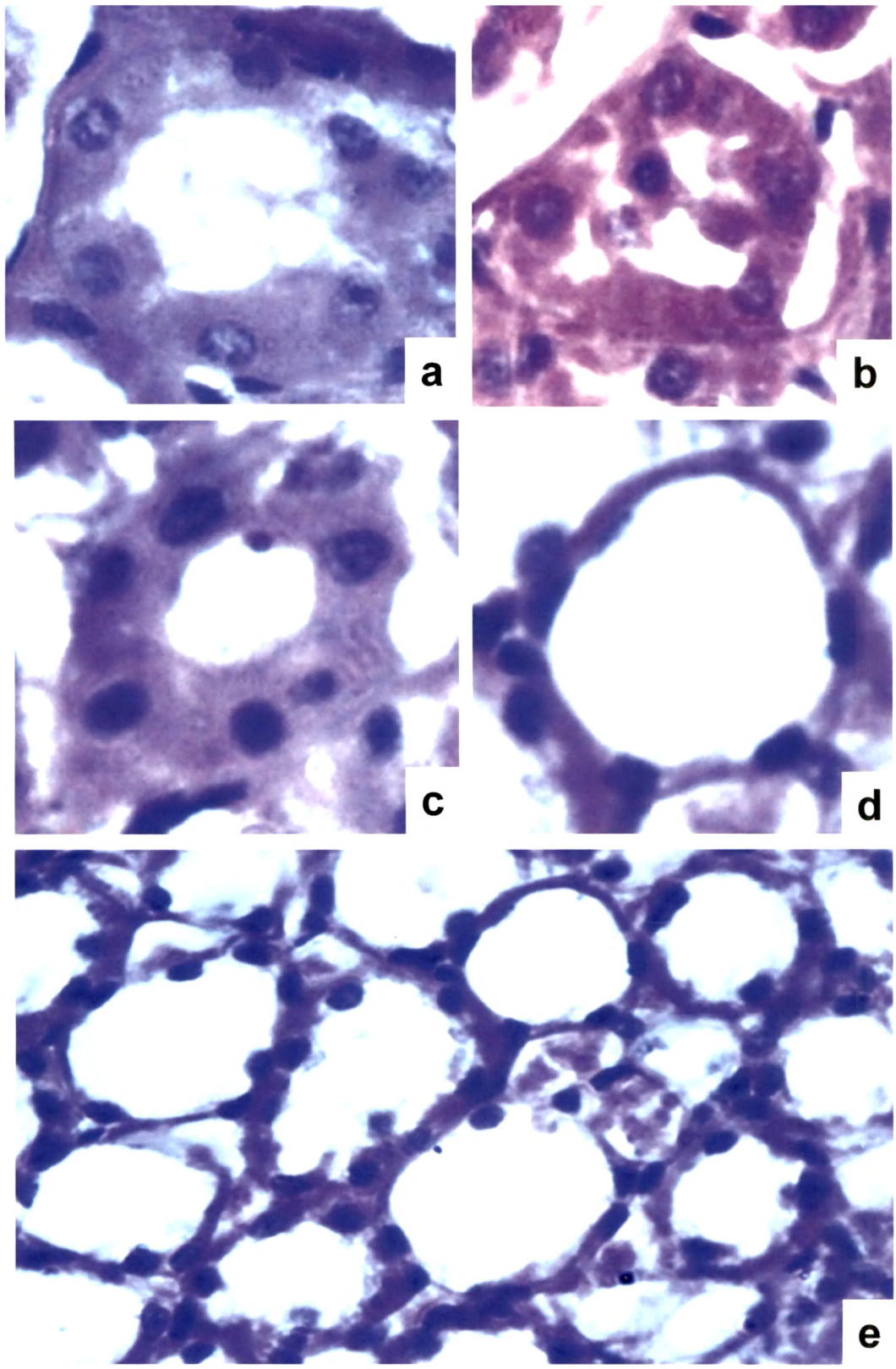

Fig. 8: An outline of the mechanisms of toxicant action leading to decrease in Glomerular Filtration Rate

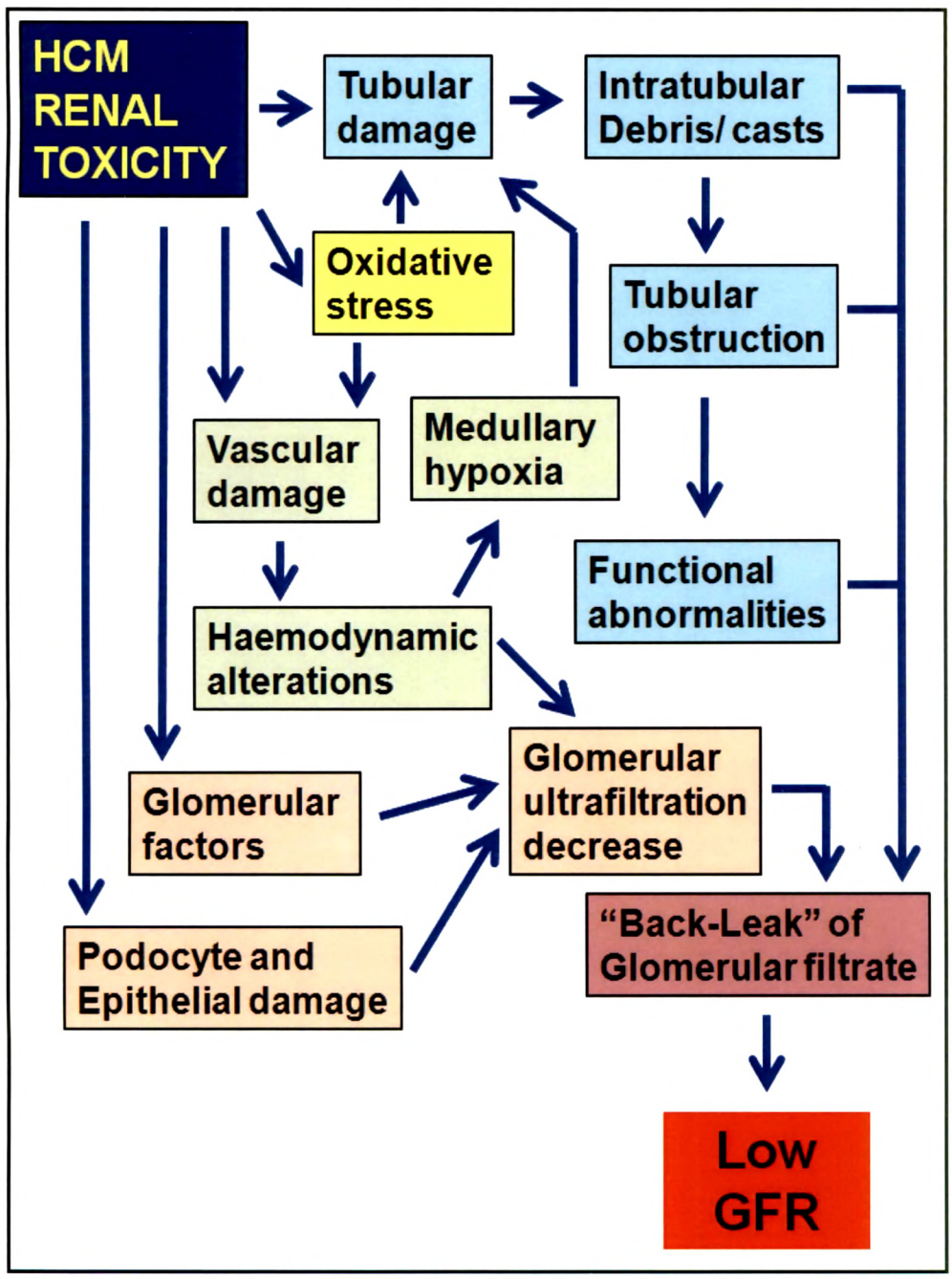

Fig. 9: Diagrammatic representation of the toxic effects on the renal tubular structure and function

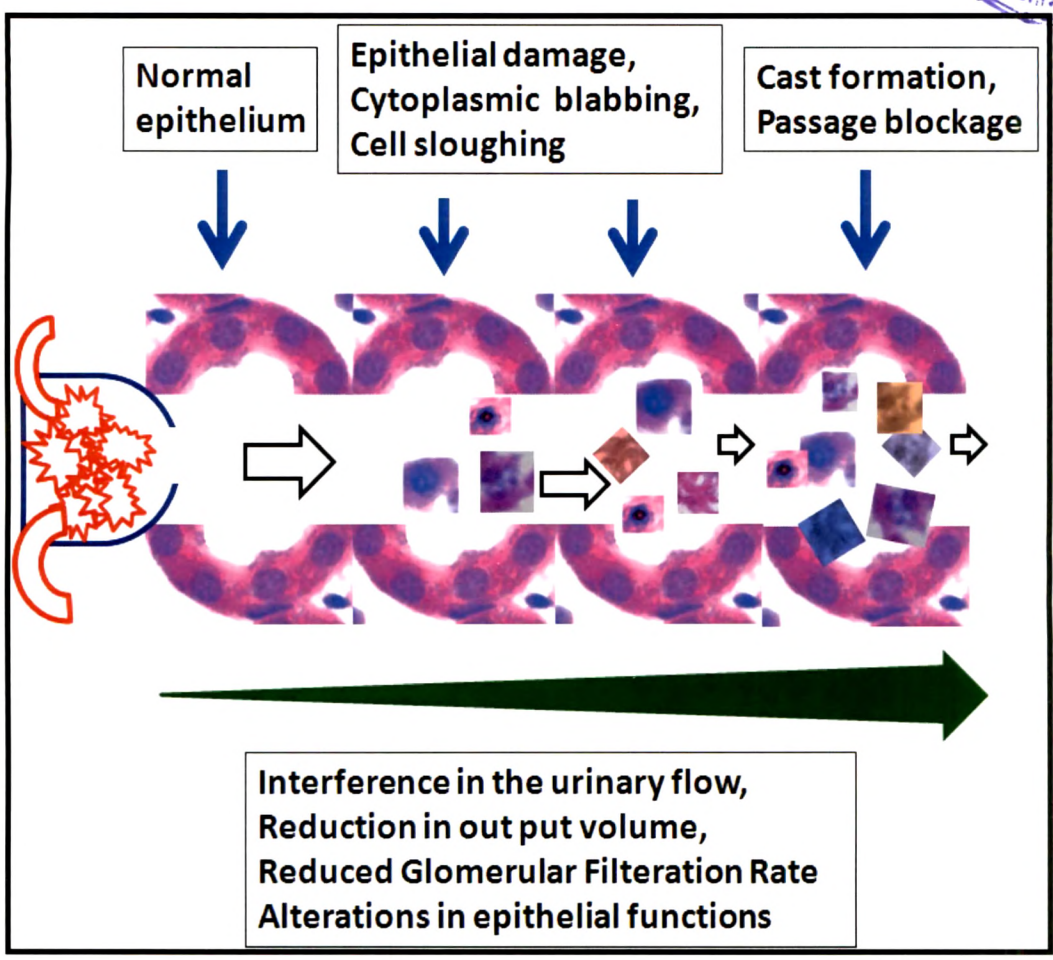

CHAPTER 4

TOXIC POTENTIALS OF HETEROGENEOUS CHEMICAL MIXTURE EXPOSURE ON THE TESTIS

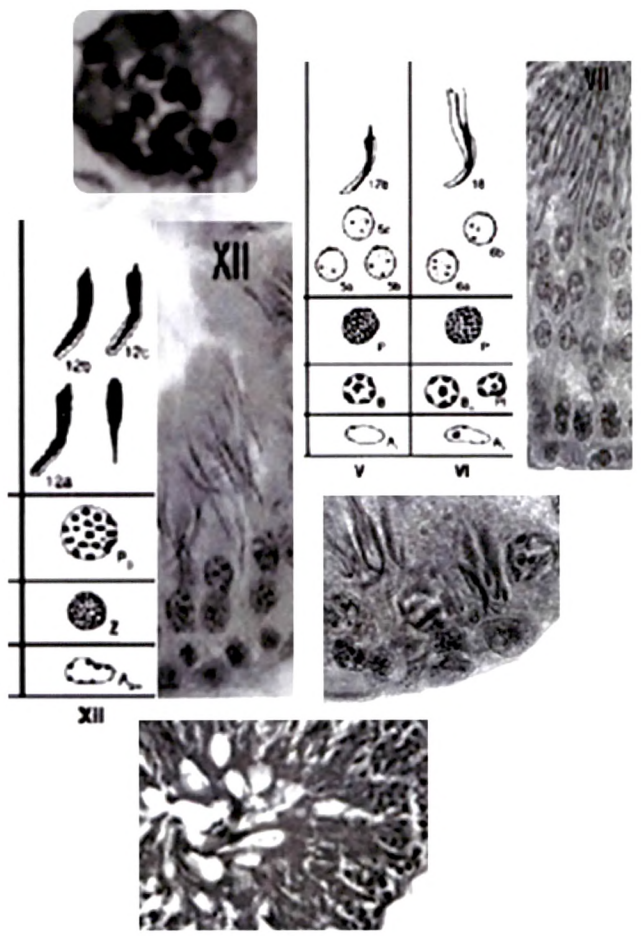

The potential of chemicals to influence the male fertility or reproduction have recently turned into a major concern of scientific issue. The evidence for adverse reproductive outcomes from exposure to chemicals is very strong and there is growing evidence for effect on male reproductive system via damaging functional and structural aspects or via disturbing the homeostasis of endocrine system (Asklund*et al.,* 2004; Bustos-Obregon and Hartley, 2008; Sikka and Wang 2008; Egbowona and Mustapha, 2011). There are thousands of structurally diverse chemical compounds present in our environment that are known to cause testicular toxicity. These chemicals include various classes of drugs, food preservatives, dyes, cosmetics, fuels, organic solvents, inorganic compounds, fertilizers and other industrial by-products. The increase of environmental chemical pollution becomes much clearer from the fact that globally there are approximately one lakh products manufactured annually and currently there are around 4 million organic compounds present for human use which has contaminated 30% of water (Bustos-Obregon and Hartley, 2008).

Our curiosity is towards the male reproductive aspects since an immense amount of work has been done under the effect of drug and chemicals on the subject of female reproductive system and that numbers of observations have reported a wide diversity of threats to woman's sexual and reproductive health. This is because after 1940, several drugs were developed as fertility potentiating agents, contraceptive pill, sleeping pills *etc.* Furthermore, a few calamities due to chemical pollution and side effects of drug resulted in early pregnancy loss, neonatal deformities, breast cancer and death. For example, thousands of mothers who had ingested thalidomide prescribed as antiemetic gave birth to children with profound disabilities, ranging from loss of hearing to cardiac defects along with malformed limbs (Miller and Stromland and; 1999) and pregnant woman who had ingested diethylstilboestrol in the mistaken belief that it would reduce the risk of miscarriage found themselves at increase risk of vaginal cancer and other diseases (Giusti *et al.,* 1995). Therefore, more attention was paid on female reproductive system to assess the effect of drugs or xenobiotics. In addition to

these varying degrees of complications caused by medical intervention, a mass of illnesses have spread as a result of increased level of environmental contaminants. As compared to this, the epidemiological records of male reproductive toxicity are much less. Moreover, the toxicity studies conducted on male reproductive system did not include adequate histological evaluation of the testis.

Some of the available reports of epidemiological and experimental studies on male reproduction were collected and analyzed. Sperm count of general male population has been deteriorating over the past few decades (Toppari *et al.,* 1996; Skakkebaek *et al.,* 2001; Saradha and Mathur, 2006). The data suggested that the semen sperm concentration of normal adult man has declined by 50 % over the 50 years of period with increase in adverse pathological conditions like, testicular cancer, hypospadia and cryptochidism (Carlsen *et al.,* 1992; Queiroz and Waissmann, 2006). It was also observed that there is a 2.1% decline in the sperm concentration per annum with 0.6% per annum decrease in sperm motility and 0.5% per annum increase in the number of morphologically abnormal sperm over the 20 year period (Creasy, 1997). Sharpe and his co-workers (1995) have tested and proposed a hypothesis for the decline in the count of sperm, based on the effect of environmental xenobiotics on developing rat testis. Despite from the fact that environmental contaminants adversely affect sexual and reproductive health, this area of investigation remains relatively underdeveloped, especially towards the mixture toxicity assessment.

Chemicals which influence the male reproductive system can act either directly or indirectly, and each class of compound may require biotransformation prior to its action (Steinberger et al, 1981; Okuno and Miyata, 2001; Scott *et al.,* 2009; Cheng *et al.,* 2011). Substances which act directly do so because of their chemical reactivity and may damage the cellular structure including damage to DNA via several different mechanisms. Those which act indirectly do so because of their similarity to some

endogenous compound i.e. hormones or because they cause modifications in physiological control mechanism important for reproduction.

The toxic effects of metals, organicals, pesticides, and other environmental contaminants are very different from each other with different mode of action. The significant toxicological effects are usually evaluated in terms of histological and biochemical lesions and the occurrence and intensity of such lesions describe the severity of toxicity. The pharmacological aspects of toxic compounds also play an important role in the generation of toxic lesions. The incidence of testicular lesions may become a direct outcome of the effect of any toxicant or it might be an indirect effect through hypothalamic-pituitary-testicular axis. The responses of various levels of spermatogenic cells are also different to different toxicants (Creasy, 1997, 2001). However, as spermatogenesis in a continuous process a minute cellular damage (histological or biochemical) in the early spermatogenic cells may be represented even as late as at the level of release of mature spermatozoa (Creasy, 2001). It has been established by several studies that the quantification of spermatogenesis is very important in evaluating toxic effects (Vachhrajani and Dutta, 1999; Hess and Nakai, 2000; Creasy, 2003; Brilhante *et al.,* 2011). Multiple histopathology markers are commonly used to describe testicular toxicity which includes germ cell sloughing, vacuolization, changes in seminiferous tubular diameter and retention of elongated spermatid in the basal compartment at stage VIII. Chemical induced sloughing of epithelium results in increased amounts of cellular debris in the lumen and may obstruct the passage of efferent ducts. The decrease in seminiferous diameter may indicate the loss of germ cell whereas increased tubular diameter may be indicative of retention of seminiferous tubular fluid (Moffit *et al.,* 2007; Vachhrajani and Pandya, 2006, 2008).

Previously, it has been shown that many chemicals have the potential to cause germ cell apoptosis, seminiferous epithelial damage and irreversible damage to Sertoli cells. Testicular damages caused by the administration of individual chemical or binary mixtures to prepubertal rats leads to serious

fertility impairment (Boekelheide, 2005; Brilhante *et al.,* 2011). Exposure of many toxicants has been associated with defects in spermatogenesis, steroidogenesis as well as reduction in weight of testis and other accessory organs. Prepubertal exposure to industrial effluent has been reported to delay the onset of puberty (Vachhrajani and Pandya, 2006). Leydig cells are present in the interstitial compartment of the testis and produce testosterone which is essential for normal spermatogenic process. The interactions among the Leydig cells, peritubular myoid cells and Sertoli cells are very important. The toxicant induced direct effect on the Leydig cells may impair the steroidogenesis. Studies from our laboratory have demonstrated that adult rats exposed to industrial effluent had disrupted Sertoli cell and Leydig cellular functions (Pandya, 2000).

Continuous exposures of chemical mixture to adult causes significant effect on the Leydig cell structure and function and reduce the capacity of production of testosterone (Hotchkiss *et al.,* 2010). Testosterone production is regulates by Lutenizing (LH) hormone secreted by pituitary and LH secretion in turn is regulated by GnRH released from the hypothalamus (Payne and Hales, 2004). Howdeshell *et al.,* (2007, 2008) demonstrated that chemical mixture altered the hypothalamic-pituitary-testicular axis. Though a great deal of understanding has developed in the mode of action of testicular toxic compounds, the primary targets and the preliminary toxic reactions/responses are yet to be determined.

Steroidogenesis is an important process going in the Leydig cells and the two important key enzymes involved in the biosynthetic pathway of testosterone are 17 ß HSD and 3 ß HSD (Penning, 1997). The activity of 17 ß HSD and 3 ß HSD have been used to study the status of testicular steroidogenesis of rats in different experimental conditions. Many researchers have demonstrated that steroidogenic enzymes activities are diminished in chemical or chemicals mixture exposed adult rats (Jana *et al.,* 2006; Murugesan *et al.,* 2007; Thyagaraju and Muralidhara, 2008).

It has been noted that Sertoli cells are the likely target of male reproductive toxicity of chemicals, a preliminary effect is seen on the peritubular membrane and blood testis barrier (Boekelheide*et al.,* 1989; Fiorini 2004). The Sertoli cells facilitate and support the physical, hormonal and nutritive development of the germ cells. They have an enormous surface area which allows them to sustain a vast number of developing germ cells. It exhibit variations in its morphology, organelle physiology and responses to hormones at different stages of seminiferous epithelium. Cyclic variation in Sertoli cell's lysosomal population and activities of acid phosphatase (ACP), alkaline phosphatase (ALP), adenosine triphosphatase (ATPase), and succinate dehydrogenase (SDH) *etc.* and microtubule organization at different seminiferous epithelial stages have been reported. Alterations in testicular microtubule assembly are suspected as one of the important mechanism of chemical induced Sertoli cell toxicity (Fiorini 2004; Bekheet, 2010). The chemicals may enter within the Sertoli cell and alter several biosynthetic processes. Therefore, disruption of Sertoli cell's normal function results in impaired spermatogenesis and ultimately subsequent germ cell loss. It becomes, therefore, necessary to identify most significant stages of seminiferous epithelium in context to toxic responses.

Despite the specialized microenvironment of testis, the testicular tissue remains vulnerable to oxidative stress due to production of reactive oxygen species (ROS) that can damage DNA, protein and Lipid (Peltola *et al.,* 1996; Turner and Lysiak, 2008). Also these ROS have been shown to have negative effects on pathway of steroidogenesis. In steroidogenic cells, ROS are principally produced by mitochondria via electron transport chain and through the process of hydroxylation of steroids (Hornsby, 1989). In addition ROS can be generated from a variety of enzymes including xanthine oxidase, NADPH oxidase and the cytochrome P450s (Hanukoglu *et al.,* 1993; Hall, 1994). In order to minimise the risk of damage caused by the ROS, the testis have developed a sophisticated array of antioxidant system comprising enzymatic and non enzymatic components. The depletion of cellular antioxidant enzyme,

increase level of ROS and lipid peroxidation were observed in many chemical induced toxicity studies at relatively higher doses in different experimental animals (Murugesan *et al.,* 2007, Mailankot *et al.,* 2009). Malondialdehyde is a marker of membrane lipid peroxidation resulting from the interaction of ROS with cellular membrane. The damage to membrane can lead to change in membrane characteristics and ultimately effects on homeostasis.

The direct effect of HCM on activities of general enzymes, steroidogenic enzymes, and antioxidant system are still unknown. Therefore, in the present study, we aimed to elucidate the effect of HCM at two different doses on histoarchitecture of testis, steroidogenesis, antioxidant system and testosterone secretary level.

RESULTS

Effects on organ weight

The variations in the testes weights of rats subject to HCM exposure and its recovery are shown in Table 1. Administration of high and low dose HCM to rats resulted in significant ($P<0.001$ and $P<0.01$ respectively) increase in the testes-to-body weight ratio (relative organ weight) when compared with vehicle treated control group III. Group VIII (high dose HCM + recovery) showed a significant ($P<0.05$) increase in relative organ weight while no such significant change was observed in Group IX (low dose HCM + recovery). However, there were no significant differences observed between control and treated groups in average organ (testes) weight of rats.

Effect on testicular steroidogenic enzyme and cholesterol level

Table 2 shows the effect of HCM on testicular steroidogenic enzyme activities, such as 3β HSD and 17βHSD. The activities of 3β HSD and 17βHSD in HCM exposed rats were significantly diminished when compared with vehicle treated control. The activities of 3β HSD and 17βHSD in recovery

group VIII showed insignificant recovery i.e. the activity is far below the normal range when compared with the control group VII. However, data of group IX suggest that withdrawal from HCM treatment proceeds towards the recovery.

Effect on testicular SDH, ALP and ACP activities

Testicular activities of general biochemistry have been recorded in Table 3. Decline in SDH and ALP activity in the high and low dose HCM treated groups was recorded as compared to the control groups. But the above noted decrement was only significant ($P<0.05$) in high dose HCM treated group IV for SDH activity when compared with vehicle treated control group. Significant recovery observed in group VIII and IX for the activity of these two enzymes as no significant decline was noted when compared with their respective control.

The ACP Activity increased ($P<0.05$) in high dose HCM treated group IV when compared with vehicle treated groups while no significant change observed in low dose HCM treated group V. Group VIII (high dose HCM + recovery) showed a significant ($P<0.05$) decrease in ACP activity while it remained normal in group IX (low dose HCM + recovery) when compared with 120 day control group VII.

Effect on Lipid Peroxidation (LPO)

Table 4 and Graph-4 compares the level of lipid peroxidation in HCM treated and recovery groups with controls. The results showed significant increase ($P<0.001$ and $P<0.05$) in LPO as measured by the amount of MDA formed after treatment with HCM (High and low dose respectively) in comparison with the vehicle treated control group. Withdrawal of high dose HCM exposure for 60 days showed some signs of recovery when compared with sixty day high dose HCM exposed group IV but the recovery was found insignificant, as the elevated difference was significant ($P<0.05$) when compared with control group VII. The results of group IX (low dose HCM +

recovery) showed the recovery pattern towards the normalization when compared with control group VII.

Effect on enzymatic and non enzymatic antioxidants

The influence of subchronic toxicity of HCM administration on non enzymatic antioxidants levels are shown in Tables 4 and 5. HCM treatment caused a decrease in the levels of testicular glutathione content and the decrement was significant ($P<0.05$) in high dose HCM treatment, compared with the control groups. Withdrawal from HCM treatment (Group VII and IX) showed a trend of recovery toward normalization. HCM treatment caused decline in the ascorbic acid content but the observed decrement was insignificant when compared with the control groups.

Table 5 provides data on testicular levels of antioxidant enzymes, such as SOD, CAT, GPx and GST in HCM treatment, withdrawal and controls groups. The activity of GST and GPx enzymes were diminished in HCM treated groups while the activity of SOD and CAT decreased insignificantly when compared with controls.

Effects on serum testosterone and cortisol concentration

Data of serum testosterone and Cortisol are presented in Table 6. Sub-chronic exposure of HCM significantly decreased the testosterone concentration when compared with vehicle treated control rats. Withdrawal from HCM treatment (group VII and IX) increased the testosterone concentrations above those of the sixty days HCM treated groups but levels were still significantly lower than control group VII. There was a significant elevation in serum cortisol level in high dose HCM exposed group in comparison to the vehicle treated control group. However, withdrawal from high dose HCM treatment for sixty days brings elevated cortisol concentration back to the normal level. Other than those noted in high dose HCM exposed group IV, no significant change was observed in serum cortisol concentration.

Effect on histology of testis

Spermatogenesis is the gradual transformation of germ cells into spermatozoa, occurs within the seminiferous tubules of the testis. This process involves cellular proliferation by repeated mitotic division, reduction division by meiotic division to produce haploid spermatids, and terminal differentiation of the spermatids into spermatozoa. In seminiferous epithelium, as the germ cells advance, older cells become associated with younger ones in specific 12- 13 day cycle. The spermatogonia undergo several mitotic divisions to produce various populations of spermatocytes (A1-A4 to intermediate and B type cells). Meiosis is an extended phase that begins after B type spermatogonia divide to produce primary spermatocytes. Meiotic prophase begins with small leptotene spermatocytes. The cells enlarge as prophase continues through zygotene, pachytene spermatocytes. Diplotene cells undergo the first meiotic division producing secondary spermatocytes. The secondary spermatocytes cells undergo second meiosis to produce round spermatids. The round spermatids are slowly transformed into elongated cells called spermatozoa. The development of spermatozoa from round spermatids is divided into 19 stages of spermiogenesis based on morphological criteria. One complete cycle of cycle of spermatogenesis in rat takes around 54-58 days and divided into approximately 4.7 cycle of seminiferous epithelium (Table 7, Fig. 6) (Leblond and Clermont, 1952; Hess, 1990).

The arrangement of the cell types that contribute to the process of spermatogenesis within the seminiferous epithelial is highly organized. A definitive orderly occurrence of epithelial wave is seen and accordingly one cycle of seminiferous epithelium is divided into 14 distinct stages. In testis, the stages are repeated in consecutive order along the length of the seminiferous tubules because the tubules are folded repetitively. A cross section of testis

will contain several hundred tubular sections, each of which can be identified as one of the 14 stages (Table 7, Fig. 6).

Since the Sertoli cells exhibit cyclic variations in their morphology relative to the spermatogenic cell type associated with it, the organization and distribution of specific cell types in the seminiferous is variable at different SE stages. Fig. 7 shows the location of spermatids which is also considered as one of the significant identification feature of particular SE stage. The round spermatids are distributed in the crypt region, following spermiation of the elongated spermatid as they begin elongation, get distributed up to the apical and of the Sertoli cytoplasm during stages XI to XIV. By the end of stage XIV the round spermatids are formed which get distributed in the crypt region while the elongated spermatid moves towards the basal epithelium for further metamorphic changes of the nucleus. The sperm head are typically adjacent to the Sertoli cell nuclei at SE stages III and IV and then begin moving to the apical surface leading ultimately to the spermiation of fully elongated curved spermatid (Fig. 7).

Due to these complications of organization of SE, for stage wise qualitataive studies, the photoGraphes of tubules of different SE stages at different experimental doses were photoGraphed at same magnifications and analysed as explained in Fig. 8. The tubule was divided into five zones encompassing the basal crypt and adluminal regions. This was obviously not based on the compartmentation by the Sertoli junctional complexes since it was not possible under light microscopy.

Although the qualitative analysis was carried out at different SE stages they are not described in that form so as to avoid repetition of observations. On day 60 in the high dose treatment group the histological lesions were more potent compared to low dose group. The summary of histological observation is presented in Table 8. Sloughing of more mature cells type resulted in tubular depopulation. This is primary indication of the damage to the Sertoli cell cytoskeletal structure. Interestingly, such sloughing was seen for more

mature cell type clearly indicating an early and severe damage to the crypt region of Sertoli cells. The spermatogenic nuclear pyknosis further led to the loss of spermatogenic cells by apoptosis. The vacuolation in the basal portion of Sertoli cell is also a primary indicator of cellular damage. In histological preparation it was evident that such vacuole in the basal portion extends and expands encapsulating the spermatogenic cell. The damage of Sertoli spermatogenic junctions in such area would result into release or large cytoplasmic mass (Table 8). The studies also showed that the round spermatids were deformed, the elongating spermatids were broken and the elongated spermatids were not released leading to increased structural abnormalities and spermiation failure. The analysis of seminiferous tubules showing regressive changes is presented in Table 9. The battery of parameters considered as representative of regressive changes are described in materials and methods sections. A total of 140 tubules per testis at different SE stages were analysed. A total of 57 and 44 % tubules exhibited various regressive changes on day 60 in high and low dose group respectively. Although recovery was seen it was partial only (38 and 25 % in respective doses).

Table 10 denotes the frequency of occurrence of different SE stages. The number of tubules at stages IX to XII and XIII and XIV significantly increased while those at stages I to IV, V to VII and VII to VIII decreased in the high dose treatment group. Fig. 9 and 10 depict the nuclear and the overall changes noted at different SE stages in various study groups. Since the control animals exhibited near normal histoarchitecture, details of those groups are not presented here.

The histological preparations nicely demonstrated the normal histoarchitecture, cellular associations and the location of various cell types at different SE stages (Plates 1 and 2). Plates 3 to 6 are lucid journey through the various SE stages. The occurrence of spermatogonia and all different spermatocyte can be clearly seen in the photographs. The stages of cells undergoing 1st meiosis and the 2nd meiosis are demonstrated appropriately for

comparison with the HCM exposed groups. The spermatid metamorphosis and the distributions of various populations of spermatids sufficiently describe the normal state of ongoing active spermatogenesis. Plate 7 illustrates the basal profile of SE where the differences in the size and shape of the Sertoli cell nucleus and the associated spermatogenic cells suggest cyclic variations in the morphology of Sertoli cell at different SE stages.

The HCM induced toxic responses were dictinct and definitive clearly suggesting the stage specific changes and also specific change in different compartment. The peritubular membranes, which are composed of myoepithelial cell and connective tissue (collagen) form primary barrier for transportation of materials across the tubule. Dissolution of this tubule was seen chiefly at stages IX to XII which led to leakage of cytoplasmic exudates, debris *etc* in the interstitium (Plate 8). Various features of cellular damage, cytoplasmic blebbing and cell sloughing are presented in Plates 9 and 10. In several tubules at stage 8 the residual bodies were not taken up by the Sertoli cell and hence were released into the tubular lumen. The luminal accumulation of cytoplasmic exudates, fluid and cellular debris was conspicuously observed in high dose HCM exposure group (Plate 11). The vacuolation of basal portion of Sertoli cell, their expansion to the crypt region leading to loss of large spermatogenic cell mass is clearly shown in Plate 12. It is obvious that these are true vacuoles and not processing artefacts.

The histological features as explained in Table 8 to 10 and Fig. 9 and 10 can be understood through the histological preparations detailed in the histological Plates 13 to 21. The damage to the developing pachytene stage primary spermatocyte was most prominently seen through different SE stages (Plates 13 and 14). The cytoplasmic dissolution leading to formation of cytoplasmic bleb and its migration towards the apical margin of the epithelium are shown in Table 14.

The retention of elongated spermatid exhibiting failure of spermiation was seen at stages XI to XIV while the deformed elongating and elongated

spermatid were seen in tubules at various SE stages (Stage 15). The chromosomal condensation and/or fragmentation were suggestive of typical cellular responses (Plate 16). Most of the spermatogonia type A in tubules at stages I to IV appeared normal while spermatogonia type B at stages IV and VI showed pyknosis. The zygotenes at stages XI to XIII were also pyknotic (Plate 16). Distinct features of cell damage were seen in pachytene primary stage spermatocytes at stages XI and XII. The cytoplasmic bleb formation, damage to the cell membrane and fragmentation of nuclear chromatin were prominently seen at stage XII (Plate 16). During the second meiotic division such chromatin exhibited karyolysis and were unable to proceed further (Plate 17). The tubule at SE stage 14 also had secondary spermatocytes dividing normally and forming primary spermatocyte.

Densely stained eosinophilic granules/ debris are also located in such cells which are indicative of ongoing necrotic process (Plate 18). In high dose HCM treated group the residual bodies taken up by Sertoli cells following spermiation were not phagocytosed and digested in the apical and crypt region and hence such densely stained bodies migrated to the basal portion of Sertoli cells through damaged cytoskeletal frame work. These were observed in the tubule of SE stages IX and X (Plate 18). Since this is an abnormality it perhaps may induce further changes in the basal cytoplasm of Sertoli cells. Although an improvement in the spermatogenesis was observed in the high dose treatment group on day 120, the cellular lesions were still persistent (Plate 19) while following withdrawal in low dose treatment group the organization of SE appeared much normal with the ongoing active spermatogenesis (Plates 20 and 21).

DISCUSSION

The present study demonstrates that HCM inhibits testosterone production reflected from the diminished value of serum testosterone level in all the HCM treated groups when compared with controls. Disruption of androgen biosynthesis in testis has been associated with increased cortisol

concentration (Bambino and Hsueh, 1981) and diminished activities of steroidogenic enzymes like 3β HSD and 17βHSD, enzymatic antioxidants such as SOD, GPx, CAT, and GST, and nonenzymatic antioxidants such as GSH and ascorbic acid (Murugesan *et al.,* 2007, Mailankot *et al.,* 2009).

Massive work exists on the neuronal pathways of the brain that trigger successful endocrine control of reproduction (Natt *et al.,* 2002; Walker and Cheng, 2005). The main pathway for the direct control of reproduction is the neurons using gonadotropin releasing hormone (GnRH) as the transmitter. These neurons have their cell bodies primarily in the hypothalamic medial preoptic area (MPOA). This neurons releases neurotransmitters as hormones in the connective link between the pituitary and the brain i.e. the GnRH released in the median eminence stimulates the release of the gonadotropin luteinizing hormone (LH) and follicle stimulating hormone (FSH) from the pituitary. Ultrastructural and histochemical work has demonstrated a consistent series of morphological events that occur upon stimulation of the cells of pituitary with GnRH. These two hormones LH and FSH play an important role in communicating to gonads. In males LH stimulates the interstitial cells located in the testes to produce testosterone, and FSH plays a role in spermatogenesis.

Cortisol is a catabolic hormone produced by adrenal glands in response to any stress. It falls into a category of hormone known as 'glucocorticoids', referring to their ability to increase or maintaining the blood glucose levels. Cortisol enhances amino acid and lipid mobilization in skeletal muscle and adipose tissue (Gablo, 2001; Wolfe 2001). Also cortisol stimulate the liver to produce the enzymes involved in the gluconeogenesis and glycogenetic pathway allowing conversion of amino acid and glycerol into glucose and glycogen (Gablo, 2001; Wolfe 2001).

Previous research has established that under certain circumstances a negative relationship exist between the hormones cortisol and testosterone. Bambino and Hsueh, (1981) showed a direct inhibitory effect of high doses of

glucocorticoids upon testicular Leydig cells, which resulted in decrease in the testosterone production and thus ultimately effect on steroidogenesis. Many researchers speculated that the increased cortisol concentration disrupted the biosynthesis pathway of testicular testosterone production (Brownlee *et al.,* 2005). The results of present study suggest that sub chronic exposure to HCM caused endocrine disruption, which may consequently lead to serious reproductive problems.

Moreover, the increased activity of testicular acid phosphatase in HCM treated rats reflects the testicular degeneration, which may likely be a consequence of increase lytic activity. The activities of SDH and ALP in testicular tissue are associated with the normal process of spermatogenesis. The activity of SDH increased markedly throughout the process of maturation of germ cell and is reported to decrease by many toxicologists under the condition of toxic insult (Fukuoka *et al.,* 1993; Zang and Lin; 2009).

The activity of testicular steroidogenic and antioxidant enzymes were markedly reduced. In view of these findings, it is proposed that an increase in free radical formation results in the inhibition of steroidogenic and antioxidant defence system during exposure to HCM.

Several lines of evidence indicate that the relations between the testicular antioxidant and the steroidogenic enzymes are physiologically relevant (Aitkin and Roman, 2008; Mandal and Dass, 2011). Free radicals react with lipids and cause peroxidative damage and enhance lipid peroxidation. The enzymatic and nonenzymatic antioxidants are the natural defence system against free radical mediated damages in various organs including testis (Aruldhas et al 2005; Murugesan et al., 2007). The observed decreased activities of enzymatic and non enzymatic antioxidants in HCM exposed groups might have increased ROS and LPO production. These data suggest that the HCM induced oxidative stress and elevated free radical generation may cause damage to cellular membrane and possibly affect the

functional integrity and power of normal function of steroidogenic process or accessory proteins involved in the cholesterol transport to the mitochondrion.

The decreased activity of SOD, observed in the present study, indicate either reduced synthesis of enzyme or its degradation in the HCM exposed groups. Similar results were observed in various toxicity studies of individual chemicals or with couple of chemicals. Decreased activities of GPx and CAT in HCM exposed groups may be attributed to in effective scavenging of hydrogen peroxide. Furthermore, CAT is exclusively present in testicular Leydig cell peroxisomes participating in intracellular cholesterol trafficking and its delivery to mitochondrion during normal steroidogenesis in adult rats. GST detoxify a broad range of xenobiotics and protect against LPO of membrane and DNA and protein damage (Rao and Shaha, 2000).

The highest concentrations of ascorbic acid occur in the pituitary, adrenal gland and gonads. Ascorbic acid play important role in steroid and peptide hormone production and its ability to protect cells from oxidative damage is also well recognized (Rao et al., 2005). Studies on toxicity of compounds revealed that the decrease serum testosterone level in rat was accompanied by decrease testicular ascorbic acid content. Therefore, the decreased ascorbic acid content in HCM exposed group may contribute to increased LPO level and decrease serum testosterone level.

Spermatogenesis is achieved by progressive proliferation and metamorphosis of spermatogenic cells in the compartmental microenvironment of Sertoli cells which exhibit stage specific variations in its structure and functions. The observed changes like cytoplasmic blebbing, cell sloughing and basal vacuole formation indicate cytoskeletal damage. It has been noted that during apoptosis, the cell cytoskeleton breaks up and causes the membrane to bulge outward which ultimately separate from the cells (Frakler and Grosse, 2008). Within the Sertoli cells the microtubules are associated with Sertoli-Sertoli and Sertoli-Spermatogenic complexes besides as general cytoskeleton (Wolosewick and Bryan, 1977). Sertoli cell interaction

is proposed to be in contact with five adjacent Sertoli cell and 47 spermatogenic cell maximum at various stages of SE (Rusell, 1983). Therefore damage to the variety of microtubules is expected to collapse the histoarchitecture of SE. The tubulobulbar complexes between elongated spermatid and Sertoli cells maintain the anchoring of spermatids as well as permit appropriate spermiation. Therefore, failure of spermiation at stage VIII clearly depicts tubulobulbar complex abnormality. The HCM is shown to potentially damage the peritubular membrane and hence may get entry into seminiferous tubule (Sertoli cell) and lead to further toxic responses. Fig. 11 describes the probable events which might lead to severe toxic responses following exposure to HCM. The HCM with in the Sertoli cell would induce oxidative stress leading to variety of functional impairments. Simultaneously structural lesions that damage the Sertoli junctional complexes permit the toxicants to enter the most protective specialized environment of adluminal compartment. It may be noted that the leptotene from the basal compartment migrate through junctional complexes into the adluminal compartment at stage IX of SE. Therefore, the Sertoli junctional complexes are under highly dynamic condition of breakage reformation and relocation at stage IX (Dym and Fawcett, 1970). Probably the HCM components find it most easy to destruct the variety of cytoskeletal element during this particular stage and thus dissociate the integrity of blood-testis-barrier. This would facilitate entry of HCM through the dismantle Sertoli junction complexes into the adluminal compartment.

Earlier studies have demonstrated that toxicant induced cytoskeletal damage is one of the significant features of cell loss and spermatogenesis impairment (Hess et al., 1988; Boekelheide et al., 1989, 2002; Vachhrajani and Dutta 1992; Sharpe et al., 1995; Vachhrajani and Pandya 2006, 2008). Probably therefore the tubules at SE stage XII and XIII are more affected in present studies.

It is also therefore possible that the pachytene stage primary spermatocytes are most vulnerable spermatogenic cell type to HCM action.

The damaged cytoplasmic and nuclear components are mostly released into the lumen of the tubule but in such tubules where the basal portion is also damaged the debris and exudates may accumulate along the basement membrane of Sertoli cell and may leak out into the interstitium through the damaged peritubular membrane (Fig. 11). Such action has been shown with some of the metallic toxicants.

The cellular debris and exudates expelled into the lumen of seminiferous tubule leads to epididymis. In present studies such products of cellular degeneration is observed in histological preparation of epididymis. Supporting the probable mode of action HCM and toxic responses of testis explained.

CONCLUSION

The HCM induced oxidative stress, metabolic impairment and steroidogenic dysfunction lead to impairment of spermatogenesis. In view of the overall toxic manifestation and the hepatic and renal toxic responses, the toxic responses of the testis appears to be severe following exposure to HCM at NOAEL dose levels for a subchronic exposure.

Experimental Groups

Groups	Treatment	Autopsy day
I	Zero (initial) day control	01
II	Control (No treatment)	61
III	Control (Vehicle treatment)	61
IV	Heterogeneous chemical mixture treated group (1% of LD_{50} dose/ animal/ day - NOAEL dose level)	61
V	Heterogeneous chemical mixture treated group (0.1% of LD_{50} dose/ animal/ day)	61
VI	Control (No treatment)	121
VII	Control (Vehicle treatment)	121
VIII	Heterogeneous chemical mixture treated group (1% of LD_{50} dose/ animal/ day) for 60 days followed by withdrawal phase of 60 days - NOAEL dose level.	121
IX	Heterogeneous chemical mixture treated group (0.1% of LD_{50} dose/ animal/ day) for 60 days followed by withdrawal phase of 60 days.	121

Values in all the following Tables are Mean± SE and statistical significance is considered and presented for (·) $P<0.05$, (+) $P<0.01$ and (#) $P<0.001$ compared withrespective vehicle control.

Table 1: Gravimetric analysis of testis

Groups	Absolute testis (both) weight (g)	Relative testis weight g/ 100 g animal
I	3.23 ±0.039	0.99 ±0.013
II	3.35 ±0.057	1.00 ±0.009
III	3.41 ±0.066	0.97 ±0.017
IV	3.15 ±0.067	1.10 ±0.034#
V	3.19 ±0.044	1.08 ±0.014+
VI	3.54 ±0.057	0.90 ±0.016
VII	3.58 ±0.080	0.88 ±0.016
VIII	3.31 ±0.047	0.97 ±0.013*
IX	3.41 ±0.059	0.93 ±0.016

Fig. 1: Gravimetric analysis of Testis

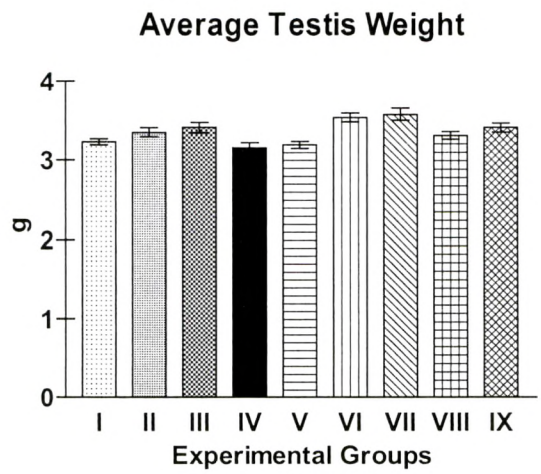

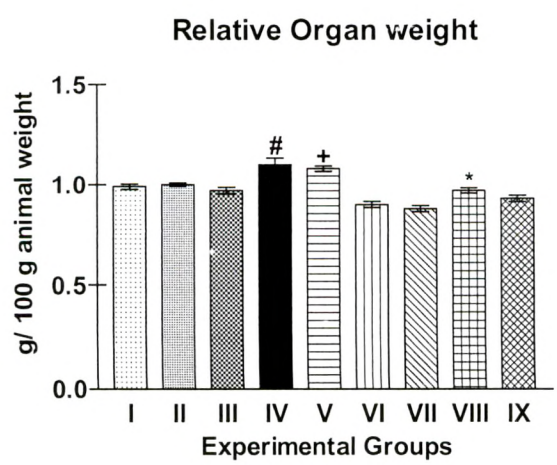

Table 2: Analysis of parameters of testicular steroidogenesis

Groups	Cholesterol (mg/ 100 mg tissue)	3 β hydroxysteroid Dehydrogenase (n mol of NAD reduced / min/ mg protein)	17 β hydroxysteroid Dehydrogenase (n mol of androstenedione formed/ mg protein/ min)
I	0.12 ±0.009	0.68 ±0.062	0.47 ±0.048
II	0.13 ±0.011	0.62 ±0.064	0.44 ±0.045
III	0.15 ±0.011	0.64 ±0.044	0.49 ±0.035
IV	0.23 ±0.019#	0.23 ±0.023#	0.19 ±0.021#
V	0.17 ±0.019	0.32 ±0.032*	0.22 ±0.030#
VI	0.15 ±0.009	0.66 ±0.060	0.45 ±0.032
VII	0.16 ±0.005	0.68 ±0.126	0.48 ±0.081
VIII	0.19 ±0.006	0.38 ±0.033*	0.27 ±0.026*
IX	0.14 ±0.009	0.44 ±0.038	0.30 ±0.025

Fig.2: Analysis of parameters of testicular steroidogenesis

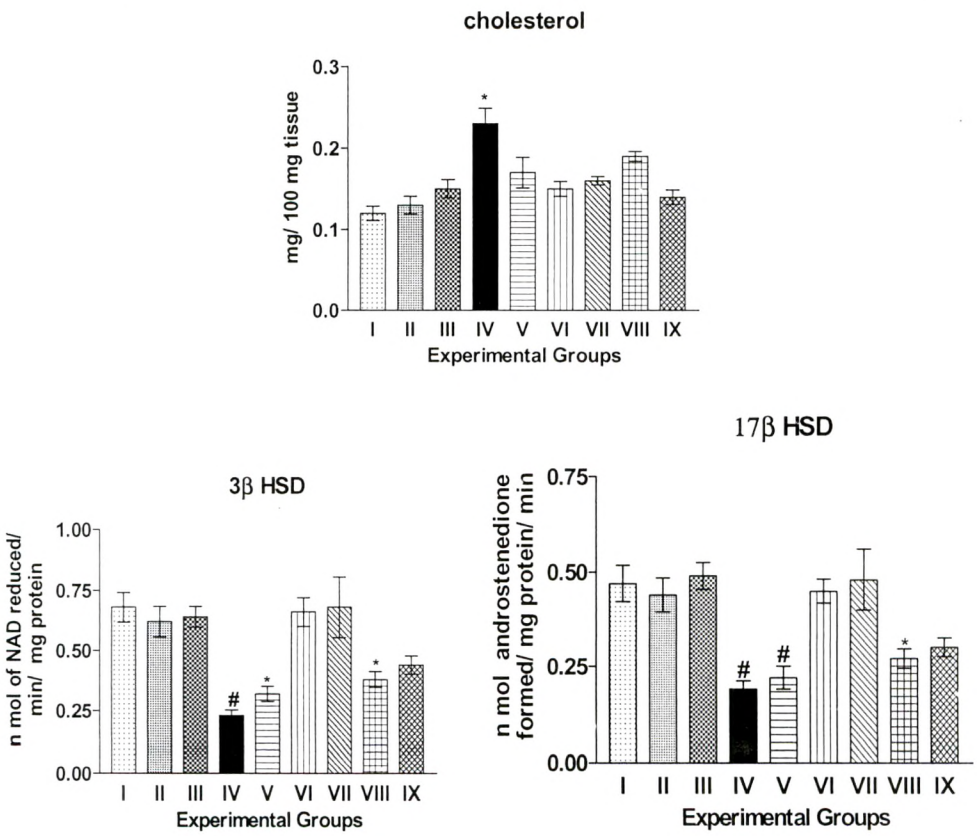

Table 3: Enzyme of general testis function

Groups	SDH (µg formazan formed/ mg protein)	ACP (µ moles of p-nitrophenol released/ mg protein/ min)	ALP (µ moles of p-nitrophenol released/ mg protein/ min)
I	11.03 ±1.80	0.11 ±0.011	0.071 ±0.011
II	11.61 ±0.83	0.11 ±0.006	0.079 ±0.007
III	12.69 ±1.10	0.11 ±0.008	0.087 ±0.010
IV	7.14 ±0.47*	0.17 ±0.015*	0.042 ±0.004*
V	8.92 ±0.32	0.11 ±0.004	0.048 ±0.002*
VI	12.38 ±0.95	0.11 ±0.009	0.077 ±0.005
VII	12.52 ±1.86	0.11 ±0.020	0.071 ±0.010
VIII	8.70 ±0.60	0.05 ±0.004*	0.052 ±0.009
IX	10.09 ±1.18	0.09 ±0.019	0.059 ±0.010

Fig. 3: Enzyme of general testis function

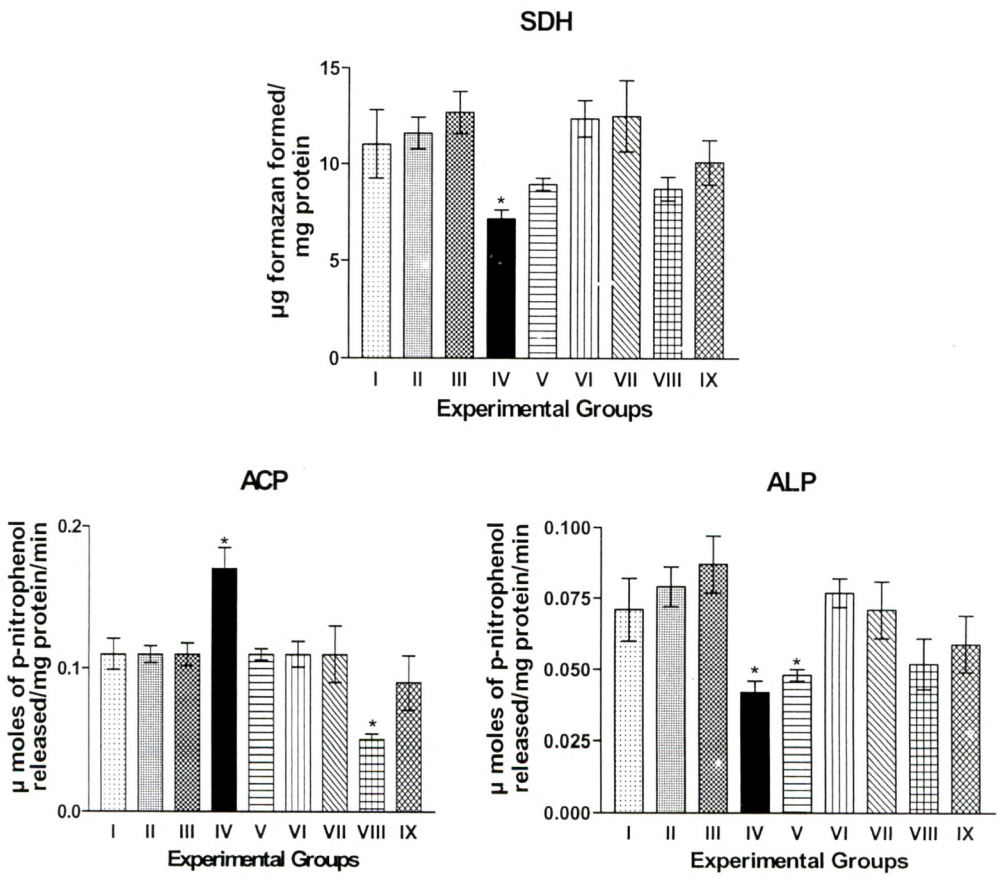

Table 4: Oxidative stress indicators of testis function

Groups	LPO (n mole MDA/ 100 mg tissue)	GSH (µg of GSH/ mg protein)	Ascorbic acid (µg/ mg tissue)	Protein (mg/ 100mg tissue)
I	51.92 ±2.62	2.48 ±0.70	0.24 ±0.025	14.21 ±1.41
II	53.63 ±3.91	3.03 ±0.51	0.25 ±0.023	15.05 ±1.31
III	55.19 ±6.33	3.53 ±0.51	0.19 ±0.042	14.84 ±0.80
IV	92.11 ±2.02#	1.10 ±0.16*	0.15 ±0.012	11.41 ±0.53
V	80.68 ±3.71*	1.51 ±0.19	0.12 ±0.016	13.41 ±0.49
VI	55.04 ±6.34	3.25 ±0.32	0.25 ±0.042	13.66 ±0.84
VII	57.22 ±7.08	3.59 ±0.63	0.26 ±0.041	14.54 ±1.51
VIII	83.75 ±5.30*	1.80 ±0.14	0.23 ±0.025	11.65 ±0.50
IX	75.67 ±7.72	1.79 ±0.57	0.34 ±0.051	13.13 ±0.81

Fig. 4: Oxidative stress indicators of kidney function

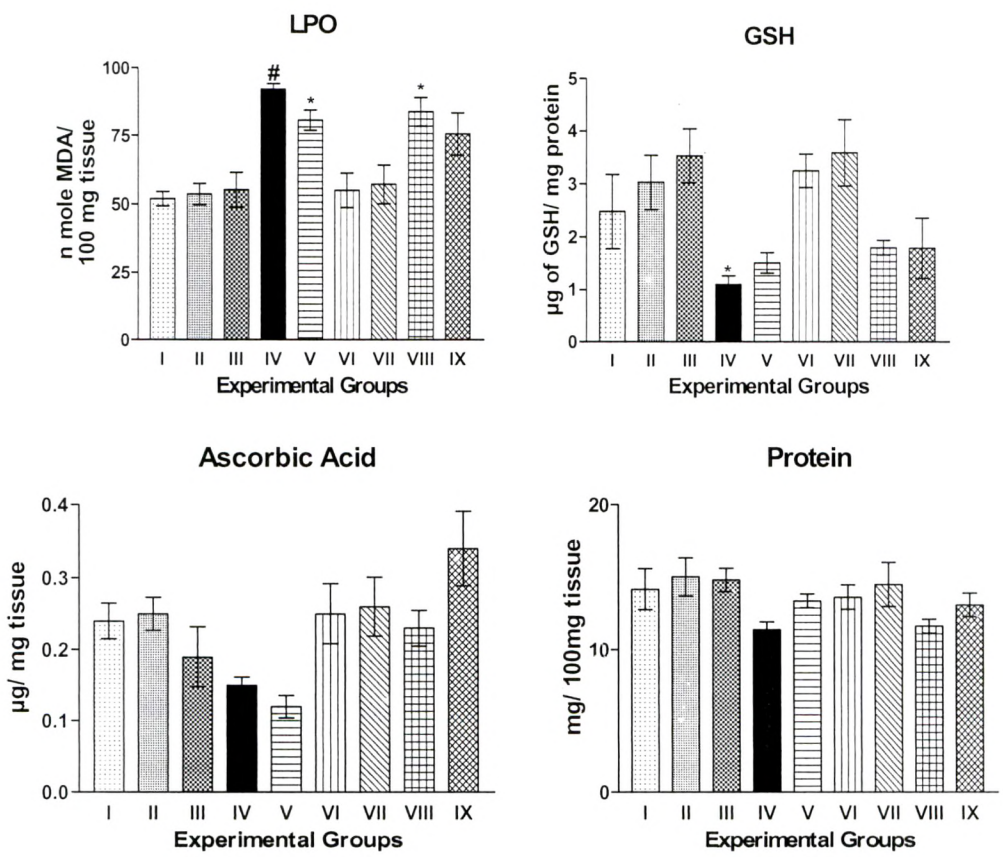

Table 5: Oxidative stress marker enzymes as indicators of testis function

Groups	SOD (Unit/ mg protein)	GPx (µg of GSH utilize/ min/ mg protein)	CAT (µ mole of H_2O_2 consumed/ min/ mg protein)	GST (µ mole CDNB-GSH conjugate formed /min/ mg protein)
I	6.49 ±0.85	4.14 ±0.41	32.77 ±3.05	4.63 ±0.70
II	5.37 ±0.36	5.28 ±0.41	33.25 ±2.93	5.78 ±0.44
III	5.23 ±0.54	4.56 ±0.46	35.17 ±6.18	5.23 ±0.59
IV	3.48 ±0.43	2.32 ±0.15*	18.30 ±1.84	2.10 ±0.15*
V	3.77 ±0.25	2.87 ±0.14	27.42 ±3.60	2.07 ±0.23*
VI	6.00 ±0.60	6.37 ±0.67	37.17 ±3.12	5.97 ±0.45
VII	6.39 ±1.60	5.27 ±0.71	36.27 ±6.66	5.12 ±1.03
VIII	2.75 ±0.42*	2.78 ±0.27+	23.50 ±2.52	4.58 ±0.74
IX	4.10 ±0.48	3.28 ±0.44	32.48 ±5.92	3.24 ±0.64

Fig.5: Oxidative stress marker enzymes as indicators of testis function

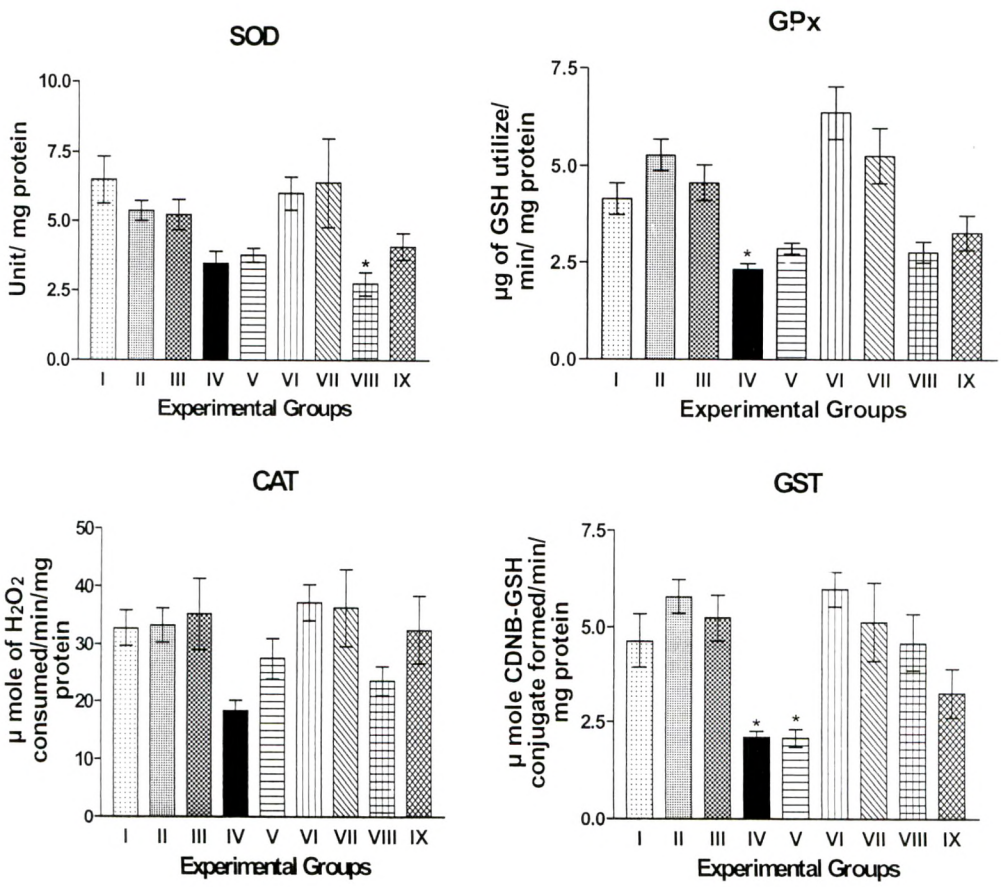

Table 6: Serum testosterone and cortisol concentration

NA: Not analyzed

Groups	Serum Testosterone (ng/ dl)	Serum Cortisol (mcg/dl)
I	NA	NA
II	NA	NA
III	195.00 ±43.04	2.42 ±0.24
IV	<<20.0#	4.65 ±0.45#
V	<<20.0#	2.55 ±0.13
VI	NA	NA
VII	184.50 ±25.63	2.42 ±0.13
VIII	55.11 ±1.65*	2.56 ±0.07
IX	49.65 ±5.84+	3.30 ±0.19

Table7: Description of different 14 stages of a seminiferous epithelial cycle in rat. The identification characters of all the 14 stages are illustrated in Fig. 11.

Stage I- VIII	Stage IX- XIV
Two steps of spermatids i.e. round and elongated spermatids are present.	Only elongated spermatids are present in the tubules, located near the lumen.
Stage I - Elongated step 15 spermatids clusters are located more towards the lumen and have a prominent bulge of dorsal-caudal aspect of acrosome (fin). - Round spermatids have a light pink stained Golgi apparatus (G).	**Stage IX** - Step 19 spermatids no longer line the lumen, and residual bodies (Rb) are seen at various levels within the epithelium. - The acrosomic system of step 9 spermatids (Ac) are elongated.
Stage II - The dorsal acrosomic fin (F) is no longer prominent as the acrosome has shifted toward the apex of the nucleus. - The Golgi apparatus of step 2 spermatid contain two proacrosomic granules (pg).	**Stage X** - The residual bodies (Rb) disappeared or relocated along the basement membrane. - The acrosomic system (Ac) of step 10 spermatid extends from the apex to the caudal region of the nucleus (segital section exhibit a V-shaped structure).
Stage III - Single acrosomic granules (Ag) are located within acrosomic vesicle of step 3 spermatids.	**Stage XI** - The step 11 spermatid features a prominent protrusion of the acrosomic system (Ac) and nucleus at a sharp angle to the caudal region of nucleus.
Stage IV - In late 4 spermatids, the acrosomic vesicle has flattened against the nuclear membrane.	**Stage XII** - The nucleus of the step 12 spermatid is more condensed and straight and thus displays a narrow width at acrosomal-nuclear junction.
Stage V - The head of step 17 spermatid is buried adjacent to the Sertoli cell nucleus.	**Stage XIII** -The acrosomic system (Ac) of the step 13 spermatid extends beyond the nuclear apex and forms a bulge on the ventral side of the nucleus. - Large diplotene (D) spermatocytes with prominent nucleoli are typical in this stage.
Stage VI - Step 18 spermatids have migrated towards the lumen and small basophilic granules (Bg) are present in their distal cytoplasm.	

Stage VII - Large basophilic granules (Bg) are located near the nuclei of step 19 (elongated spermatid: mark very prominent curvature of late spermatid nucleus) spermatids that line the lumen.	**Stage XIV a** - The first meiotic division is recognized by the presence of large meiotic Figures(M) with clumps of chromatin forming scattered patterns in the centre of the spermatocyte cytoplasm.
Stage VIII - The acrosomic system (Ac) and nucleus of step 8 spermatid are positioned toward the basal pole of the cytoplasm. - Residual bodies (Rb) from the cytoplasmic lobe are layered between the step 19 spermatid nuclei and round spermatids. - The Sertoli cell nucleus is positioned away from the basement membrane.	**Stage XIV b** - Secondary spermatocytes (SS) are present and typically larger than the round spermatids. - Meiosis II id detected by the presence of smaller, centrally located meiotic Figuresthat forms dense cluster of chromatin (M).

Fig.6: Seminiferous Epithelial stages and transitions in the spermatogenic cycle of rat testis (Hess, 1990)

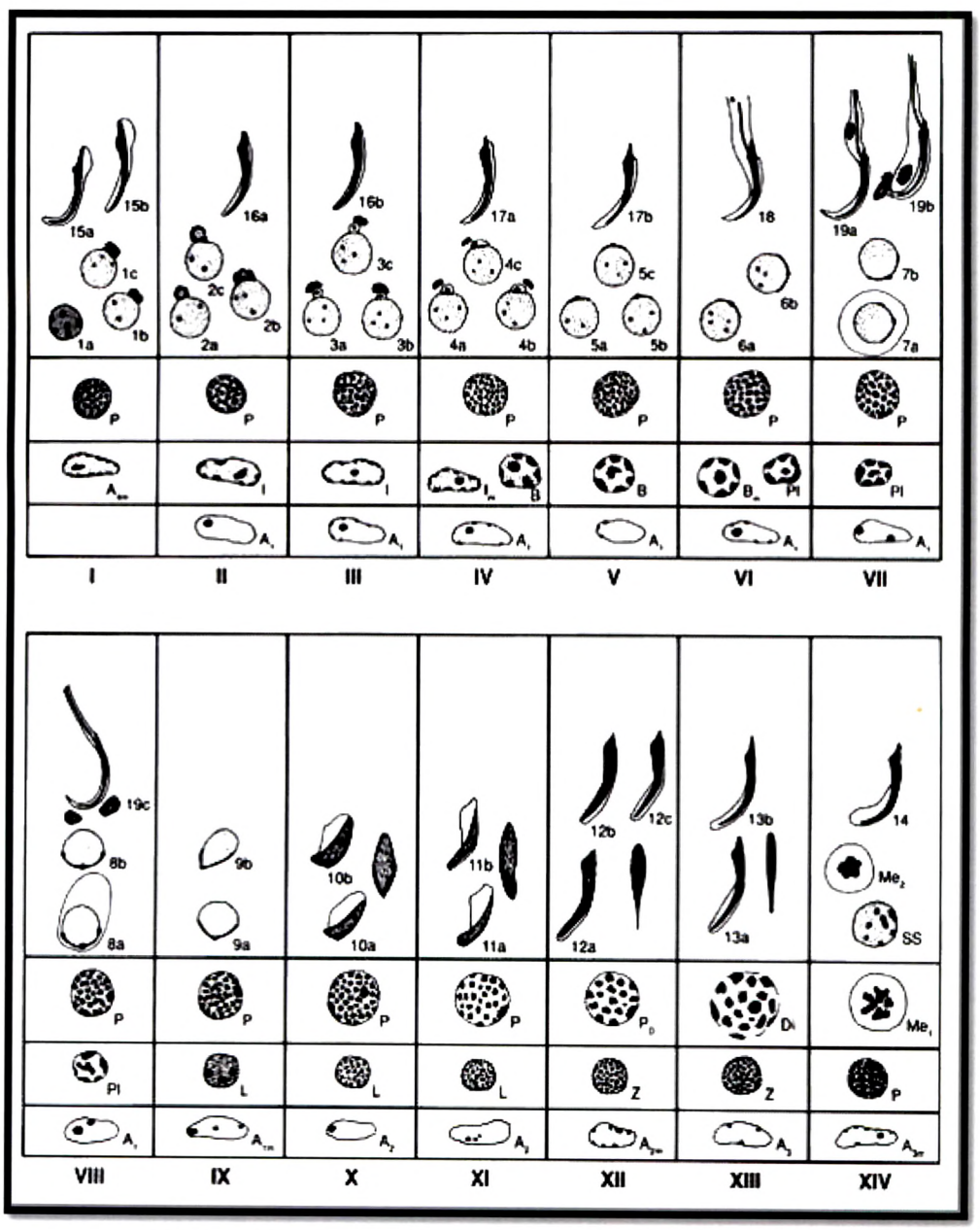

Fig. 7: Diagrammatic representation of the progression of the spermatogenesis. The approximate location of different spermatogenic cells in the epithelium is indicated. The arrow shows movement of spermatids in the epithelium.

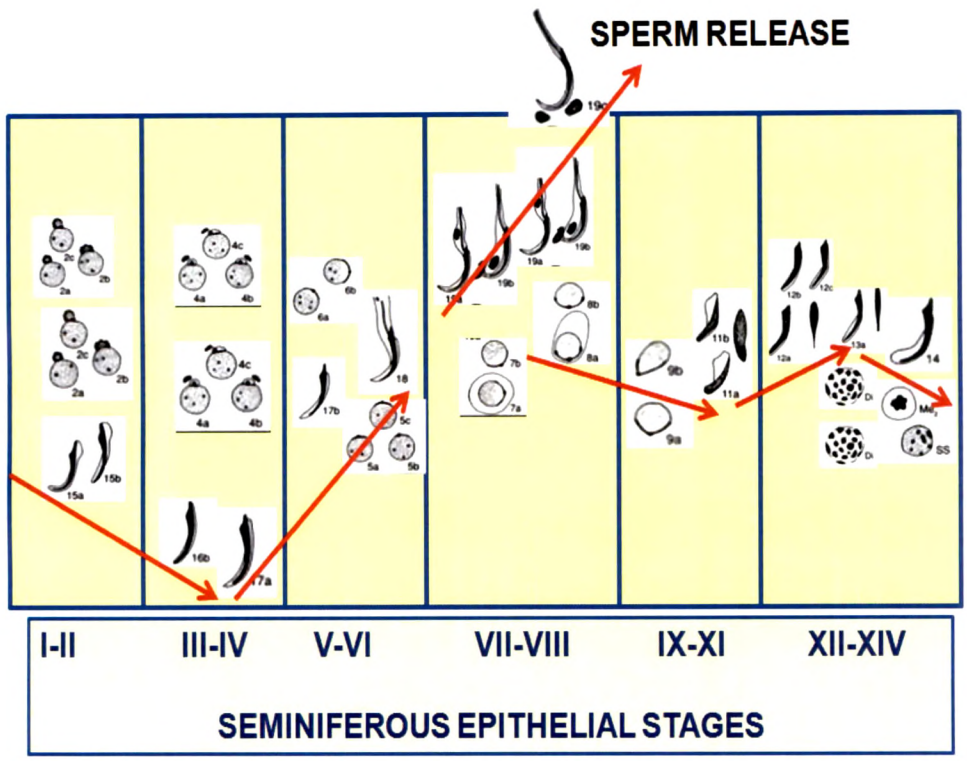

Fig. 8: Diagrammatic representation of the compartmentation of the seminiferous tubule. The qualitative analysis was carried out accordingly at different stages.

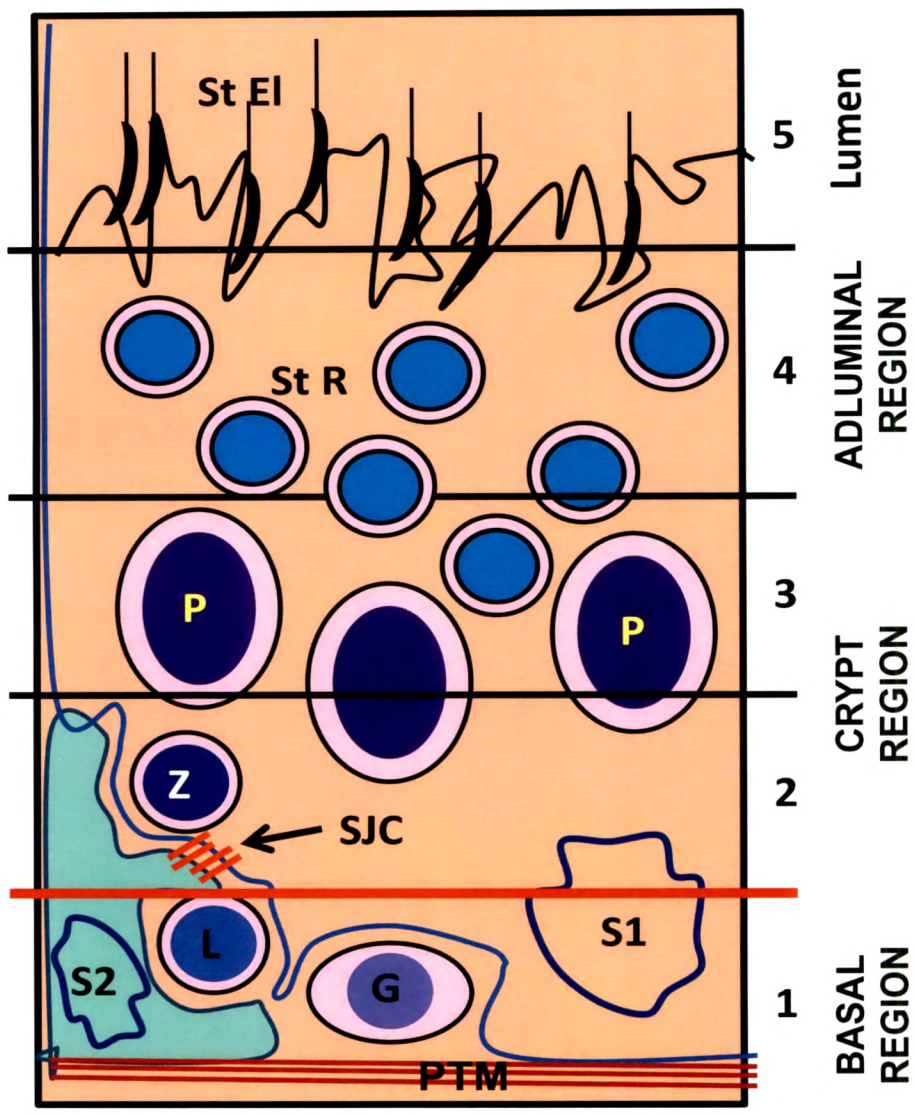

Table 8: Summary of histological observations

Histological changes	EXPERIMENTAL GROUPS								
	I	II	III	IV	V	VI	VII	VIII	IX
Damage in basal portion of tubules	-	-	+	+++	++	-	+	++	+
Damage in adluminal portion of tubules	-	-	+	++++	+++	-	+	++	++
Spermatogenic nuclear pyknosis	-	-	-	+++	++	-	+	++	+
Spermatogenic nuclear karyorrhexis	-	-	-	++	+	-	-	+	+
Cytoplasmic vacuolation	-	-	+	+++	++	-	+	++	+
Cytoplasmic blebbing	-	+	+	+++	++	-	+	+	+
Cell sloughing	-	-	+	++++	++	-	+	++	+
Retention of residual bodies	-	-	-	+++	++	-	-	+	+
Eosinophilic masses	-	-	-	+++	++	-	-	++	+
Deformation of round spermatids	-	-	+	+++	++	-	-	++	+
Deformation of elongating spermatids	-	-	-	++++	+++	-	-	+++	++
Presence of broken sperms	-	-	-	++++	+++	-	-	+++	++
Premature release of spermatids	-	-	+	+++	++	-	+	++	+
Delayed spermiation	-	-	-	++	++	-	-	+	+
Clogging of the spermatozoa flagella	-	-	-	++	+	-	-	+	+
Interstitial oedema	-	-	+	+++	++	-	-	+	+

Microscopic observation based semi quantitative analysis where, (-): no effect, (+): less effect, (++): moderate effect, (+++): high effect, (++++): very high effect

Table 9: Analysis of seminiferous tubules showing regressive changes

SE Stages	Tubules scored	Experimental Groups								
		I	II	III	IV	V	VI	VII	VIII	IX
I-IV	40	2	4	3	20	16	3	4	14	10
V-VI	20	1	1	2	12	08	3	3	10	7
VII-VIII	20	1	2	3	08	08	4	4	5	2
IX-XI	30	3	3	4	22	12	2	3	12	8
XII-XIII	20	3	2	3	13	14	2	3	9	6
XIV	10	2	3	2	5	4	1	2	4	2
TOTAL (I-XIV)	140	12	15	17	80	62	15	19	54	35
(% Value)	100	8.5	10.7	12.1	57.1	44.2	10.7	13.6	38.6	25

Table 10: Frequency of occurrence of seminiferous epithelial stages

GROUPS	SEMINIFEROUS EPITHELIAL STAGES				
	I-IV	V-VI	VII-VIII	IX-XII	XIII-XIV
I, II and VI (Control)	22.80 ±0.65	14.70 ±0.60	31.10 ±0.75	19.80 ±0.47	11.60 ±0.48
III and VII (Vehicle Control)	22.30 ±0.70	15.10 ±0.64	30.40 ±0.69	20.00 ±0.42	12.20 ±0.49
IV	15.30 ±1.15	11.30 ±0.47	26.10 ±0.59	28.80 ±0.85	18.50 ±0.37
V	23.10 ±1.41	12.20 ±0.55	25.50 ±0.73	25.10 ±0.69	14.10 ±0.64
VIII	21.30 ±1.51	13.40 ±0.50	27.20 ±0.74	24.40 ±0.83	13.70 ±0.52
IX	28.00 ±0.99	14.30 ±0.60	25.40 ±0.60	19.90 ±0.50	12.40 ±0.50

Fig. 9: Summary of histological observations based on the nuclear changes at different SE stage groups.

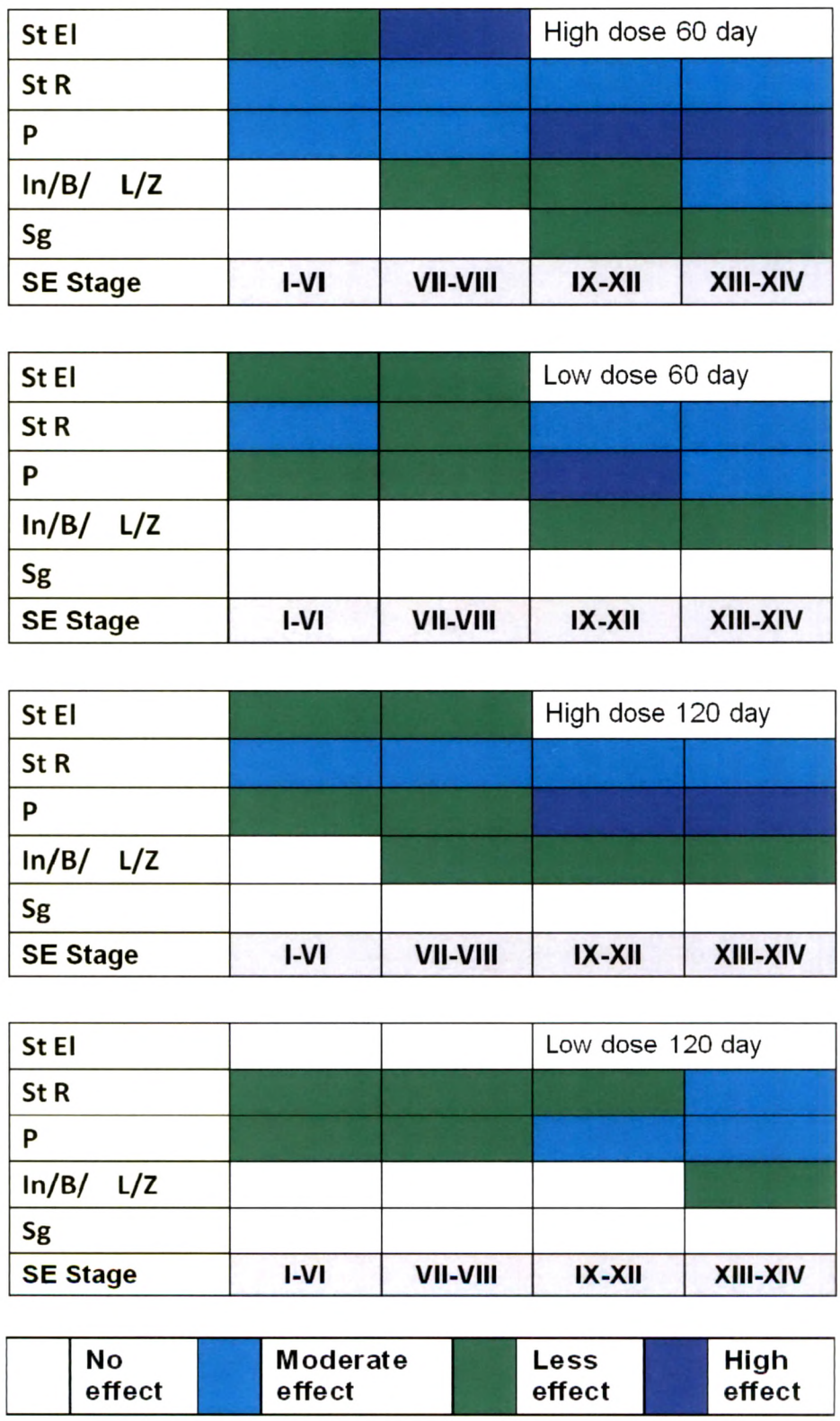

Fig. 10: Summary of histological observations

15	16	16	17	17	18	19	19	Low dose 60 day					
1	2	3	4	5	6	7	8	9	10	11	12	13	14
P	P	P	P	P	P	P	P	P	P	P	P	D	SS
In	In	In	In	B	B	PI	PI	L	L	L	Z	Z	P
A	A	A	A	A	A	A	A	A	A	A	A	A	A
I	II	III	IV	V	VI	VII	VIII	IX	X	XI	XII	XIII	XIV
SEMINIFEROUS EPITHELIAL STAGES													

15	16	16	17	17	18	19	19	High dose 60 day					
1	2	3	4	5	6	7	8	9	10	11	12	13	14
P	P	P	P	P	P	P	P	P	P	P	P	D	SS
In	In	In	In	B	B	PI	PI	L	L	L	Z	Z	P
A	A	A	A	A	A	A	A	A	A	A	A	A	A
I	II	III	IV	V	VI	VII	VIII	IX	X	XI	XII	XIII	XIV
SEMINIFEROUS EPITHELIAL STAGES													

	No effect		
	Less effect (+)		Moderate-High effect (+++)
	Less-Moderate effect (++)		Very High effect (++++)

Fig. 10 (Contd): Summary of histological observations

15	16	16	17	17	18	19	19	Low dose 120 day					
1	2	3	4	5	6	7	8	9	10	11	12	13	14
P	P	P	P	P	P	P	P	P	P	P	P	D	SS
In	In	In	In	B	B	PI	PI	L	L	L	Z	Z	P
A	A	A	A	A	A	A	A	A	A	A	A	A	A
I	II	III	IV	V	VI	VII	VIII	IX	X	XI	XII	XIII	XIV
SEMINIFEROUS EPITHELIAL STAGES													

15	16	16	17	17	18	19	19	High dose 120 day					
1	2	3	4	5	6	7	8	9	10	11	12	13	14
P	P	P	P	P	P	P	P	P	P	P	P	D	SS
In	In	In	In	B	B	PI	PI	L	L	L	Z	Z	P
A	A	A	A	A	A	A	A	A	A	A	A	A	A
I	II	III	IV	V	VI	VII	VIII	IX	X	XI	XII	XIII	XIV
SEMINIFEROUS EPITHELIAL STAGES													

	No effect		
	Less effect (+)		Moderate-High effect (+++)
	Less-Moderate effect (++)		Very High effect (++++)

Fig. 11: Diagrammatic representation of the mode of action and toxic responses of testis. The toxicant penetrate through the tubule, disrupt Sertoli-Sertoli and Sertoli-spermatogenic cell junctional complexes,get distributed in the adluminal compartment of the tubule and influence meiotically dividing cells direcetly or through the Sertoli cell. Damage to peritubular membrane may lead to leakage of exudates in the interstitium.

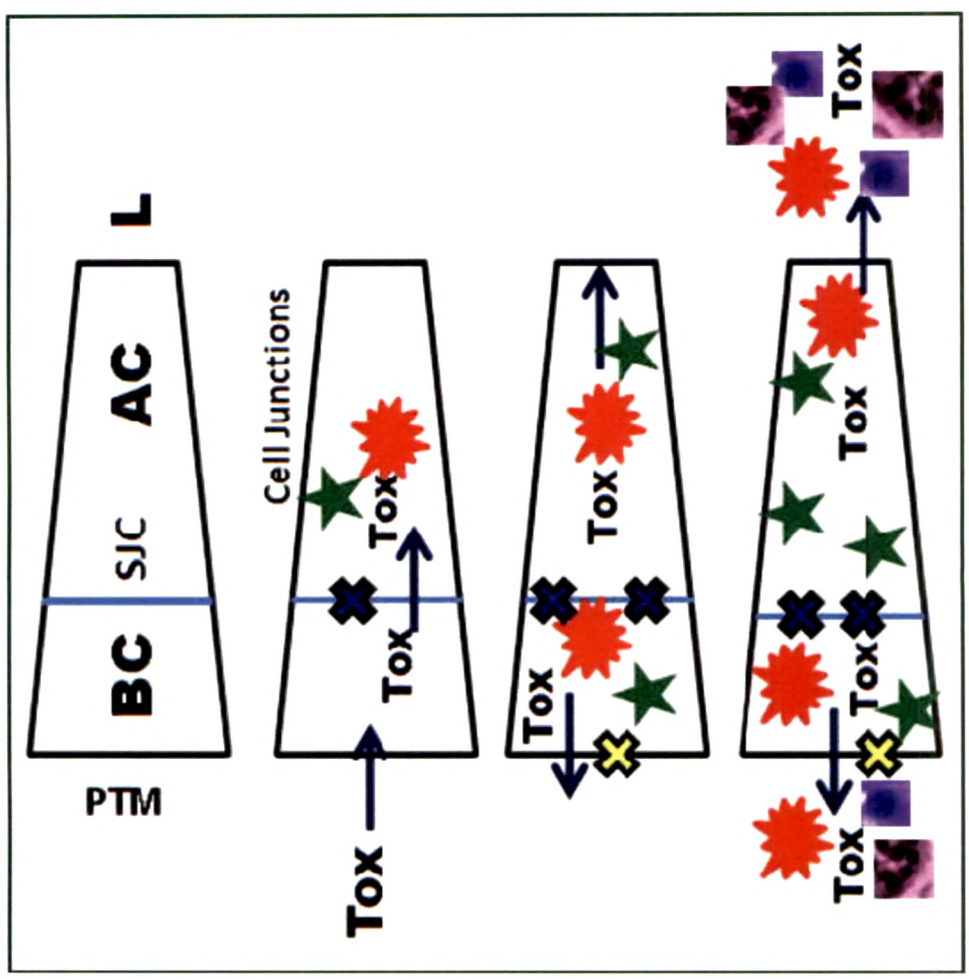

PLATE 1

Showing the transections of the testis from the adult control rat.

The Figures demonstrate normal histoarchitecture where the compactly arranged seminiferous tubules are lined by the peritubular membrane. The germinal epithelium shows the appropriate cellular organization where spermatogenic cells of progressive developmental stages are successively organized from the base to the lumen of the tubule. The interstitium is distinct. a, b: 200X, c,d: 400X

PLATE 1

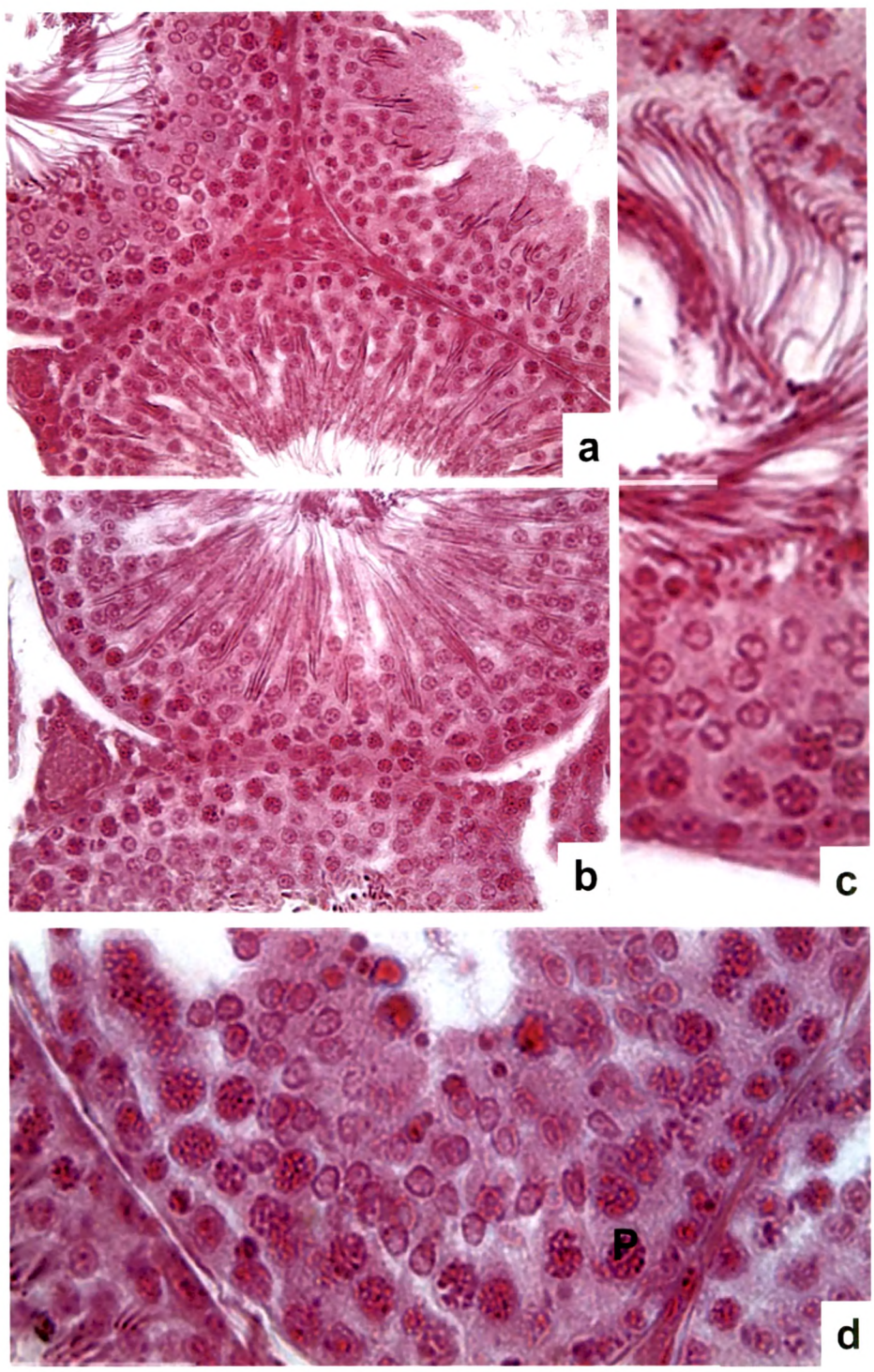

PLATE 2

Transection of testis demonstrates appropriate organization of germinal epithelium where the variation in the height of epithelium is clearly seen. This variation is due to differences in the spermatogenic cell associations.

a to f : 200X

PLATE-2

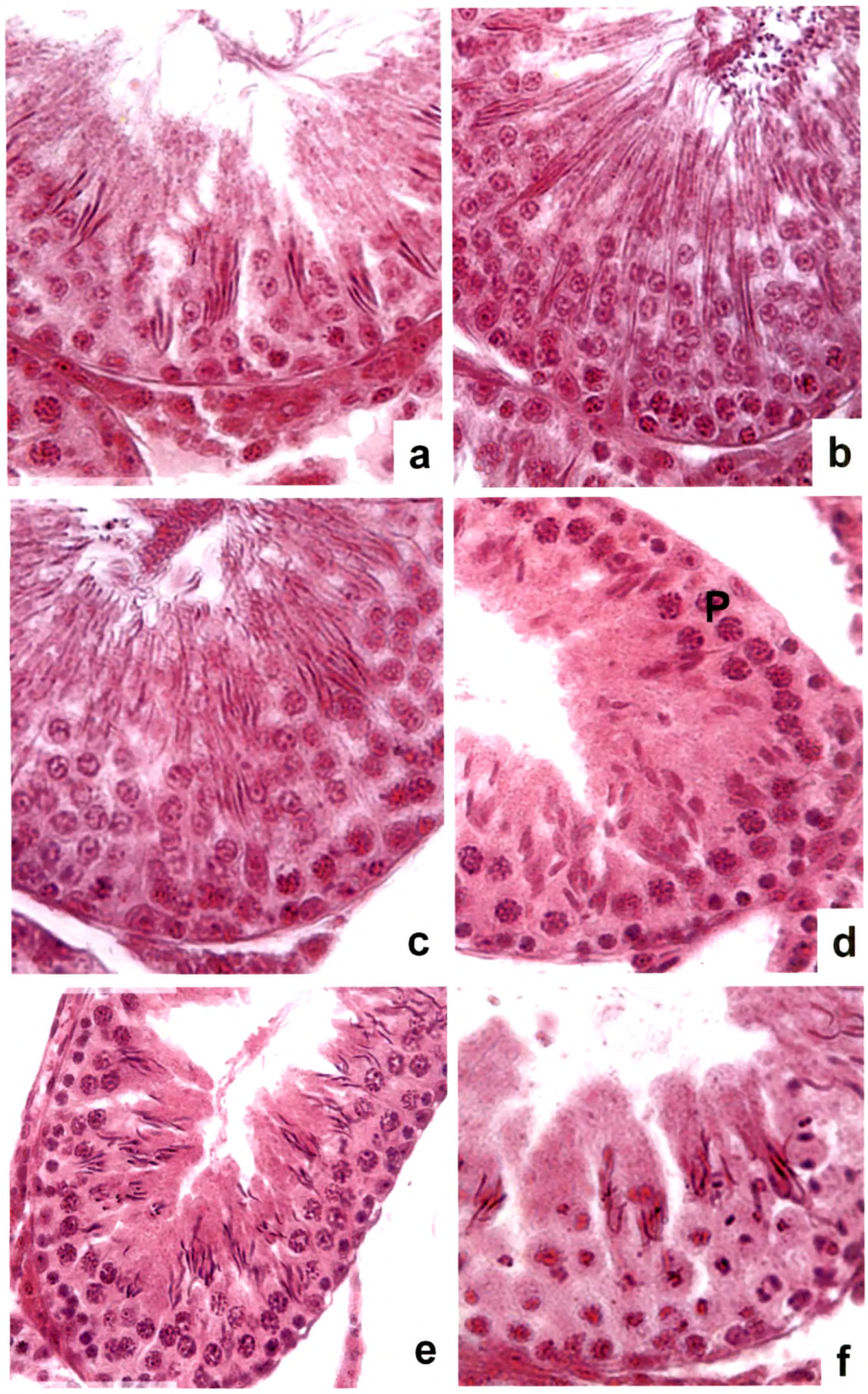

PLATE 3

Plates 3 to 6 describe the spermatogenic cellular associations at I to XIV stages of seminiferous epithelium (SE)

The SE stages I to VI are shown in Plate 3. With the progression of spermatogenesis, the location of spermatogenic cell and therefore the organization of their epithelium is modified. Note the variations in the type of the spermatogenic cells associated with the Sertoli cells, size of their nuclei and their location in the epithelium. The spermatogonia type A (A), intermediate (IM) and B (B) as well as the leptotenes are located at or near the basement membrane. The early pachytenes and the round spermatids are located in the crypt region while the elongated spermatids particularly at SE stage I, II and V are located in the crypt region, at stages III and IV in the basal region and in the adluminal region at SE stage VI.

a to f : 200X

PLATE 3

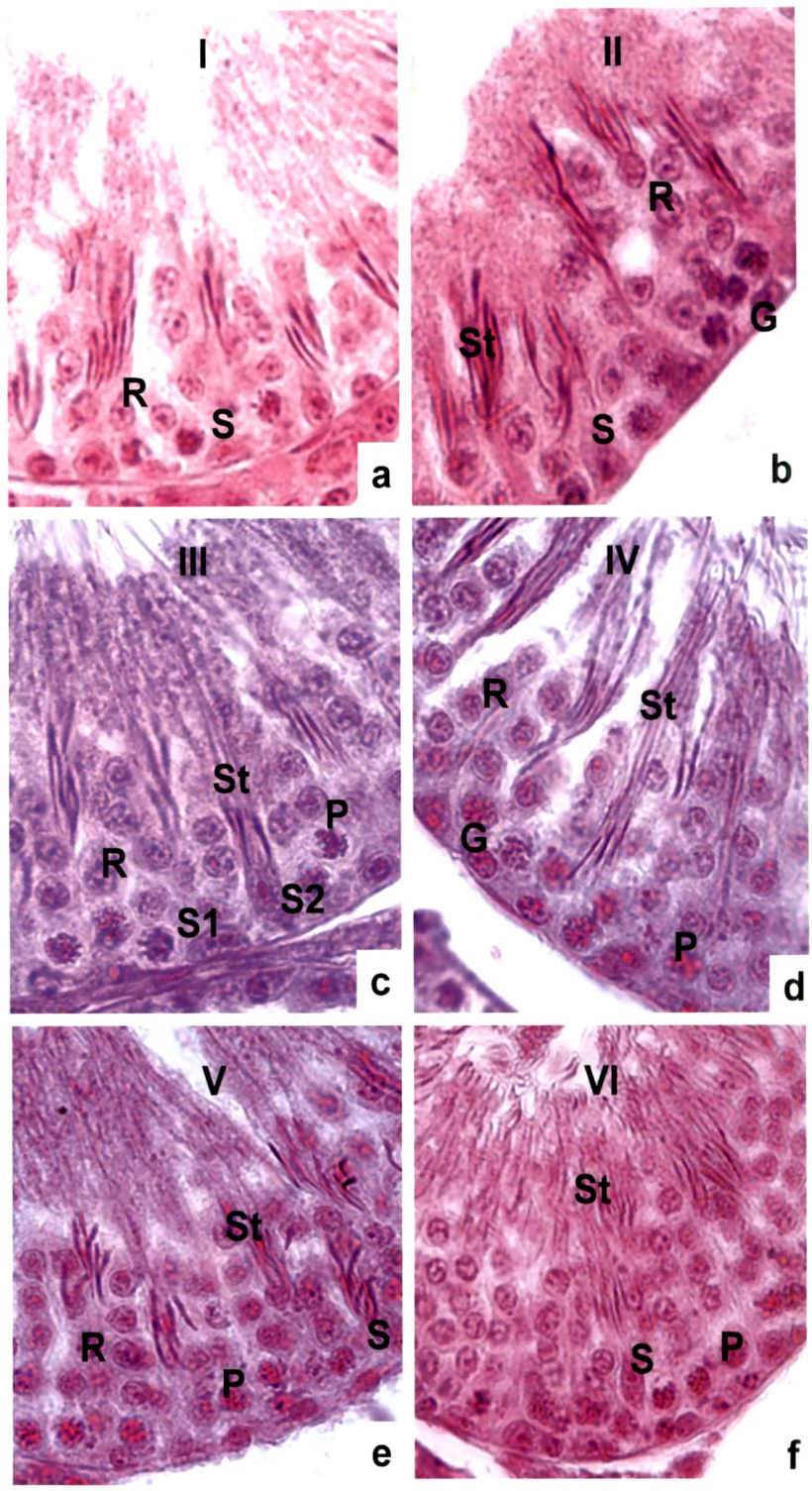

PLATE 4

The photographs describe the spermatogenic cell association at SE stages VII to IX. The spermatids progressively metamorphose from round to early elongating stages. During these stages spermeiogenesis occurs. The elongated spermatids located in the adluminal region progressively move at apical end to get ready for release. During this period the cytoplasmic remnant is released as residual body near the epithelial margin towards the lumen (stage VIII a) upon complete release of spermatozoa from lumen the residual bodies are taken up by the apical cytoplasm of Sertoli cell and phagocytosed to form phagolysosome (stage VIII b). These residual bodies are mostly destroyed in the apical and crypt region of Sertoli cell cytoplasm by the completion of the stage.

The beginning of the elongation of the round spermatids is designated as stage IX and by that time the cytoplasm is cleared of the residual bodies.

a,b : 400X, c to f : 200X

PLATE 4

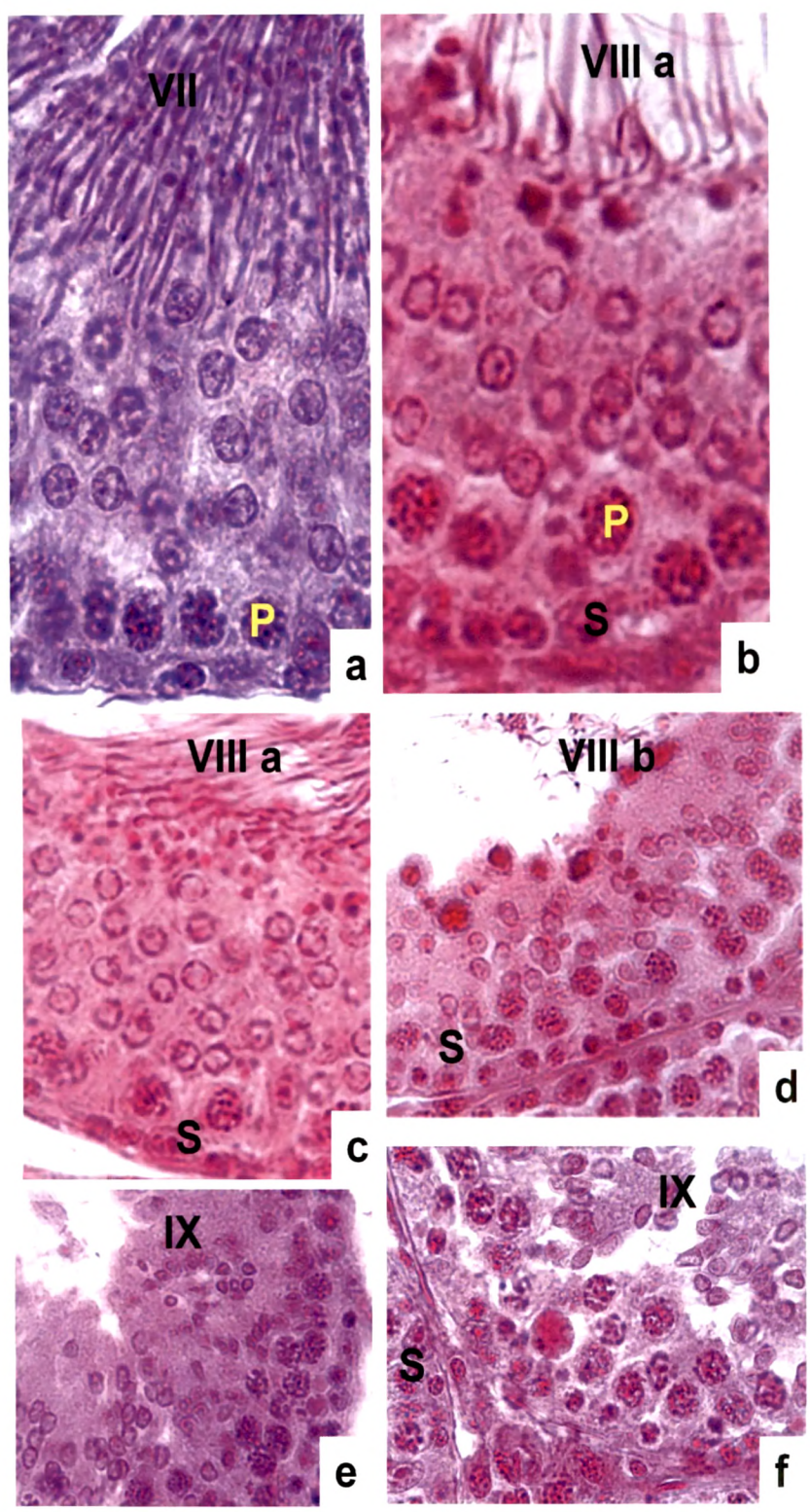

PLATE 5

The photographs showing cellular associations at SE stages IX to XIII.

The events are prominently marked by elongation of the spermatid and hence only one population of spermatid is seen at SE stages IX to XIV. Since the round spermatids occupy large space the height of the epithelium at SE stages I to VIII is grater than at stages IX to XIV. The leptotenes are converted to zygotenes and the late pachytenes progress further to diplotene stage of the first meiosis. The elongating spermatids are located in the crypt region and their cytoplasm extends beyond the Sertoli cell cytoplasm.

a to g: 400X

PLATE 5

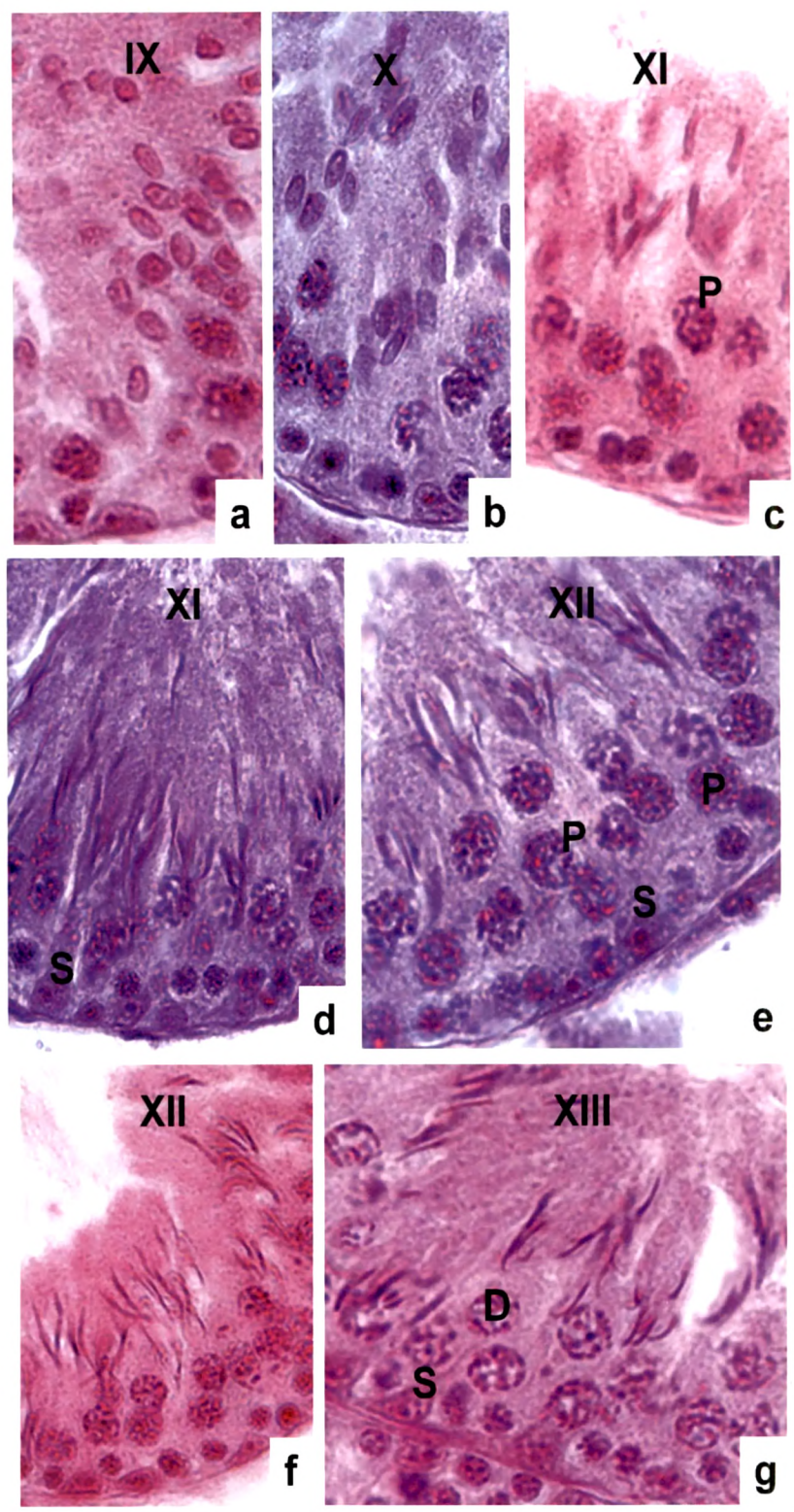

PLATE 6

The photographs showing spermatogenic cellular association at SE stages XIII, XIV and I.

During this period the last phase of first meiotic division is completed that forms secondary spermatocyte (XIV a) which further undergoes second meiosis (XIV b) to form round spermatids (XIV c). The chromatin organization at diplotene (D) at SE stages XIII and that at diakinesis (Di) at SE stage XIV a are distinctly seen as identification features of the stage. The mitotic features of second meiosis are prominently seen.

The photograph f shows SE stage I thatimmediately follows SE stage XIV c for the reference of cell associasions and distribution of cell types.

a, b, c, d, e, f : 400X

PLATE 6

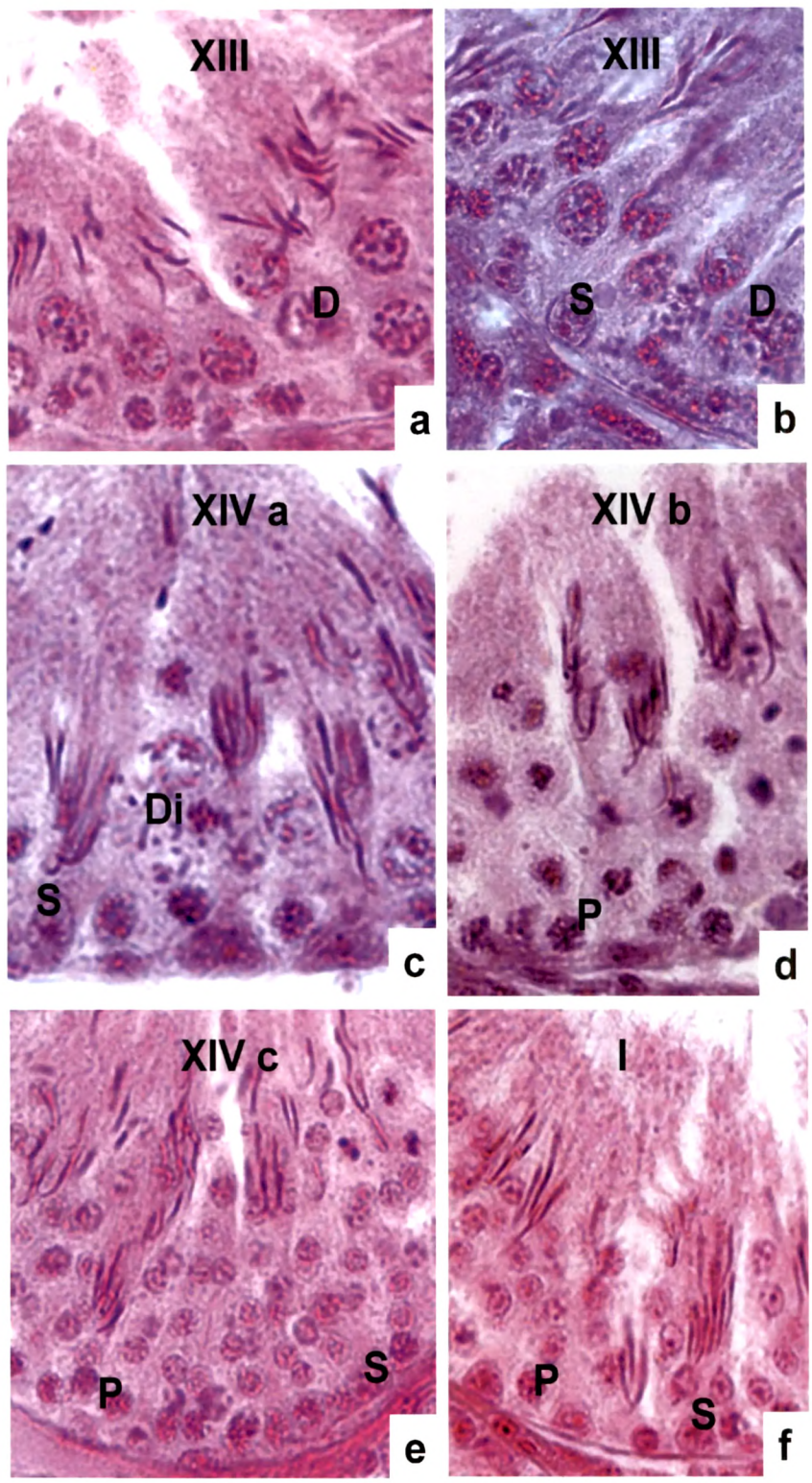

PLATE 7

The Sertoli cels exhibit morphological variations depending upon the various cellular associations at different stages of seminiferous epithelium. Interestingly, the nuclear morphology is also modified. This is distinctly demonstrated in this Plate where the morphological features of the Sertoli nuclei (S) are shown. In b, the nuclei on the left is lying along the peritubular membrane while that on the right still has a close association with elongated spermatids and hence is arranged vertically like that noted in the photo a.

a to f : 1000X

PLATE 7

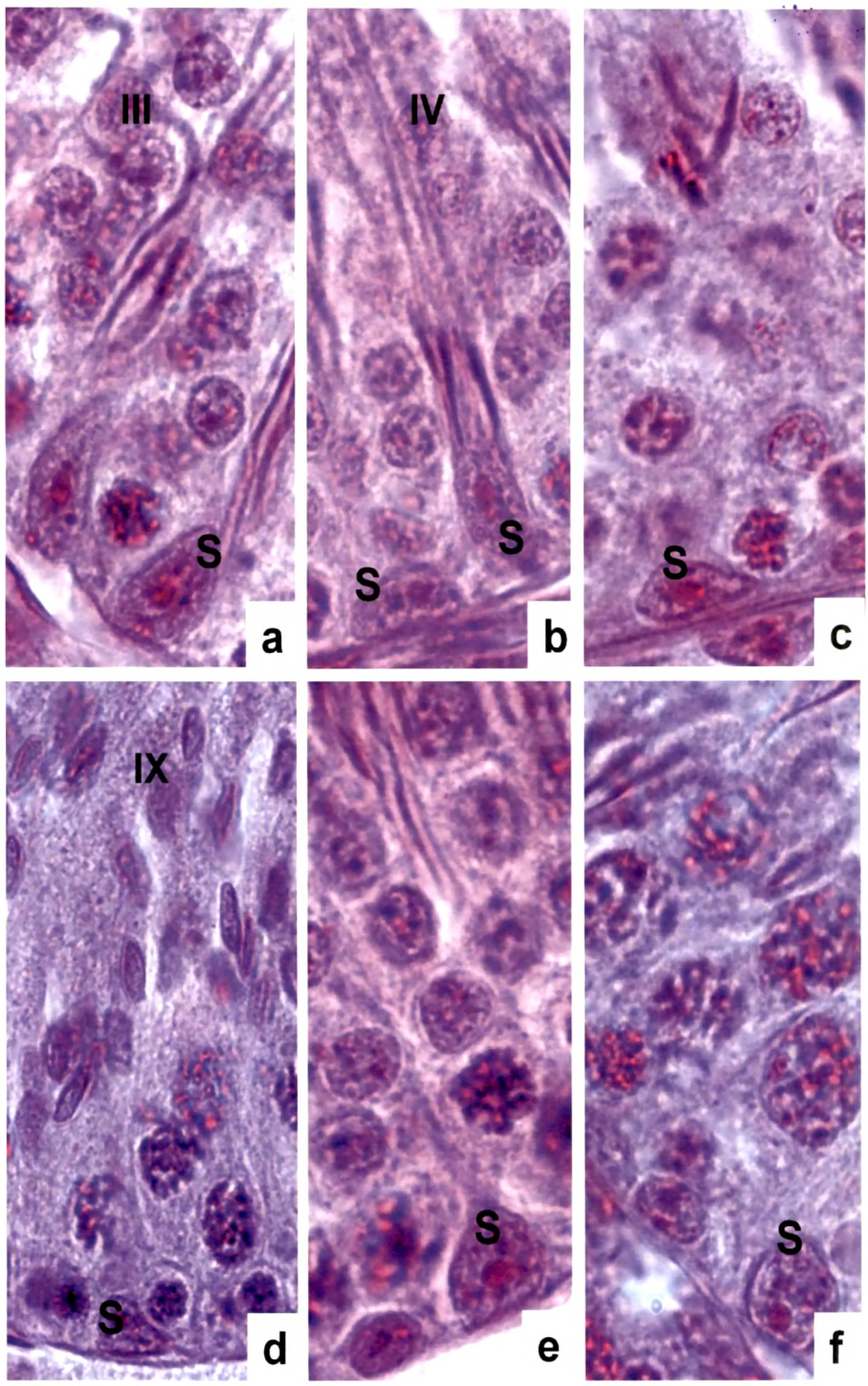

PLATE 8

The seminiferous peritubular membrane in rat consists of single layer of myoepithelial cell and the collagen fibers located externally. It also forms primary barrier for transportation of materials acroos the tubules.

a Depicts the structural integrity of peritubular membrane in the testis of control rat. 1000X

b, c and d The basal profile of the seminiferous tubules of the rat exposed to high dose of toxicant for 60 days shows damage to the integrity of the peritubular membrane. In photo d, leakage from the tubule into the interstitium is also seen. 400X

e, f and g Extensive loss of integrity of the seminiferous peritubular membrane demonstrating accumulation of cytoplasmic dissolution products towards the base of the tubule which may leak out into the interstitium. 400X

h and I Showing the edematous interstitium (IE). h: 400X, i: 200X

PLATE 8

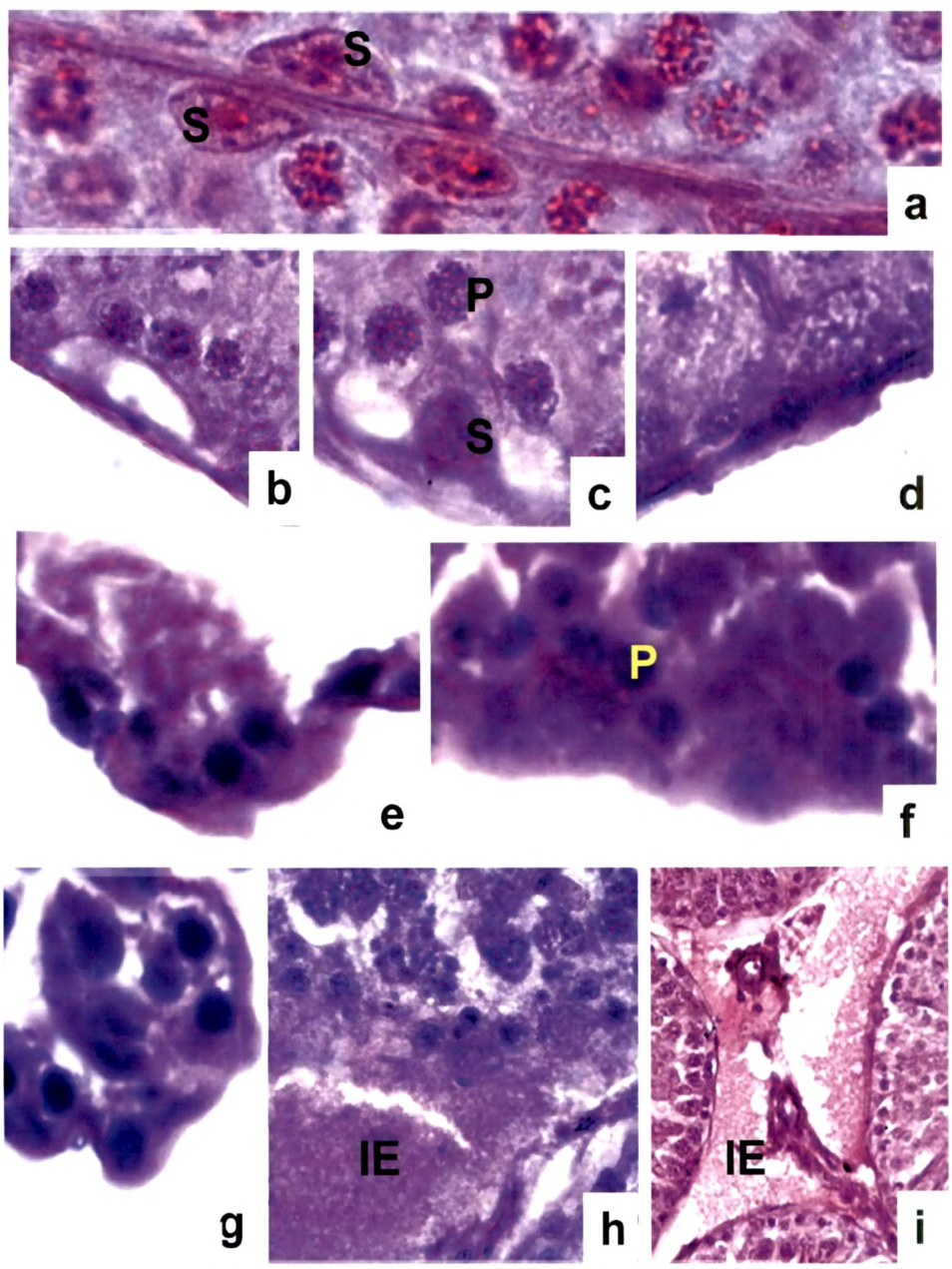

PLATE-9

Showing the transection of testis of rat treated with high dose of heterogenous chemical mixture for 60 days.

a The spermatogenic cellular associations at different stages demonstrate that structural integrity of the epithelium is affected and several zygotenes and pachytenes at stage XII were pycnotic. 400X

b At stage XIV cytoplasmic blebbing is seen and the elongating spermatids are detached from the epithelium and show premature release from the epithelium. 400X

c At stage VIII, the elongated spermatiols have just got released. However, the distribution of pachytene is inappropriate. Some of them were located in the apical portion or sloughed withim the lumen. 400X

PLATE-9

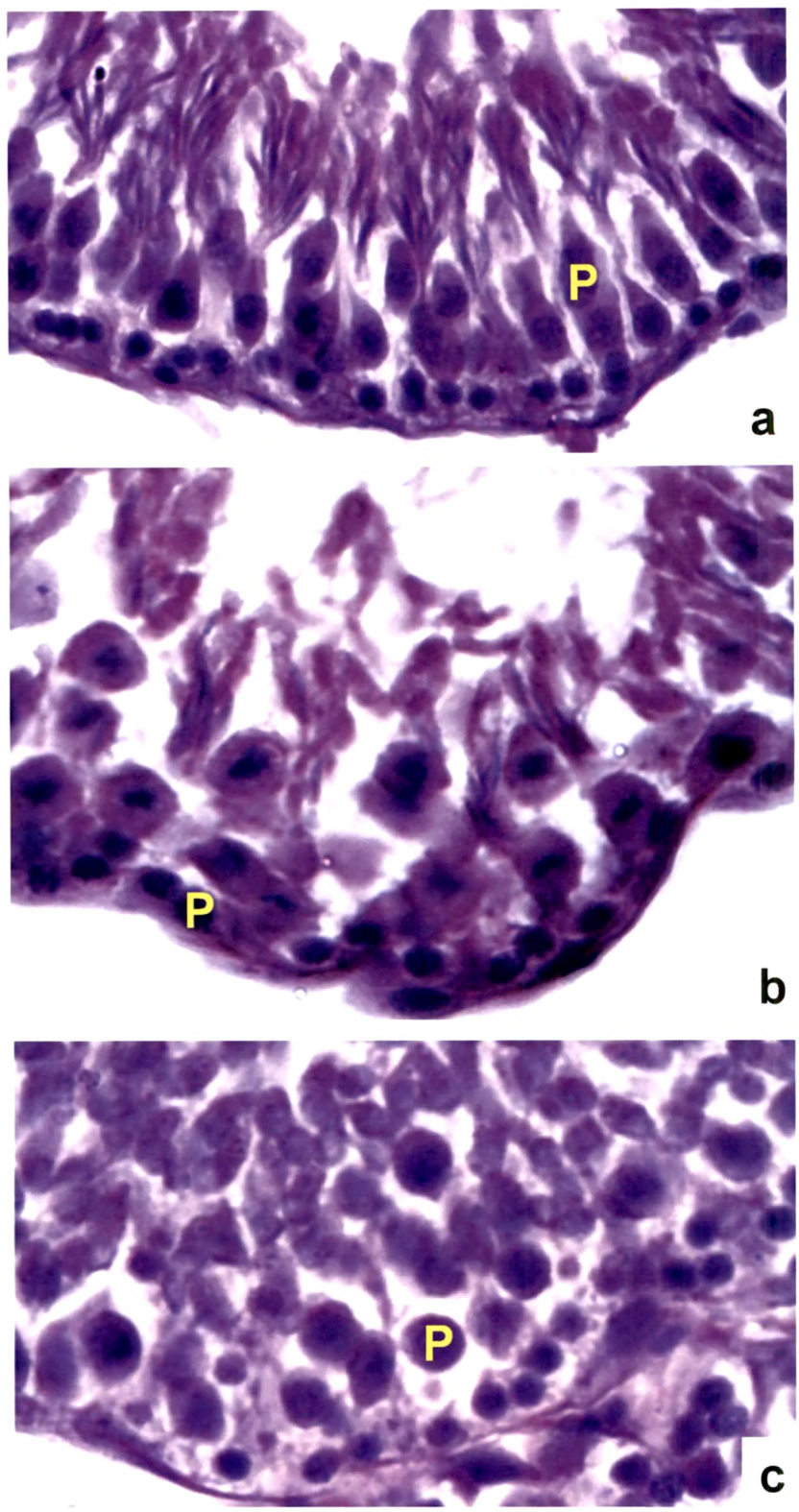

PLATE 10

Cytoplasmic blebbing and cell sloughing are prominent responses of the Sertoli cells to the toxic insult. This is regarded as feature where the damaged spermatogenic cell and the degenerating cytoplasmic masses are released into the lumen.

a to d The high dose of heterogenous chemical mixture exposure for 60 days lead to extensive sloughing and loss of more mature spermatogenic cells particularly at stages IX to XIV.

e,f and g The low dose exposure for 60 days also shows similar features. In several cases the residual bodies released during at spermiation at SE stage VIII were not taken up by the Sertoli cells and were released into the lumen. e,f,g : 200X

PLATE 10

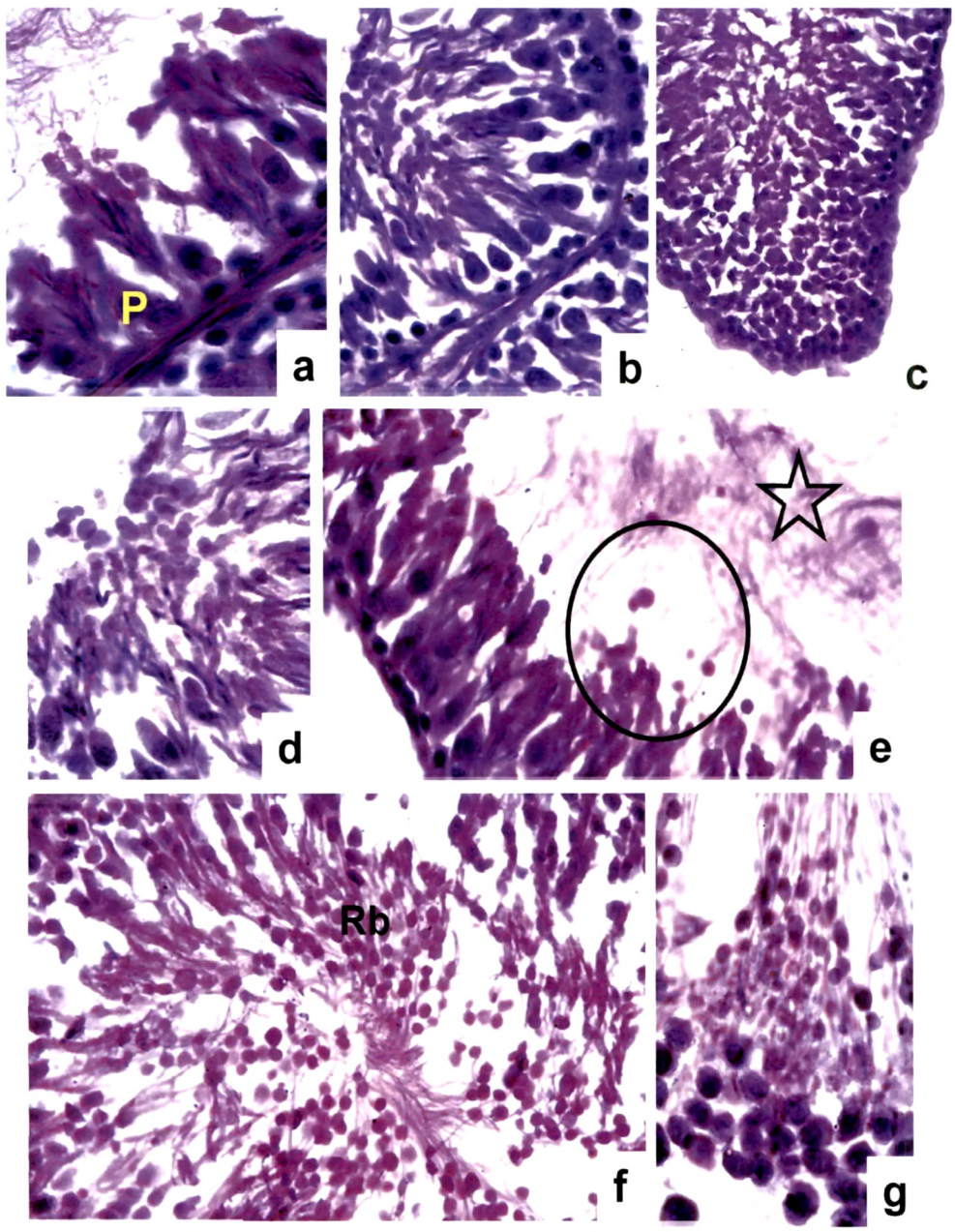

PLATE 11

The luminal accumulation of cytoplasmic exudates, fluid and cellular debris are prominent features of Sertoli cells toxic responses. It was more conspicuously observed in high dose exposure group. The lumen of the tubules at different stages was almost completely filled up with the debris and the fluid exudate. a, b: 200X and c,d and e: 400X

f The occurance of vacuoles in between the epithelia filled with debris and fluid indicate critical damage to Sertoli cytoplasm. It is clearly seen that the nuclei of degenerating cells are located along such vacuoles which will lead to their detachment from the epithelium and final release into the lumen. 400X

g This shows a cytoplasmic mass which has accumulated cell debris and necrotic nuclei. Such clumps were located in different regions of the epithelium in the high dose group. 400X

h Severe depopulation of the spermatogenic cells lead to condition correlated with Sertoli only syndrome. However, here a few primary spermatocytes were also seen. 200X

PLATE 11

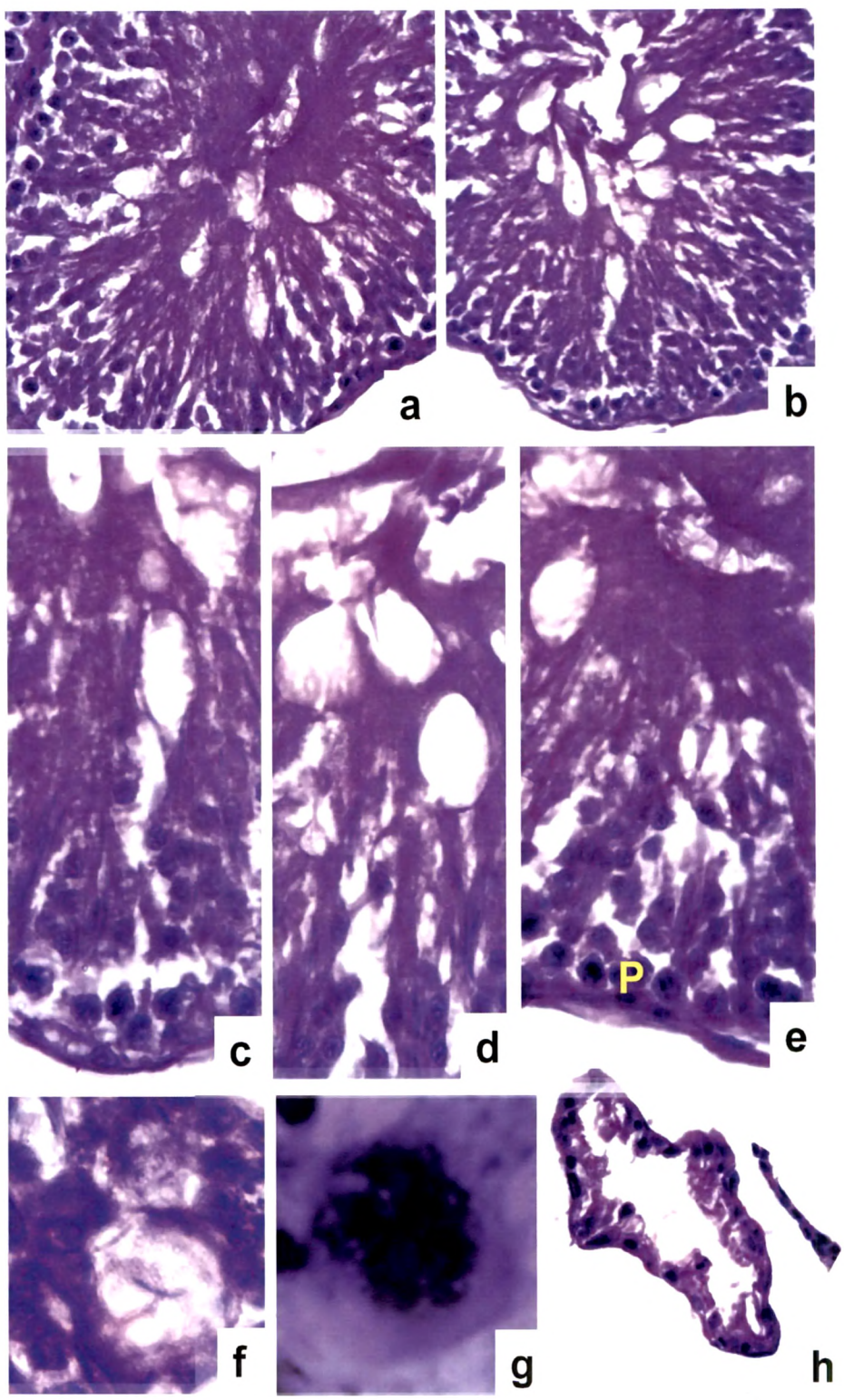

PLATE 12

Vacuolation in the basal cytoplasm of Sertoli cells is also important feature of toxic responses.

a and b Shows the basal profile of Sertoli cell of the control testis where the Sertoli cell cytoplasm is quite granular, distinct and surrounds the spermatogenic cells.1000X

c, d and e The toxicant exposure lead to formation of vacuolation in the basal cytoplasm of Sertoli cells following exposure to toxicant for 60 days.1000X

f and g The extension of vacuolation may indicate typical histological changes as depicted in these photographs. In photo f the smaller vacuoles fuse together to form large vacuole which will tend to dissociate the junctional complexes. In photo g, the extension and expansion of the vacuolated region is shown (arrows) which will ultimately lead to the dissociation of large number of cellular associations into the lumen. f: 1000X ,g : 400X

PLATE 12

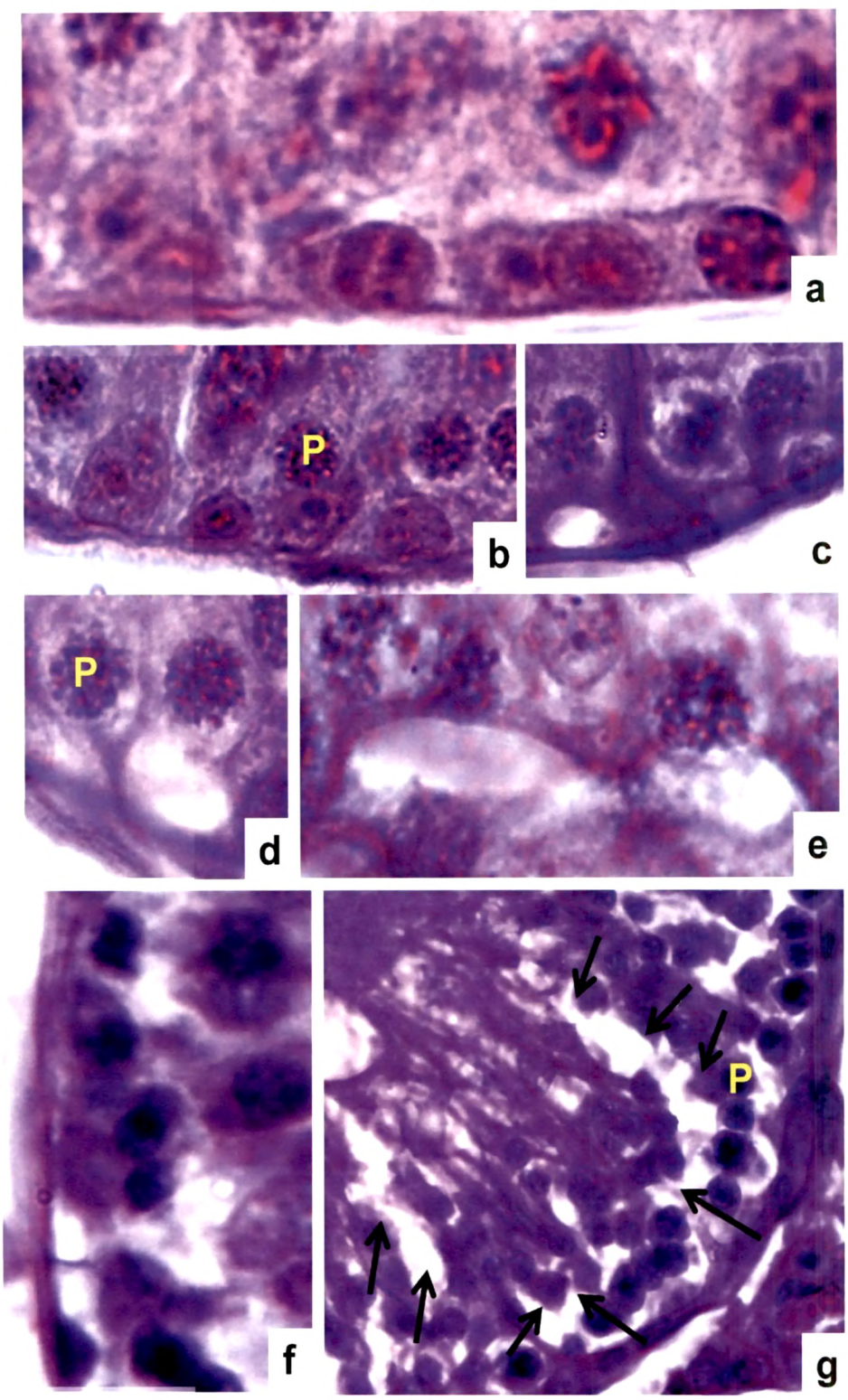

PLATE-13

The prominent effect of high dose heterogenous chemical mixture exposure for 60 days were noted at SE stage IX-XIV. The vacuolation in basal and crypt region as well as cytoplasmic blebbing and release of elongating spermatids as clumps were seen. 600X

PLATE-13

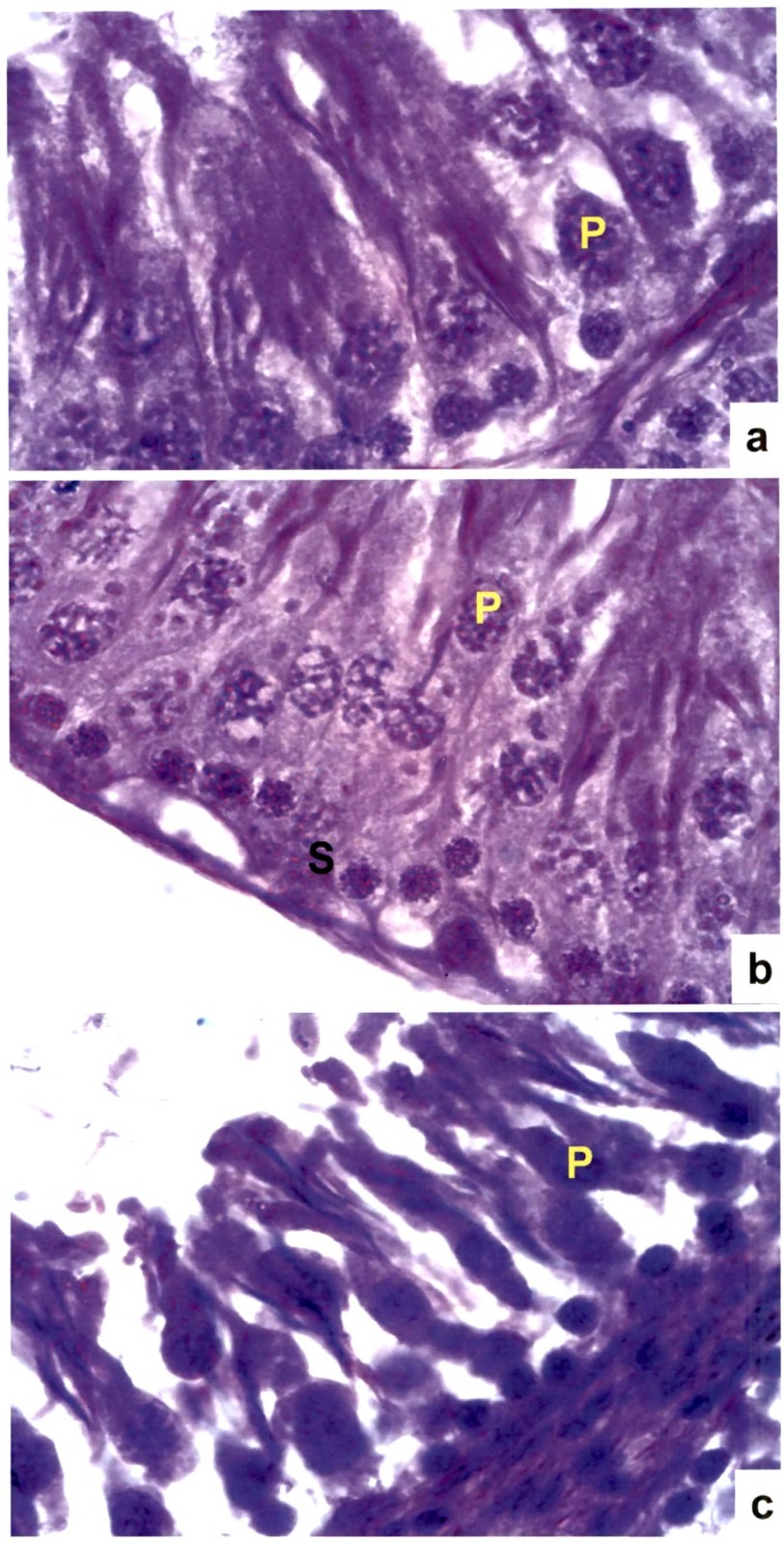

PLATE 14

a and b The toxicant exposure at low dose for 60 days also lead to conspicuous degenerative changes at stages IX to XIV although in several cases it was less prominent compared to the high dose exposure group.

a, b: 1000X

c The cytoplasmic dissolution (thick arrow) formation of cellular debris (thin arrow) and the extension of vacuole (star) exhibit the progressive migration of the degenerative cell content from the crypt to the apical end of the epithelium. This photograph clearly depicts how the degenerative nuclei is sloughed off and is indicative of extensive cytoskeletal damage. 1000X

PLATE 14

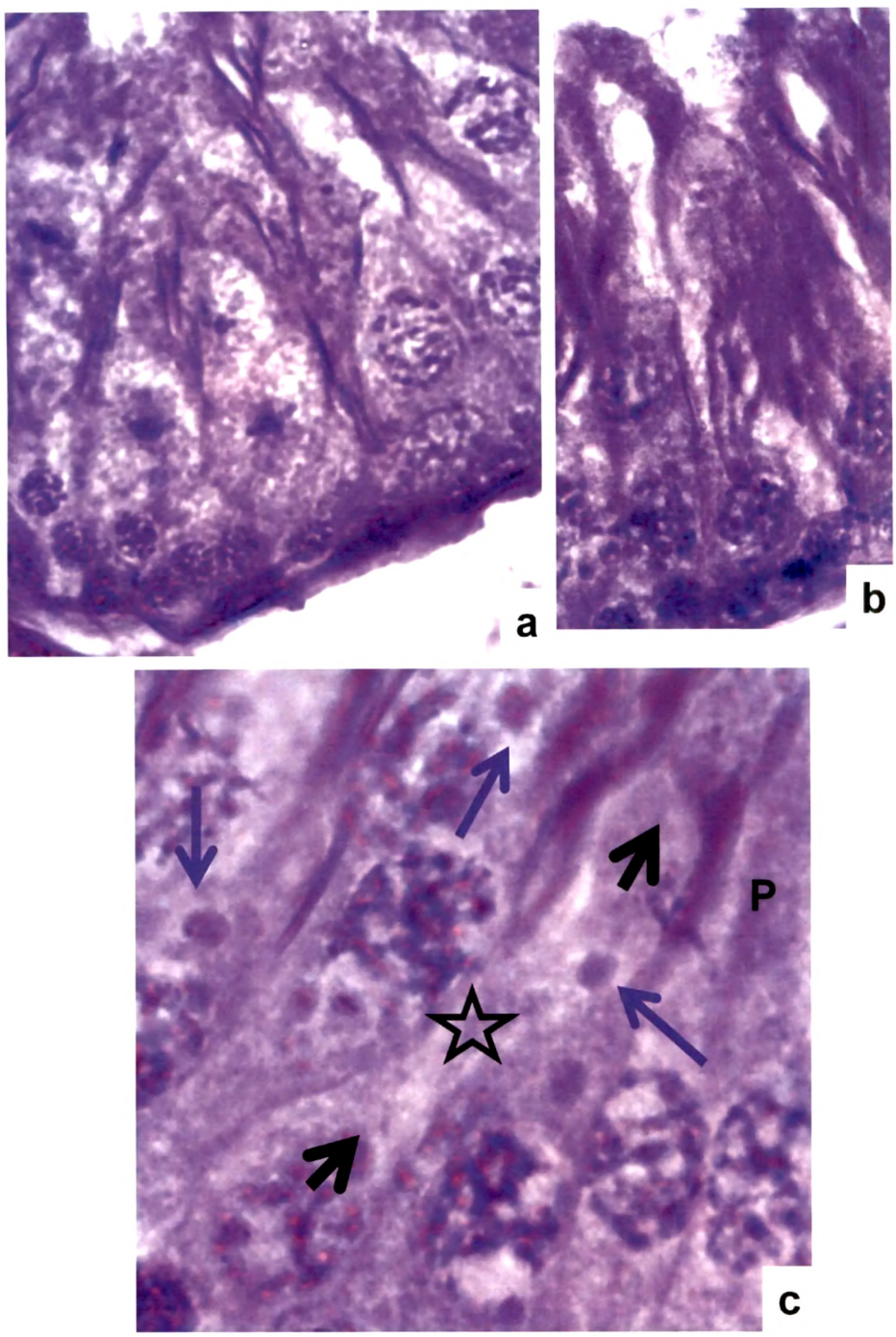

PLATE 15

The status of spermatids and late meiotic chromosomes is shown where the sperm abnormalities are clearly depicted.

a, b Showing the status of meiotic chromosomes at SE stage XIV; the fragmentation is clear in high dose 60 day treatment group in photo a (thinl arrow). While, following recovery in the same group, the normal meiotic chromosomes were seen. a: 400X, b: 1000X

c to g Depicting various spermatid abnormalities in the treatment groups. In photo d and e, SE stage XIV shows broken heads of elongating spermatids (encircled) and retension of elongated spermatid (thick arrow) which did not get released at SE stage VIII previously Also shown in photo a). Several elongated spermatids exhibited deformed head morphology. d, f: 400X, c, e, g: 1000X

The sperm head anomalies were confirmed in the epididymal spermatozoa preparations (Chapter 5 on Epididymis and Spermatology)

PLATE 15

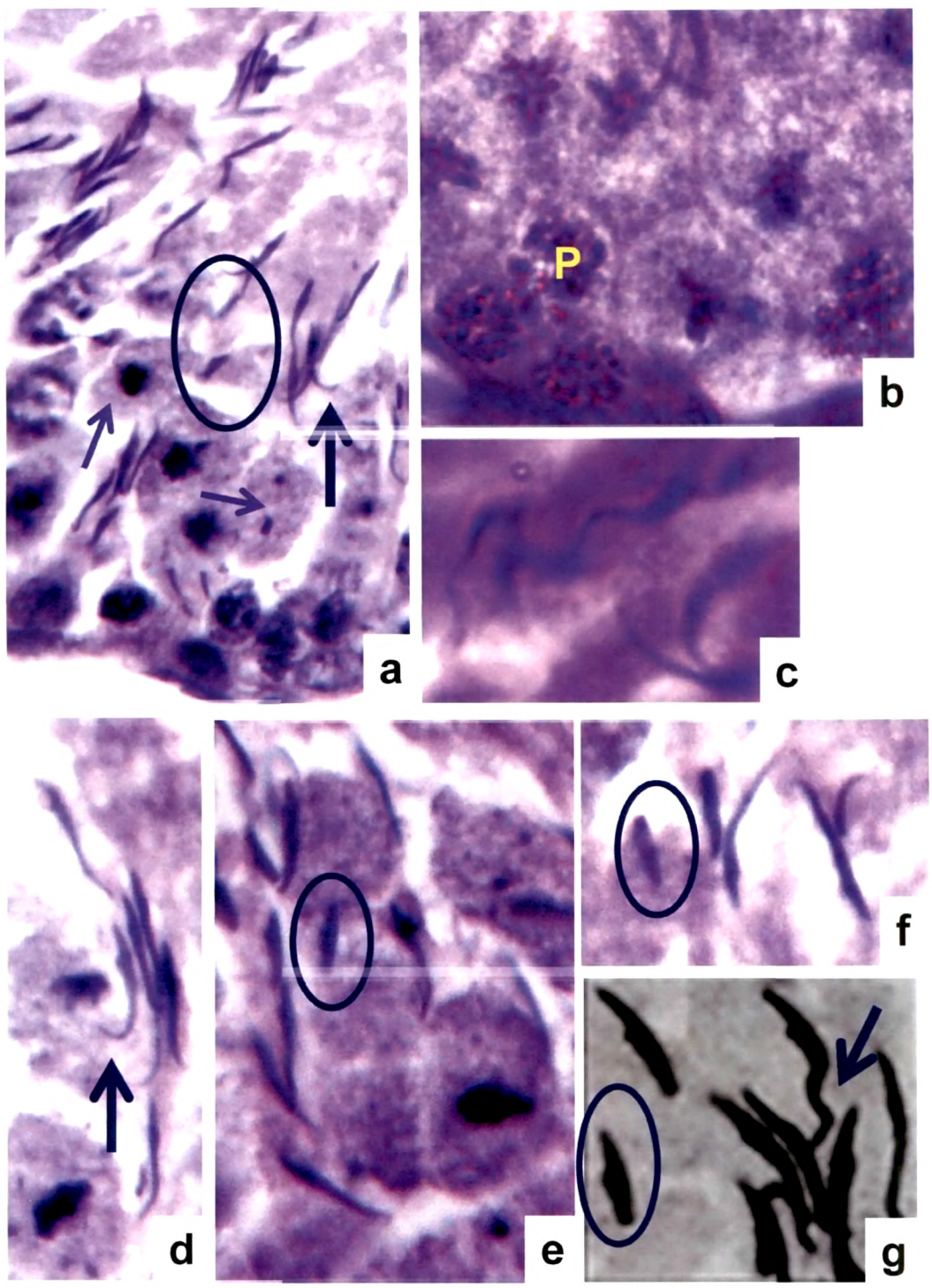

PLATE 16

The chromosomal anomalies are typical feature of toxic responses of a cell which may also indicate apoptosis status.

a,b and c The normal nuclei of zygotenes stage (a), pachytene stage (b) and diakinesis stage (c) of primary spermatocytes undergoing first meiotic division are shown. Note the typical loose flowery arrangement of chromatin at pachytene stage and marginal/ peripheral arrangement at diakinesis stage. S; Sertoli cell nucleus.

d, e and f Typical apoptotic features demonstrated by late pachytene primary spermatocyte undergoing final stage of first meiotic division. The chromatin fragmentation is clear in all as well the cytoplasmic degeneration. The damage to cell and leakage of contents is seen (arrow head). In photo e, the constrictions at more than one place (thin arrow) are suggestive of the blebbing.

g to k Other nuclear changes are seen in pachytene (g, h, i), leptotene (j) and zygotene (k) primary spermatocytes undergoinig first meiotic division. Compare the chromosome distribution, staining intensity and over all content for pachytene stage in photo b (control) and h (treatment group) and zygotenes in photo a (control) and k (treatment group).

All photographs: 1000X

PLATE 16

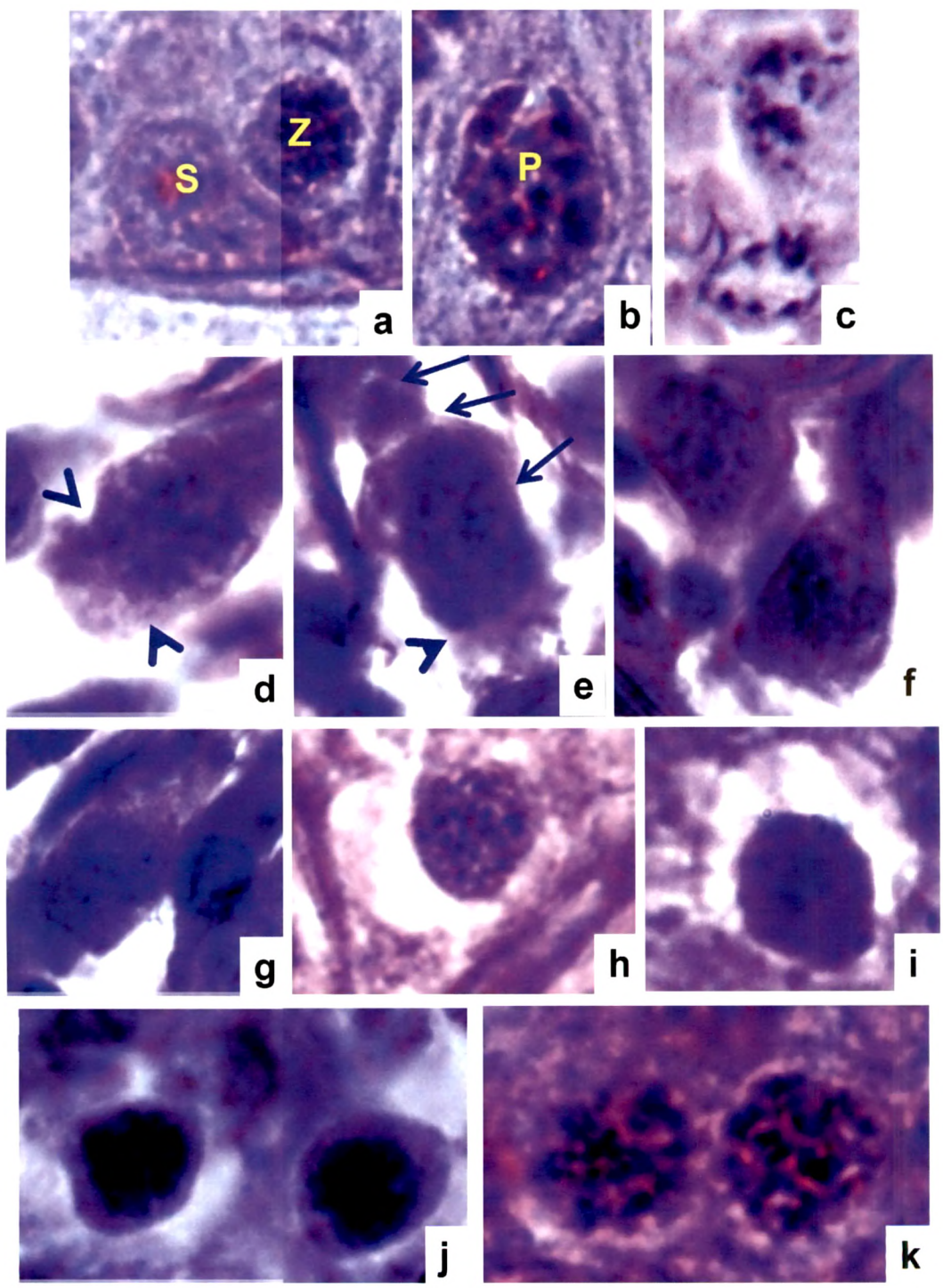

PLATE 17

a to i Showing the choromosal fragmentation as indicator of potential toxic effecet of heterogeneous chemical mixture on the spermatogenic cells. Photo a-e and g are the chromosomes of secondary spermatocytes undergoing second meiotic division (SE stage XIVb). Photo f and h are clumps of chromosomes found in SE stage XIII-XIV tubules therefore they are that of late primary spermatocyte stage. A clump of early pachytene at SE stage III suggests severe pyknosis.

j and k Highly eosinophilic cytoplasmic mass observed in the heterogeneous chemical mixture exposed group on day 60. A large multinucleated body was seen at SE stage XII while the other shown in photo k was seen at SE stage VI. The cell types present are different as seen clearly from the nuclear staining.

PLATE 17

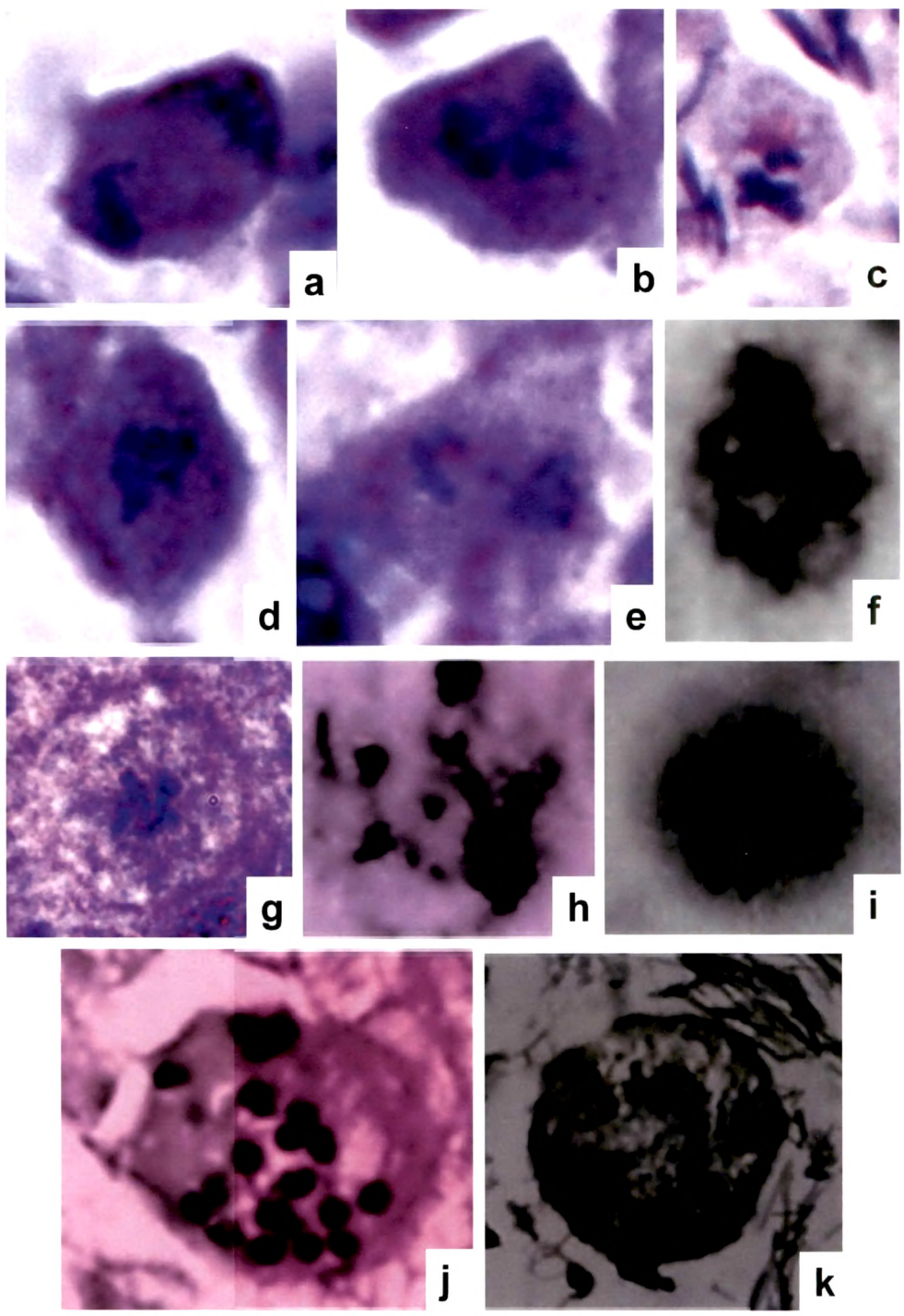

PLATE 18

Following the withdrawl phase in the high dose treatment group, the tubules at the stage I to VIII exhibited partial recovery while those at stage I to XIV shows persistant demage.

a At stage IX the phagolysosomes have not completely shattered the residual bodies and these are distributed in the basal cytoplasm of Sertoli cells. These are suppose to induce specific response by Sertoli cells. 600X

b At the stage XIV the anomalies of second meiosis are seen where the chromatin fragmentation is clear. The epithelium was indicative of degenerative changes. 400X

c At SE stage-III the changes in the basal compartment are clearly seen. However, the elongated spermatids are located at their normal position. The population of the round spermatid was still less. 400X

PLATE 18

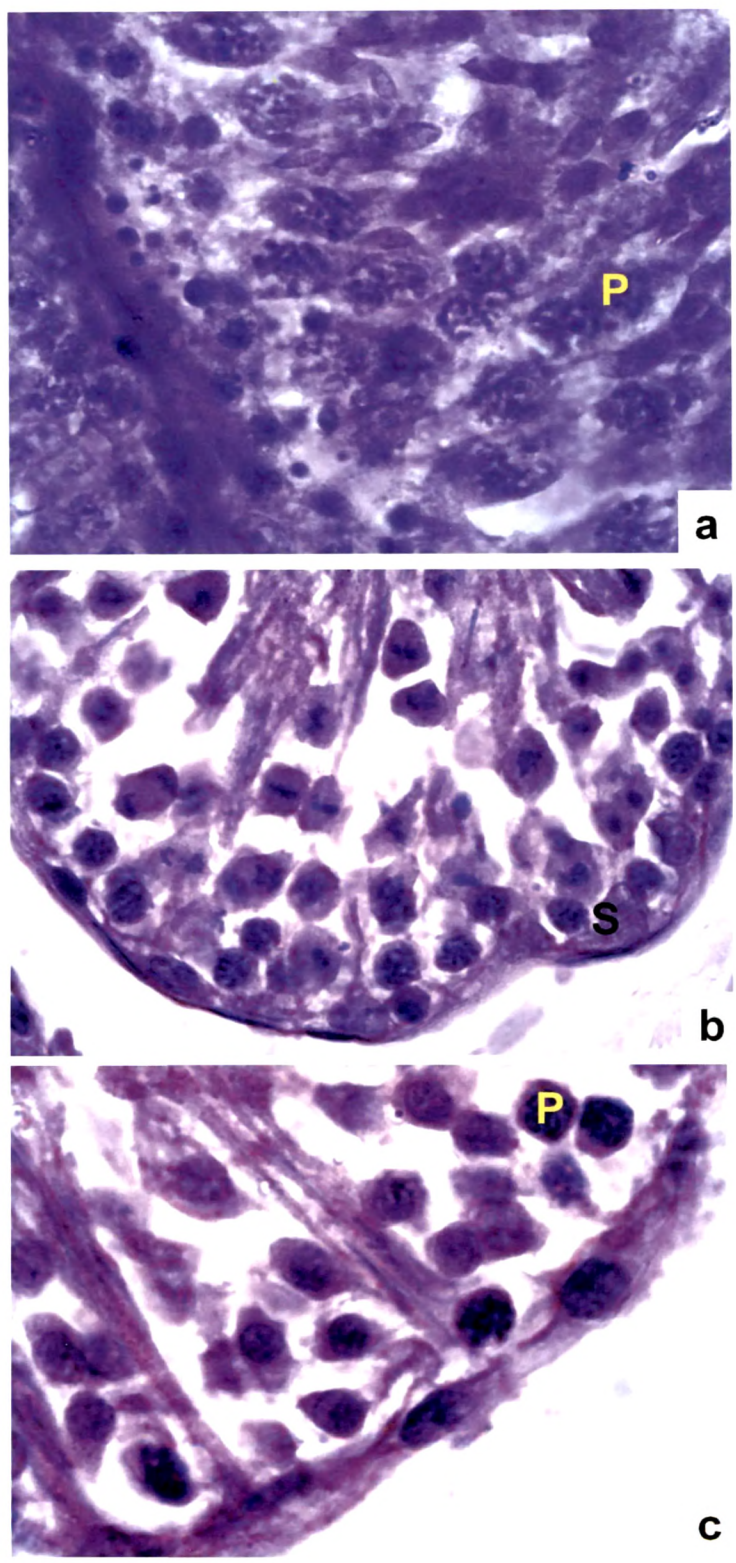

PLATE 19

Following the withdrawl phase in the high dose treatment group, the tubules at different SE stages exhibited partial recovery.

a A tubule at stage VIII showing prominent vacuolation and degeneration in the pachytene region. The residual bodies are quite large. 400X

b A large vacuole is seen in the basal portion of the tubule which has displaced the arrangement of elongated spermatids. 400X

c A tubule at stage XIV showing detachment of several meiotically dividing cells and dislodging of the elongating spermatids. 400X

d A tubule at stage IV showing comparatively better status of the epithelium and normal histoarchitecture. 400X

PLATE 19

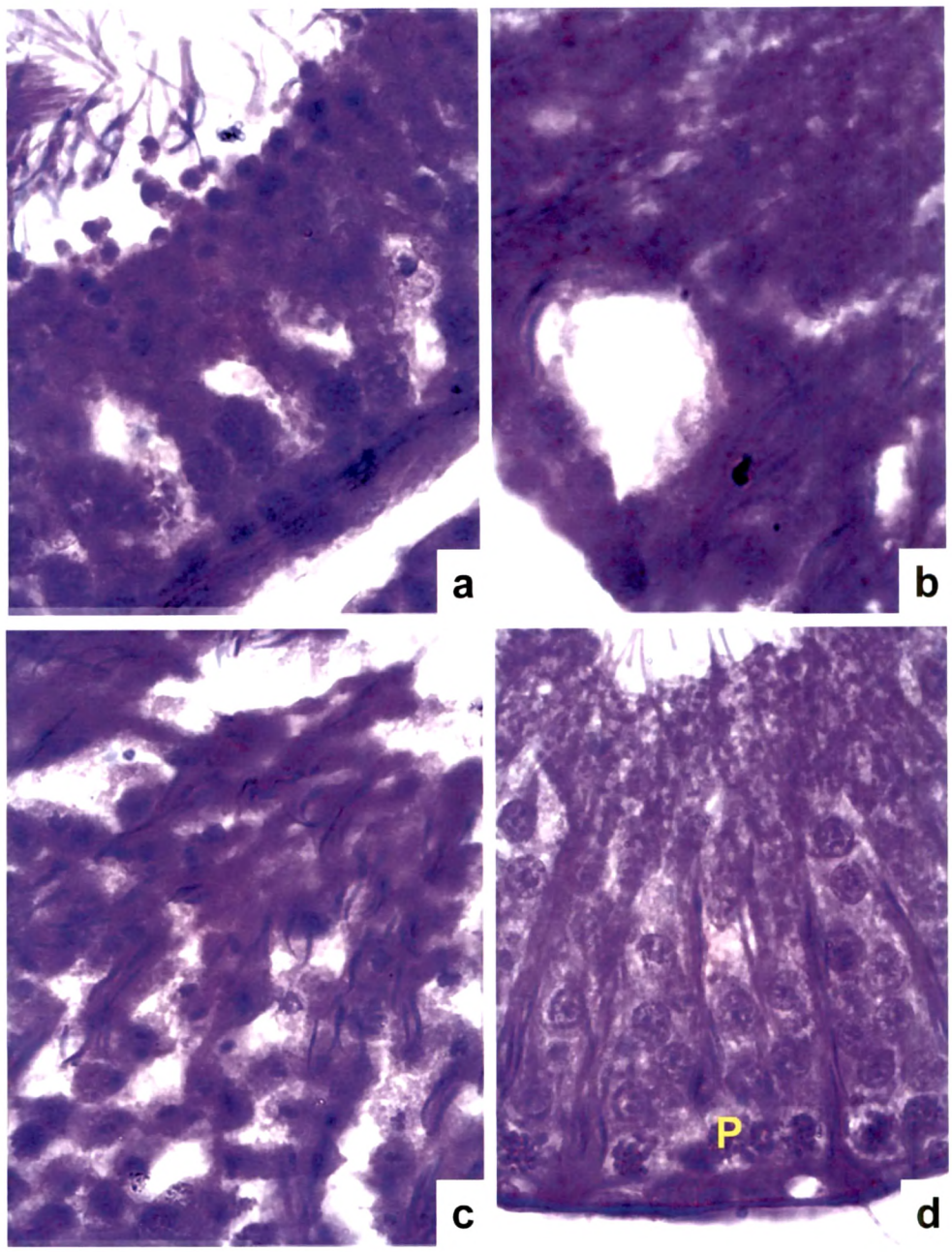

PLATE 20

Following the withdrawl phase in the low dose treatment group, the tubules at different SE stages exhibited much better recovery and almost normal progression of spermatogenesis.

a A tubule at stage IV-V shows only marginal damage in the baso-crypt region. The spermatogonia are undergoing mitosis, the round and elongated spermatid nuclei appear normal and are distributed appropriately. 400X

b A tubule at stage early XI shows basal vacuolation in the cytoplasm of Sertoli cells. All the spermatogenic cell types are normal. A bit thickening of the peritubular membrane is seen. 400X

c A tubule at SE stage XIII shows persistent moderate changes in the baso-crypt region. The nuclei of early pachytenes are normal. 400X

PLATE 20

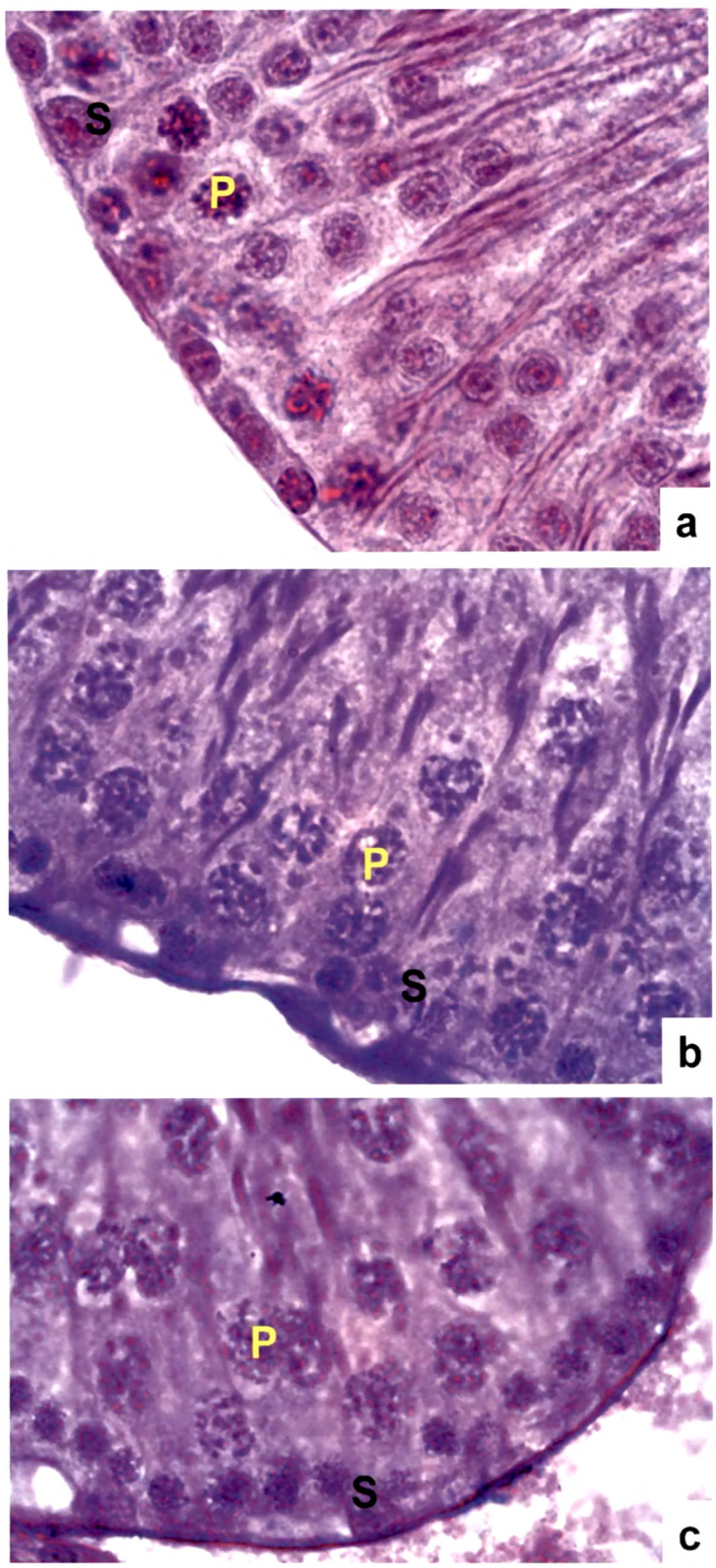

PLATE 21

In the low dose treatment group on day 120, following withdrawal of the treatment, recovery was almost complete in some of the tubules.

The tubules at SE stages V (a), XIII (b) and III (c) show normal number of spermatogenic cells and progression of the spermatogenesis.

In photo a, the number of early pachytes is indicative of normal progression of mitotic divisions in the spermatogonia during the recovery phase.

All photographs 400X

PLATE 21

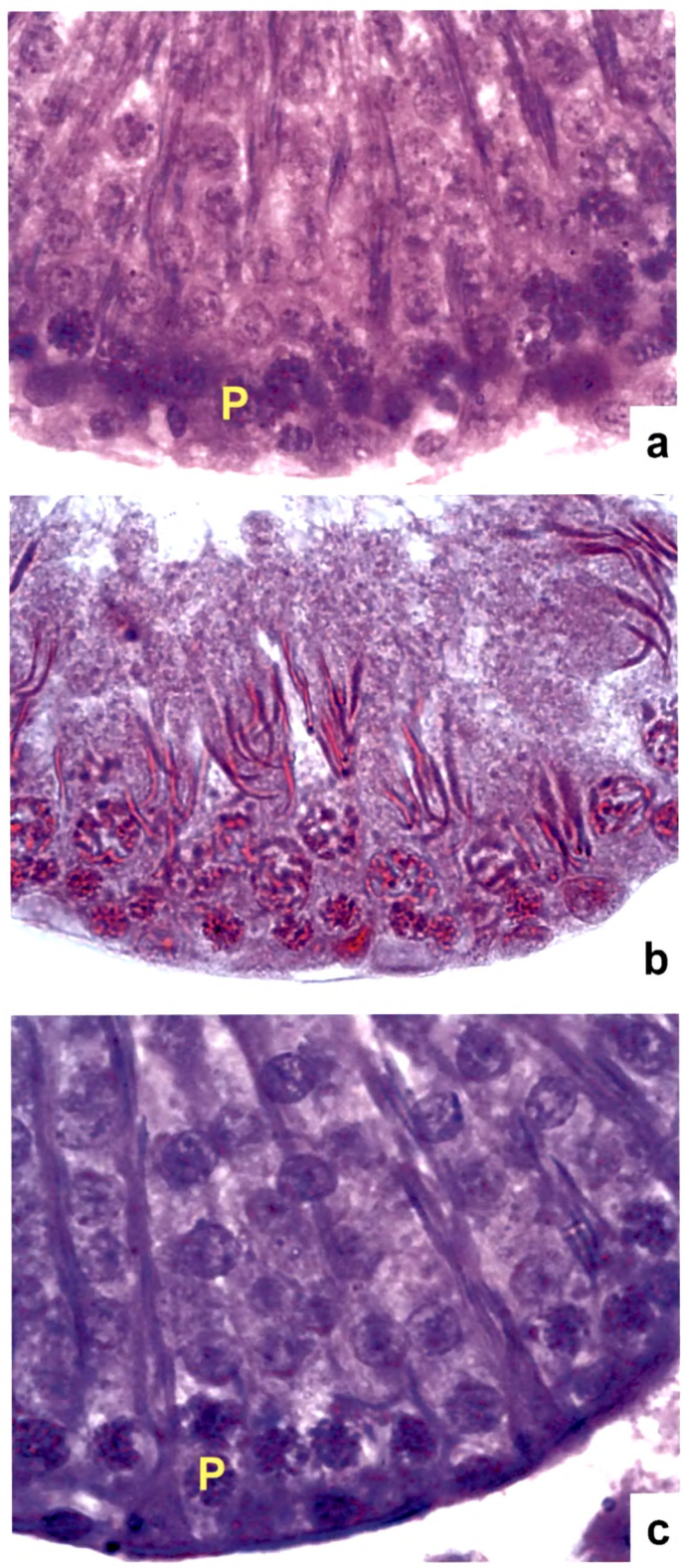

CHAPTER 5

TOXIC POTENTIALS OF HETEROGENEOUS CHEMICAL MIXTURE EXPOSURE ON EPIDIDYMIS AND OTHER ACCESSORY ORGANS

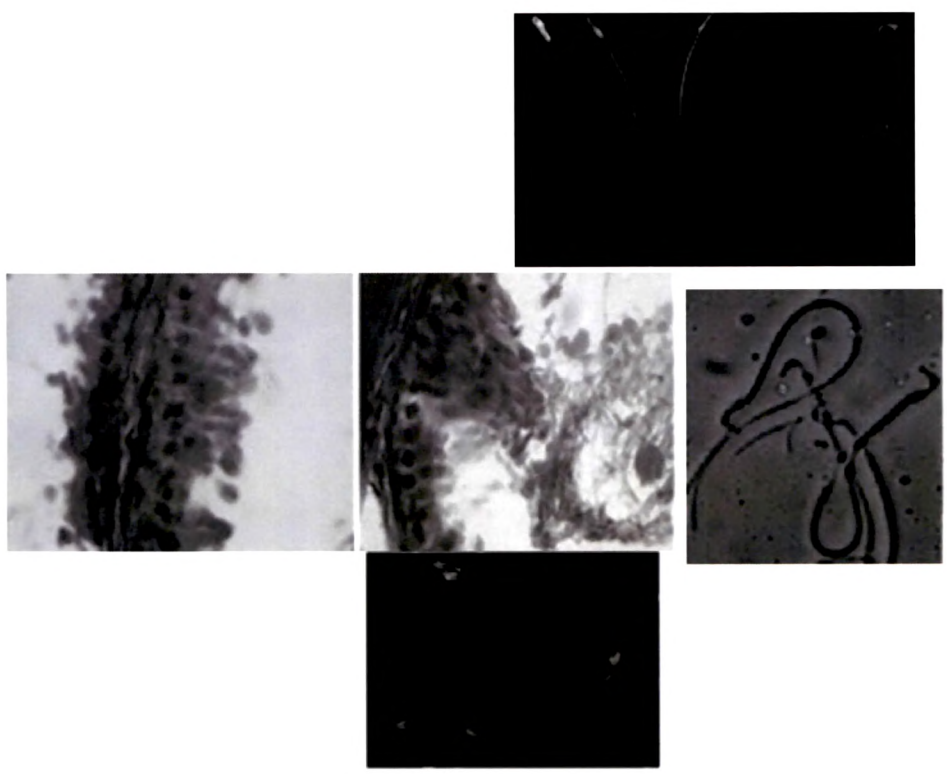

General environmental exposures are typically to heterogeneous chemical mixture (HCM) and much lower than those found in industrial or agricultural work places. The studies indicate that assessing the risk of chemicals one-at-a-time will underestimate the potential harm of mixtures (Jadav *et al.,* 2007; Syberg *et al.,* 2008). For all the experimentations, the relationship exist between potentials of chemical exposures and reproductive toxicity, defining the exposure that produces the effect is critical. People could be affected by mixtures of chemicals that are currently considered harmless based on their individual toxicities.

Spermatozoa leave the testicular environment and enter into the long tubule of epididymis. During transit through the epididymis the spermatozoa gain the maturity and acquire progressive motility and the ability to fertilize ova (Foley, 2001). A morphologically normal spermatozoa arising from the testis may turn out to be functionally deficient and hence unable to fertilize an ova. Therefore, epididymis is considered an important organ for investigations in male reproductive toxicological studies. Several parameters, such as sperm characteristics (motility, count and morphology), and hormone levels (testosterone, follicle stimulating hormone, Lutenizing hormone and cortisol) as well as histopathological observations of reproductive organs has been assessed in reproductive toxicity testing of chemicals.

In light of recent evidences, many chemical exposures result in explicit alterations in epididymal sperm transit, it seems reasonable to suspect reductions in the fertilizing capacity of sperm (Hess, 1999; Pina-Guzman *et al.,* 2009). It is obvious now that many chemicals can alter the structure and function of the epididymis via direct and indirect mechanism of actions. The current study investigates the ability of environmental chemicals to cause epididymal and other reproductive accessory organs toxicity. The parameters investigated to evaluate the effect of HCM on epididymis sperm were motility, count, hypoosmotic swelling test (HOS), viability and percentage head and tail

abnormality along with histopathology and measurement of several biochemical parameters.

The studies of accessory glands (i.e. seminal vesicle and prostate) are of significance since their secretions contribute largely to the semen. Seminal vesicular and prostatic secretions are important for semen coagulation, stability of chromatin and suppression of immune activity of the female reproductive tract. Therefore, the indices of accessory sex organs function in males such as acid phosphatase activity in the prostate and fructose in seminal vesicle were also studied.

RESULTS

Organ weight

No significant changes were observed in the weights of accessory organs; caput and cauda epididymis, seminal vesicle and prostate compared to control groups (Table 1, 10 and 11).

Sperm count

The average sperm count in cauda epididymis was found to be 88 ± 5.24 million in vehicle treated control rats. A significant decrease ($P < 0.01$) in the sperm count was observed in rats exposed to high HCM dose when compared with that of control rats. As shown in Table 2 a moderate but not significant decrease (63 ±7.03 million per ml) in sperm count was observed in low dose HCM treated rats (Fig. 2). In recovery groups (sixty days after cessation of HCM exposure), further decrement was observed when compared with sixty days HCM treated groups and the sperm count was significantly ($P<0.001$) decreased in recovery groups when compared with control group. The average sperm count was found to be 47 ±6.37 and 55 ±3.50 million in groups VIII and IX respectively when compared with that of control group VII.

Sperm Motility

The motility of cauda epididymis sperm of HCM treated group IV and V decreased significantly ($P<0.001$) as compared to vehicle treated control group III. At the end of the withdrawal phase, sperm motility recovered in group VIII and IX when compared with 60 day HCM exposed groups, but was still significantly ($P<0.001$) lower than the control groups VII.

Sperm Viability

Cauda epididymal sperm viability was significantly ($P<0.001$) reduced in high dose HCM treatment as compared to control group III. However, the recovery was obtained in withdrawal groups VIII and IX. In both the withdrawal groups, complete recovery was noted and was very much comparable to control values.

Hypoosmotic swelling test

Percentage of swollen spermatozoa (positive response or/ normal sperm) detected after HOS test are shown in Table 3. Under vehicle treated control group III, the positive response reached to 72.45 ±0.92 while in high dose HCM treated group, only 61.75 ±1.54 were swollen ($P<0.05$ as compared to control group III). This effect of HCM was fully recovered in withdrawal groups when compared with control group.

Sperm- Acridine orange and ethidium bromide staining test

The acridine orange and ethidium bromide assay was used to undertake the effect of HCM on sperms (Table 4 and 5). The fluorescence microscopic analysis results are shown in Plates 1 and 2, and two distinct types of cells can be recognized under fluorescence: live cells (green) and apoptotic or necrotic cells (yellowish orange). Consistent with the results by the trypan blue staining, viability decreased in high (significantly) and low dose HCM treated groups. The results indicated 37.45 ±1.31 ($P<0.01$) and 32.13 ±0.84 percentage of apoptotic and/or necrotic sperms at high and low dose of HCM respectively. This effect of HCM was partially recovered in

withdrawal groups when compared with sixty days HCM treated groups. In recovery study, the results indicated 29.72 ±1.06 ($P<0.05$) and 23.10 ±0.77 % of apoptotic and/or necrotic sperms in group VIII and IX when compared with the control group VII. The results suggested that the recovery was not comparable to control groups.

The assessment of sperm morphology with acridine orange and ethidium bromide assay under fluorescence microscope revealed that with high dose of HCM, the number of alterations in sperm morphology was significantly increased (Table 5). A significant increase in sperm head defects was observed in high dose HCM treated group while sperm tail defects were not significant when compared with control groups. Similarly low dose HCM treatment increased the head defects but the value was insignificant when compared with the vehicle treated control group. In recovery group, no significant changes were observed in head and tail defects except in group VIII (high dose HCM treated + recovery), where marginal increase in head defects were noted.

Effect on epididymal glycerylphosphorylcholine (GPC)

HCM treatment resulted in significant suppression of caput and cauda epididymal glycerylphosphorylcholine when compared with the control group III (Table 6 and Fig. 6). In caput epididymis of group VIII and IX, slight recovery was observed while cauda epididymis showed further suppression ($P<0.01$) of glycerylphosphorylcholine instead of recovery.

Effect on epididymal protein content

The protein levels in the caput and cauda epididymis decreased after sixty days of HCM treatment in group IV and V as compared to control group III. However, this decrease was significant ($P<0.05$) only in cauda epididymis. No sign of recovery was observed in protein content in groups VII and IX (withdrawal).

Effect on epididymal lipid peroxidation (LPO)

Surprisingly, considerable decrement in LPO levels were observed in HCM treated group (Table 7). In cauda this decrease was significant in high dose and insignificant in low dose HCM treated group. Similarly, caput epididymis showed non significant decrease in LPO in high and low dose HCM treated group when compared with control group VII i.e. withdrawal of the HCM treatment for sixty days showed recovery in LPO when compared with HCM treated groups.

Effect on epididymal enzymatic and non enzymatic antioxidants

Tables 7, 8 and 9 depict that the content of non enzymatic antioxidants such as GSH, ascorbic acid and activities of enzymatic antioxidants such as SOD, GPx, CAT and GST were declined upon HCM treatment (group IV and V) when compared with vehicle treated control (group III) in both caput and cauda epididymis. Withdrawal of the HCM treatment for sixty days showed recovery in few antioxidant parameters but, the recovery was not comparable.

Effect on epididymis histology

The epididymis is a tightly-coiled tube which connects the testis to the vas deferens. On the basis of histological difference, the epididymis is divided into three main regions: caput (head), corpus (body), and cauda (tail). Histologically the caput is characterized by a thin myoepithelium while cauda has a thicker myoepithelium, as it is involved in absorbing fluid. Epididymis consists of pseudostratified columnar to cuboidal epithelium of six major cell types: principal, basal, clear, narrow, apical and halo cells. Each region carries out distinctive function of early and late sperm maturation events and also serves as storage site for matured sperm. Therefore, the contribution of different cell types in various regions is also different. The luminal microvilli (stereocilia) of the principal cells are elongated in the caput region while in the cauda region they appear like brush border. The tubules are surrounded by 2

to 3 layers of myoid cells and connective fibres; the thickness of which is increased in caudal region (Plate 3). The histological observations were categorized into the specific changes observed in cytoplasm, nucleus, as well as in the lumen of epididymis. Nuclear pyknosis was observed on day 60 in high dose treatment group particularly in the caput region. The epithelial cell height was significantly decreased in the caput region and marginally in cauda (Plate 4, 5). The clogging of stereocilia was conspicuous in caput region while in the caudal region meshwork of damaged ciliary processes and spermatozoa tail could be observed (Plate 6 and 7). In the caput region cytoplasmic blebbing was enormous, basal cytoplasmic vacuoles and cytoplasmic degenerative changes were obvious (Plates 4-6). The lumen had comparatively much less spermatozoa bundles compared to that found in the control animals both on 60 and 120 days (Plates 4,7 and 9). The lumen of several tubules were largely blocked by sloughed off spermatogenic celis and cellular debris of testicular and epididymal origin (Plates 4, 5 and 7). Following withdrawal phase there was an improvement in the histoarchitecture of epididymis particularly at low does exposed (Plates 8, 9). The histological features are described in detail with the plates.

Effect on seminal vesicles fructose content

Fructose content in seminal vesicle decreased marginally after HCM treatment in toxicity as well as in recovery study when compared with the control groups (Table 10, Fig. 10).

Effect on prostate- Acid Phosphatase

No significant change in prostatic acid phosphatase activity was observed in any of the groups of toxicity and recovery study (Table 11 and Fig. 11).

DISCUSSION

Sperm count is one of the most sensitive tests for assessment of spermatogenesis (Wyrobek, 1983; Foster *et al.,* 2010). Our result showed that treatment with HCM at high and low dose levels; reduced the total sperm count. Histological structure of the testis confirm this, where it revealed spermatogenesis impairment and degeneration and atrophy of seminiferous tubules after HCM treatment. This ultimately results in the elimination of more mature cells of spermatogenesis and thus culminates into reduction in daily sperm production. These finding are in agreement with those of Sinclair *et al.* (2000) and Nair *et al.* (2008) who found that the number of spermatocytes, spermatids and Leydig cells were significantly decreased with the administration of several environmental chemicals and thus reduced sperm count.

Sperm motility assessments are an integral part of reproductive toxicity test and considered as a reproductive end point parameter. Microenvironment and distinct biochemical processes of the testes and epididymis are highly synchronized to assure the proper development and maturation of the sperm and the acquisition of functional characteristics i.e. motility and the fertilizing capacity (Cornwall, 2009). With chemical exposures, disruption of this balance may occur, producing alterations in properties of sperm such as motility; chemicals have been identified that affect sperm motility and ultimately reduce fertility (Benoff, 2000; Chowdhury, 2009; Yuan *et al.,* 2010). Decline in sperm motility after HCM administration may be due to its direct action on spermatogenesis process or due to indirect action via androgen insufficiency. Interestingly, sperm motility increased in all withdrawal groups but it did not reach up to the normal level. The results indicated that the sperm motility was revived in recovery group.

In rats, a complete spermatogenic cycle is approximately 54-58 days and thus reduction/cessation of sperm production takes about this much time (Leblond and Clermont, 1952; Hess, 1990). Differentiating germ cells are extremely susceptible to cytotoxic chemicals and although Leydig cells and Sertoli cells survive during most cytotoxic conditions but could suffer functional damage (Moffit *et al.,* 2007). HCM exposure resulted in premature sloughing of germ cells with marked alteration in Sertoli cells cytoplasm. Sloughing of germ cells was observed in approximately all stages of the cycle. Sloughed spermatids were usually found as clusters or in close association to one another in lumen as they normally would exist in tubule suggesting that cells remained connected to each other by their intracellular bridges. Thus the process of germ cell sloughing may have contributed to the long term effects of HCM observed even on day 120.

Several authors have reported that quality of sperm production has been adversely affected following exposure of certain chemicals (Haouem *et al.,* 2008; Okumuru et al. 2009; Pina-Guzman *et al.,* 2009; Foster *et al.,* 2010). An increase in morphologically abnormal sperm has been considered as evidence that the chemical has gained access to the germ cells (U.S. EPA, 1986). Toxicologic testing of chemicals on male reproduction has relied on subjective categorization of sperm head and tail defects in either stained preparation by fluorescent microscopy or fixed, unstained preparation by phase contrast microscope (Ombelet *et al.,* 1995; Menkveld et al 2011). Moreover, assessment of sperm viability is one of the basic elements to evaluate the functional status of epididymis. It is especially important in those samples where many sperms are immotile, to distinguish between live and dead sperm.

In present study, percentage of abnormal sperm forms were significantly increased in HCM treated groups. The observed increased sperm abnormalities are due to aberrations in the process of spermatogenesis (Saba

et al., 2009). This occurred as a result of toxic injury of HCM to seminiferous tubules as postulated from the histological investigations of testis. Similar results were reported with certain metal and organochlorine compounds (Li *et al.,* 2001; Kini *et al.,* 2009; Reddy *et al.,* 2010). Only head sperm cells abnormality had the highest occurrence, followed by bent tail, curve tail and only tail of all the sperm abnormality observed. Although, rats in the HCM treatment groups had higher percentages of these abnormalities, only head sperm abnormality was significant while rest of the abnormalities were within range of that observed in the rats of the controls groups. These abnormalities arise as a result of a fundamental problem with the process of sperm development (spermeiogenesis) where abnormal sperm developed from damaged seminiferous tubules.

The primary cell type throughout the tubule is the principle cell which constitutes 80%-85% of the epithelium and it is responsible for bulk of the proteins that are secreted into the lumen (Leung *et al.,* 2004). The principle cells also play an important role in absorption of fluid. The principle cells forms tight junctions with one another known as blood- epididymis barrier which creates an immunoprotective sheath within the epididymis for further maturation of sperm. The basal cells are the second most common cell type after principle cell and some studies suggested its major role in regulating the electrolyte and water transport. However, narrow, apical and clear cells contain the vacuolar H^+-ATPase and secrete proton into the lumen of the epididymis and thus participates in its acidification (Kujala *et al.,* 2007). Clear cells are also known to play the role of endocytic cells and may be responsible for removal of proteins from the epididymis. Halo cells appear to be the primary immune cell in the epididymis.

Although an objective quantitative studies of different epithelial cell was not carried out, the variations were qualitatively evaluated both in the caput and cauda regions. The changes in the principle cell were observed as basal

vacuolations, eosinophilic cytoplasm, microvili disruption and cytoplasmic blebbing were significant in high dose group indicative of damage to the blood epididymal barrier since the accumulated toxicants may disrupt microtubules. In the caudal region there was a comparative increase in number of halo cells which are lymphocytic and monocytic in origin. It is proposed that increase in halo cell number is relative to the variation in the composition of luminal content (Robaire and Hermo, 1988). In cauda epididymis the number of clear cells increased which is thought to be associated with phagocytic activity (Transler et al., 1988). In histological preparations the density of abnormal spermatozoa, sloughed cell and the cytoplasmic debris were high while that in the cauda region these were comparatively less, indicative of active phagocytosis by clear cells in that region. Akbarsha and Sivasamy (1998) demonstrated an increase in halo and clear cells following phosphomidon exposure. The function alterations of principal cells are demonstrated due to general endocrine dysfunction and the mediation via hormonal axis (Akbarsha and Averal 1998). The damage to microvili indicates impaired ability of fluid reabsorption. The histological findings provide sufficient indication of structural alterations that would lead to functional impairments in specific regions of the epididymis. Thus the microenvironment of the epididymal lumen is significantly modified which may not be appropriate for the structural and functional potentiation of spermatozoa during the transit.

In control rats, the concentration of GPC is higher in caput region than in cauda, and this finding agrees with previous studies of Hoffmann and Killian (1981) and Wang et al. (1981). Atreja and Anand (1985) reported that the activity of phosphalipase A_2 enzyme is involved in the synthesis of GPC. The decrease in tissue GPC concentration after HCM treatment may be due to the impaired synthesis of the phospholipase A_2. Because the synthesis and secretion of GPC are under androgenic control, the decrease in testosterone level is attributed to the decrease in GPC concentration. As GPC play a major role in maintaining sperm membrane stability, the low level of GPC observed after HCM administration may have an adverse effect on sperm viability,

motility and morphology. The changes in GPC levels are transient as they are reversed towards normalcy after withdrawal of HCM treatment for next sixty days.

Polyunsaturated fatty acid and phospholipids of spermatozoa are highly susceptible to peroxidation (Sanocka and Kurpisz, 2004), leading to morphological alterations and loss of membrane integrity of the sperm (Pina-Guzman *et al.,* 2009). Thus sperms are very susceptible to ROS attack which result in decreased sperm viability, presumably, by rapid loss of intracellular ATP leading to axonemal damage, increase morphology defects in tail and mid piece and deleterious effect on sperm capatiation and acrosomal reaction. Lipid peroxidation of sperm membrane is considered to be the key mechanism of this ROS induced damage leading to reduced sperm viability and induced morphological alterations (Aziz *et al.,* 2004).

Also, both decrease motility and increased sperm DNA damage can result from high reactive oxygen species level. Action of ROS on sperm resulted in decrease in sperm motility and loss of membrane integrity. The capacity of epididymis and spermatozoa to generate reactive oxygen species (ROS) has been described (Aitken etal., 1989). Although these ROS play a modulator role in sperm hyperactivation and capacitation, several studies have also indicated that they are involved in producing defects in sperm function via direct or indirect action (Griveau *et al.,* 1995; Pina-Guzman *et al.,* 2009; Bansal and Bilaspuri, 2011). Treatment with HCM in this study significantly decreased the endogenous antioxidant level, which is in agreement with previous finding of Aboua *et al.,* 2009. They reported that organic hydroperoxides exposure impaired the endogenous antioxidant activity and reduced sperm motility. Similarly, decrease in sperm count and motility as well as altered activity of steroidogenic enzymes have been reported in various metal toxicity studies (Mukherjee and Mukhopadhyay, 2009; Chowdhury, 2009).

Fructose, a readily glucosable sugar is produced mainly by the seminal vesicle and is used as an energy source by the sperm for its motility. In present study, the observed very slight decrease (almost normal) in fructose values suggest that HCM treatment caused no marked changes in secretary processes of seminal vesicle.

CONCLUSION

The findings of the present investigation suggest that HCM exposure at NOAEL leads to alteration in sperm count, sperm motility and viability. The histological observation supports the findings in biochemical changes. HCM effectively produced oxidative stress in different regions of epididymis.

Experimental Groups

Groups	Treatment	Autopsy day
I	Zero (initial) day control	01
II	Control (No treatment)	61
III	Control (Vehicle treatment)	61
IV	Heterogeneous chemical mixture treated group (1% of LD_{50} dose/ animal/ day - NOAEL dose level)	61
V	Heterogeneous chemical mixture treated group (0.1% of LD_{50} dose/ animal/ day)	61
VI	Control (No treatment)	121
VII	Control (Vehicle treatment)	121
VIII	Heterogeneous chemical mixture treated group (1% of LD_{50} dose/ animal/ day) for 60 days followed by withdrawal phase of 60 days - NOAEL dose level.	121
IX	Heterogeneous chemical mixture treated group (0.1% of LD_{50} dose/ animal/ day) for 60 days followed by withdrawal phase of 60 days.	121

Values in all the following Tables are Mean± SE and statistical significance is considered and presented for (*) $P<0.05$, (+) $P<0.01$ and (#) $P<0.001$ compared withrespective vehicle control.

Table 1: Gravimetric analysis of epididymis

Groups	Absolute Epididymis weight (g)	Relative epididymis weight (g/ 100 g animal)
I	1.30 ±0.040	0.40 ±0.011
II	1.45 ±0.047	0.43 ±0.015
III	1.48 ±0.070	0.42 ±0.018
IV	1.25 ±0.036	0.44 ±0.018
V	1.34 ±0.044	0.46 ±0.013
VI	1.56 ±0.044	0.39 ±0.010
VII	1.57 ±0.069	0.38 ±0.020
VIII	1.41 ±0.058	0.41 ±0.016
IX	1.44 ±0.037	0.39 ±0.009

Fig. 1: Gravimetric analysis of epididymis

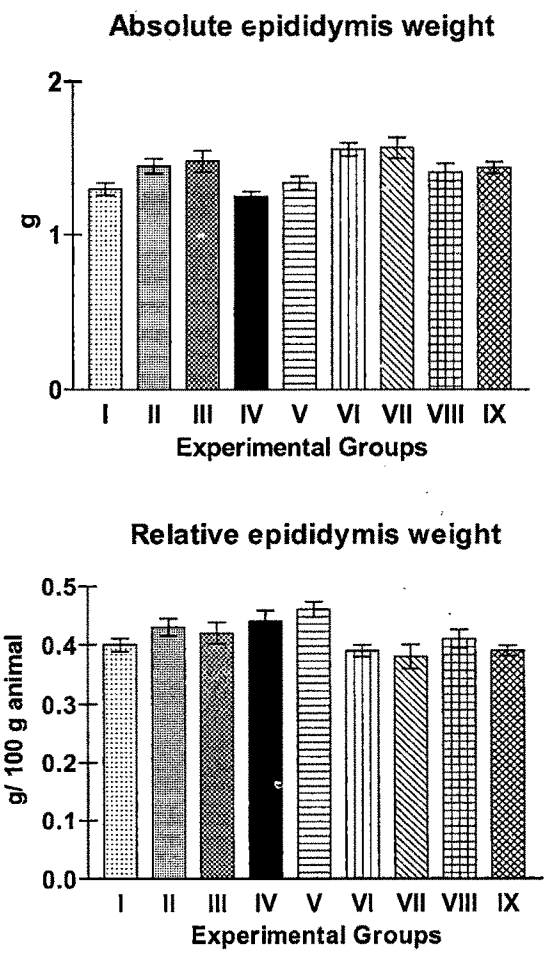

Table 2: Quantitative spermatological analysis

Groups	Sperm Count (Cell X 10^6/ Cauda Epididymis)	Sperm Motility (%)	Sperm viability test with trypan blue	
			Live sperm (%)	Dead sperm (%)
I	83 ±5.97	70.25 ±1.33	78.68 ±1.66	21.32 ±1.66
II	98 ±7.70	72.12 ±1.83	72.69 ±2.14	27.31 ±2.14
III	88 ±5.24	68.33 ±1.78	76.42 ±2.39	23.58 ±2.39
IV	51 ±5.25^{+}	41.16 ±1.03$^{\#}$	60.59 ±3.86$^{\#}$	39.41 ±3.86
V	63 ±7.03	54.33 ±1.29$^{\#}$	67.19 ±2.68	32.81 ±2.68
VI	95 ±4.61	78.95 ±2.62	76.84 ±2.05	23.16 ±2.05
VII	97 ±7.05	73.78 ±1.81	73.45 ±2.58	26.55 ±2.58
VIII	47 ±6.37$^{\#}$	52.55 ±1.33$^{\#}$	70.02 ±1.09	29.98 ±1.09
IX	55 ±3.50$^{\#}$	60.84 ±1.50$^{\#}$	79.38 ±2.54	20.62 ±2.54

Fig. 2: Quantitative spermatological analysis

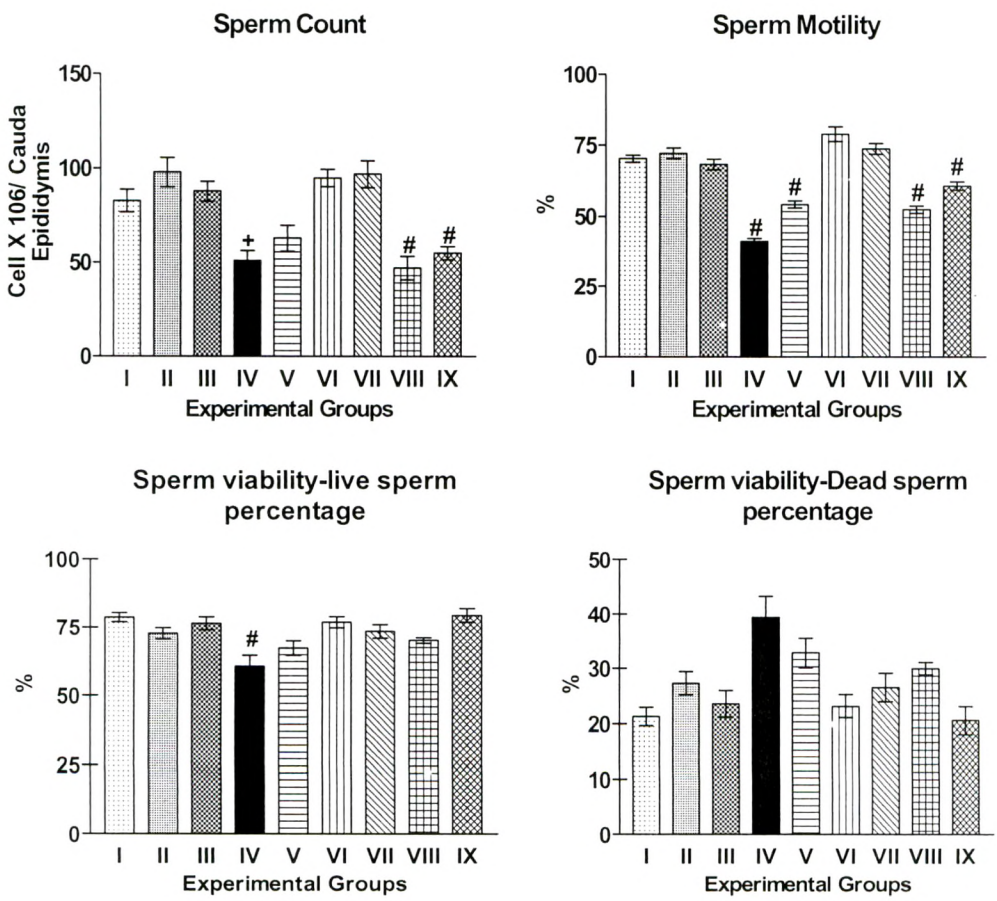

Table 3: Sperm hyposomotic swelling test

Groups	Sperm Hypo-Osmotic Swelling (HOS) test	
	Positive Response to HOS	Negative Response to HOS
I	72.94 ±1.55	27.06 ±1.55
II	69.97 ±0.97	30.03 ±0.97
III	72.45 ±0.92	27.55 ±0.92
IV	61.75 ±1.54*	38.25 ±1.54*
V	63.92 ±1.20	36.08 ±1.20
VI	72.59 ±1.51	27.41 ±1.51
VII	73.80 ±2.73	26.20 ±2.73
VIII	70.86 ±2.40	29.14 ±2.40
IX	72.24 ±3.13	27.76 ±3.13

Fig. 3: Sperm hyposomotic swelling test

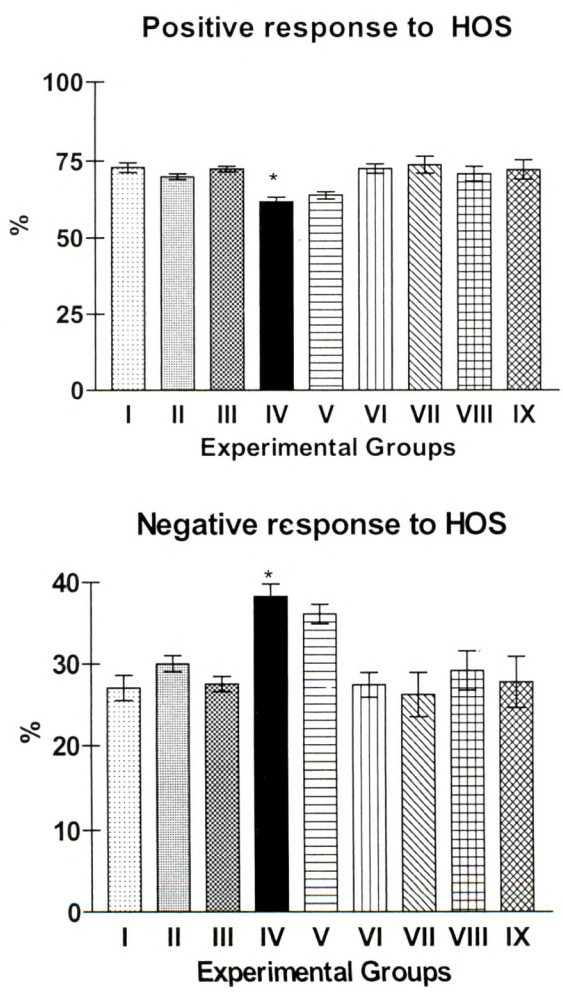

Table 4: Sperm morphology analysis to show normal and necrotic cells

Sperm- Acridine orange and ethidium bromide (AOEB) staining		
Groups	**Normal Sperm**	**Apoptotic or Necrotic Sperm**
I	71.50 ±1.91	28.50 ±1.91
II	74.38 ±1.59	25.62 ±1.59
III	70.80 ±1.87	29.20 ±1.87
IV	62.55 ±1.31^{+}	37.45 ±1.31^{+}
V	67.87 ±0.84	32.13 ±0.84
VI	76.66 ±1.37	23.34 ±1.37
VII	77.37 ±1.66	22.63 ±1.66
VIII	70.28 ±1.06*	29.72 ±1.06*
IX	76.90 ±0.77	23.10 ±0.77

Fig. 4: Sperm morphology analysis to show normal and necrotic

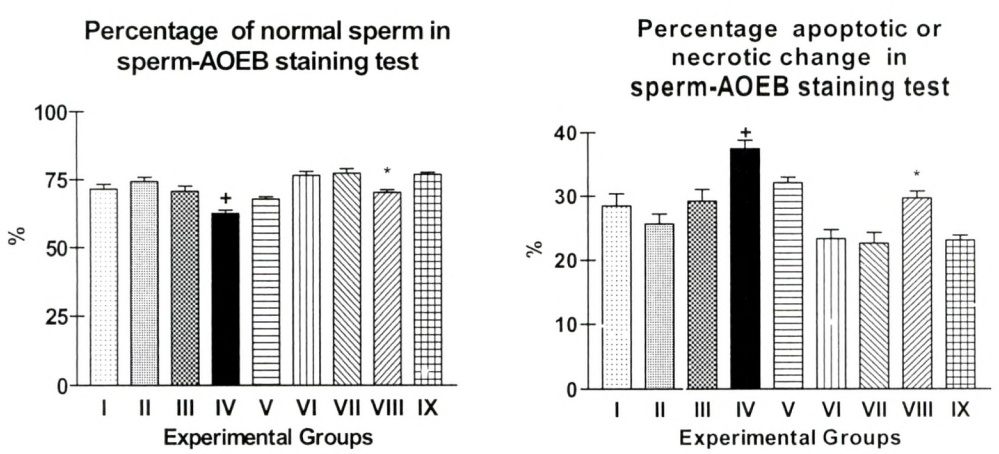

Table 5: Sperm morphological abnormality analysis

Sperm- Acridine orange and ethidium bromide staining				
Groups	**Only Head**	**Only Tail**	**Bent Tail**	**Curve Tail**
I	6.15 ±0.80	6.69 ±0.93	10.13 ±1.56	5.53 ±1.50
II	3.90 ±0.61	6.41 ±1.71	7.52 ±1.15	7.78 ±2.06
III	2.77 ±0.56	6.17 ±0.78	12.45 ±1.33	7.81 ±0.71
IV	9.86 ±1.00$^{\#}$	7.69 ±0.38	12.74 ±0.96	7.16 ±0.83
V	4.72 ±0.89	6.77 ±0.24	12.02 ±0.95	8.62 ±1.17
VI	4.43 ±0.70	3.92 ±0.76	9.22 ±0.97	5.78 ±0.36
VII	2.20 ±0.79	3.87 ±0.86	10.06 ±1.30	6.50 ±1.16
VIII	4.82 ±1.09	3.85 ±0.84	13.04 ±0.93	8.01 ±1.18
IX	2.51 ±0.57	3.54 ±0.73	10.21 ±1.13	6.84 ±0.76

Table 6: General biochemical analysis in epididymis

	Epididymal Glycerylphosphorylcholine (mg/ 100 mg tissue)		Epididymal Protein (mg/ 100mg tissue)	
Groups	Caput	Cauda	Caput	Cauda
I	0.68 ±0.09	0.49 ±0.07	9.18 ±1.05	10.03 ±0.87
II	0.61 ±0.04	0.46 ±0.04	8.54 ±0.54	9.75 ±1.14
III	0.72 ±0.10	0.46 ±0.04	8.63 ±0.71	10.44 ±0.71
IV	0.43 ±0.04	0.11 ±0.01$^{\#}$	6.47 ±0.73	6.69 ±0.42*
V	0.38 ±0.04*	0.22 ±0.06*	7.01 ±0.55	6.68 ±0.62*
VI	0.73 ±0.05	0.49 ±0.03	8.95 ±0.88	9.90 ±0.73
VII	0.72 ±0.06	0.48 ±0.03	8.86 ±1.01	9.72 ±0.80
VIII	0.40 ±0.07	0.22 ±0.03^{+}	5.18 ±0.53*	5.72 ±0.74*
IX	0.54 ±0.08	0.22 ±0.05^{+}	5.44 ±0.24	6.04 ±0.20*

Fig. 6: General biochemical analysis in epididymis

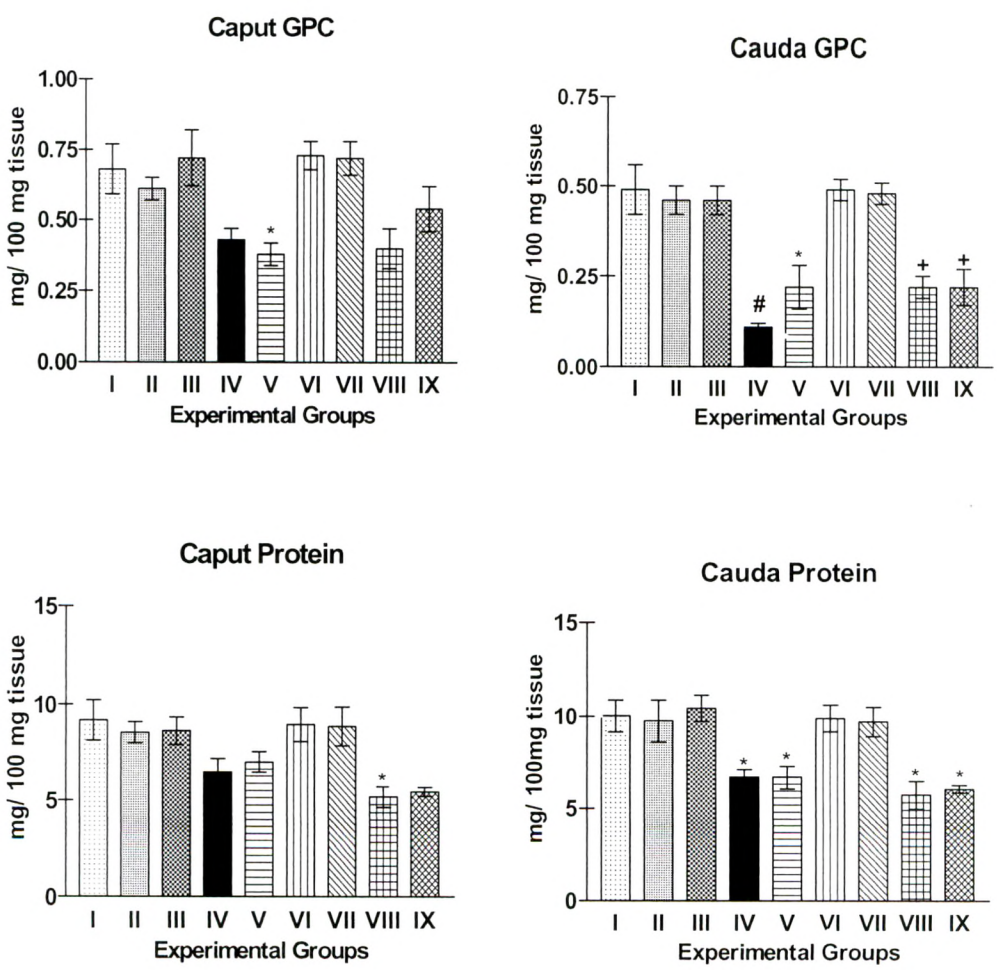

Table 7: Status of oxidative stress in epididymis

	Epididymal LPO (n mole MDA/ 100 mg tissue)		Epididymal GSH (µg of GSH/ mg protein)	
Groups	**Caput**	**Cauda**	**Caput**	**Cauda**
I	31.65 ±1.75	33.19 ±6.68	1.95 ±0.20	2.07 ±0.32
II	34.64 ±1.85	39.74 ±7.80	1.85 ±0.23	2.06 ±0.12
III	36.63 ±1.78	39.70 ±4.69	1.69 ±0.21	2.28 ±0.14
IV	24.88 ±1.83	18.28 ±1.64*	0.80 ±0.22	0.53 ±0.19#
V	27.49 ±2.48	28.05 ±2.09	1.23 ±0.33	0.98 ±0.29*
VI	37.96 ±5.21	30.43 ±1.96	1.91 ±0.20	2.00 ±0.28
VII	38.58 ±4.45	38.64 ±3.90	2.12 ±0.37	2.59 ±0.27
VIII	27.30 ±2.59	28.28 ±1.27	1.33 ±0.38	0.30 ±0.06#
IX	29.77 ±1.89	29.48 ±1.91	1.38 ±0.43	0.85 ±0.37#

Fig. 7: Status of oxidative stress in epididymis

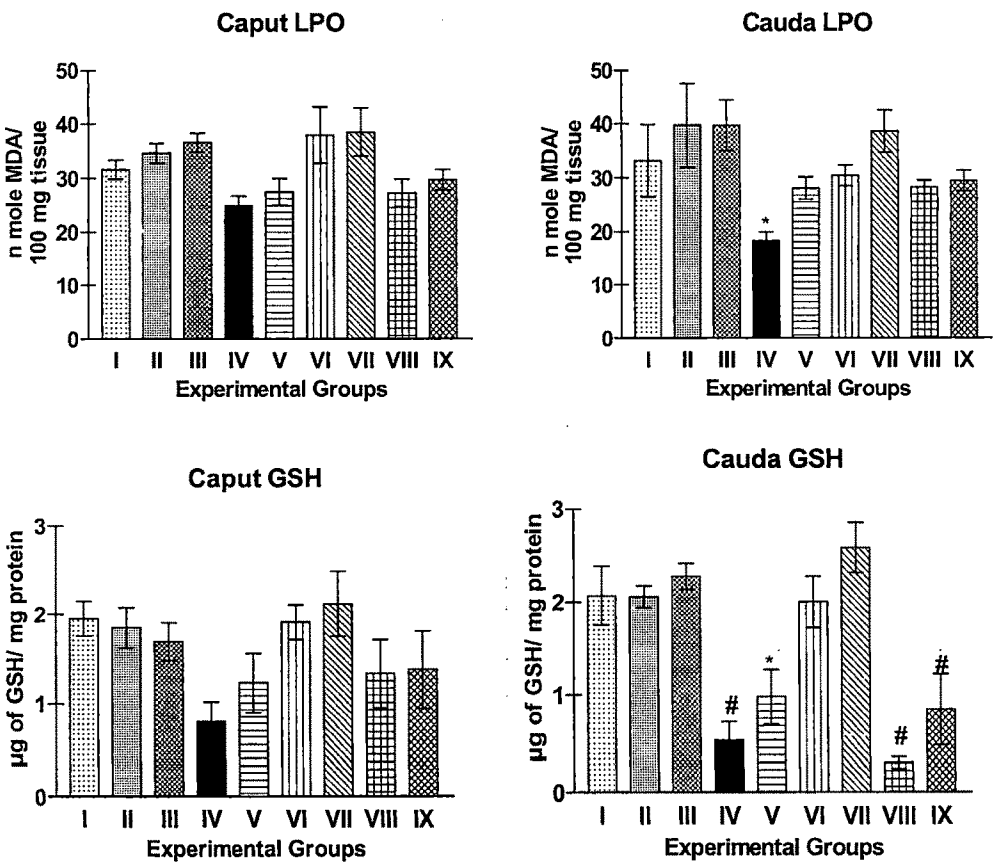

Table 8: Status of oxidative stress in epididymis (Enzymes)

	Epididymal SOD (Unit/ mg protein)		Epididymal GPx (µg of GSH utilize/ min/ mg protein)	
Groups	Caput	Cauda	Caput	Cauda
I	3.77 ±0.51	2.15 ±0.25	3.09 ±0.60	3.80 ±0.28
II	3.93 ±0.60	2.33 ±0.61	2.50 ±0.49	3.40 ±0.41
III	3.74 ±0.71	2.67 ±0.23	2.93 ±0.34	3.39 ±0.42
IV	2.52 ±0.81	1.41 ±0.25	1.32 ±0.57	2.83 ±0.30
V	2.40 ±0.35	1.70 ±0.54	2.02 ±0.45	2.95 ±0.31
VI	2.73 ±0.29	2.84 ±0.28	2.82 ±0.49	2.84 ±0.12
VII	2.06 ±0.51	2.97 ±0.38	3.48 ±0.53	3.68 ±0.23
VIII	1.05 ±0.30	0.55 ±0.14#	1.85 ±0.78	0.72 ±0.31#
IX	1.69 ±0.68	0.90 ±0.14+	1.90 ±0.53	0.99 ±0.69#

Fig. 8: Status of oxidative stress in epididymis (Enzymes)

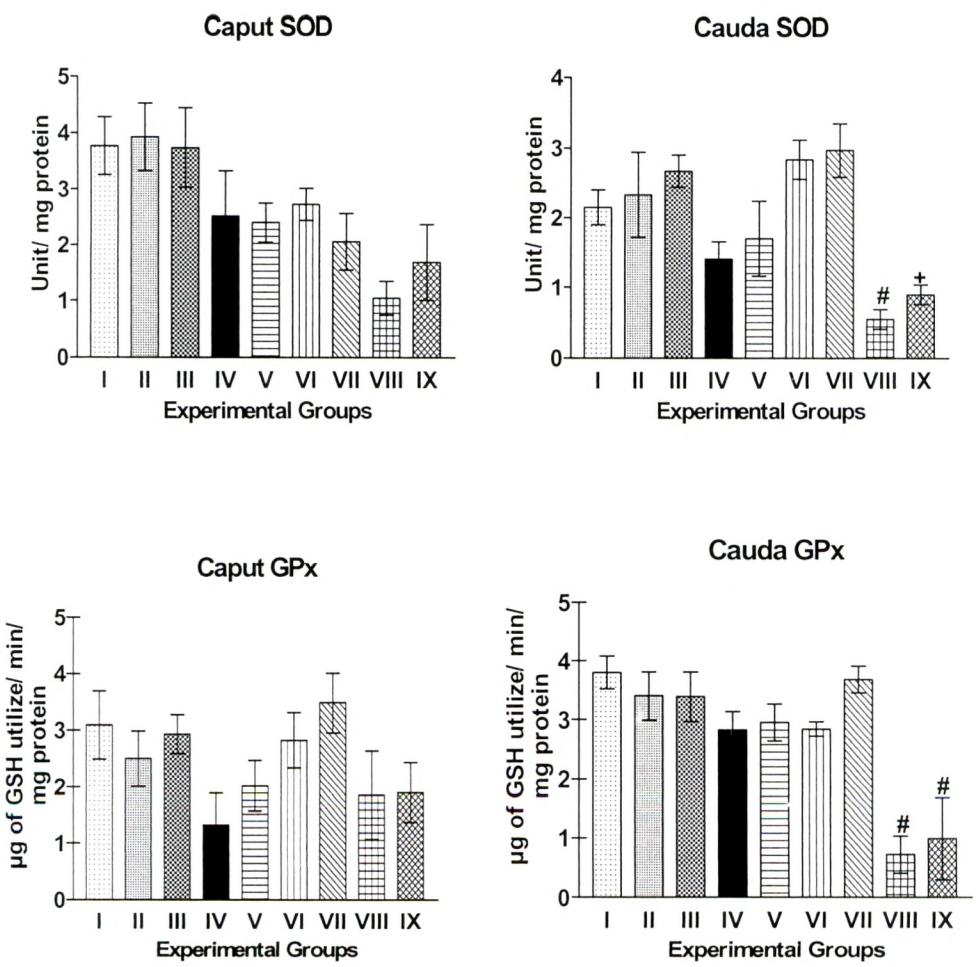

Table 9: Status of oxidative stress in epididymis (Enzymes)

	Epididymal Catalase (μ mole of H_2O_2 consumed/ min/ mg protein)		Epididymal GST (μ mole CDNB-GSH conjugate formed /min/ mg protein)	
Groups	**Caput**	**Cauda**	**Caput**	**Cauda**
I	23.70 ±3.03	25.45 ±3.72	3.77 ±0.38	2.77 ±0.42
II	21.72 ±3.86	27.15 ±2.99	3.68 ±0.71	2.31 ±0.20
III	20.00 ±3.39	23.42 ±2.21	2.88 ±0.44	2.28 ±0.24
IV	11.39 ±0.92	11.43 ±1.40*	0.92 ±0.22*	1.62 ±0.36
V	14.14 ±1.11	15.26 ±0.32	1.09 ±0.11*	1.71 ±0.29
VI	19.27 ±2.69	25.50 ±1.98	3.22 ±0.35	2.67 ±0.36
VII	20.72 ±2.73	26.13 ±2.94	3.00 ±0.36	2.77 ±0.35
VIII	7.21 ±0.73*	13.09 ±1.97*	0.81 ±0.08^{+}	0.59 ±0.06^{+}
IX	14.05 ±2.24	11.26 ±2.19^{+}	1.03 ±0.26*	1.06 ±0.48*

Table 9: Status of oxidative stress in epididymis (Enzymes)

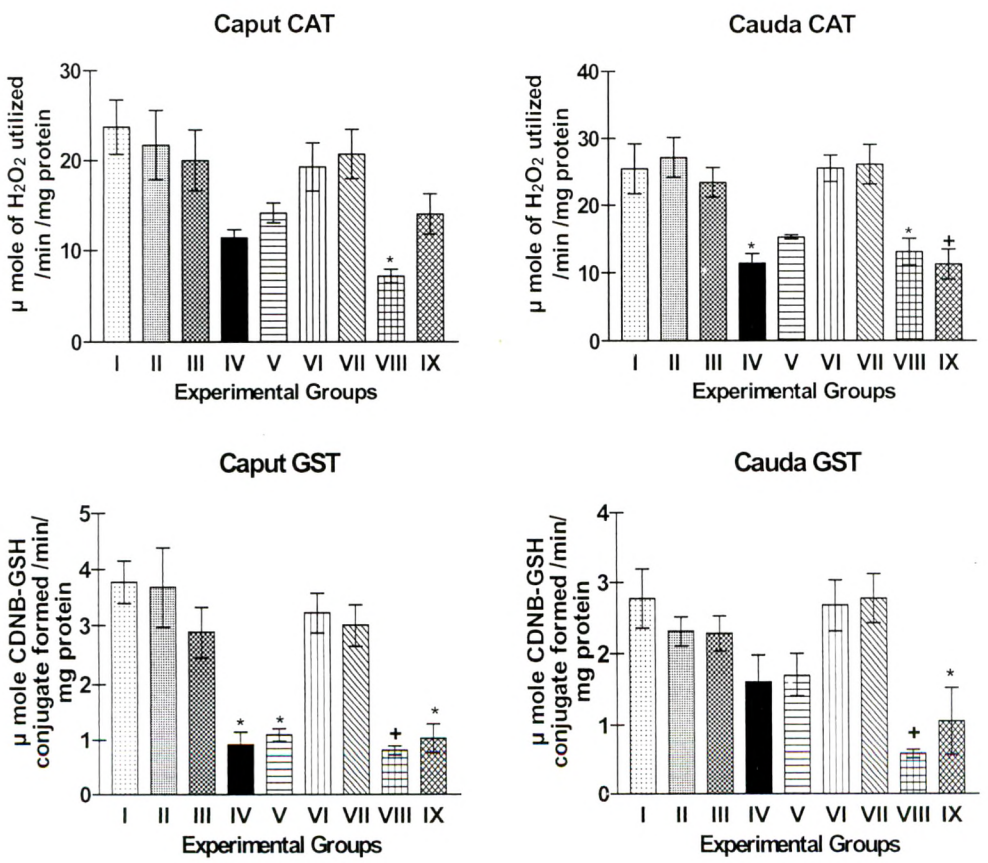

Table 10: Gravimetric and biochemical indicators of seminal vesicle functions

Groups	Seminal Vesicles Fructose content (µg/ mg tissue)	Seminal Vesicle Absolute weight (g/ animal)	Seminal Vesicle Relative weight (g/ 100 g animal)
I	6.94 ±0.71	1.42 ±0.051	0.44 ±0.015
II	8.13 ±0.59	1.47 ±0.034	0.44 ±0.014
III	8.99 ±0.77	1.52 ±0.020	0.43 ±0.005
IV	6.25 ±0.73	1.40 ±0.052	0.49 ±0.017
V	6.73 ±0.81	1.35 ±0.028	0.46 ±0.010
VI	8.03 ±0.19	1.53 ±0.025	0.39 ±0.007
VII	7.61 ±0.60	1.50 ±0.041	0.37 ±0.010
VIII	5.98 ±0.64	1.42 ±0.053	0.42 ±0.014
IX	6.17 ±0.29	1.37 ±0.033	0.37 ±0.012

Fig. 10: Gravimetric and biochemical indicators of seminal vesicle functions

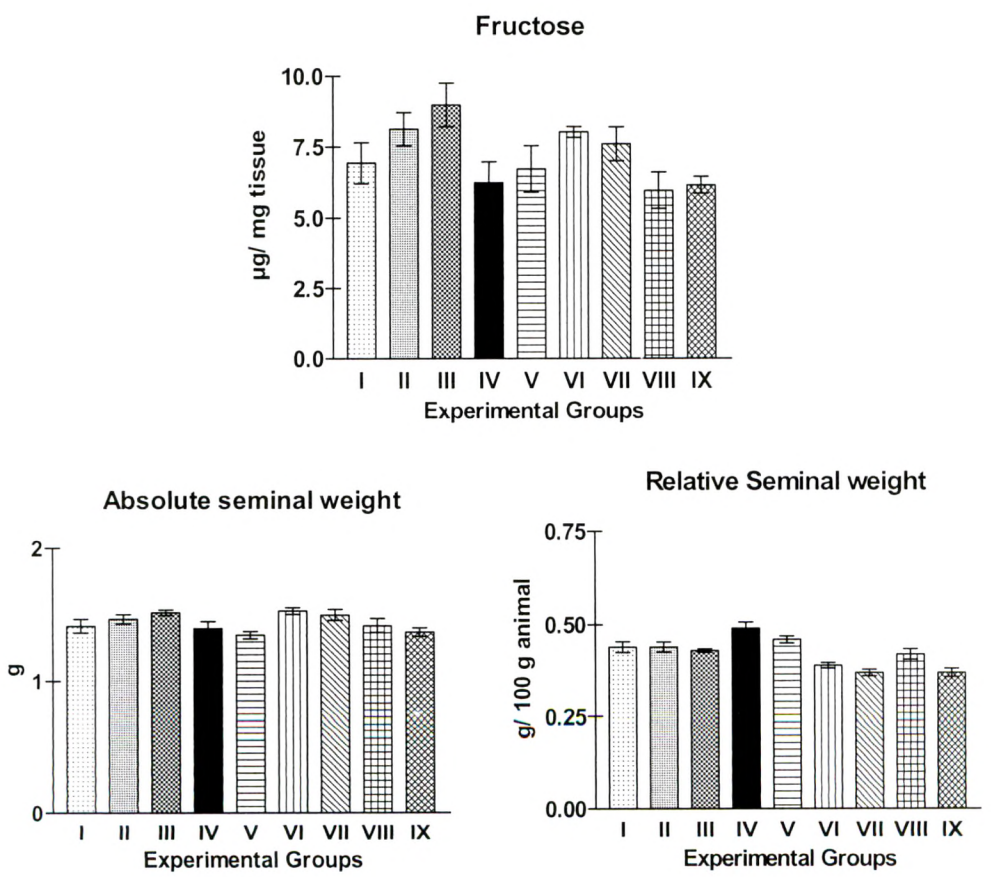

Table 11: Gravimetric and biochemical indicators of prostate functions

Groups	Prostate- Acid Phosphatase (µ moles of p-nitrophenol released/ mg protein/ min)	Prostate- Protein Content (mg/ 100mg tissue)	Absolute Prostate weight (g/ animal)	Relative Prostate weight (g/ 100 g animal)
I	0.14 ±0.012	13.54 ±0.53	0.77 ±0.030	0.24 ±0.012
II	0.11 ±0.012	14.77 ±0.96	0.80 ±0.013	0.24 ±0.006
III	0.11 ±0.023	13.70 ±1.01	0.78 ±0.019	0.22 ±0.006
IV	0.16 ±0.012	11.81 ±0.65	0.73 ±0.015	0.25 ±0.006
V	0.14 ±0.004	12.22 ±0.42	0.70 ±0.022	0.24 ±0.007
VI	0.15 ±0.015	13.22 ±0.54	0.84 ±0.017	0.21 ±0.004
VII	0.14 ±0.009	12.57 ±0.51	0.82 ±0.021	0.20 ±0.005
VIII	0.11 ±0.015	13.27 ±0.64	0.79 ±0.024	0.23 ±0.007
IX	0.15 ±0.013	11.63 ±0.62	0.73 ±0.025	0.20 ±0.007

Fig. 11: Gravimetric and biochemical indicators of prostate functions

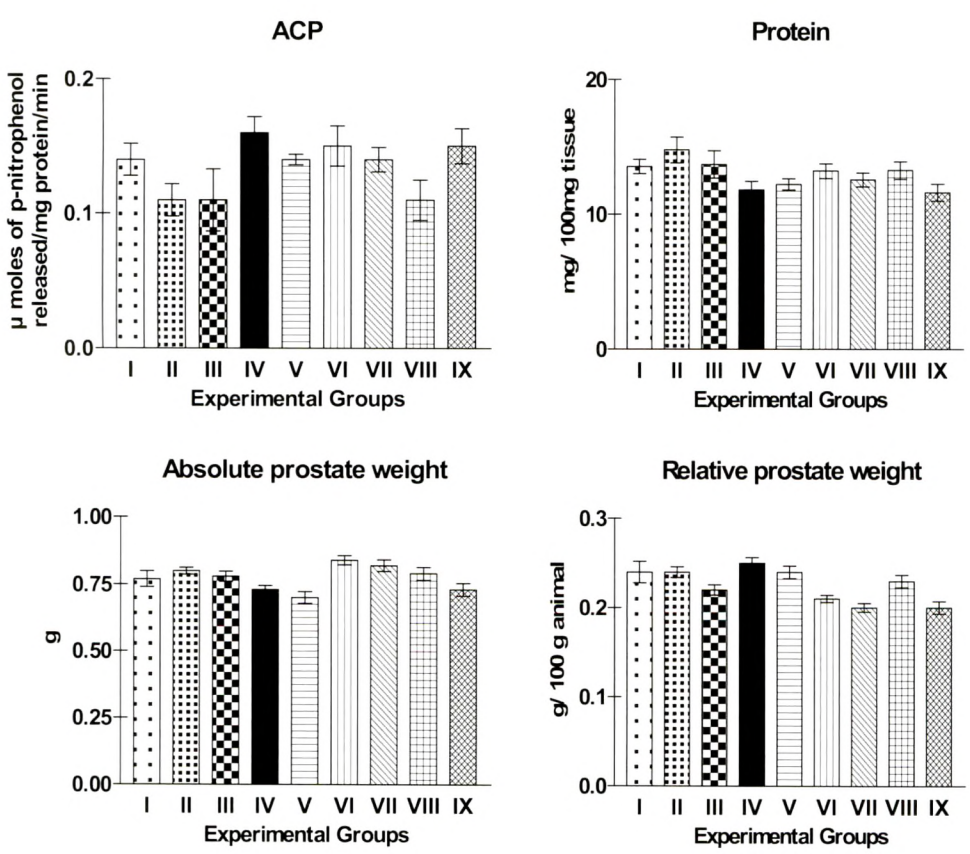

PLATE 1

a: Acridine orange and ethidium bromide stained normal spermatozoa of rat observed under fluorescence microscope.

b and d Sperms showing bent tail and head less tail abnormalities

c Sperms showing abnormalities in head region

e Detached head, non viable sperm

PLATE 1

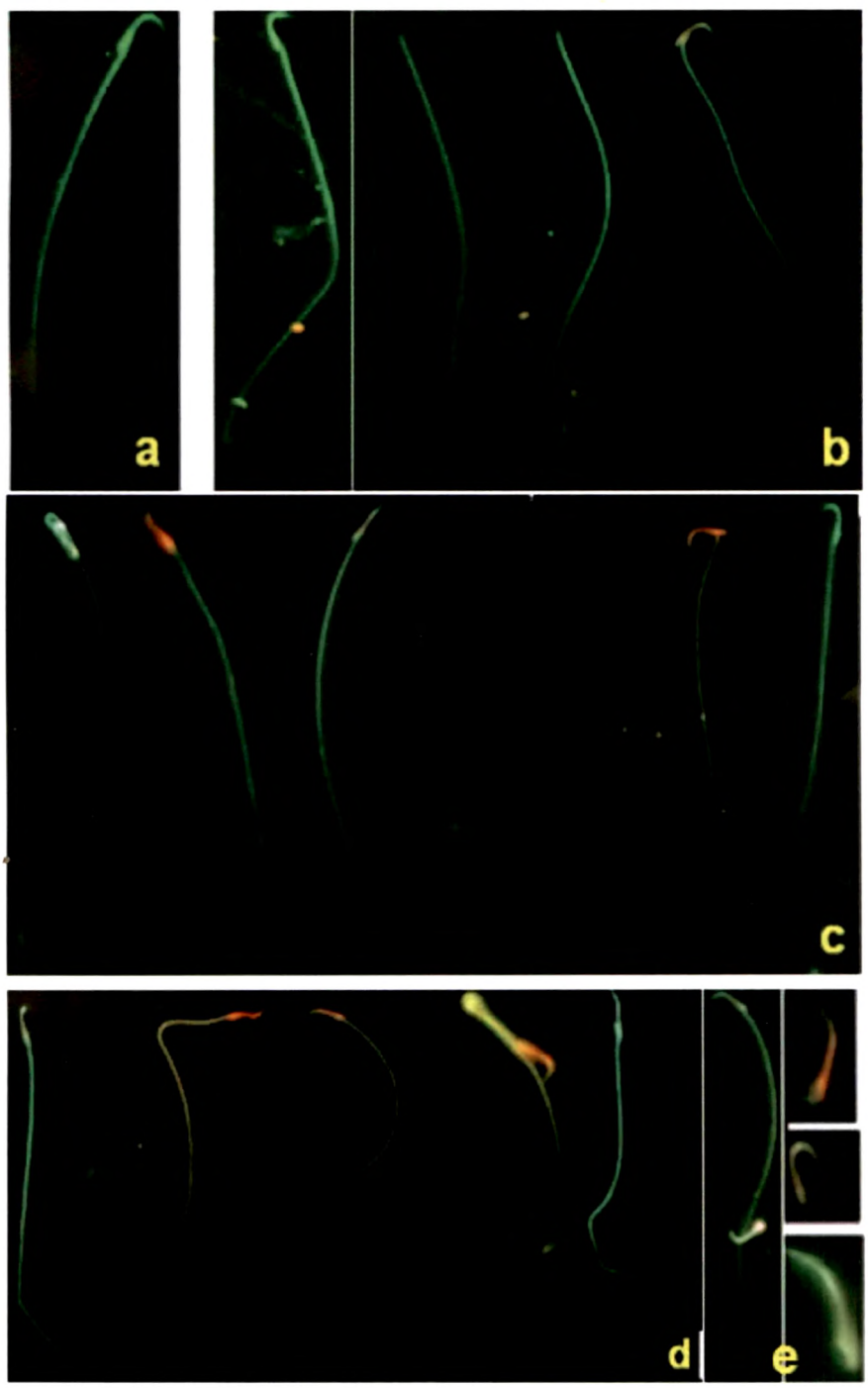

PLATE 2

a Acridine orange and ethidium bromide stained normal spermatozoa (emitted green fluorescence) of control groups rats observed under fluorescence microscope.

b The picture shows the effect of HCM on sperms. The abnormal sperm emitted reddish yellow fluorescence.

C The photograph shows the normal sperm (curve tail) and abnormal sperm (straight tail) after application of hypo osmotic swelling.

PLATE 2

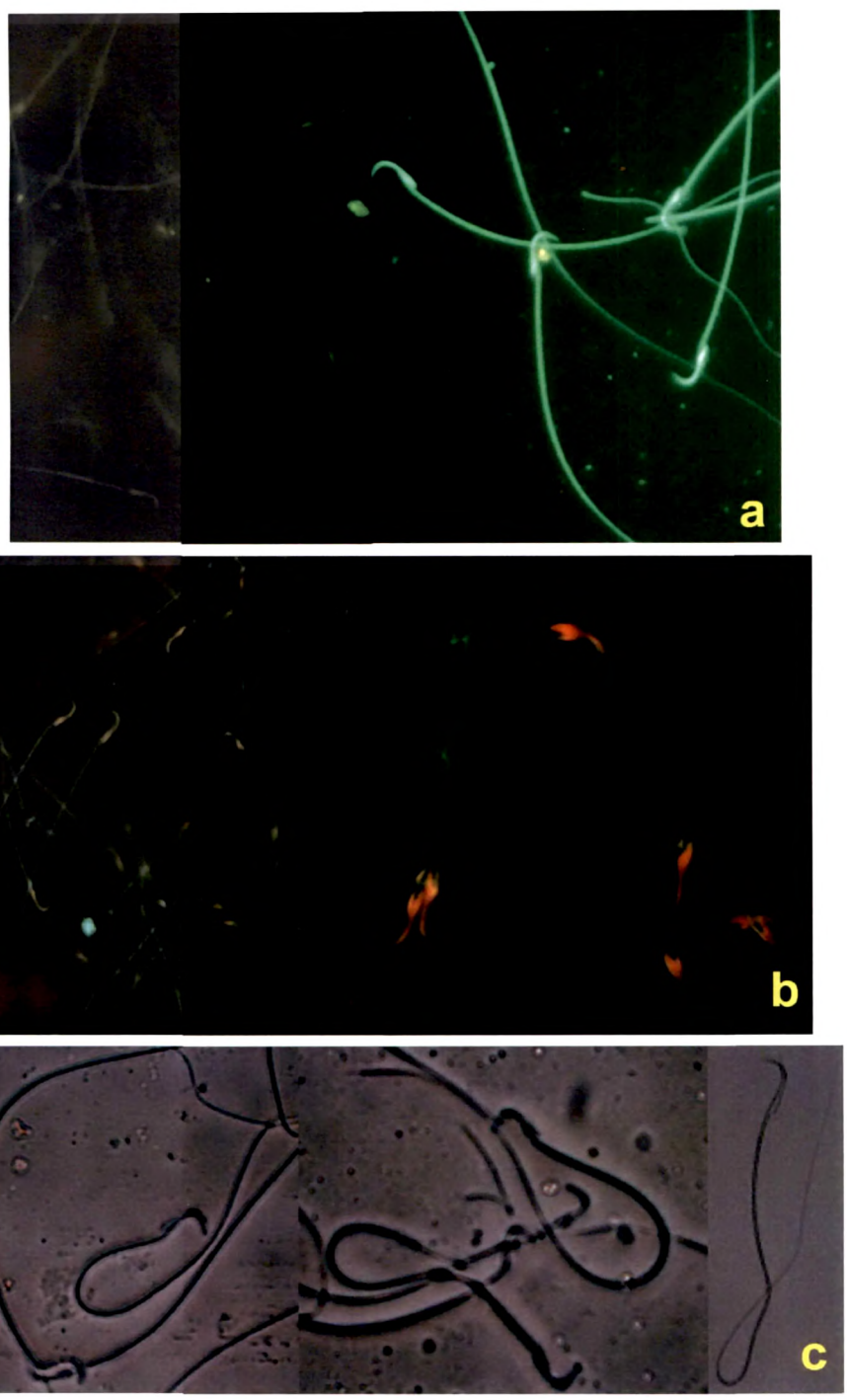

PLATE 3

Showing the histological features of epididymis of control rats.

a, b and c The epithelial lining of the caput epididymis is shown where the nuclei of principal cells are prominent, the luminal margins are wavy and exhibit dense stereocilia. The peritubular membrane also appears to be normal. All 400X

P: Principal cell, B: Basal cell, A: Apical cell, St C: Stereocilia

d The thin epithelium of cauda epididymis is seen where the lumen has sufficient number of spermatozoa (Sz). 400X

PLATE 3

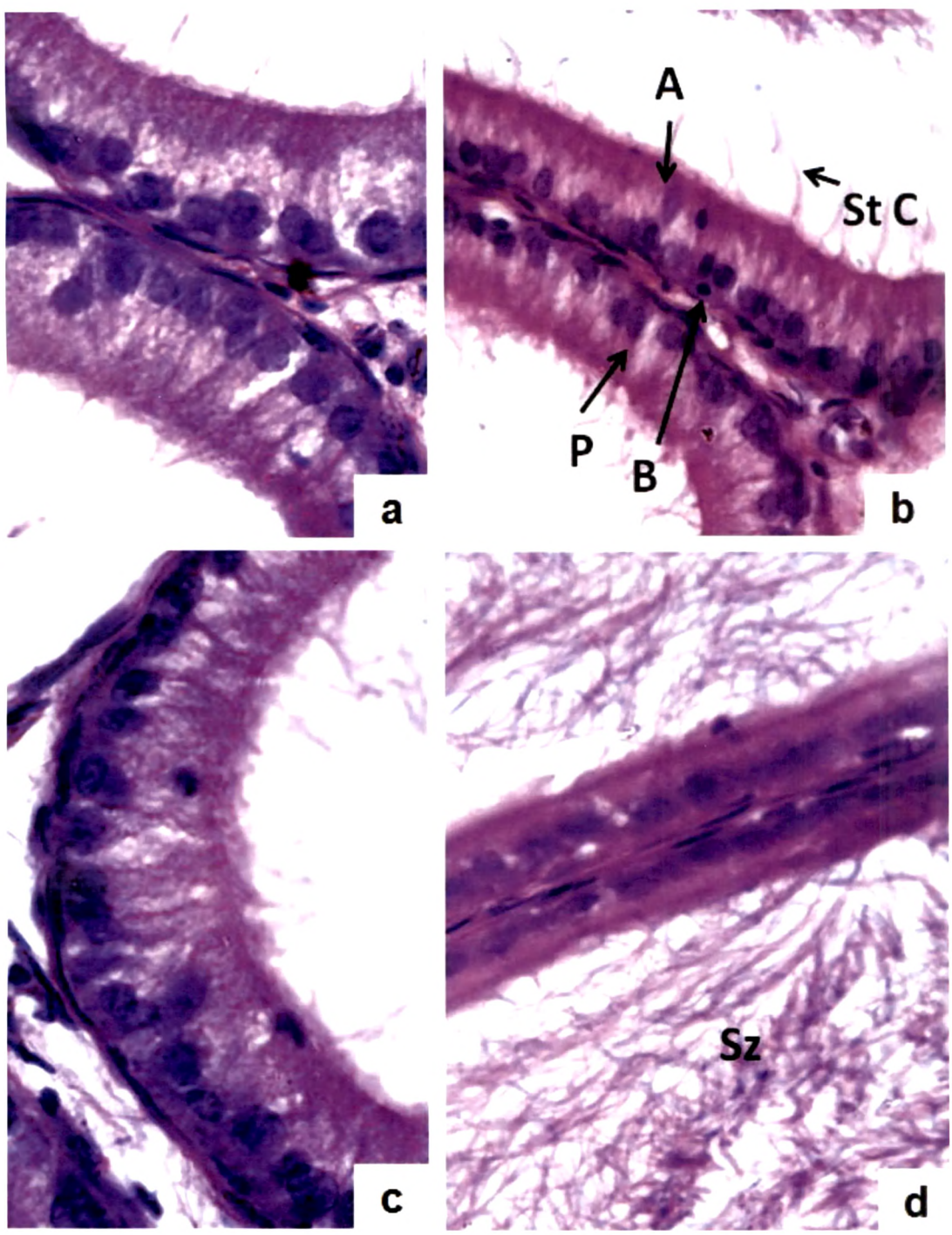

PLATE 4

Showing the caput epididymis of rat exposed to high dose of heterogeneous chemical mixture for 60 days.

a Most of the tubules had very little amount of spermatozoa and such portions were filled with fluid or cellular debris. This photo shows the region of initial part of the caput. The basement membrane is thick and interstitial edema is seen. The fluid exudates have filled up the lumen. The principal cells are vacuolated in the basal portion. 200X

b, d From the apical margin of the epithelium, the release of cytoplasmic blebs are clearly seen. The nuclei of the principal cells appear normal. b 200X, d 400X

c, e The highly eosinophilic apical margin and clogging of stereocilia are prominently seen. The principal cells also show marked vacuolation

PLATE 4

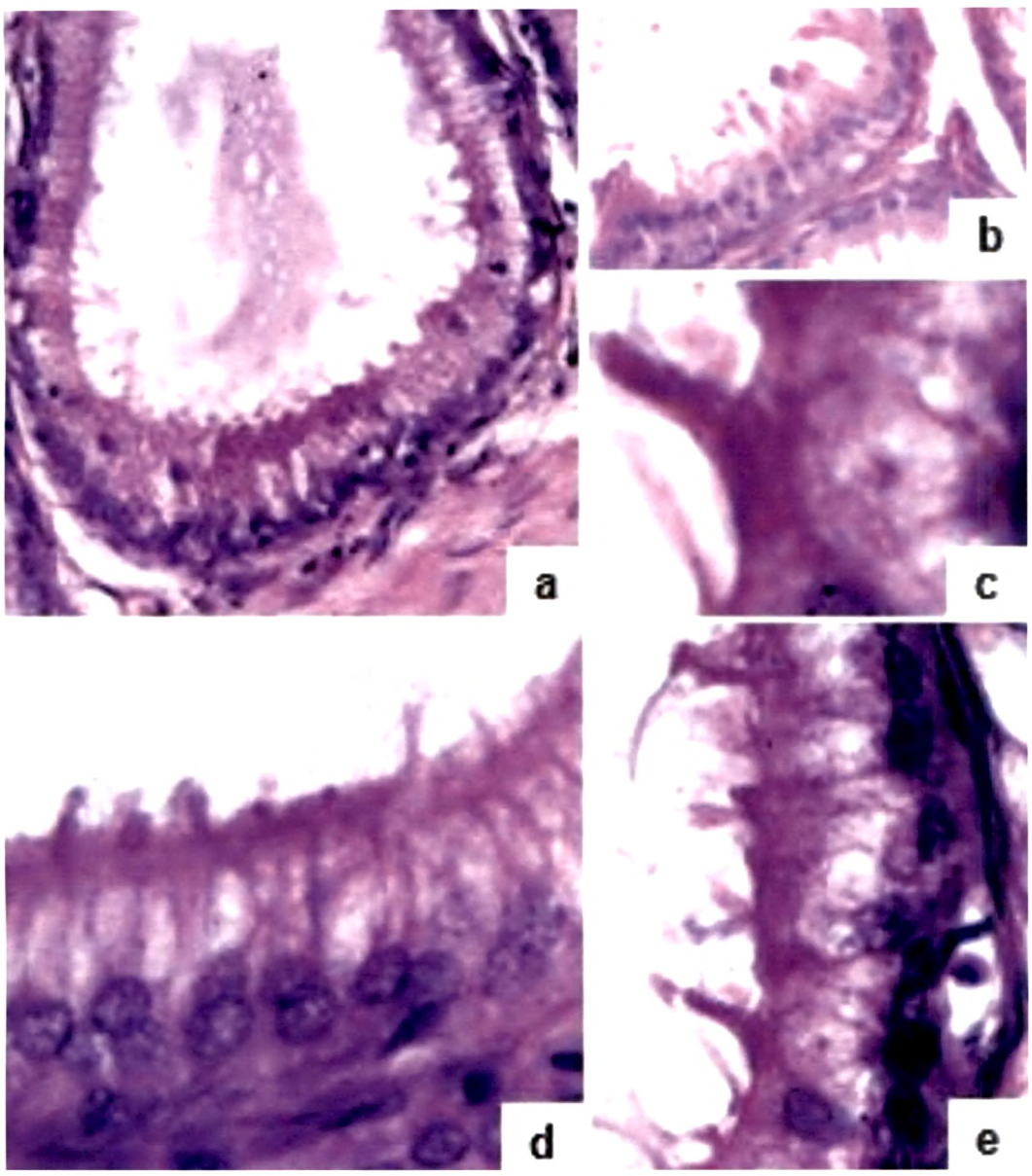

PLATE 5

Showing the caput epididymis of rat exposed to high dose of heterogeneous chemical mixture for 60 days.

a The apical cytoplasm is highly eosinophilic showing cytoplasmic blebbing (CB). Large vacuoles (V) in the epithelium are between the cells suggesting the breakage of cytoplasmic bridges. The degenerating cell debris including that from apoptotic cells are encapsulated in large vacuoles and taken to the apical cytoplasmic membrane where they are release as or along with cytoplasmic blebs (open arrow) . 400X

b, c Some of the features in these epithelia are similar to those described in the above photograph. Additionally, the increase in the population of Halo cells (H) is indicative of inflammatory/ immune responses in b. Supranuclear vacuolation is suggestive of lipoic inclusions. both 400X

d Formation of large vacuolated bodies with several nuclei and cellular debris suggest an apoptotic mass (open star). Such structures fuse together to form larger ones and release out of the epithelium. 400X.

PLATE 5

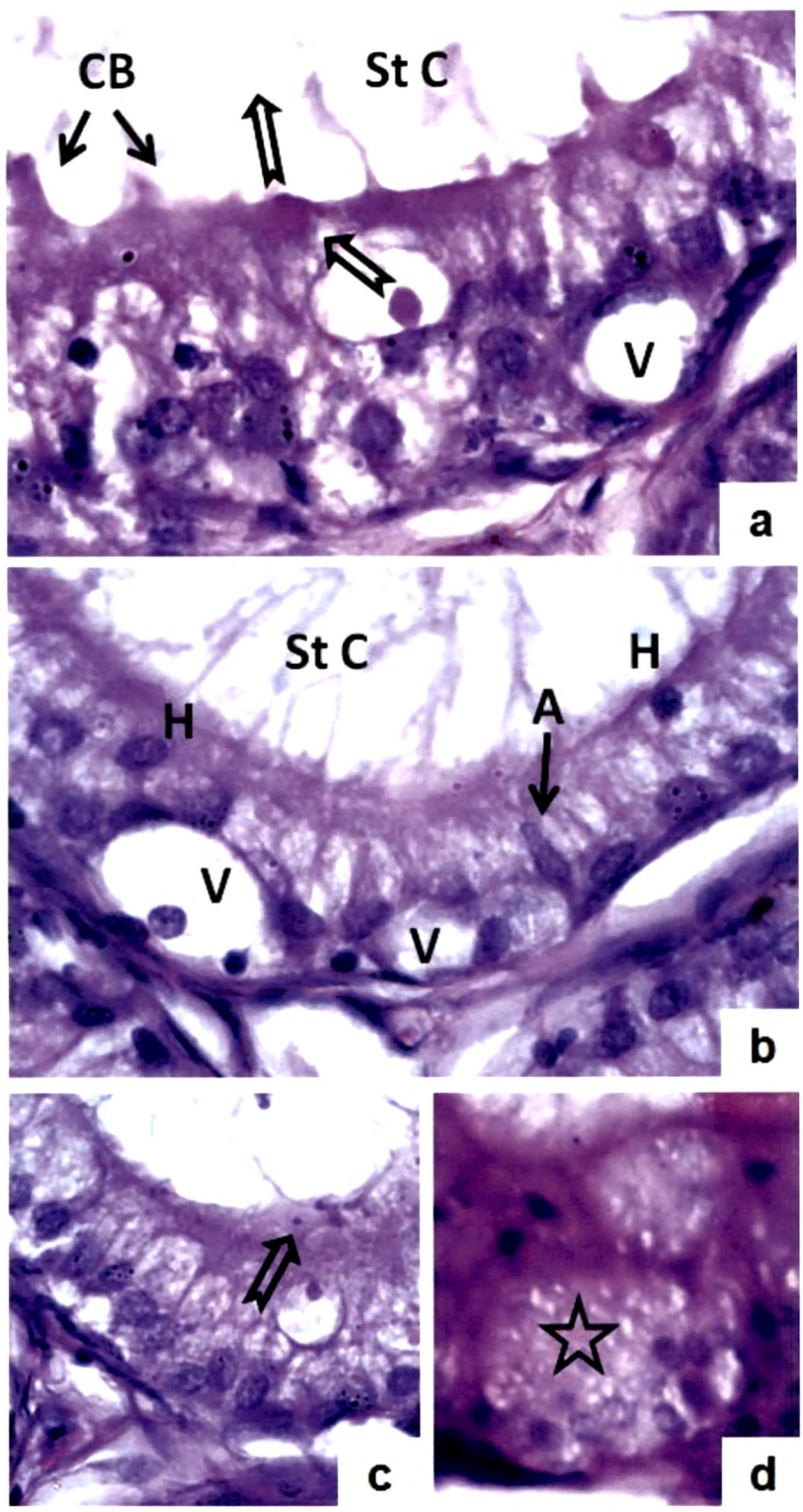

PLATE 6

Showing the caput epididymis of rat exposed to high dose of heterogeneous chemical mixture for 60 days.

a. The cells that could not undergo cytokinesis formed apoptotic body and were taken towards apical margin for release in to the lumen. 400X

b. The apical margin of the epithelium is highly eosinophilic (star) and vacuolated. Several Halo cells (H) are also seen in the outer margin of the epithelium. 400X.

c. The disorganization of the epithelium is prominently seen in this photograph. The cellularity of the epithelium is also distorted. Since the peritubular membrane is damaged the possibility of interstitial cell (like macrophages and lymphocytes) infiltration increases. The cytoplasm of principal cells is highly vacuolated and the vacuoles are of different sizes (open arrow heads). The degenerating nuclei (thick arrow) and cell debris are engulfed in the large vacuoles are being taken towards the apical membrane for release in to the lumen of the duct (open arrow). 400X

PLATE 6

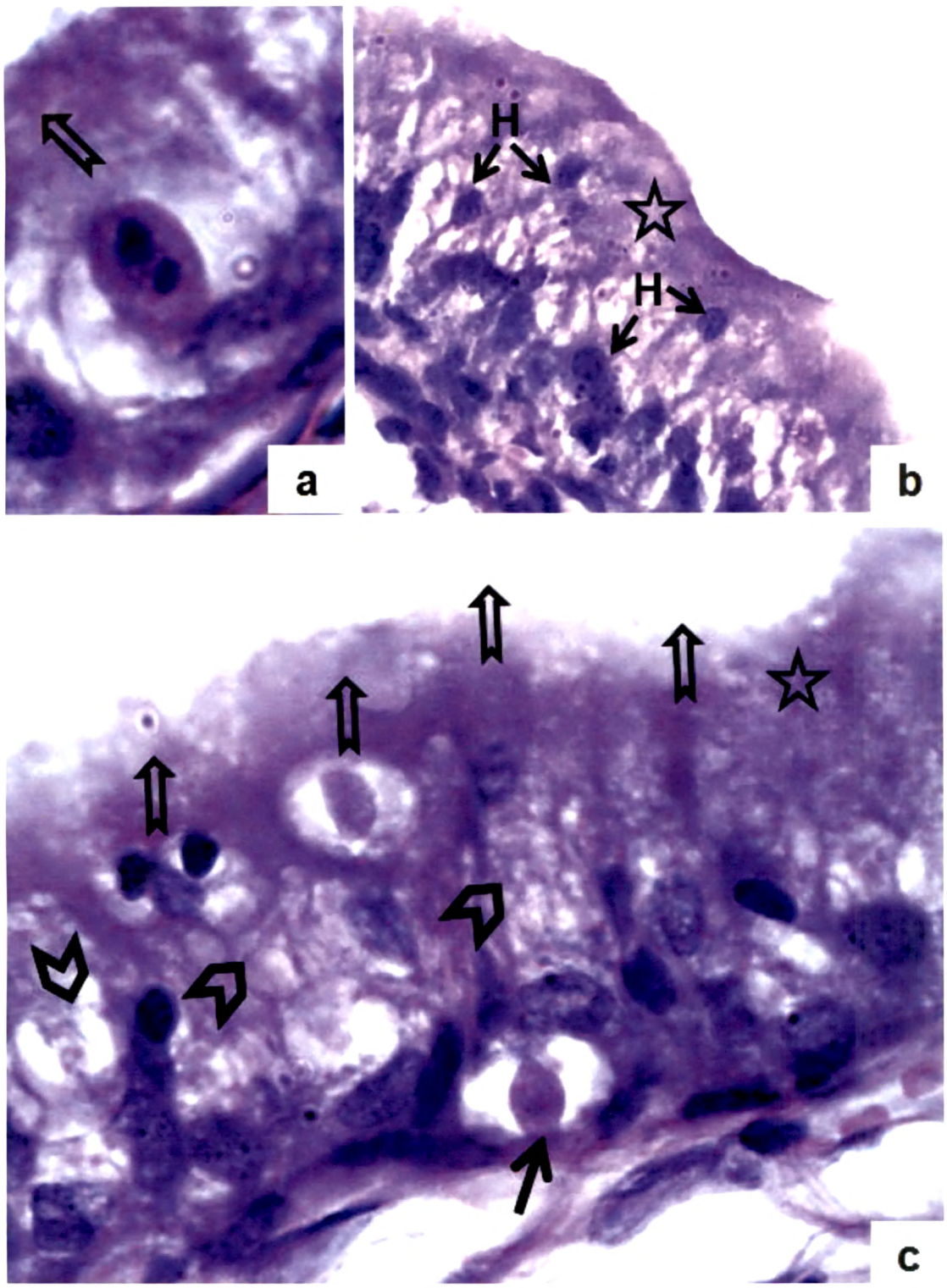

PLATE 7

Showing the cauda epididymis of rat exposed to high dose of heterogeneous chemical mixture for 60 days.

a, b The epithelium is almost entire and the peritubular membrane is also intact. However, the membrane exhibits partial thickening which may be seen as connective tissue enlargement. The lumen is enormously filled with spermatogenic cellular debris, degenerating cytoplasmic masses, cytoplasmic blabs and the residual bodies not taken up by the Sertoli cells during sperm release, and spermatozoa clumps. Such observations made in the testicular histology are confirmed in the epididymal preparations. 200X

c, d The cauda epididymal Principal cell apical margin is shown which is highly eosinophilic with clogged stereocilia. The fragments of spermatogenic cells and spermatozoa are trapped in between. The morphologically abnormal spermatozoa are also seen. 400X

PLATE 7

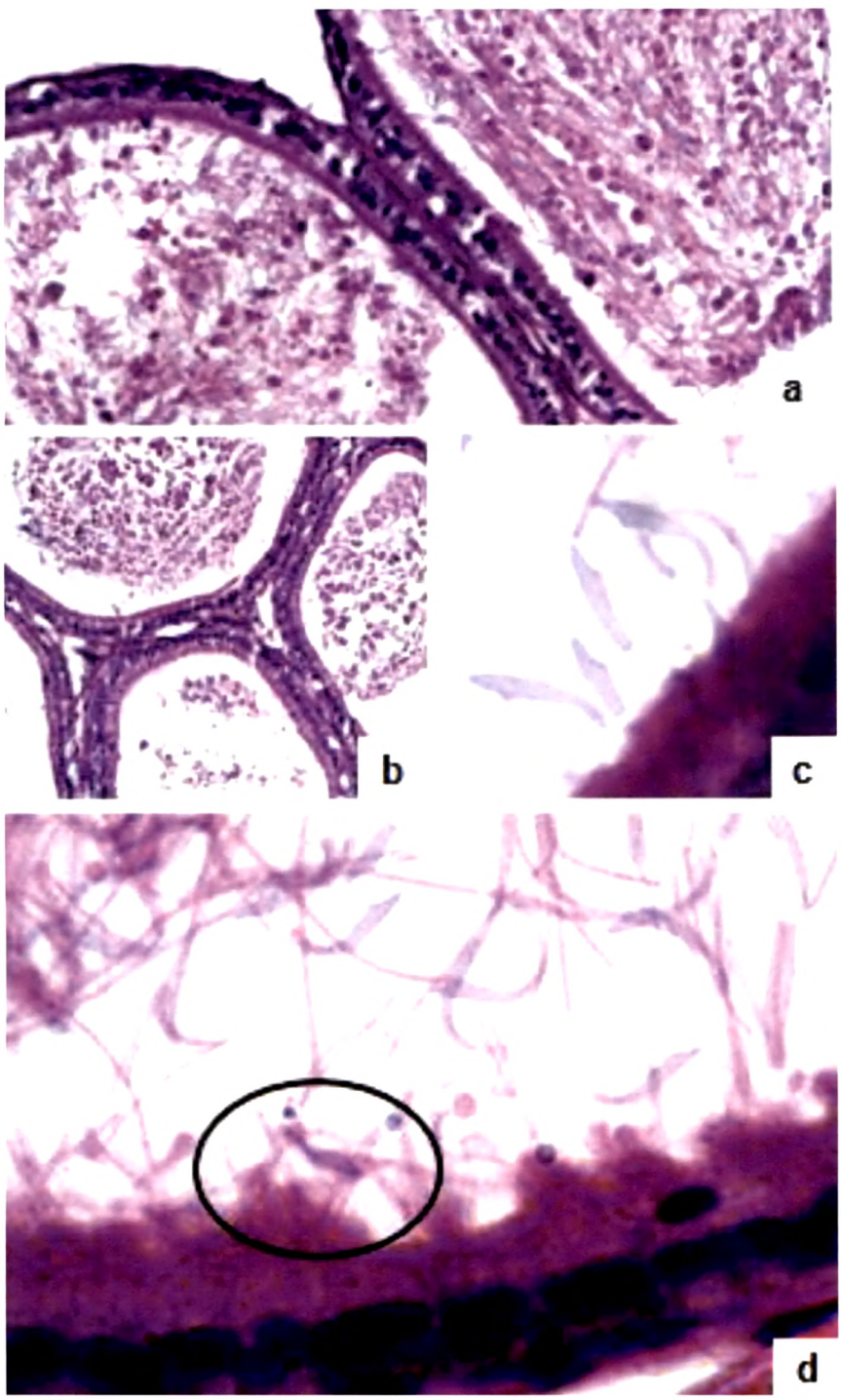

PLATE 8

Showing the caput epididymis of rat exposed to high dose of heterogeneous chemical mixture for 60 days followed by further 60 days of withdrawal.

a The epithelium exhibits significant recovery from the damage induced by the toxicant mixture. The number of H cells is enormous and these are located at the apical margin signifying their role as immune responsive cells. The stereocilia appear quite normal. 400X

b. The organization of nuclei of principal cells and supranuclear vacuoles are suggestive of normal histoarchitecture of caput epithelium. However, the apical margin is eosinophilic and the stereocilia are clogged. The lumen also has traces of edema/ exudates accumulation. 400X.

PLATE 8

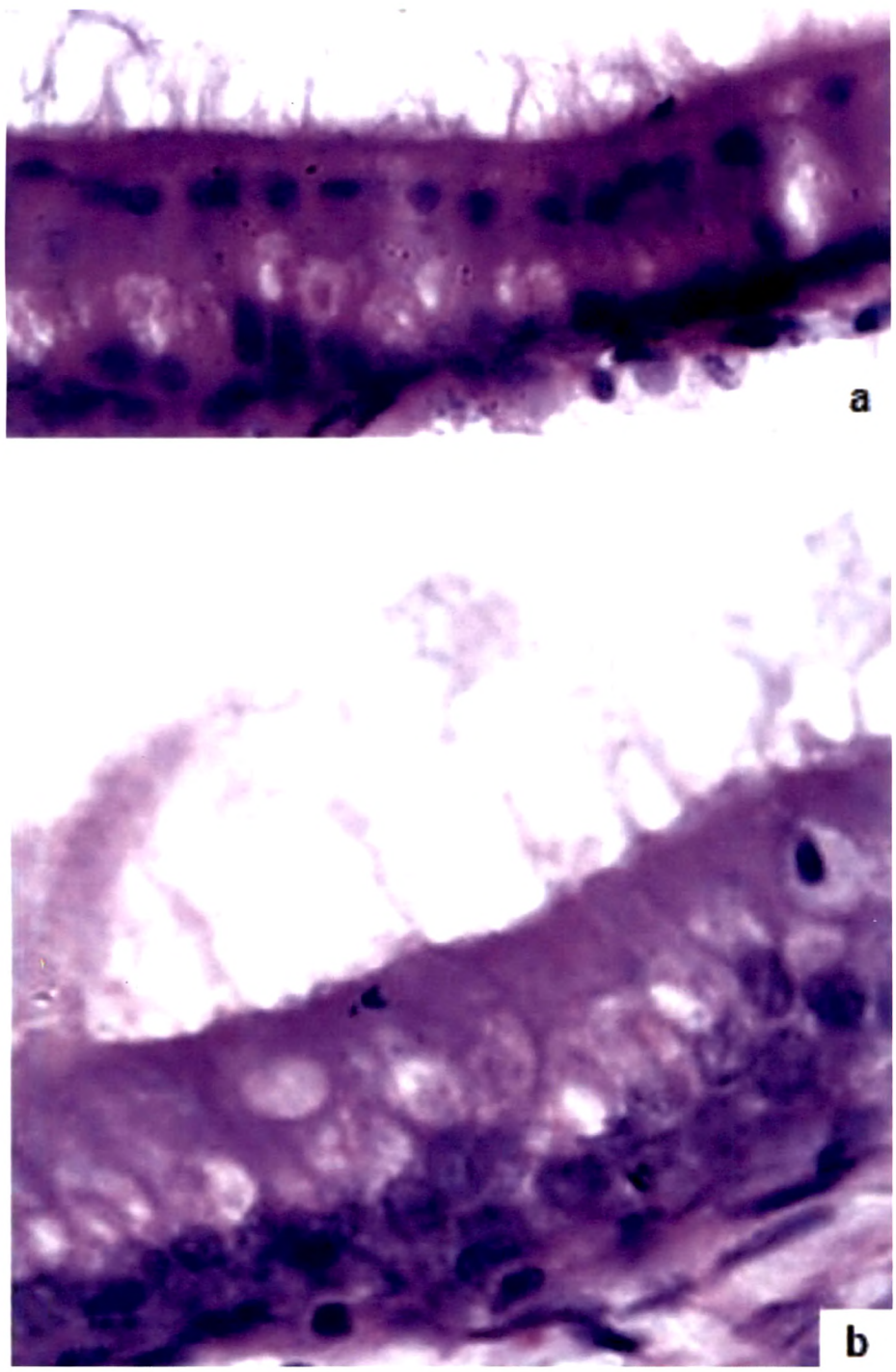

PLATE 9

Showing the epididymis of rat exposed to heterogeneous chemical mixture for 60 days followed by further 60 days of withdrawal.

During the treatment and withdrawal phases the pattern of changes remained quite similar in all the group only the intensity was different and thus exhibited, to some extent, dose and duration related toxic responses.

a, c: The cauda epididymis epithelium in the high dose 120 day group showed improvement but a few cells were still undergoing degenerative changes. The flagella of the spermatozoa were clumped and clogged and therefore indicate persistent effect in the epididymis which result in to high rate of spermatozoa morphological abnormalities like broken tail and isolated heads. 400X

b,d The caput epithelium exhibits almost normal architecture. The spermatozoa also appear normal in content. 400X.

PLATE 9